

Proceedings of the  
NEACRP Specialists' Meeting on

**APPLICATION OF CRITICAL EXPERIMENTS AND  
OPERATING DATA TO CORE DESIGN  
VIA FORMAL METHODS OF  
CROSS SECTION DATA ADJUSTMENT**

**Snow King Resort  
Jackson Hole, Wyoming, U.S.A.  
September 23-24, 1988**



---

**ARGONNE NATIONAL LABORATORY, ARGONNE, IL**

94050001

NEACRP-L-307

PROCEEDINGS OF THE  
NEACRP SPECIALISTS' MEETING  
ON APPLICATION OF CRITICAL EXPERIMENTS AND OPERATING DATA  
TO CORE DESIGN  
VIA FORMAL METHODS OF CROSS SECTION DATA ADJUSTMENT.

Snow King Resort  
Jackson Hole, Wyoming, U.S.A.  
September 23-24, 1988

David C. Wade  
Program Chairman

Administrative Arrangements

Lori DeLuca  
Eileen Johnson  
Karen Leffler

## PREFACE

Over the past decade, powerful formalisms have been developed to bring integral quantity measurements from critical assemblies to bear on core design via adjusted cross section sets. In general, these formalisms:

- rest on the use of functional derivatives computed using generalized perturbation theory, and
- constrain the cross section adjustments via covariance matrices among the measured differential and measured integral data.

These formalisms have the operational virtues of bringing the whole past history of integral experiments to bear on design and operation decisions thereby:

- expanding the relevant integral data base beyond a specific Engineering Mockup Critical experiment, and
- allowing design benefits to accrue prior to construction of a specific Engineering Mockup Critical experiment (or of generation of actual power reactor integral data).

Of major importance, they replace ad hoc procedures by:

- providing a formal means for estimating uncertainties in the calculational design predictions.

Moreover, extensions of this methodology to include depletion-dependent generalized perturbation theory should in the future allow data from operating plants to be brought to bear on design and operating decisions within the same framework as are the critical experiment data.

It was proposed and approved at the 1987 NEACRP Meeting in Helsinki that a specialists meeting be held in the fall of 1988 to review the status of applications of the formal methodology to practical problems of fast reactor design and operation. Applications in the thermal reactor field were also encouraged, though the meeting was not aimed at reload strategies for thermal reactors.

The meeting was organized by Argonne National Laboratory and was held on September 23-24, 1988 at the Snow King Resort in Jackson Hole, Wyoming, following the ANS Topical on Reactor Physics. Thirty-one specialists were in attendance, representing reactor programs in seven countries.

Over two days, fifteen papers were presented and discussed in four technical sessions. Applications of the data adjustment methodology to LMFBR design issues--including spatial dependencies and burnup effects--were treated at length. They indicated a diversity of approaches under consideration in the various national programs. Several papers were presented on theoretical aspects and on directions of future application focus.

This proceedings is comprised of the full-length papers presented in the technical sessions plus the rapporteur's synopses of the content of papers and discussions in each session.

The meeting produced a statement of current status of the field and a set of recommendations to the NEACRP. These are presented in the following section.

As a participant, I found the technical exchange to be substantive and stimulating. The data adjustment methodology as a tool for design is quite evidently coming into the mainstream in all the national LMFBR programs represented; the fascinating thing is that the underlying motivations differ and the implementation approaches are still undergoing exploration--as evidenced by the wide diversity in details of the application method. I believe the meeting was timely and that the collection of papers will be widely read and referenced over the next several years as the methodology continues to mature.

I wish to thank all participants for their attendance and for sharing their points of view and their insights. Especially I thank the rapporteurs for their insightful condensation of the presentations and discussions--done on a very short schedule. Finally, on behalf of all participants I express our thanks to the NEACRP for sponsoring the meeting and to the NEA Secretariate for administrative assistance.

David C. Wade  
Program Chairman



## Conclusions and Recommendations to the NEACRP

The conclusions and recommendations of the conference--as jointly agreed by all in attendance--are as follows.

### Status

- 1) Formal methods of data adjustment are in widespread use in the world's LMFBR programs as a means to apply critical experiments results to design.
- 2) Irradiation operating and/or startup data from Phenix, SPX-1, and PFR are also being applied via data adjustment methods.
- 3) The required calculational tools have been developed and are in place, in most countries, to apply data adjustment to design and operating activities.
- 4) The application of the methodology to the thermal reactor program in France has been initiated to guide cross section evaluation in the thermal range.
- 5) The application to design is achieved in diverse ways in the several LMFBR programs:
  - adjustment of the cross sections on a fine group level,
  - adjustment of the cross sections on a coarse group level,
  - adjustment of quantities previously calculated with unadjusted cross sections through the use of sensitivity vectors,
  - cross section adjustment followed by use of bias factors and uncertainties.
- 6) Use of the methodology has lead to improvement in calculational predictions (reduced  $\frac{E-C}{E}$ ) for integral measurements and leads to reduction in the estimated uncertainties--generally by factors of 2 to 6.
- 7) Use of sensitivity profiles in designing integral experiments is being increasingly employed.

### Recommendations

- 1) The worldwide integral data base constitutes a valuable resource for the improvement of calculated design quantities--which supplements the worldwide differential data base. Efforts conducted within the framework of the NEACRP should explore the possibility of a combined integral data base for common availability.

- 2) Improvement in covariance data are needed across the board:
  - The quantification of the modeling uncertainties and correlations has received the least attention to date and needs more work.
  - The ENDF-VI differential data covariance files are expected to provide improvement over the ENDF-V files; and the JEF-2 files will contain some covariance data.
  - The covariance matrix for the integral experiment data base is crucial to determining improved values of the calculated quantities and is being constructed with special effort.
- 3) The importance of thermal/hydraulics effects has been indicated. Extension of the methodology to thermal/hydraulic and structural effects should be explored in the future.
- 4) It is recommended that a follow-up meeting on this subject be organized in two or three years.

## Table of Contents

	<u>Page</u>
PREFACE .....	ii
CONCLUSIONS & RECOMMENDATIONS TO THE NEACRP .....	iv
<b>Technical Program</b>	
<u>Session 1</u>	
Chairman: A. Gandini (ENEA/VEL, Italy)	
Rapporteur: W. Poenitz (ANL, U.S.A.) .....	1
THE CARNAVAL-IV FORMULAIRE - METHODS, PERFORMANCES AND PRESENTS TRENDS OF DEVELOPMENT	
M. Salvatores, CEA, Cadarache .....	3
THE ADJUSTED CROSS-SECTION SET, FGL5 PRODUCTION, PERFORMANCE AND PROBLEMS	
John L. Rowlands, UKAEA AEE, Winfrith .....	31
ADJUSTMENT OF JENDL-2 CROSS SECTION AND PREDICTION ACCURACY OF FBR CORE PARAMETERS USING JUPITER INTEGRAL DATA	
T. Takeda, M. Takamoto, A. Yoshimura, Osaka University	
K. Shirakata, PNC, .....	39
UNCERTAINTY REDUCTION REQUIREMENTS IN CORES DESIGNED FOR PASSIVE REACTIVITY SHUTDOWN	
D. C. Wade, ANL .....	59
<u>Session 2</u>	
Chairman: Y. Orechwa (ANL, U.S.A.)	
Rapporteur: T. Takeda (Osaka Univ., Japan) ...	75
A DATA BASE FOR THE ADJUSTMENT AND UNCERTAINTY EVALUATION OF REACTOR DESIGN QUANTITIES	
P. J. Collins, C. A. Atkinson, W. P. Poenitz, R. M. Lell, ANL ....	77
UTILIZATION OF EXPERIMENTAL INTEGRAL DATA FOR THE ADJUSTMENT AND UNCERTAINTY EVALUATION OF REACTOR DESIGN QUANTITIES	
W. P. Poenitz and P. J. Collins, ANL .....	97
USE OF SUPERPHENIX START-UP EXPERIMENT FOR DATA ADJUSTMENT A NEW APPROACH	
J. C. Cabrillat, M. Salvatores, CEA, Cadarache	
G. Palmiotti, CISI, Ingenierie.....	125
PREDICTION UNCERTAINTY ANALYSIS BY USE OF SENSITIVITY-BASED METHODOLOGY IN THE NUCLEAR DESIGNING OF A LARGE FAST BREEDER REACTOR	
T. Kamei, Nippon Atomic Industry Group Co., Ltd.	
T. Takeda, Osaka University	
K. Shirakata, PNC .....	145

Table of Contents (Cont.)

	<u>Page</u>
<u>Session 3</u>	
Chairman: K. Skirakata (PNC, Japan)	
Rapporteur: J. Rowlands (UKAEA AEE, U.K.)	165
RECENT INTEGRAL EXPERIMENTS DESIGNED TO IMPROVE HIGHER ACTINIDE DATA TO MEET DESIGN TARGET ACCURACIES	
A. D'Angelo, ENEA-CASACCIA	
M. Salvatores, CEA, Cadarache	167
UNCERTAINTY IN THE BURNUP REACTIVITY SWING OF FAST REACTORS	
H. Khalil, ANL and T. J. Downar, Purdue University	187
NUCLEAR DATA QUALIFICATION FOR THERMAL NEUTRON REACTORS	
H. Tellier, CEN, Saclay	213
TOPICS IN DATA ADJUSTMENT THEORY AND APPLICATIONS	
R. N. Hwang, ANL	227
<u>Session 4</u>	
Chairman: D. Wade (ANL, U.S.A.)	
Rapporteur: D. Hwang (ANL, U.S.A.)	271
ADJUSTMENT METHODS FOR SYSTEM DESIGN AND OPERATION IMPROVEMENT	
A. Gandini, ENEA/VEL, CRE, Casaccia	273
EXTENDED COVARIANCE DATA FOR THE ENDF/B-VI DIFFERENTIAL DATA EVALUATION	
R. W. Peelle, ORNL and D. Muir, LANL	305
RAPPORTEUR'S SYNOPSES OF SESSION CONTENT	
Session 1	317
Session 2	319
Session 3	321
Session 4	325
APPENDIX 1	
List of Participants	329



**SESSION I**

**September 23, 1988**

**Chairman: A. Gandini (ENEA/VEL, Italy)**

**Rapporteur: W. Poenitz (ANL, U.S.A.)**



SPECIALIST'S MEETING ON THE  
APPLICATION OF CRITICAL EXPERIMENTS AND OPERATING DATA TO  
CORE DESIGN VIA FORMAL METHODS OF CROSS-SECTION DATA ADJUSTMENT  
JACKSON-HOLE, SEPTEMBER 23/24, 1988

THE CARNAVAL-IV FORMULAIRE - METHODS, PERFORMANCES  
AND PRESENTS TRENDS OF DEVELOPMENT

by

M. SALVATORES

CEA IRDI/DEDR/DRP/SPRC Cadarache

ABSTRACT :

In this paper we will give the principles of application and practical implementation of CARNAVAL-IV.

We will give for granted the basic principles of the cross section adjustment procedures used to establish the French core formulaire CARNAVAL-IV. Sensitivity analysis techniques will also not be reviewed.

As far as performances, we will concentrate on the results obtained at the SUPER PHENIX start-up.

The lessons that have been learned during these years, are at the basis of the present core formulaire development. We will give a survey of the major points, and two among them will be described in detail in two companion papers at this meeting.



## 1 - INTRODUCTION

The CARNAVAL formulaire has been established to be used by the Fast Reactor core designers. At the origin of its developement it was supposed to provide adjusted data, able to reproduce the neutron balance in a large enough range of spectra / 1 /. The adjustment procedure was of the type of those proposed as early as 1964 / 2 /.

Successive versions of CARNAVAL have been developed, enlarging the experimental data base, each version having as starting point the previously developed version. The version "four" (CARNAVAL-IV), was developed in time (1977) to be used for the definition of the critical enrichments of SUPER PHENIX. At that time, the major new points were the adjustments of fission products and minor actinide data / 3 /. However, during the years it had become evident that basic data adjustments did cover only part of the designer requirements. In fact, even if the prescription was to use for design the adjusted data with the same calculation tools used to analyse the experiments used to adjust the data, this general rule was difficult to apply effectively to all design parameters : control rod worth, power distributions, reactivity coefficient etc. In fact, to avoid calculation method bias, only the so-called "clean core parameters" had been used to adjust data, and in particular the fundamental mode components of the critical neutron balance (buckling, major isotope spectrum indexes,  $K_{\infty}$ ) / 1 /. Moreover, the problem of bias factors and associated uncertainties had become crucial, in the performance assessment of design calculations, in particular in terms of safety margins.

The results of the investigations, was the definition of a set of bias factors and uncertainties for the major design parameters, to be used together with the adjusted data. The complete set (calculation methods, multigroup basic data, bias factors and uncertainties) forms the actual CARNAVAL-IV system.

We will review first this more recent part of the CARNAVAL formulaire development, and we will discuss its performances, as seen at the SUPER PHENIX start-up. Finally, we will give the trends for the present developments.

## 2 - AFTER AN ADJUSTMENT, WHAT IS LEFT ?

Whatever the adjustment technique used, the result of a cross section adjustment can be resumed as a set of multiplication factors to be applied to multigroup data (or to basic parameters, if the adjustment procedure is applied to basic parameters, as it is done in the "consistent" method / 4 /) in such a way that  $\sigma^* = f\sigma$ ; a revised set of E-C\* values, where C\* is the integral parameter calculated value with the adjusted  $\sigma$  set ( $\sigma^*$ ), and "a posteriori" variance-covariance matrices on cross sections,  $B_{\sigma^*}$ , on integral parameters,  $B_{C^*}$ , with eventual correlations among cross sections and integral parameters,  $B_{\sigma^*C^*}$ .

If the statistical adjustment procedure is used, based on Lagrange multipliers / 5 /, this results has a precise meaning, statistically well founded. Interpretation and use of those results can vary, without altering the basic outcome of the procedure.

The mathematics behind these procedures being well known and understood (see, among many references, / 5 / and / 6 /), we will concentrate on the practical problem of the "use" of the results of an adjustment, and, in particular, on the strategy followed to define the CARNAVAL-IV formulaire.

## 3 - HOW TO EXTRAPOLATE TO A REFERENCE DESIGN CONFIGURATION

The major problem related to cross section adjustment, is the assessment of its range of applicability. In other words, the "art" of the physicists is to provide f factors which are as far as possible, independant of set of integral experiment used, or, at least, to provide "rules" to extrapolate the results obtained in critical experiments to a reference design configuration. On the first point, any adjustment which is made on system (or composition) independent parameter (such as a resonance parameter or a nuclear temperature characterising an evaporation spectrum of secondary neutrons / 4 /), is preferable to an adjustment made on a multigroup cross section, which is composition dependent (e.g. via the flux weighting). However, even in the most favorable case, a very large data base of representative experiments are necessary.

The concept of a "representative" integral experiment, is related to the type of integral parameter and to the type of reference (design) configuration of interest.

Most of the cross-section adjustments performed in the 70's, were directed towards well defined reference systems (such as SUPER PHENIX). One tried then to provide an integral data base, varying parametrically the spectrum characteristics of the different experimental configurations, in order to "bracket" the spectrum characteristics of the reference system / 1 /. A more quantitative approach to define the "representativity" of an experiment has been proposed and used / 7, 8 /.

Whatever the approach (qualitative or quantitative) to define the representativity of a set of experiments in terms of their extrapolation to a reference system, one has to define the practical rules of extrapolation for a variety of integral parameters.

These rules amount essentially to define, besides the set of adjusted (infinite dilution) multigroup cross sections and associated unadjusted self-shielding factors (or sub-group parameters, for heterogeneous lattices calculations), bias factors and uncertainties which apply to each individual integral parameter.

In the case of CARNAVAL-IV, we have distinguished three categories of integral parameters, for which different rules have been used to extrapolate the results of the critical experiments.

The first type of parameter is the one for which integral experiments (clean core experiments) were performed and used to adjust cross-sections. As indicated above, this case is represented by the neutron balance (or, more generally, the  $K_{eff}$ ) of the so-called "clean core" (a core made up only with fuel and no singularities such as control rods, control rods followers, special subassemblies, etc...).

The second type of parameter is the one for which integral experiments (mock-up type experiments) have been performed, but not used to adjust cross-sections. Typical examples are control rod worths and reactivity coefficients (e.g. Na void reactivity). The third type of parameters (composite integral parameters) is the one for which integral experiments are not directly available in critical facilities, and which involve several components each depending by different data. Typical examples are the reactivity loss per cycle and the power distributions.

For each category we used the following strategies to set up bias factors and uncertainties.

### 3.1 - "Clean core" integral parameters

For this type of parameters ( $K_{eff}$ ,  $K_{\infty}$ ,  $B^2$ , spectrum indexes) to extrapolate the results obtained to a reference design configuration, the procedure followed at Cadarache has been to characterize each configuration with an indicator, which, for the spectrum-dependent integral parameters has been defined as a spectrum-dependent parameter value  $r$ . In this way, for each integral parameter that has been measured in  $M$  different configurations characterized by a different value of the parameter  $r$ , a graph can be constructed of  $(E-C)/C$ , which results after adjustment as a function of  $r$ . Since the reference power reactor configuration is also characterized by a well-defined  $r$  value, interpolation allows definition of an appropriate bias factor with its associate uncertainty, mainly related to the experimental uncertainties  $\Delta E_j$ . The parameter chosen for all the integral quantities that characterize the critical balance is :

$$r = \frac{\overline{v\Sigma_f}}{\xi\Sigma_s} \quad (6)$$

The physical meaning of this parameter is discussed in Reference / 8 /. Moreover, to illustrate the relevance of the chosen parameter in the case of the core critical balance, in Figs. 1, 2 and 3 the behavior of some major component of that balance is given as a function of the  $r$  parameter. This approach has allowed minimization of the uncertainties related to the bias factor assessment for a reference reactor or for similar reactors of different composition e.g., core enrichment or steel content.

The parametric approach has been particularly successful in the case of the critical mass, as fairly small uncertainties have been associated, as a result of this procedure, with the critical mass definition of SUPER PHENIX / 9 /. It should be stressed, however, that the successful application of this procedure is related to the performance of an ad hoc integral experiment program, related to a well-defined integral parameter class as has been the case in the so-called R-Z program at the MASURCA facility / 1 /.

In Figs. 4 and 5 we indicate two examples of the results of the parametric approach in the case of  $K_{\text{eff}}$  and critical buckling measurements. The experimental points correspond to only a few of the experimental configurations of the R-Z program ; nevertheless the figure show the type of bias factors that can be deduced from this program, corresponding to the two enrichment zones of SUPER PHENIX 1 and their related uncertainties. It is interesting to note that the parametric approach, as far as representativity of the integral experiments, can be shown to be equivalent to a "sensitivity profile similarity" approach. In fact , in Figs. 6 and 7 we show the energy sensitivity profiles of  $K_{\text{eff}}$  to  $^{238}\text{U}$  sigma absorption and sigma inelastic variations for several configurations, corresponding to different values of the r parameter. The sensitivity profiles show a monotonic evolution as a function of the r value, which ensures that no unexpected basic data uncertainty effects will show up in the reference configuration. Of course, care should be exercised in choosing the experiments, with verification of the sensitivity profiles and with physical judgment.

### 3.2 - Mock-up type integral experiments

In the case of control rod worths, bias factors and uncertainties are derived from specific integral experiment programs. The experimental programs in this field are often of a mock up type. In fact, the rod sizes and compositions and the core environment are simulated. However, the control-rod experiments, when they are not performed in a complete core mock-up, are difficult to extrapolate to larger core sizes, since the control-rod reactivity can have a different sensitivity to the data uncertainties in a large reference core and in a typical critical assembly configuration.

In the case of the SUPER PHENIX-1 design calculations the overall uncertainty of  $\pm 13\%$  has been defined taking into account (1) an uncertainty of the calculation of a central control rod in small-to-medium size reactors (up to  $\sim 3000$  l of core volume) and the interactions of two control rods (interaction factors  $f = \rho_{1+2}/(\rho_1 + \rho_2) \approx 1.2$ ), deduced from integral experiments (uncertainty =  $\pm 6\%$  without bias factors) : (2) the supplementary uncertainty due to the extrapolation to larger size cores ( $\pm 4\%$ ) ; and (3) the uncertainty of the calculation method (detailed geometry representation of the rod in exact core geometry),  $\pm 3\%$ . All three uncertainties were simply added together.

In the case of the Na void reactivity coefficient, experiments performed in critical facilities have been used to assess bias factors and uncertainties. A method of biasing individual components (radial and axial leakage, non-leakage component) has been developed /10/, and widely used for design purposes. In table 1 , bias factors obtained for the different Na void components, and their related uncertainties are given for the case of SUPER PHENIX.

However, in the case of the Na void coefficient, calculation method uncertainties play a major role. In fact, in critical experiments and in power reactors, the Na void component calculations are affected by different types of uncertainties. In particular, heterogeneity, modelisation and streaming problems are somewhat different. Moreover, temperature and fuel cycle effects (e.g. fission product effects) are typical of a power reactor and not directly accessible in critical experiments.

In table 2 we show the method uncertainties, for the case of a SUPER PHENIX type LMFBR, which have been combined with the residual uncertainties after application of the bias factors deduced from experiments, and given in table 1 .

### 3.3 - "Composite" integral parameters

#### 3.3.1 - The reactivity loss per cycle

The uncertainty of the reactivity loss per cycle  $\Delta\rho_C$ , is obtained starting from the following simplified decomposition :

$$\begin{aligned}\Delta\rho_C &\cong \sum \Delta N_i (v\sigma_f - \sigma_a)_i \phi\phi^+ - N_{FP}\sigma_{FP}\phi\phi^+ \\ &= \Delta\rho_{HI} + \Delta\rho_{FP},\end{aligned}$$

where  $i = 1, \dots, I$  ( $I$  = total number of fissile and fertile isotopes) and :

$$\Delta N_i = (N_{t=t_F})_i - (N_{t=t_0})_i = N_F^i - N_0^i ;$$

$t_F - t_0$  being the total irradiation time. FP is the index of a lumped pseudo-fission-product isotope.

The actual decomposition for a SUPER PHENIX type reactor, is given in the following table (for an irradiation time of 480 full-power days) :

$\Delta\rho_{HI} \cong -0.7 \% \Delta K/K$
$\Delta\rho_{FP} \cong -2.3 \% \Delta K/K$
$\Delta\rho_C \cong -3.0 \% \Delta K/K$

The uncertainty of the fission-product component can be obtained, starting from isolate fission-product integral experiments and from irradiated fuel oscillation experiments. The present uncertainty of a SUPER PHENIX type reactor has been estimated to be  $\pm 16 \%$  (in reactivity).

For the heavy isotope component,  $\Delta\rho_{HI}$ , a simplified calculation (in fundamental mode) of the relative contribution of the different heavy isotopes gives, in the case of Pu of PWR origin for a 480 FPD (full-power days) irradiation in a SUPER PHENIX type reactor, the results in Table 3. The  $\Delta\rho_C$  values are obtained with a fundamental mode calculation :

$$\Delta\rho_{ci} = \frac{\Delta N_i (\nu\sigma_f - \sigma_a)_i}{\nu\Sigma_f}$$

The standard deviation of the  $\Delta\rho_{HI}$  component due to  $\Delta N_i$  and  $\sigma$  uncertainties can be obtained formally as the sum of two components :

$$E_{HI} = \sqrt{E_{\sigma}^2 + E_{\Delta N}^2}$$

The  $\delta(\Delta N_i)/\Delta N_i$  can also be expressed in terms of cross-section uncertainties, using the generalized perturbation theory in the nuclide field :

$$\frac{\delta\Delta N_i}{\Delta N_i} = \frac{\delta N_F}{N_F^i} \frac{N_F}{\Delta N_i} = \frac{N_F}{\Delta N_i} \sum_j S_j^i \delta\tau_j / \tau_j$$

where  $\delta\tau_j / \tau_j$  are the reaction rate uncertainties, which contribute to the uncertainty of the final number of nuclei of the heavy isotope  $i$ , and  $S_j^i$  are sensitivity coefficients.

In conclusion, if the uncertainties associated with the main reaction rates in the CARNAVAL-IV core formulaire (after adjustment) are used (see Table 4) one obtains the following uncertainty for  $\Delta\rho_{HI}$  :

$$E_{HI} \cong 0.65 \% \frac{\Delta K}{K}$$

which amounts to a substantial 25 % of the nominal  $\Delta\rho_C$ -value.



### 3.3.2 - Power distributions

In general, the uncertainty of power distribution predictions is related to the experiment/calculation comparison of reaction rate distributions, measured in critical facilities.

A detailed breakdown of the power components is necessary to appreciate the different contributions to the uncertainty, which varies according to the different types of subassemblies, and, for the same type, differs according to their position in the core.

In Table 5 we show the breakdown of a core fuel subassembly power for a large LMFBR into its components (fission power,  $\gamma$ -heating, kinetic energy released to materials due to elastic and inelastic interactions). In Table 6 we show the distribution of the total subassembly power in axial subregions.

The reaction rate uncertainties given in Table 4 are representative of the average residual uncertainties, after cross-section adjustments, of the measured reaction rates of the experimental programs on MASURCA.

These uncertainties are larger for subassemblies close to interfaces or special subassemblies (i.e. close to control rods) and, in general, in any case where strong gradients are observed. For  $\gamma$ -heating and kinetic energy release, uncertainty values of 15 and 20 %, respectively, are generally quoted, except close to interfaces where the photon transport phenomena are often approximated in standard calculations and a larger (i.e.  $\pm 40$  %) uncertainty has been suggested. When these uncertainty values are used together with the information in Tables 5 and 6, the results of Table 7 are obtained.

#### 4 - PERFORMANCES OF CARNAVAL-IV AT THE SUPER PHENIX START-UP

The "physical" performances of data adjustments, i.e. the indications which have proved to be physically well founded, have been reviewed elsewhere / 11 /.

In that reference, we recalled that the present state of the art allows us to state that the "brute force" adjustments have left the place to "physical" adjustments.

Here, we will recall only briefly here a few major results obtained at the SUPER PHENIX start-up, which have been discussed in detail elsewhere / 9, 12 /.

They concern the critical mass and the control rod worth.

For the critical mass, after application of the bias factor deduced according the procedure indicated in paragraph 3.1, a C-E close to zero (and within the experimental uncertainties) has been observed both for the minimum critical mass core and for the working core / 9 /. On the contrary, a substantial discrepancy has been observed on the control rod worth. The C/E value varies slightly with the rod configuration type. However, a general overestimation of the calculations of the order of  $8 \div 10$  % has been observed, which cannot be attributed to calculation (e.g. transport effects) or to model (e.g. heterogeneity effects) problems. Both these last two effects have been carefully studied and the present uncertainty is thought to be not larger than  $\sim \pm 3$  %, if the most sophisticated calculation methods are used.

The residual discrepancy could at least in part be attributed to systematic errors in the measurements.

A review of  $\beta_{\text{eff}}$  calculated values does not seem to indicate there a major source of uncertainty, even if this point has still to be experimentally proved.

The experimental techniques used (MSM method with a reference rod drop calibration reactivity, corrected for space effects), does not seem to be affected by large systematic errors, even if statistical uncertainties are not negligible.

For these reasons, we have looked into basic data effects, which are very large for control rod worth in large cores / 8, 13 /.

The first step that we have taken was to investigate known deficiencies of the CARNAVAL-IV (i.e. possible sources of compensation in the analysis of the reactivity of clean cores) and to assess their impact on the control rod worths of SUPER PHENIX.

In particular, it is known that the structural material cross-sections were adjusted in CARNAVAL-IV only in a "global" way. Systematic integral experiments have been performed only after the completion of the formulaire and have not been taken into account, other than to confirm a global performance of the stainless steel cross-section in the reactivity evaluation. However it is known that, in particular for iron, CARNAVAL-IV has both  $\sigma_c$  and  $\sigma_{tr}$  strongly underestimated ( $\sim 50\%$  and  $25\%$  above 100 keV respectively).

One more known deficiency is the  $\sigma_{tr}$  of oxygen in the energy region corresponding to  $\sim 400$  keV. For that resonance, the data (unadjusted) used in CARNAVAL-IV are underestimated (of  $\sim 10 \div 15\%$ ), due to forward scattering bias not accounted for.

Finally, the capture cross-section of B-10 (unadjusted) is too high above  $\sim 200$  keV by approximately  $\sim 10\%$ . If these indications, due exclusively to a better knowledge of basic data, are used together with the sensitivity coefficients given (in six energy groups) in tables 8 and 9, one obtains the interesting result that the calculated control and rod worth is lowered by  $\sim 5\%$  and the critical balance does change only by  $\sim 0.2\%$   $\Delta K/K$ . In other words, a substantial improvement is obtained on the C/E value for the control rod worths, without affecting significantly the excellent performance of CARNAVAL-IV in terms of critical mass prediction.

## 5 - FUTURE TRENDS

The experience gained in the development and use of the CARNAVAL-IV formulaire, has indicated a number of guidelines for the future work.

In fact, in the frame of the European collaboration on Fast Reactors, it has been decided to proceed to development of a unified core formulaire / 14 /.

A clear necessity is to use a more modern and improved data base. This data base will be the version 2 of the JEF file / 15 /, which will hopefully minimize the needs for drastic cross-sections adjustments, allowing in that way to enlarge "naturally" the domain of applicability of any new formulaire.

However, new integral experiments will be used to improve the basic data performances. These new experiments are of different types :

a) Clean integral experiments already performed in the recent past and not yet fully exploited. This is the case for exemple of  $K^\infty = 1$  systems with large amounts of structural materials, performed both in Italy (RB-2/TV) and in France (ERMINE, CADARACHE).

b) Start-up experiments, such as the experiments performed at SUPER PHENIX.

Both these types of experiments have already been used in a preliminary adjustment procedure, starting from CARNAVAL-IV, and the results are given in a paper presented at this meeting / 16 /.

c) Integral experiments explicitly designed to investigate parametrically integral parameters up to now only investigated with mock-up experiments. This is the case of the CONRAD program experiments, devoted to control rod studies, in which the parametrical aspect is formally associated to the definition of a representativity indicator, the eigenvalue separation SVP (or the analogous PAP parameter / 8 /).

d) Mixed critical and power reactor experiments, for specific" composite" integral parameter assessment. A significant exemple is the case of a combined use of the critical integral experiments program BALZAC-HI and PHENIX irradiation experiments, to reduce the uncertainty on the reactivity loss/cycle.

A separate paper at this meeting presents the results of such analysis, again starting from the CARNAVAL-IV data / 17 /.

Finally, it is important to stress the role of the integral data banking effort, which is essential for a future efficient use of these enlarged data bases.

At CADARACHE, a first version of an integral data bank (BDI) is operational. This version contains most of the fundamental mode experiments (clean core experiments), which were used to develop CARNAVAL-IV, and it is being extended to power reactor experiments (PHENIX irradiation experiments and SUPER PHENIX start-up experiment) and to other European critical experiment programs (SNEAK, RB-2/TV, ZEBRA).

As a conclusion, we think that data adjustments will certainly play an essential role in the future, and the convergence of integral and differential data which is more and more achieved / 11 /, is a clear indication in that sense.

#### 6 - REFERENCES

- / 1 / J.Y. BARRE et al., Proc. Int. Conf. Physics of Fast Reactors, Tokyo, October 16-23, 1973, CONF-731015, p. 396, International Atomic Energy Agency (1973).
- / 2 / G.P. CECCHINI et al. Proc. Geneva Conference, P/267 Vol. 2 (1964).
- / 3 / J.P. CHAUDAT et al. Trans. Am. Nucl. Soc. 27, 877 (1977).
- / 4 / A. D'ANGELO, Nucl. Sci. Eng. 65, 477 (1978).
- / 5 / A. GANDINI.
- / 6 / D. SMITH.
- / 7 / L.N. USACHEV et al. Proc. Int. Conf. Neutron Physics and Other Applied Purposes, Harwell, September 25-29, 1978, CONF-780921, p. 181, International Atomic Energy Agency (1978).

- / 8 / G. PALMIOTTI, M. SALVATOIRES, Nucl. Sci. Eng. 87, 333 (1984).
- / 9 / M. SALVATOIRES, Proc. ANS Topical Meeting, Paris April 1987, Page 907, Vol. II (1987).
- / 10 / C.L. BECK et al. Proc. Int. Meet. on Fast Reactor Safety and Related Physics, Chicago (1976).
- / 11 / M. SALVATOIRES "Differential and Integral Experiments : An Overview of Accomplishments" Proc. Int. Conf. on Nuclear Data for Basic and Applied Science, Santa Fe (1985).
- / 12 / J.C. CABRILLAT et al., "Methods and Data Development from the SUPER PHENIX start-up experiments analysis". Proc. of the 1988 Reactor Physics Conference, Jackson Hole (1988).
- / 13 / M. SALVATOIRES, G. PALMIOTTI, Annals of Nucl. En. 12, 291 (1985).
- / 14 / M. SALVATOIRES et al., Development of a common European scheme for fast reactor core calculations. From basic data to experimental validation, ibidem.
- / 15 / M. SALVATOIRES, C. NORDBORG, The JEF evaluated data file. Validation of the version 1 and version 2 development status, ibidem.
- / 16 / J. CABRILLAT, M. SALVATOIRES, this meeting.
- / 17 / A. D'ANGELO, M. SALVATOIRES, this meeting.

TABLE 1

Na VOID BIAS FACTORS OBTAINED FROM EXPERIMENTS

Bias factors		
Radial leakage	Axial leakage	Spectral + Production
$0.98 \pm 0.10$	$1.04 \pm 0.04$	$0.95 \pm 0.03$

TABLE 2

Na VOID METHOD UNCERTAINTIES

Effect	Uncertainty by component		
	Spectral	Axial leakage	Radial leakage
Design method	$\pm 5$	$\pm 5$	$\pm 5$
Transport	$\pm 5$	$\pm 5$	$\pm 5$
Heterogeneity + modelization	$\pm 5$	$\pm 5$	$\pm 5$
Streaming	0	$\pm 5$	$\pm 3$
Temperature	$\pm 2$	0	0
FP effect	+ 1	0	0
TOTAL (%)	$\cong \pm 10$	$\cong \pm 10$	$\cong \pm 10$

TABLE 3

FUNDAMENTAL MODE CALCULATION OF THE ISOTOPE CONTRIBUTION TO THE REACTIVITY LOSS IN A LARGE LMFBR (PWR ORIGIN FUEL, 480 FPD IRRADIATION)

	$N_t = 0$	$N_{t=tF}$	$\Delta\rho_{ci}$ (pcm)	$\nu\sigma_f - \sigma_a$	$\nu\sigma_f$
$^{238}\text{U}$	0.0071	0.00674	1190	- 0.21	0.12
$^{239}\text{Pu}$	0.000746	0.0007785	1450	2.88	5.19
$^{241}\text{Pu}$	0.000153	0.000111	- 2900	4.44	7.37
$^{240}\text{Pu}$	0.000305	0.000326	+ 70	0.20	1.07
$^{242}\text{Pu}$	0.000066	0.000067	- 2	- 0.11	0.72
$^{238}\text{Pu}$	0.000014	0.000012	- 30	1.15	2.52
$^{235}\text{U}$	0.000029	0.000019	- 300	2.17	4.05
$^{241}\text{Am}$	-	0.0000063	- 120	- 1.25	0.97
TOTAL			- 642		

pcm =  $10^{-5}$   $\Delta K/K$ .

TABLE 4

INDICATIVE CARNAVAL-IV FORMULAIRE PERFORMANCES FOR MAJOR REACTIONS AND ISOTOPES

	$\delta\nu\sigma_f/\nu\sigma_f$ (%)	$\delta\sigma_a/\sigma_a$ (%)	$\delta\sigma_c/\sigma_c$ (%)
$^{238}\text{U}$	$\pm 5$	$\pm 5$	$\pm 2.5$
$^{239}\text{Pu}$	$\pm 2$	$\pm 6$	$\pm 10$
$^{241}\text{Pu}$	$\pm 6$	$\pm 10$	$\pm 12$
$^{240}\text{Pu}$	-	-	$\pm 12$
Structural materials	-	$\pm 25$	$\pm 20$



TABLE 5  
TYPICAL CORE SUBASSEMBLY POWER DECOMPOSITION  
FOR A LARGE LMFBR

Isotope	Fission Contribution	(n, $\gamma$ ) Capture Contribution	Kinetic Energy Contribution	
$^{235}\text{U}$	2.1	-		
$^{238}\text{U}$	10.3	6.2		
$^{239}\text{Pu}$	68.4	1.6		
$^{240}\text{Pu}$	3.9	0.4		
$^{241}\text{Pu}$	3.5	-		
Others	-	1.8		
TOTAL (%)	88.2	10	1.8	= 100

TABLE 6  
AXIAL POWER DECOMPOSITION OF A STANDARD FUEL  
SUBASSEMBLY AT THE CORE CENTER

Zone	Power fraction (%)
Axial blanket (30 cm both sides of fuel height)	2.7
Center of fuel column (2/3 of total height)	71.2
Fuel column edge (both sides of central 2/3 fuel column)	26.1

TABLE 7

POWER UNCERTAINTIES OF DIFFERENT TYPES OF CORE SUBASSEMBLIES

Parameter	Fuel subassembly			Fertile subassemblies
	Far from control rods	Adjacent to control rods	At core/blanket interfaces	
Max. linear power	$\pm 3$	$\pm 4$	$\pm 5$	First row : $\pm 12\%$ Second row : $\pm 20\%$ Third row : $\pm 30\%$
Integrated power	$\pm 3.5$	$\pm 6$	$\pm 6$	

TABLE 8

SENSITIVITY COEFFICIENTS OF ROD RING WORTHS IN SPX-1, DUE TO + 10 %  
VARIATION OF  $\sigma$

Group	$\sigma_c^{Fe}$			$\sigma_{tr}^{Fe}$			$\sigma_{tr}^{Ox}$		
	RI (*)	RE (*)	RI+RE (*)	RI	RE	RI+RE	RI	RE	RI+RE
1	0.01	0.02	0.01	- 0.8	- 0.3	- 0.2	- 0.7	- 0.1	- 0.2
2	0.0	0.01	0.0	- 0.7	- 0.2	- 0.2	- 0.9	- 0.2	- 0.3
3	- 0.02	0.04	0.0	- 1.1	- 0.6	- 0.4	- 1.6	- 0.5	- 0.6
4	- 0.01	0.02	0.0	- 0.2	- 0.1	- 0.1	- 0.2	- 0.1	- 0.1
5	- 0.04	0.07	- 0.02	- 0.2	- 0.1	- 0.1	- 0.1	0.	- 0.1
6	0.0	0.0	0.0	0.	0.	0.	0.	0.	0.

Group	$\sigma_f^{Pu-239}$			$\sigma_c^{U-238}$			$\sigma_{tr}^{U-238}$		
	RI	RE	RI+RE	RI	RE	RI+RE	RI	RE	RI+RE
1	- 1.9	- 0.6	- 1.1	0.01	+ 0.04	+ 0.03	- 0.8	- 0.8	- 0.3
2	- 2.3	- 1.0	- 1.7	- 0.02	+ 0.2	+ 0.1	- 0.8	- 0.8	- 0.3
3	- 3.8	- 2.1	- 3.0	- 0.7	+ 0.4	- 0.03	- 1.5	- 1.5	- 0.6
4	- 0.5	- 0.7	- 0.5	- 0.6	+ 0.5	- 0.1	- 0.3	- 0.3	- 0.2
5	+ 0.5	- 0.9	+ 0.01	- 0.9	+ 0.6	- 0.3	- 0.1	- 0.1	- 0.1
6	+ 0.2	- 0.1	+ 0.1	- 0.1	+ 0.05	- 0.04	0.	0.	0.

(\*) RI : inner rod ring worth  
RE : outer rod ring worth

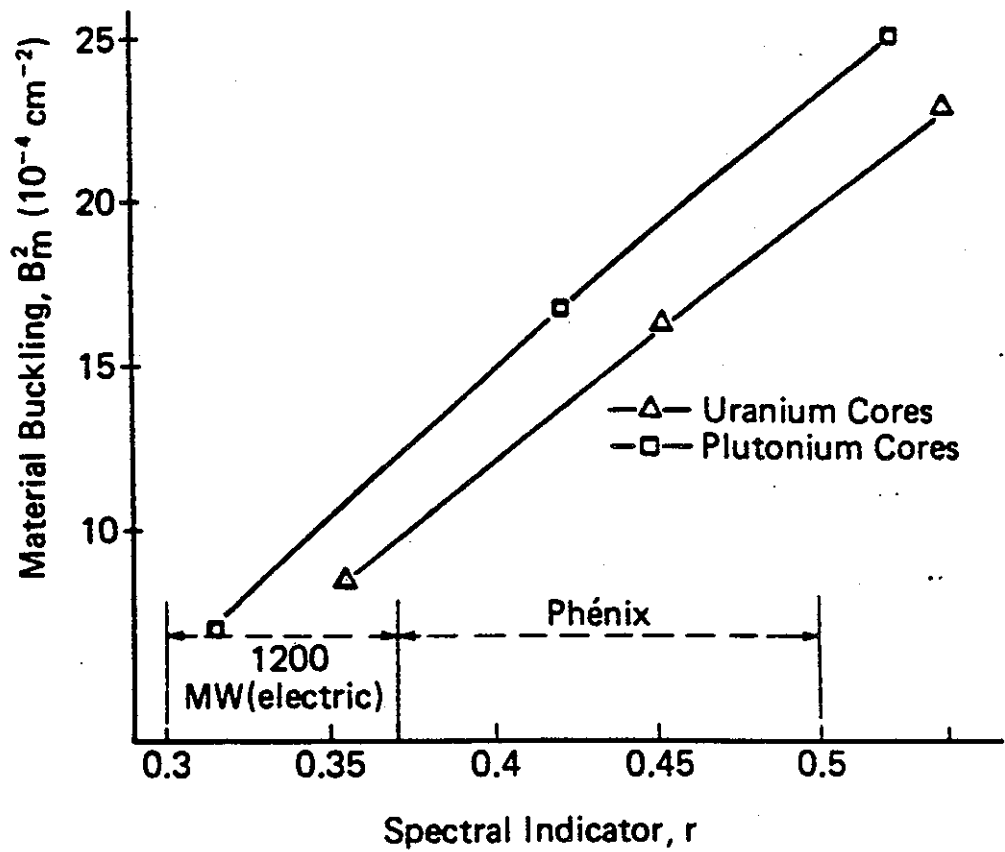


Fig. 1. Material buckling as a function of the spectral indicator  $r = \nu\Sigma_f/\xi\Sigma_s$ .

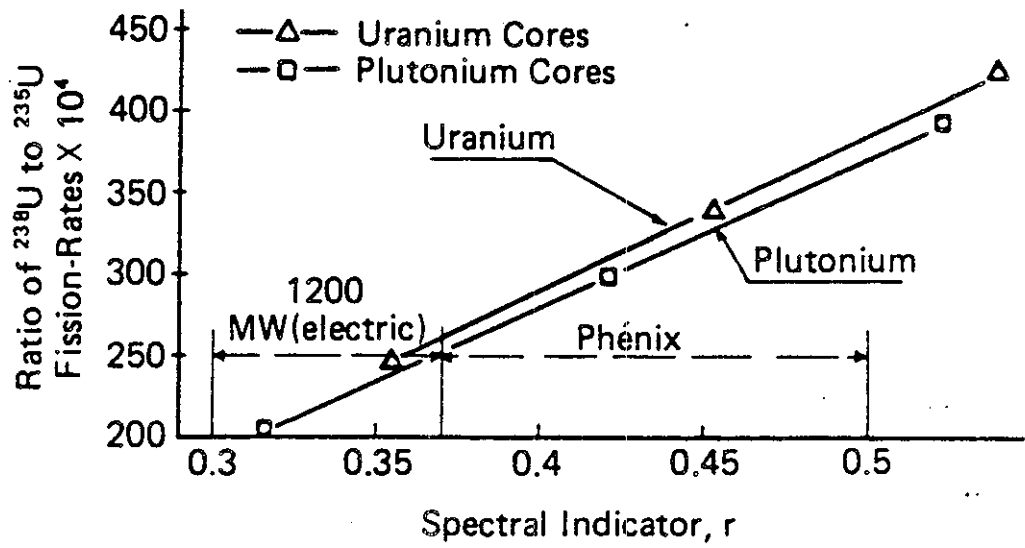


Fig. 2. Ratio of  $^{238}\text{U}$  fission reaction rate to  $^{235}\text{U}$  fission reaction rate as a function of the spectral indicator  $r = \nu\Sigma_f/\xi\Sigma_s$ .

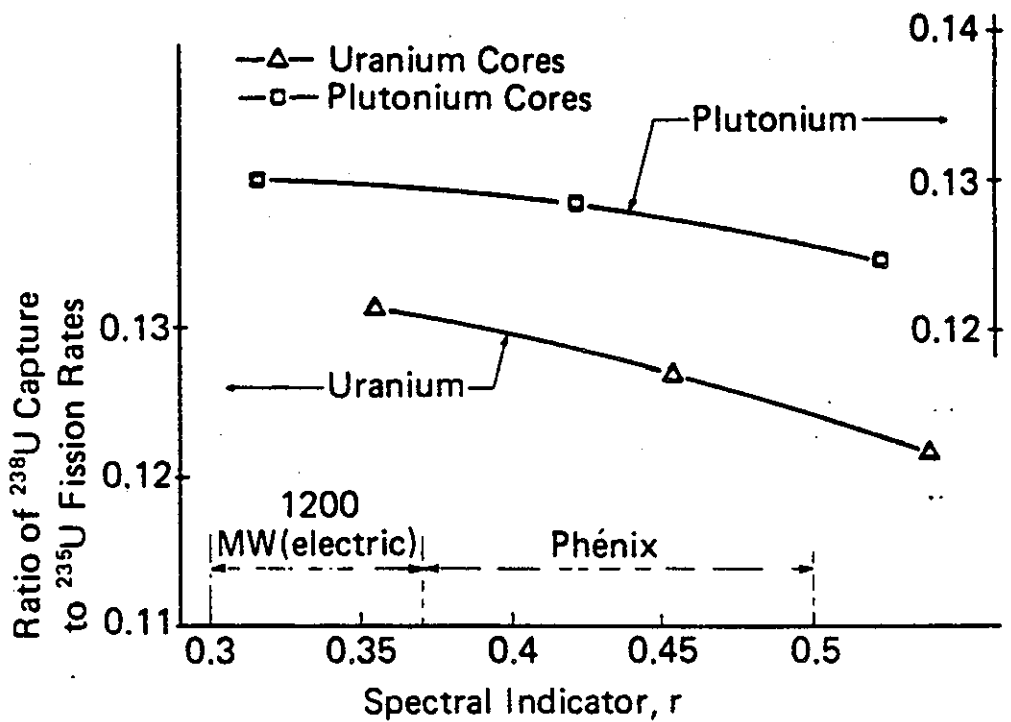


Fig. 3. Ratio of  $^{238}\text{U}$  capture reaction rate to  $^{235}\text{U}$  fission reaction rate as a function of the spectral indicator  $r = \nu \overline{\Sigma}_f / \xi \overline{\Sigma}_s$ .

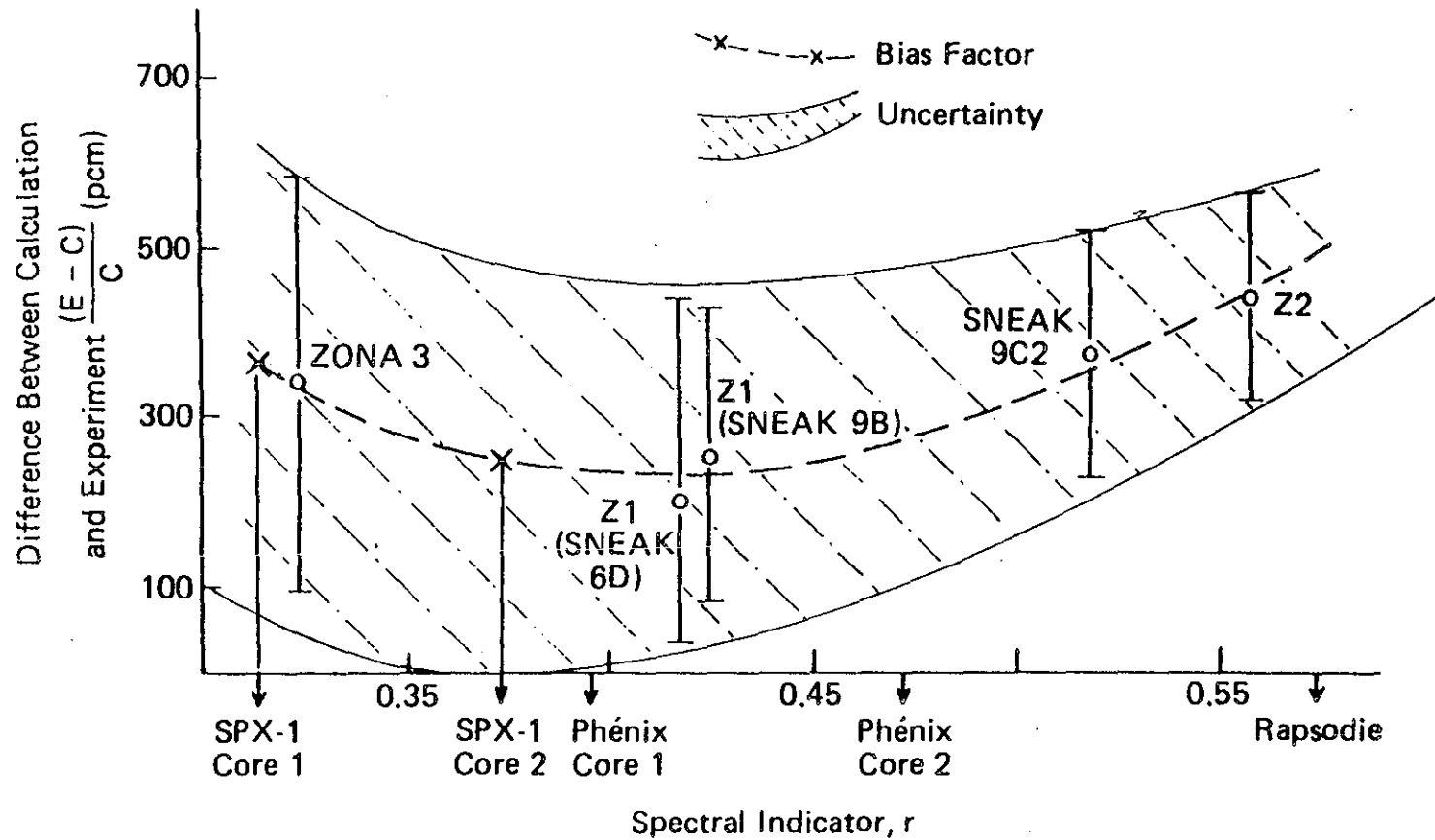


Fig. 4. Residual  $(E - C)$  values of  $k_{eff}$  after adjustment of some experiments of the  $R-Z$  program and the resulting bias factors for different reference plutonium-fueled LMFBRs (SPX-1 = Super Phénix 1).

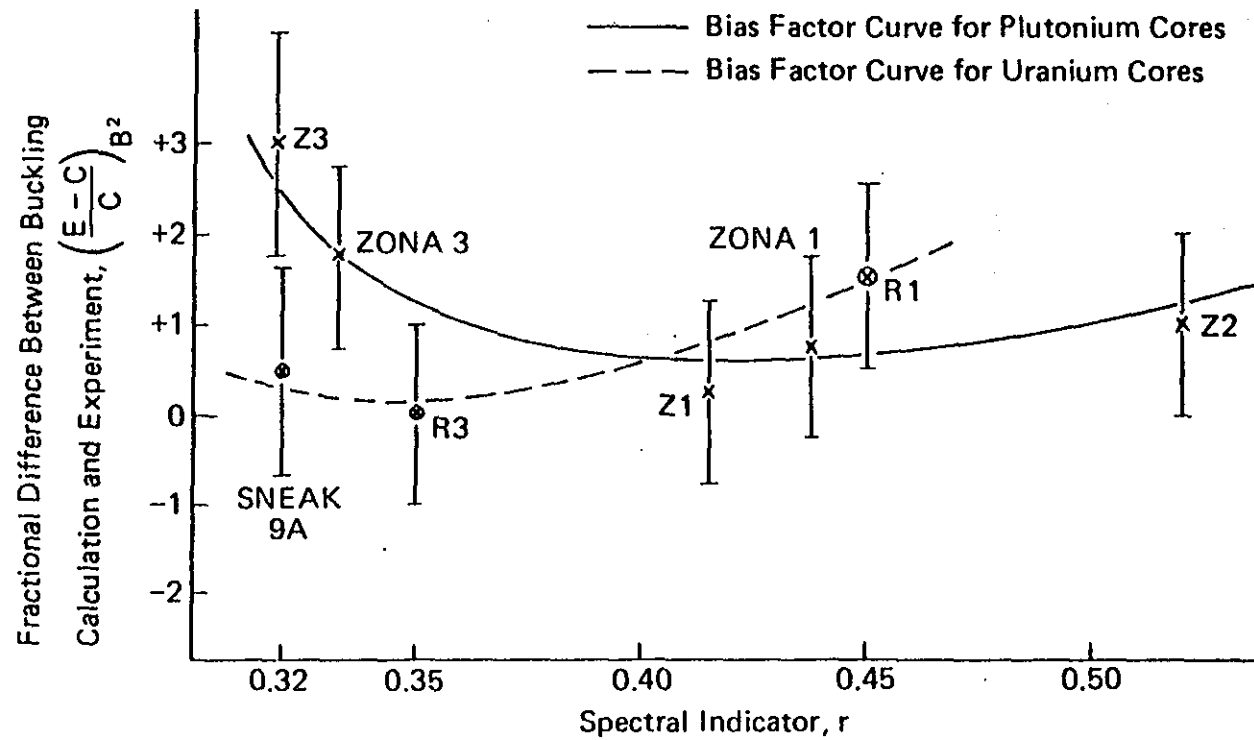


Fig. 5. Residual  $(E - C)/C$  values of  $B^2$  after adjustment of some experiments of the  $R-Z$  program and the resulting bias factor curves for uranium and plutonium cores.



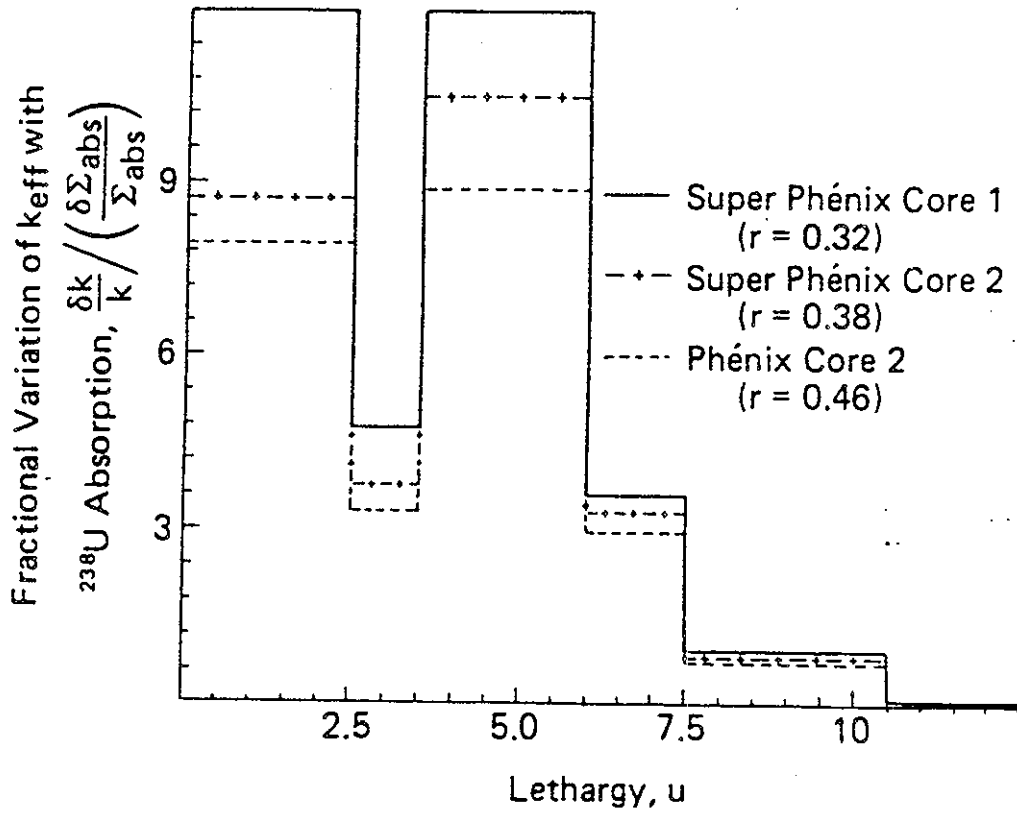


Fig. 6. Energy sensitivity profiles of  $k_{eff}$  of  $^{238}\text{U}$   $\Sigma_{absorption}$  variations for different configurations.

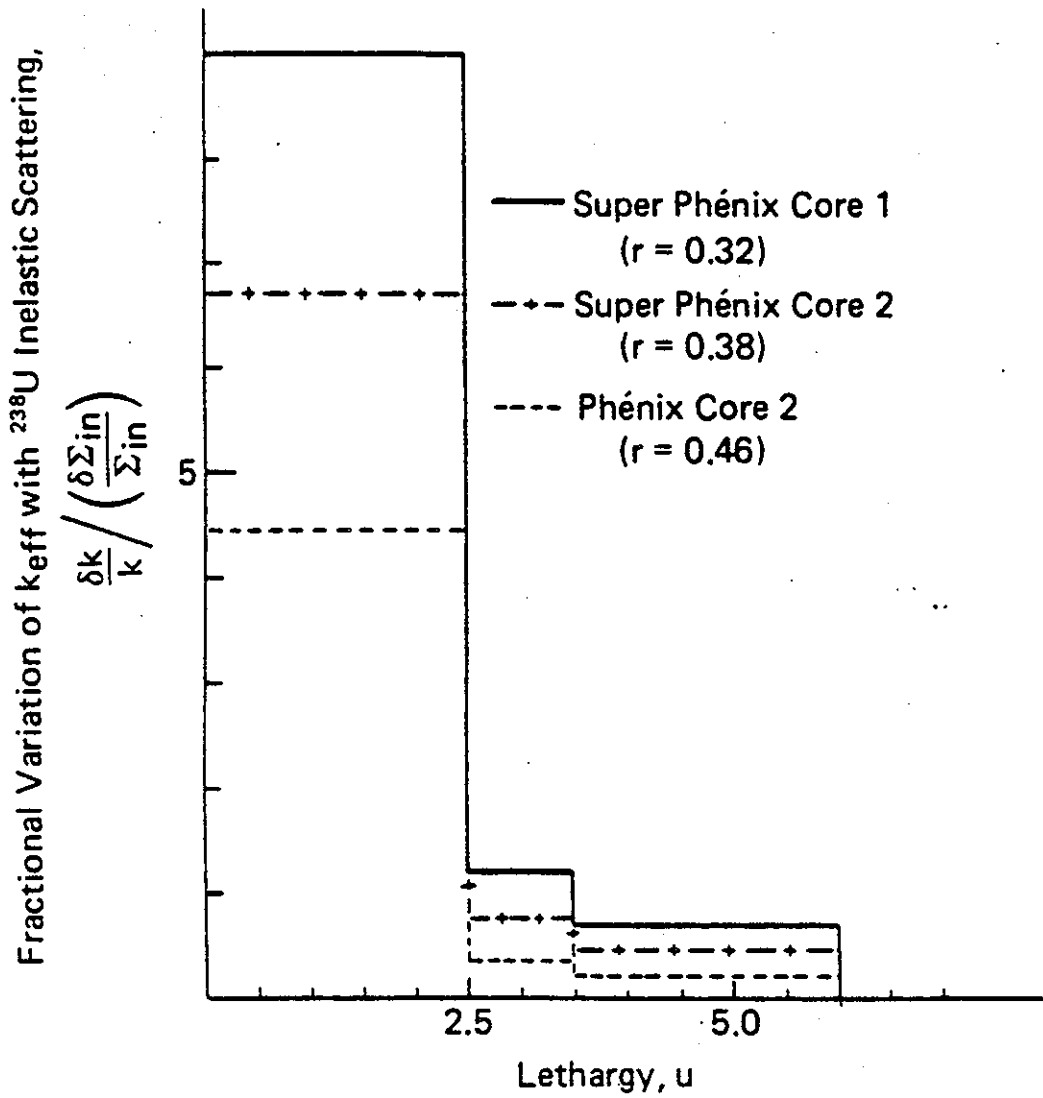


Fig. 7. Energy sensitivity profiles of  $k_{eff}$  to  $^{238}\text{U}$   $\Sigma_{inelastic}$  variations for different configurations.



THE ADJUSTED CROSS-SECTION SET, FGL5  
PRODUCTION, PERFORMANCE AND PROBLEMS

John L. Rowlands  
UKAEA AEE Winfrith  
Dorchester, Dorset, UK

ABSTRACT

The paper describes aspects of the way in which the adjusted cross-section set FGL5 was produced, problems encountered in its production and problems which have become evident since it was produced.

INTRODUCTION

Cross-section adjustments can be made either to improve predictions for a particular reactor type using a particular calculational method (in which case the adjustments partly compensate for methods approximations) or they can aim to improve calculations made using them, independently of the reactor type and calculational method. Our aim has been to produce adjusted cross-sections of the second type. The cross-section adjustments are chosen to be consistent with the uncertainties by providing a least squares fit to the differential cross-section and integral measurements. Individual cross-section adjustments might not be improvements but the combined set of adjustments results in improved predictions of reactor properties, particularly for the class of properties used to adjust the data. The accuracy of prediction should be no worse for any property because the cross-sections are adjusted taking into account uncertainties. This is the aim. The extent to which a general improvement in accuracy is achieved depends on the extent to which uncertainties in the integral measurements and approximations in the calculational methods are recognised and taken into account. It also requires the fitting to be made to a wide range of characteristics measured on assemblies having different compositions and with different neutron spectra so that the different contributions to discrepancies between measurement and calculation can be separated (by material and energy range).

It is the systematic errors which are important; that is, errors which affect all of the measurements of a particular type in about the same way. Such errors can also be correlated between different types of integral measurement. An example of a systematic error which was not recognised when the FGL5 set was produced<sup>1</sup> is the ZEBRA pin-plate discrepancy. There is a discrepancy of about 0.5% between the Keff values calculated for plate geometry assemblies and pin geometry assemblies in ZEBRA and this discrepancy is still not understood.

Measurements made in the ZEBRA plate geometry cores (which have plutonium metal plates) predominated in the integral data used to produce FGL5 and a simple (one dimensional) cell model was used to calculate them. This simple model results in systematic underestimates of  $K_{eff}$  for plate geometry cores, relative to pin geometry cores, of about 1%, and there is a corresponding effect on relative reaction rates.

Simplifications are made in the adjustment of cross-sections. For example, an average adjustment is made in a broad energy range (the FGL5 adjustments were calculated in 10 energy groups only). Although, in principle, a fine energy representation can be used (with individual resonance parameters being adjusted and detailed secondary energy and angular distributions parametrised and adjusted) a broad group approach is more usual. Indeed, most integral properties are sensitive only to the average cross-section changes in broad energy intervals, and some are sensitive only to combinations of cross-sections, rather than individual cross-sections. Thus it can be acceptable for some materials and energy ranges to treat just the total inelastic scattering cross-section as a variable and to decide separately how the change is to be partitioned between the primary cross-section and the secondary distribution. However, high resolution neutron spectrum measurements can enable the detailed structure of cross-sections to be adjusted.

The usual approach to cross-section adjustment (to take account of core neutronics measurements) is to linearise the dependence of the integral properties on cross-section changes:

$$\frac{\delta P_j}{P_j} = \sum_i \left( \frac{\partial P_j}{\partial \sigma_i} \cdot \frac{\sigma_i}{P_j} \right) \frac{\delta \sigma_i}{\sigma_i} \quad (1)$$

where  $\left( \frac{\partial P_j}{\partial \sigma_i} \cdot \frac{\sigma_i}{P_j} \right)$ , is the sensitivity of property  $j$  to

changes in cross-section,  $\sigma_i$ . In the production of FGL5 this linear dependence was assumed but the adjustments were carried out in stages so as to allow for the use of broad energy groups and for non-linearities. The adjustment equations then involve bias terms to allow for the earlier stages of adjustment.

When FGL5 was produced the uncertainties in the differential cross-sections were assessed as being large compared with the uncertainties in integral measurements, such as  $K_{eff}$ . The cross-section libraries which are now being produced, ENDF/B VI, JENDL-3 and JEF-2, are of a much higher accuracy. If cross-section adjustments are to be applied which are independent of approximations in the calculational methods and of systematic errors in the integral measurements then we need to look carefully at both. There is still a place, however, for those adjustments to nuclear data which allow a routine calculational method to be correlated with integral

experiments such as those measured on an operating reactor. It must be recognised, though, that such adjustments can only be expected to improve the prediction of the fitted properties, and not other properties. Fitting reactor operational characteristics, such as burnup variations, might not improve the prediction of safety characteristics.

#### ADJUSTMENT OF DIFFERENTIAL CROSS-SECTIONS ON THE BASIS OF BROAD GROUP PRIMARY CROSS-SECTION ADJUSTMENT FACTORS

The approach adopted was to obtain a smooth fit to the broad group adjustment factors and apply this to the differential (or fine group) cross-section. In the case of the U-238 resonance region a new set of resonance parameters was selected, with values chosen to reproduce the broad group adjustment factors. In the case of U-235 and Pu-239 just the infinite dilution cross-sections were altered and not the resonance shapes of cross-sections. This was also done for structural materials, chromium, iron and nickel, but for these cross-sections the adjustment should have been made to the resonance parameters or in a way which ensures that the scaling is physically consistent.

Changes to elastic and inelastic scattering cross-sections should be examined to see whether there is information which would guide the allocation of the change to primary cross-section or secondary energy or angular distribution. In FGL5 the changes were only made to the primary cross-sections.

Following this first cycle of adjustments the integral properties are recalculated and a new fit made which includes the first cycle of adjustments as biases in the equation for the best fit.

This procedure allows non-linearities in the dependence of integral parameters on cross-section changes to be allowed for and the effect of the transition from broad group adjustments to continuous energy adjustments to be examined, as well as the allocation of the adjustment to primary cross-sections and secondary distributions. In the case of FGL5 three stages of adjustment were carried out.

- (a) U-238 capture and fission
- (b) General adjustment
- (c) Minor additional adjustments to remove residual biases.

No revisions were made to the sensitivities at each step, the assumption being that sensitivities need not be calculated to high accuracy. Not all of the cross-sections for which adjustments were indicated were adjusted, only those adjustments having a significant effect. However, it is important in the adjustment procedure that all sources of uncertainty are represented even though the resulting adjustments to the data are negligibly small.

## UNCERTAINTY DATA

Formalisms for the representation of cross-section uncertainties, and programs for processing them to group form, are available, and covariance data for the more important cross-sections are included in the most recent evaluations. Uncertainty data for integral measurements are also usually provided, although the components which are systematic to a measurement technique, or to different techniques (such as half-lives in reaction rate measurements) are not generally identified in reports of measurements. For the production of FGL5 such systematic errors were treated by means of "systematic error variables" and the contribution of each variable to the uncertainty in a measurement was estimated together with the standard deviation of the variable. This was done only for the ZEBRA measurements although similar systematic errors are present in all integral measurements. A covariance matrix could be generated from the systematic error variables but we found it easier to work out uncertainty estimates in this way.

Reaction rate ratio measurements have been made in ZEBRA using foils and fission chambers. Typical of the uncertainties assumed for the foil and solid state track recorder measurements taken into account in the production of FLG5 are the following values derived for ZEBRA core 12 (MZB).

Table 1

Cell Average Reaction Rate Ratios Measured in ZEBRA Core 12 and the Assumed Uncertainties

Ratio	Values	Uncertainties	
		% Random	% Systematic
F <sub>8</sub> /F <sub>5</sub> Foils	0.02301	1.1	0.9
SSTR	0.02258	1.7	-
F <sub>5</sub> /F <sub>9</sub> Foils	1.067	1.4	0.9
SSTR	1.065	1.7	-
C <sub>8</sub> /F <sub>9</sub> Foils	0.1424	1.0	1.1
SSTR	0.1421	1.1	1.1

The IRMA International Reaction Rate Measurement Technique Intercomparisons indicate that the uncertainties given here are underestimates.

A reassessment of the uncertainties in reaction rate ratio measurements is needed, together with an assessment of the correlations between measurements made using each technique and in each facility.

The quantity which enters into the adjustment is the ratio of calculation to experiment. The correlations in the uncertainties associated with approximations in calculational methods are difficult to assess. These approximations are particularly relevant to the more heterogeneous ZEBRA plate geometry cells. Uncertainties which are systematic to all calculations, such as the use of the transport approximation for whole core calculations are less important than those which have a different effect in power reactor calculations and analyses of critical facility experiments. Use of Monte-Carlo methods to give an independent set of C/E values is one approach to this problem but it cannot be assumed that the Monte-Carlo results are free from approximation because the cross-section processing for the Monte-Carlo code could introduce errors (for example, in the treatment of resonance structure).

The good consistency which has been obtained for the calculation of  $K_{eff}$  values and reaction rate ratios in all ZEBRA plate geometry assemblies studied since FGL5 was produced shows that the errors which are present, in both calculational methods and experimental techniques, are strongly correlated between different cores. To allow for uncertainties associated with approximations in the calculational methods a systematic error should be assumed for particular geometries and associated with particular reactions. For example, a systematic uncertainty in the prediction of fission in plutonium plates of about 1% and of capture in uranium metal plates of about 1% should be assumed. There will be a corresponding systematic (and correlated) uncertainty in  $K_{eff}$  predictions. Uncertainties in the treatment of leakage (possible additional streaming effects) should also be allowed for in terms of a systematic uncertainty in the leakage fraction of about 1% and a corresponding uncertainty in  $K_{eff}$ . These could be treated by means of "systematic error variables" (and incorporated into the integral data covariance matrix, if required). The above figures are given as illustrative only.

The calculation of small sample and small region reactivity perturbation effects is subject to uncertainties because of the perturbation of the flux spectrum (or adjoint flux spectrum) outside the region which is treated explicitly in the cell or supercell calculation (and the corresponding effect of the outside region on the cell or supercell flux spectrum). For materials with a strong reactivity effect, such as a fissile material addition or subtraction, the cell boundary effect is small, but for materials such as sodium the



region boundary effects can be significant. It is better to use the results of measurements in which a large zone has been perturbed or the results of progressive changes in zones of different size from which the boundary effect can be separated out. Whole core sodium voiding experiments (such as the ZEBRA Cadenza experiments) can be calculated more accurately.

#### INTEGRAL DATA USED IN THE PRODUCTION OF FGL5

It is best to include in the fit the widest possible range of integral measurements for which uncertainties can be reliably estimated (including calculational methods uncertainties). In the production of FGL5 the following types of measurement were included:

- (a)  $K_{\infty}$  in zero leakage zones.
- (b)  $K_{eff}$  in uranium and plutonium fuelled assemblies.
- (c) Buckling measurements in critical and subcritical systems.
- (d) Central reaction rate ratios: in particular  $F_8/F_5$ ,  $F_9/F_5$ ,  $C_8/F_5$ .
- (e) Spectrum measurements.
- (f) Small sample reactivity measurements for fissile and fertile materials (and exploratory studies including sodium, structural materials and moderators).

Reaction rate distributions in two zone cores and across core-blanket boundaries were not included in the fit because of uncertainties about the accuracy of calculational methods at interfaces. Only the bucklings derived from reaction rate distributions measured away from boundaries were included. There are problems associated with Sn order, anisotropy of scattering, finite mesh effects and, more importantly, cell mismatch effects. If these effects are being treated then there is no reason why parameters additional to the buckling should not be included.

Sodium voiding measurements in zones were not included. This was because of uncertainties in the treatment of effects at zone boundaries. The standard cell calculational method treats the cell as a component in an infinite array and this method has also been used for normal and sodium voided cells. If a method is used which treats zone boundary effects then such experiments could be included.

Control rod reactivity measurements and the effects of control rods on reaction rate distributions were also not included, again because of uncertainties in the approximations made in the calculational methods used to treat control rod heterogeneity and spectral transients in neighbouring regions. If the control rods have homogeneous compositions (or if the calculational methods are accurate) then these measurements could be included.

Doppler coefficient measurements were not included, but the SEFOR Doppler measurements were used to check the final adjusted set. Measurements of neutron spectra made using the Time of Flight technique and proportional counters were included. The Time of Flight measurements extended to energies below 1eV thus giving information about the spectrum calculated for the Doppler energy region. Treatment of Doppler measurements would have required an explicit dependence of the fit on average values of resonance parameters in energy ranges (and not just infinite dilution cross-section scaling factors as for FGL5). The spectrum measurements were averaged in broad groups. (The detail of the measurements was not taken into account explicitly in the fit).

#### STRATEGY OF ADJUSTMENT

Firstly, it is important to include as wide a range of types of integral measurement as possible and measurements made using as many different techniques and as many facilities as possible so as to reduce the effect of unrecognised systematic errors. Secondly, careful consideration should be given to possible systematic errors which could affect all measurements of a particular type and errors which could be common to different types of measurement.

Having assembled the sensitivities, studies should be made of the effect of omitting types of integral measurement from the fit and of the effect of varying assumptions about uncertainties. Inconsistent integral measurements will be revealed by these studies and these must then be examined. Integral measurements which result in cross-section adjustments which are large compared with the assumed standard deviations should be given careful consideration. Over 100 different fits were tried before the final selection was made for FGL5. It was only when adjustments were confirmed by different types of integral measurement that we were confident in making them and even then, the fact that similar adjustments were being made to the cross-sections of different materials suggests that many of the individual adjustments are not significant. For example there was a tendency for all capture cross-sections below about 25Kev and scattering cross-sections above 25Kev to be reduced. This trend was present even when the fit was made to Keff alone but it was reinforced when the spectrum measurements were included in the fit.

#### CONCLUSIONS

The adjusted cross-section set FGL5 has given good predictions for a wide range of properties measured in ZEBRA Assemblies, including sodium voiding coefficients, and the predictions of other properties, such as the SEFOR Doppler coefficient measurements, are good. Adjustments made to iron cross-sections have similarities to those made to fit the iron shielding benchmark. However, it has become clear that there are additional sources of uncertainty which were not recognised when FGL5 was produced. These are associated with the

calculational methods used for plate geometry cells, (which is probably resulting in FGL5 overestimating  $K_{eff}$  by about 1% for an LMFBR) and underestimation of uncertainties in reaction rate ratio measurements.

The conclusions are that careful attention must be given to sources of systematic error in the integral measurements, including those associated with calculational methods, and that proper account of the correlations in these must be taken into account.

The fit resulting in FLG5 did not include distributed properties (apart from buckling), control rod worths and flux distribution perturbations caused by control rods, sodium voiding measurements in zones, and Doppler measurements. These could now be included by using the more accurate calculational methods now available and extending the nuclear data parameters in the fit to include resonance parameters.

#### REFERENCE

- 1 J.L. Rowlands et al. The Production and Performance of the Adjusted Cross-section Set, FLG5. Proc. Int. Symp. on Physics of Fast Reactors Vol III p 1133 Tokyo (1973).

## ADJUSTMENT OF JENDL-2 CROSS SECTION AND PREDICTION ACCURACY OF FBR CORE PARAMETERS USING JUPITER INTEGRAL DATA

Toshikazu Takeda, Masanori Takamoto, Akira Yoshimura  
Osaka University, Department of Nuclear Engineering  
Yamada-oka 2-1, Suita, Osaka, Japan

Keisho Shirakata  
Power Reactor and Nuclear Fuel Development Corporation  
9-13, 1-Chome, Akasaka, Minato-ku, Tokyo, Japan

### ABSTRACT

The JUPITER integral data have been utilized to adjust the 16 group cross section set produced from JENDL-2. The diffusion coefficient, individual excitation levels of the  $^{238}\text{U}$  inelastic scattering,  $\beta_{\text{eff}}$  and the fission spectrum were considered in the adjustment in addition to conventional cross sections. The contribution of each cross section to the change of C/E of core performance parameters and to prediction uncertainties was investigated.

The prediction uncertainties of core performance parameters of a 1000MWe FBR core were also estimated using the adjusted cross section.

### I. INTRODUCTION

In the core design of a large liquid-metal fast breeder reactor (FBR), it is desirable to reduce the uncertainties of design parameters. Along that line, much experimental and analytical efforts have been performed. The JUPITER I and II, collaboration between the US and Japan, provided us with many valuable experimental information for homogeneous, and radial heterogeneous FBR cores.

In Japan the bias factors, the ratios of calculation to experiment have been utilized in core design calculations of FBR: The FCA (fast critical assembly) facility of the Japan Atomic Energy Research Institute and the Mozart program carried out using the Zebra facility were used to obtain the bias factors for the designs of the experimental reactor JOYO and the prototype fast reactor MONJU. There were extensive studies for the cross section adjustment methods by Kuroi and Mitani.<sup>1</sup> However the cross section adjustment has not been applied to real core designs. Recently cross section adjustment study has been started to get reliable data from the nuclear data user sides. This is because the bias factors have large spatial dependence in large fast critical assemblies, and the uncertainties of the core design parameters for real FBR cores become large.

In Chap. II the analysis results of fast critical

assemblies are described. The cross section adjustment results are shown in Chap. III. The prediction uncertainty of core parameters in a real FBR core of 1000MWe is estimated in Chap. IV.

## II. ANALYSIS OF INTEGRAL EXPERIMENTS

The JUPITER (Japanese-United States Program of Integral Tests and Experimental Researches) program<sup>2</sup> is the joint physics large LMFBR core critical experiment program between U.S. DOE and PNC, Japan, using the ZPPR facility at ANL-Idaho. ZPPR-9 and -10, assembled for the JUPITER-I program, were conventional homogeneous two-zone cores of 650~850MWe-size. ZPPR-9 was a clean physics benchmark, and ZPPR-10 was a series of engineering benchmarks with hexagonal core boundary, i.e., ZPPR-10A through -10D, that included control rod positions and/or control rods. ZPPR-13, assembled for the JUPITER-II program, was a radial heterogeneous core. Cross sectional views of these cores are shown in Fig. 1.

Physics parameters of these assemblies were measured, and analyzed in Japan by the method shown in Fig. 2. A 70 group cross section set was produced from the JENDL-2 library using TIMS-1 and PROF-GROUCH-G2.<sup>3</sup> The base cell calculations are based on 1-D cell calculations, and the base core calculations are based on 7-group diffusion calculations with Benoist's diffusion coefficients using one mesh point per drawer in the XY plane and ~5cm mesh intervals in the axial direction. The 7-group calculations were done for criticality, reaction rate and control rod worths, and the 18-group calculations were used for sodium void worths. The XYZ model was applied to all calculations except for control rod worths. For control rod worths, XY calculations were applied with axial buckling corresponding to the core height. As the corrections to the base calculation we considered the 2-D cell correction, cell interaction correction, 3-D transport correction, energy collapsing correction and mesh correction. The details of these corrections are shown in Ref. 4.

Results of analysis are summarized in TABLE I for main physics parameters.<sup>5</sup> The criticality is predicted fairly well for all assemblies, and the difference in C/E value between assemblies is less than 0.4%, in spite of their different core sizes and different control rod patterns. The C/E value for control rod reactivity worth is from 0.94 to 1.06. However, it is observed that the C/E value becomes higher with core radius, and the C/E value for the outermost ring is 4~12% higher than that for the central rod. As for the reaction rate ratio, C/E values for 25F/49F ( $^{235}\text{U}$  fission/ $^{239}\text{Pu}$  fission), 28C/49F and 28F/49F are 1.03~1.06, 1.05~1.10 and 0.97~1.01, respectively. The reaction rate distribution of  $^{239}\text{Pu}$  fission shows a tendency of C/E value to become higher with core radius. The point-by-point C/E value become higher gradually with radius up to about 6% at the outer core relative to the core center. Approximately the same tendency was also observed for the  $^{235}\text{U}$  fission,  $^{238}\text{U}$  fission and  $^{238}\text{U}$  capture rate distributions. The

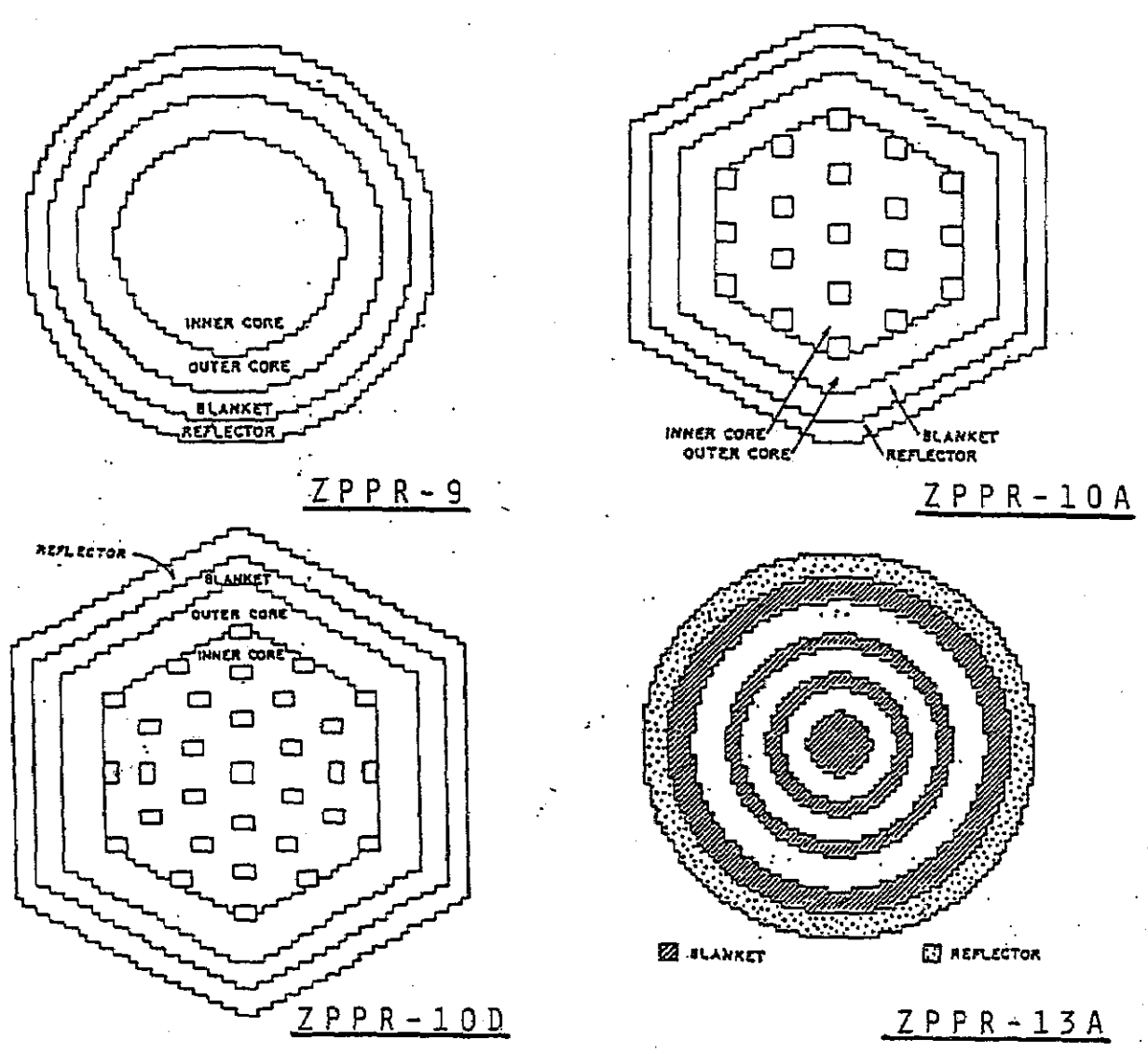
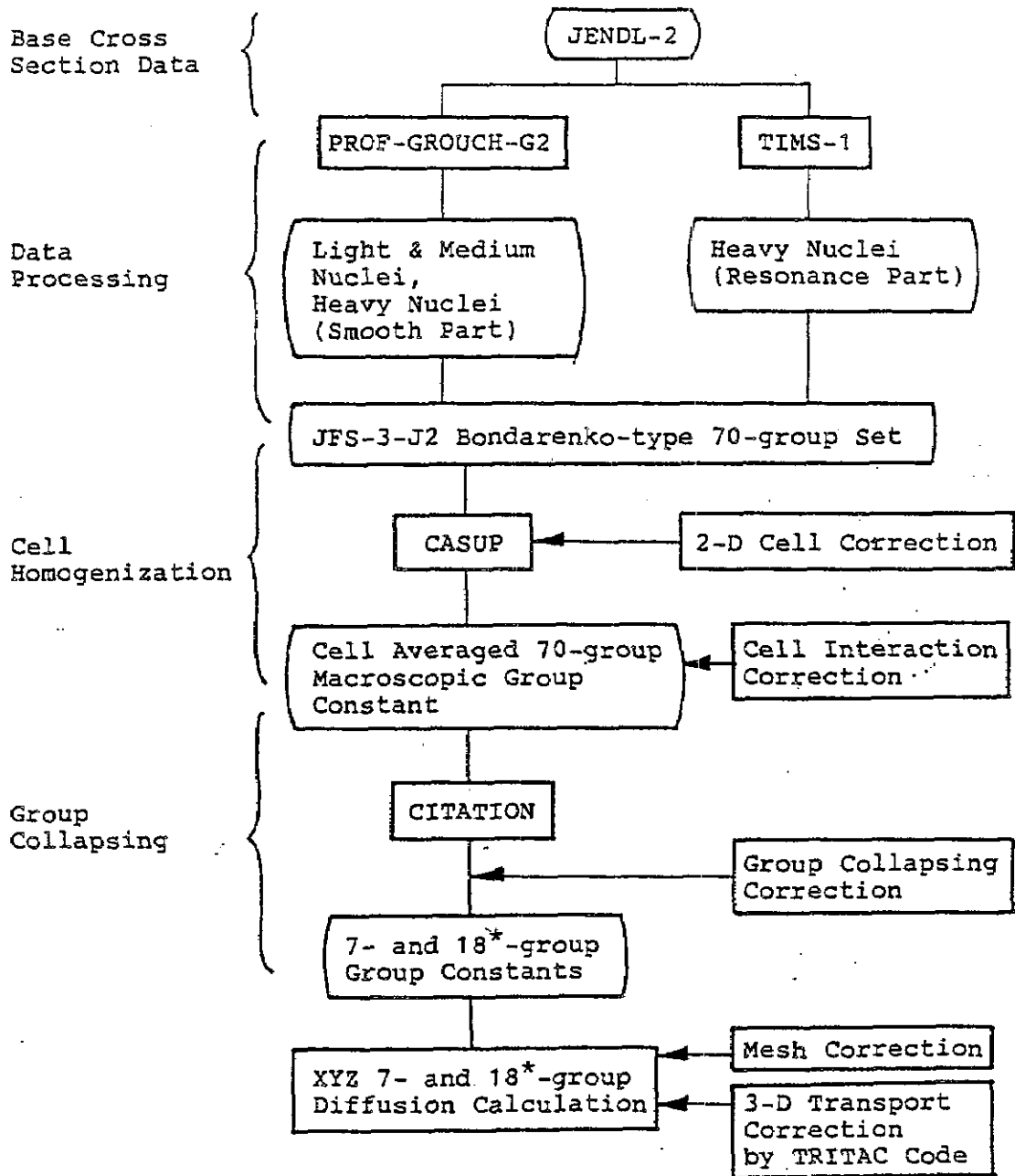


Fig. 1 Cross Sectional Views of the Cores



\* Sodium Void Calculation

Fig.2 The Method of Analysis for the Physics Parameters

sodium void worth is overestimated by 5~40%.

The use of the new JENDL-3T library did not improved these C/E discrepancies<sup>6</sup>(see TABLE II):  $k_{eff}$  decreased by ~0.7%, and 28C/49F increased by ~5%. Then, the disagreement between the experiment and the calculation become larger, compared to JENDL-2. Thus, in order to increase the accuracy of the calculation we have to rely on cross section adjustment.

TABLE I  
C/E and Standard Deviation of Core Performance Parameters  
before and after adjustment

Core Performance Parameters	C/E Value		Standard Deviation( % )			
	Before	After	Ve	Vm	GMG	GM'G
ZPPR-9 $k_{eff}$	0.999	1.001	0.04	0.50	2.97	0.35
ZPPR-10A $k_{eff}$	0.996	1.004	0.04	0.49	2.36	0.34
ZPPR-10D $k_{eff}$	0.996	0.997	0.04	0.49	2.86	0.34
ZPPR-13A $k_{eff}$	0.999	1.002	0.04	0.49	2.13	0.35
ZPPR-9 Doppler UO <sub>2</sub>	0.905	0.917	1.00	10.00	6.81	4.56
ZPPR-9 Na-Void( 9.3x 40.6) <sup>1)</sup>	1.045	0.993	0.70	10.00	24.04	5.20
ZPPR-9 Na-Void(30.7x 40.6)	1.101	1.036	0.70	10.00	33.68	6.04
ZPPR-9 Na-Void(30.7x101.8)	1.278	1.170	0.70	10.00	53.37	8.65
ZPPR-10D CR.Worth, Core Center	0.943	1.023	2.00	4.40	8.35	3.15
ZPPR-10D CR.Worth, 3rd CR Ring <sup>2)</sup>	1.128	1.033	0.50	2.20	7.68	1.61
ZPPR-9 25F/49F <sup>3)</sup>	1.027	1.000	1.00	2.20	4.36	1.40
ZPPR-9 28F/49F	0.988	0.993	2.00	2.20	14.86	2.27
ZPPR-10D 25F/49F	1.057	1.022	1.00	2.20	4.44	1.43
ZPPR-10D 28C/49F	1.088	1.031	1.00	2.20	8.02	1.52
ZPPR-10D 28F/49F	1.009	1.019	2.00	2.20	14.07	2.20
ZPPR-13A 25F/49F	1.033	1.011	1.00	2.20	3.23	1.30
ZPPR-13A 28F/49F	0.967	0.991	1.50	2.20	4.92	1.85
ZPPR-13A 28C/49F	1.058	1.007	1.00	2.20	6.80	1.60
ZPPR-9 RRD.49F, IC Midpoint <sup>4)</sup>	1.009	1.005	0.90	2.20	0.32	0.09
ZPPR-9 RRD.49F, IC Edge	1.029	1.014	0.90	2.20	1.17	0.29
ZPPR-9 RRD.49F, OC Midpoint	1.041	1.018	0.90	2.20	4.77	0.74
ZPPR-10A RRD.49F, IC Midpoint	1.018	1.015	0.90	2.20	0.25	0.09
ZPPR-10A RRD.49F, IC Edge	1.020	1.003	0.90	2.20	1.68	0.46
ZPPR-10A RRD.49F, OC Midpoint	1.041	0.999	0.90	2.20	4.06	1.11
ZPPR-10D RRD.49F, IC Midpoint	1.010	1.003	0.90	2.20	0.68	0.16
ZPPR-10D RRD.49F, IC Edge	1.019	0.996	0.90	2.20	3.19	0.52
ZPPR-10D RRD.49F, OC Midpoint	1.031	0.991	0.90	2.20	8.67	1.23
ZPPR-13A RRD.49F, 2nd Fuel Ring <sup>5)</sup>	1.032	1.019	0.80	2.20	1.72	0.48
ZPPR-13A RRD.49F, 3rd Fuel Ring	1.069	1.030	0.80	2.20	4.81	1.29

1) Sodium void region, radius(cm) X height(cm)

2) CR Worth(3rd CR Ring)/CR Worth(Center CR)

3) Reaction rate ratio, F:fission, C:capture, 49:<sup>239</sup>Pu, 25:<sup>235</sup>U, 28:<sup>238</sup>U

4) Reaction rate distribution, <sup>239</sup>Pu fission rate,

normalized to unity at core center, IC:inner core, OC:outer core

5) Normalized to unity at fuel ring 1



TABLE II  
Average Difference between Calculations and Experiments  
of the Reaction Rate Ratios for 1-D Benchmark Tests

Reaction Rate Ratio	Pu-core (%)			U-core (%)		
	JENDL-2	-3T	Difference	JENDL-2	-3T	Difference
$K_{eff}$	-0.2	-1.0	-0.8	0.3	1.1	0.8
49F/25F	-3	-1.5	1.5	-1.5	-1.3	0.2
28C/49F	1	5	4	-5	5	10
28F/25F	6	13	7	4	11	7

### III. ADJUSTMENT OF CROSS SECTION

The 16-group cross section set obtained from JENDL-2 was adjusted using the C/E values of the core performance parameters of ZPPR-9, 10 and 13. Sensitivity coefficients were calculated by the generalized perturbation theory code SAGEP based on diffusion theory on 2-D RZ geometry.<sup>7</sup> The cross section covariance matrix was produced by modifying the covariance file evaluated by Drischler and Weisbin.<sup>8</sup> The standard deviations are listed in TABLE III. The standard deviation for each excitation level of the  $^{238}\text{U}$  inelastic scattering was taken as 70%, and that for diffusion coefficient as 5%.

The cross section adjustment was performed by using the method developed by Kuroi-Mitani,<sup>1</sup> in which the calculational method error is considered by adding it to the experimental error. The method uncertainties used are listed in TABLE IV. The cross sections for the elements listed in TABLE V are adjusted. For the fission spectrum, the temperature of Maxwell distribution was chosen as the adjustment parameter. The diffusion coefficients were also adjusted because there is uncertainty in the  $P_1$  scattering cross section  $\Sigma_s^4$  used in the definition of transport cross section  $\Sigma_{tr} = \Sigma_t - \Sigma_s^4$ . For the adjustment of the  $^{238}\text{U}$  inelastic scattering cross section, 26 individual excitation levels and a continuum region were divided into four groups: the 1st group corresponds to the 1st and the 2nd levels, the 2nd group the 3rd to the 9th levels, the 3rd group the 10th to the 16th levels and the 4th group the continuum region as shown in TABLE VI. The scaling factor  $\beta_{eff}$  was also adjusted because the measured control rod worth is converted to  $k_{eff}$ . For the control rod worth, the method uncertainty is large because there is an error of about 4% in the estimated scaling factor  $\beta_{eff}$ . When we consider this large error in the adjustment of control rod worth for each rod pattern, the spatial dependence of the C/E values (not the C/E value itself) is not improved by the adjustment. Then, as utilized by Kamei and Kato<sup>9</sup>, we took the ratio of control rod worths at the core center and off-center positions, and adjusted the ratio because there will be no scaling factor uncertainty.

TABLE III  
Standard Deviation of 16-Group Cross Sections  
used for Adjustment(%)

energy group	upper energy	<sup>8</sup> O scat	<sup>11</sup> Na cap	<sup>26</sup> Fe cap	<sup>235</sup> U cap	<sup>235</sup> U fis	<sup>238</sup> U cap
1	10.0 E+6	1.2	50.0	20.0	64.3	3.2	50.1
2	6.07 E+6	1.3	50.0	20.0	61.2	3.0	51.8
3	3.68 E+6	1.1	50.0	20.0	60.0	3.0	26.8
4	2.23 E+6	1.2	40.8	20.0	60.0	2.3	16.2
5	1.35 E+6	1.1	36.6	14.2	46.2	2.3	23.9
6	8.21 E+5	2.4	36.6	15.6	33.8	3.2	15.7
7	3.88 E+5	2.2	50.0	18.9	22.4	2.8	12.5
8	1.83 E+5	1.4	18.1	12.5	37.0	2.8	8.7
9	8.65 E+4	1.4	20.8	12.5	9.8	2.9	5.3
10	4.09 E+4	1.4	13.6	9.2	8.8	3.2	9.9
11	1.93 E+4	1.4	23.2	10.5	9.3	3.8	13.6
12	9.12 E+3	1.4	11.9	17.8	8.0	5.0	11.2
13	4.31 E+3	1.4	12.2	24.8	7.6	5.4	10.0
14	2.03 E+3	1.4	12.2	24.2	7.6	4.9	10.1
15	9.61 E+2	1.4	10.7	23.3	7.8	3.2	7.9
16	4.54 E+2	1.4	1.0	1.0	10.5	1.9	0.5

energy group	<sup>238</sup> U fis	<sup>238</sup> U $\nu$	<sup>240</sup> Pu cap	<sup>241</sup> Pu fis	<sup>239</sup> Pu cap	<sup>239</sup> Pu fis	<sup>239</sup> Pu $\nu$
1	3.2	0.0	13.6	2.3	60.0	3.2	1.2
2	3.1	1.1	19.0	4.4	60.0	3.1	1.4
3	3.0	1.4	15.6	3.4	60.0	3.0	1.0
4	2.3	1.6	10.7	3.8	60.0	2.3	0.6
5	2.6	1.6	7.0	4.6	37.8	2.5	0.4
6	3.7	1.6	24.8	7.5	9.5	3.2	0.6
7	3.5	1.6	20.8	7.5	12.0	2.8	0.8
8	7.9	1.6	34.7	4.1	16.7	2.9	0.8
9	7.9	1.6	37.3	2.7	11.4	3.1	0.8
10	108.0	1.6	11.1	4.0	7.4	3.2	0.8
11	109.6	1.6	9.8	5.1	8.5	4.1	0.8
12	109.6	1.6	9.1	5.3	7.8	4.0	0.8
13	0.0	0.0	11.1	9.3	13.6	4.0	0.8
14	109.7	1.6	9.6	12.9	17.9	4.0	0.8
15	109.6	1.6	1.7	12.6	11.4	4.0	0.8
16	109.5	1.6	4.0	0.7	9.0	4.0	0.8

scat: scattering cap: capture fis: fission  $\nu$ :  $\nu$  value

TABLE IV  
Uncertainty of Neutronics Parameters due to  
Method Error and Experimental Error

Error	Criticality		Control rod worth		Reaction rate distribution
	A	B	A	B	A and B
Method error					
Processing of nuclear data	0.3*		3.0*		1.0*
Cell(Assembly) calculation modeling	0.3	0.2	2.0	1.0	1.0
Neutron Streaming	0.2	0.1	1.0		1.0
Cell interaction	0.1	0.0	2.0	1.0	1.0
Core calculation	0.1		1.0		1.0
Total Uncertainty	0.5	0.4	4.4	3.6	2.2
Experimental Error	0.04		4.3**		1.0

A : Typical critical assembly (ZPPR-10D)

B : Target LMFBR

\* : Expressed in %

\*\* :  $\beta_{eff}$  Uncertainty of 4.0% included

The C/E values before and after the adjustment are also listed in TABLE I. The cross section change is shown in TABLE VII. The spatial discrepancy for the reaction rate distribution and the control rod worth was remarkably improved: The 12% discrepancy between the control rod worths at the core center and the core edge in ZPPR-10D was reduced to 3%. The element-wise contribution to this improvement is shown in TABLE VIII. The increase of diffusion coefficient of about 4% has ~53% contribution. This is because the sensitivity of control rod worth is large at the core center compared to that at the core edge as shown in TABLE IX, and has strong spatial dependence. This spatial dependence is caused by the following fact. The change of diffusion coefficient has small effect on the flux distribution when there is no control rod. When there

is a core center rod, the increase of diffusion coefficient by 10% decrease the flux distribution around the core center by about 7%. However, when there are control rods at core edge, the flux distribution change is rather small as shown in Fig.3. In the heterogeneous core ZPPR-13A the sensitivity is opposite in sign at the core center and at the core edge. For the reaction rate distribution the sensitivity to diffusion coefficient has different trend (see TABLE X). While the sensitivity of the control rod worth is large at the core center, that of the reaction rate distribution large at the core edge. This is because the reaction rate distribution is normalized at the core center.

Besides the diffusion coefficient, the  $^{238}\text{U}$  capture cross section and the  $^{239}\text{Pu}$  fission cross section have large contributions of 25% and 16% to the improvement of the spatial discrepancy of control rod worth.

TABLE V  
Cross Sections used for adjustment

Nuclide	Reactions			
	Capture	Fission	$\nu$ value	Scattering
$^{235}\text{U}$	⊙	⊙	⊙	
$^{238}\text{U}$	⊙	⊙	⊙	⊙
$^{239}\text{Pu}$	⊙	⊙	⊙	
$^{240}\text{Pu}$	⊙			
$^{241}\text{Pu}$		⊙		
$^{26}\text{Fe}$	⊙			
$^{11}\text{Na}$	⊙			
$^{8}\text{O}$				⊙

Others

\*  $\beta$  eff

\* diffusion coefficient

\* temperature parameter T of the Maxwell distribution for the  $^{239}\text{Pu}$  fission spectrum  $x$

\* excitation levels and the continuum region of the  $^{238}\text{U}$  inelastic scattering

TABLE VI  
Energy Level Structure of  $^{238}\text{U}$  Inelastic Scattering

Calculated Group	No.	Energy (MeV)		
		JENDL-2	JENDL-3T	
1	1	0.0447	0.0449	
	2	0.148	0.148	
2	3	0.301	0.307	
	4	0.520	0.518	
	5	0.680	0.680	
	6	0.732	0.731	
	7	0.790	0.776	
	8	0.838	0.827	
	9	0.939	0.927	
	3	10	0.968	0.950
		11	1.006	0.966
12		1.047	0.993	
13		1.076	1.037	
14		1.100	1.060	
15		1.123	1.077	
16		1.150	1.107	
17		1.190	1.129	
18		1.210	1.150	
19		1.246	1.169	
20		1.274	1.223	
21	1.313	1.243		
22	1.361	1.270		
23	1.401	1.279		
24	1.437	1.290		
25	1.470	1.378		
26		<u>1.415</u>	1.415	
4	Continuum region ( above 1.5MeV )			

TABLE VII  
Relative Change of Cross Sections by Adjustment ( % )

Energy group	<sup>11</sup> Na cap	<sup>26</sup> Fe cap	<sup>235</sup> U cap	<sup>235</sup> U fis	<sup>238</sup> U cap	<sup>238</sup> U fis	<sup>240</sup> Pu cap	<sup>239</sup> Pu cap
1	-1.35	1.51	0.43	-0.22	-8.43	1.55	-1.22	2.81
2	-1.35	1.51	0.66	-0.27	1.64	1.67	-2.41	2.81
3	-1.35	1.51	0.56	-0.39	1.45	2.05	-1.23	2.81
4	-0.33	1.51	0.56	-0.45	-1.20	1.67	-1.27	2.81
5	-0.06	1.96	0.53	-0.73	-6.83	1.43	-0.77	5.25
6	-0.18	1.93	0.44	-1.37	-3.53	0.88	3.15	3.90
7	-0.39	3.18	0.31	-1.67	-2.11	0.49	5.75	5.90
8	-0.25	2.22	0.55	-2.26	-2.05	0.21	10.28	8.31
9	-0.22	1.38	0.10	-3.30	-2.35	0.05	10.90	2.39
10	-0.22	0.69	0.09	-4.08	-6.96	2.08	2.90	4.07
11	-0.22	0.66	0.08	-4.69	-9.93	2.11	1.00	4.11
12	-0.43	1.07	0.07	-5.71	-7.98	2.11	2.18	3.96
13	-0.49	0.71	0.07	-6.02	-7.37	0.00	2.29	6.87
14	-0.49	-0.46	0.06	-5.44	-8.78	2.11	1.33	7.85
15	-0.43	-0.46	0.06	-2.94	-6.25	2.11	0.15	3.60
16	0.00	0.00	-0.01	-1.53	-0.26	2.10	-0.04	-1.76

Energy group	<sup>239</sup> Pu fis	<sup>239</sup> Pu $\nu$	Dif.* Coef.	<sup>238</sup> U Lev.1	<sup>238</sup> U inelastic scattering Lev.2	<sup>238</sup> U inelastic scattering Lev.3	<sup>238</sup> U inelastic scattering Lev.4
1	-0.67	0.31	3.70	3.61	4.39	-0.13	15.64
2	-0.81	0.57	3.75	4.37	5.00	-0.66	19.16
3	-1.19	0.29	3.86	4.17	4.04	-2.75	18.29
4	-1.12	0.01	3.93	1.58	1.09	-7.58	13.26
5	-1.62	-0.27	3.94	-0.65	0.82	-7.63	0.00
6	-2.53	-0.47	4.33	0.16	3.32	0.00	0.00
7	-2.25	-0.61	4.36	-7.95	2.49	0.00	0.00
8	-1.83	-0.61	4.29	-18.94	0.00	0.00	0.00
9	-1.38	-0.61	4.10	-16.45	0.00	0.00	0.00
10	-1.19	-0.61	3.97	0.00	0.00	0.00	0.00
11	-1.09	-0.61	3.85	0.00	0.00	0.00	0.00
12	3.56	-0.61	3.74	0.00	0.00	0.00	0.00
13	3.56	-0.61	3.69	0.00	0.00	0.00	0.00
14	3.56	-0.68	3.71	0.00	0.00	0.00	0.00
15	3.56	-0.61	3.68	0.00	0.00	0.00	0.00
16	3.56	-0.61	3.68	0.00	0.00	0.00	0.00

\* diffusion coefficient  
cap: capture fis: fission  $\nu$ :  $\nu$  value  
Lev.1-4 : <sup>238</sup>U inelastic scattering,  
1st-4th group (TABLE VI)

TABLE VIII  
Element-Wise Contribution to the C/E Change  
due to Adjustment

(1) Control Rod Worth Ratio (3rd ring / center) in ZPPR-10D

CROSS SECTION		ALTERATION ( % )	CONTRIBUTION ( % )
<sup>80</sup> O	SCT	-0.12	1.45
<sup>238</sup> U	CAP	-2.07	24.61
	Inel. Lev. 1*	-0.41	4.83
	Lev. 2*	0.05	-0.62
	Lev. 3*	-0.23	2.69
	Lev. 4*	0.54	-6.46
<sup>239</sup> Pu	FIS	-1.35	16.08
Diffusion Coefficient		-4.54	53.84
Fission Spectrum		-0.40	4.76
Total		-8.42	100.0

(2) Sodium-Void Worth in ZPPR-9

CROSS SECTION		ALTERATION ( % )	CONTRIBUTION ( % )
<sup>80</sup> O	SCT	0.16	-3.12
<sup>238</sup> U	FIS	0.06	-1.30
	CAP	-3.33	66.84
	FIS	0.12	-2.35
	$\nu$	-0.09	1.82
	Inel. Lev. 1*	2.18	-43.82
	Inel. Lev. 2*	-0.20	4.08
	Inel. Lev. 3*	0.99	-19.83
	Inel. Lev. 4*	-2.48	49.81
<sup>239</sup> Pu	CAP	1.05	-21.04
	FIS	-3.02	60.07
		0.72	-14.54
	$\beta_{eff}$	-1.06	21.24
Total		-4.98	100.0

\* Inel. Lev.1-4 : <sup>238</sup>U inelastic scattering,  
1st-4th group ( TABLE VI )

The overestimation of the <sup>238</sup>U capture to <sup>239</sup>Pu fission rate ratio of about 8% was also improved to 3% due to the change of the relevant cross sections as shown in TABLE VII. The <sup>238</sup>U capture cross section is decreased below 1MeV, but the <sup>239</sup>Pu fission cross section is also decreased above 10keV.

TABLE IX  
Sensitivity Coefficients of Control Rod Worth with respect to  
Diffusion Coefficient (\*10E-2 )

	ZPPR9 center	ZPPR9 2nd ring	ZPPR10D center	ZPPR10D 3rd rig	ZPPR13A center	ZPPR13A 3rd ring
1	2.387	0.080	1.061	0.058	1.149	-0.431
2	5.831	0.489	4.019	0.184	5.488	-0.529
3	11.161	1.417	9.177	0.342	10.920	-0.618
4	12.931	1.358	10.484	-0.103	15.451	-0.889
5	11.652	0.924	9.233	-0.439	13.618	-0.598
6	23.613	2.503	20.590	-0.457	23.162	-0.554
7	23.549	3.128	20.134	0.270	24.187	-0.971
8	18.208	3.235	16.706	0.937	19.553	-1.168
9	12.259	2.379	10.675	1.151	14.812	-1.290
10	8.545	1.965	6.938	1.458	7.727	-0.896
11	5.085	1.506	4.381	1.340	5.998	0.032
12	2.803	0.890	1.857	0.888	2.087	-0.195
13	1.471	0.083	0.416	0.335	0.156	-0.275
14	2.877	1.968	2.578	1.990	1.711	1.037
15	1.545	0.945	1.099	1.300	0.977	0.167
16	1.067	0.211	0.246	0.661	0.518	-0.442
total	144.984	23.081	119.594	9.915	147.511	-7.620

TABLE X  
Sensitivity Coefficients of <sup>239</sup>Pu Fission Rate Distribution  
with respect to Diffusion Coefficient (\*10E-2 )

	ZPPR9 IC	ZPPR9 OC	ZPPR10D IC	ZPPR10D OC
1	-0.073	-0.211	-0.096	-0.292
2	-0.232	-0.682	-0.365	-1.101
3	-0.510	-1.507	-0.874	-2.568
4	-0.570	-1.687	-1.041	-3.032
5	-0.499	-1.482	-0.936	-2.729
6	-0.997	-2.963	-1.963	-5.683
7	-0.934	-2.778	-1.778	-5.165
8	-0.695	-2.080	-1.377	-3.972
9	-0.429	-1.285	-0.816	-2.347
10	-0.262	-0.791	-0.447	-1.274
11	-0.129	-0.388	-0.244	-0.693
12	-0.058	-0.170	-0.075	-0.221
13	-0.024	-0.065	-0.011	-0.033
14	-0.056	-0.161	-0.074	-0.207
15	-0.031	-0.079	-0.011	-0.017
16	-0.019	-0.041	0.014	0.072
total	-5.518	-16.370	-10.094	-29.262

IC : Inner Core      OC : Outer Core



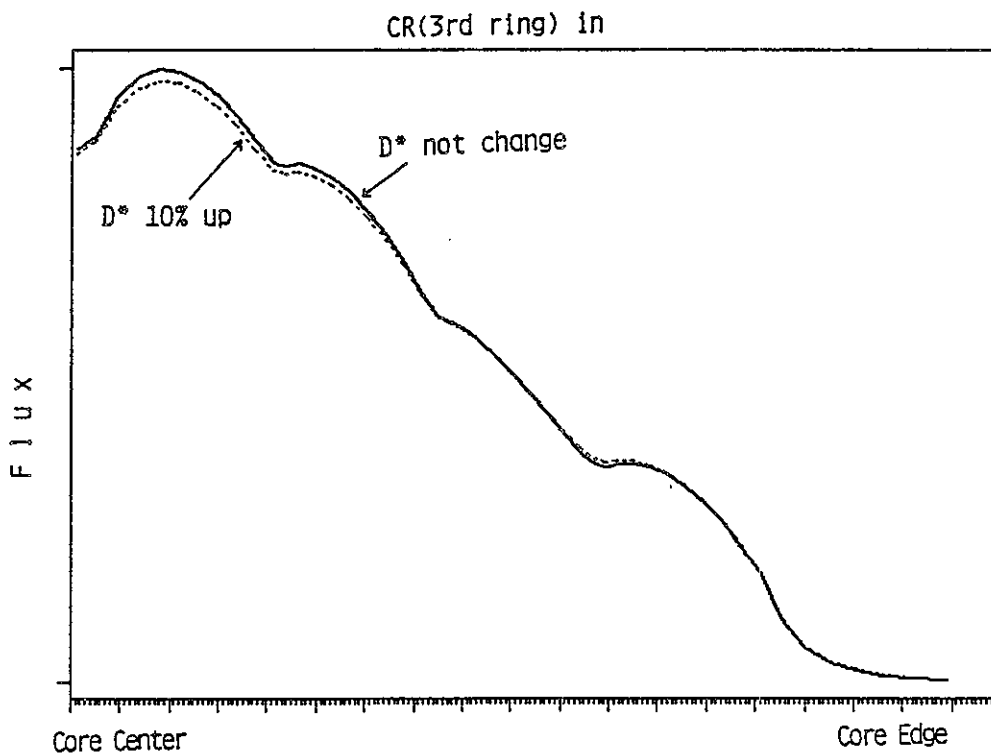
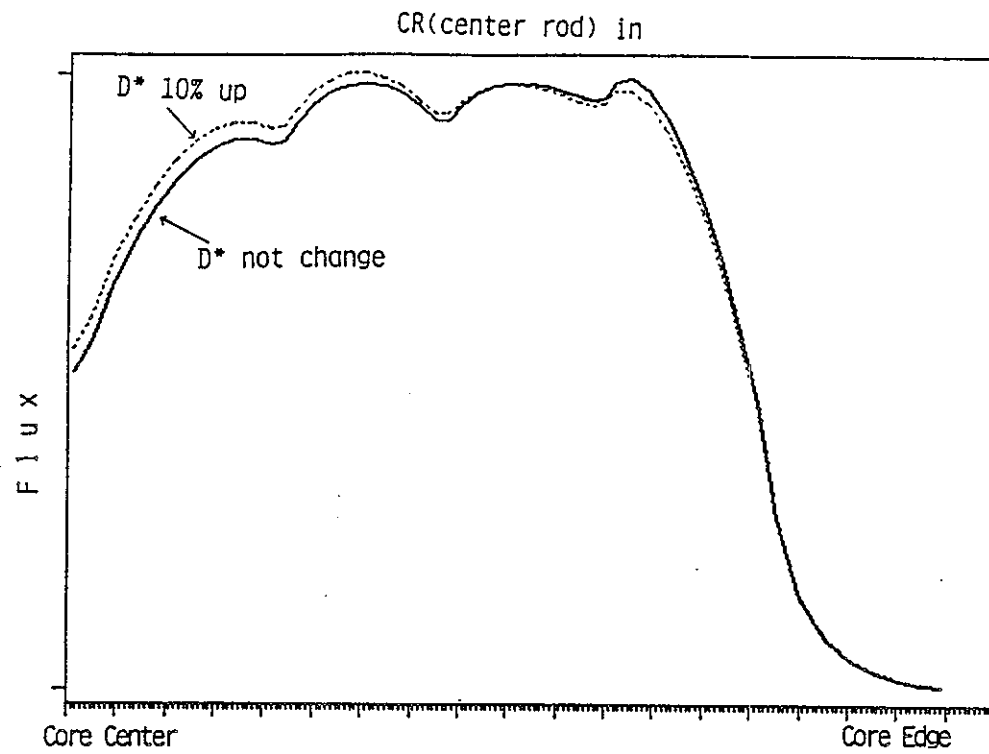


Fig.3 Flux Distribution Change due to 10% Increase of Diffusion Coefficient

The improvement of the 4~28% overestimation of sodium void worth was due to the change in the  $^{239}\text{Pu}$  fission and capture cross sections, and the  $^{238}\text{U}$  capture and inelastic scattering cross sections as shown in TABLE VIII. The change of the  $^{238}\text{U}$  capture and the  $^{239}\text{Pu}$  fission cross sections below 5keV have large effect because the sensitivities are larger in these energy range as shown in Fig.4.

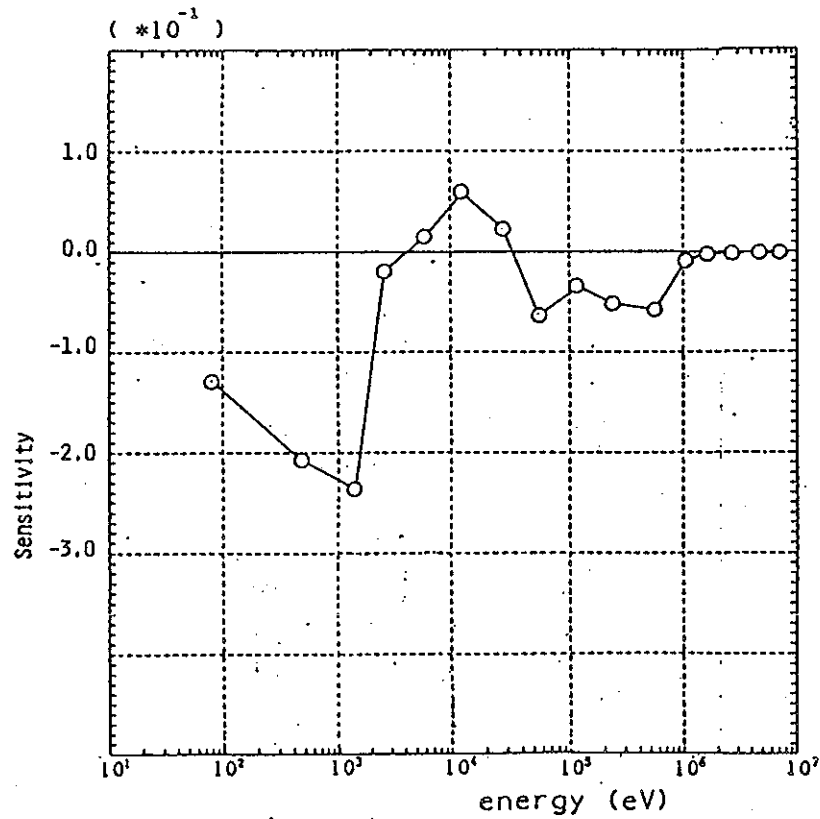
In the following we compare the uncertainties of core parameters used for the adjustment. TABLE I also lists the uncertainties (standard deviation) due to the experimental error  $V_e$ , method error  $V_m$  and the cross section error. The last uncertainty is evaluated by GMG where G is the sensitivity coefficient and M is the cross section covariance data. All (C/E-1) values should be smaller than or nearly equal to the sum of  $V_e+V_m+GMG$ , because the C/E discrepancy should be illustrated from the points of the above uncertainties. The values in TABLE I satisfy this condition. The uncertainty due to cross section is 2.5% for  $k_{eff}$ . This uncertainty is dramatically reduced after the adjustment. The control rod worth uncertainties are also reduced from 8% to a few percent. TABLE XI lists the element-wise contribution to the GMG value for  $k_{eff}$ , the control rod worth ratio at the core center and the core edge, and 28C/49F of ZPPR-10D. For control rod worth, diffusion coefficient,  $^{238}\text{U}$  inelastic scattering,  $^{238}\text{U}$  capture cross sections have large contributions. For  $k_{eff}$ , the  $^{238}\text{U}$  capture and inelastic scattering,  $^{239}\text{Pu}$  fission cross sections have large contributions.

TABLE XI  
Element-Wise Component of Core Parameter Uncertainty  
due to Cross Section Error in ZPPR-10D

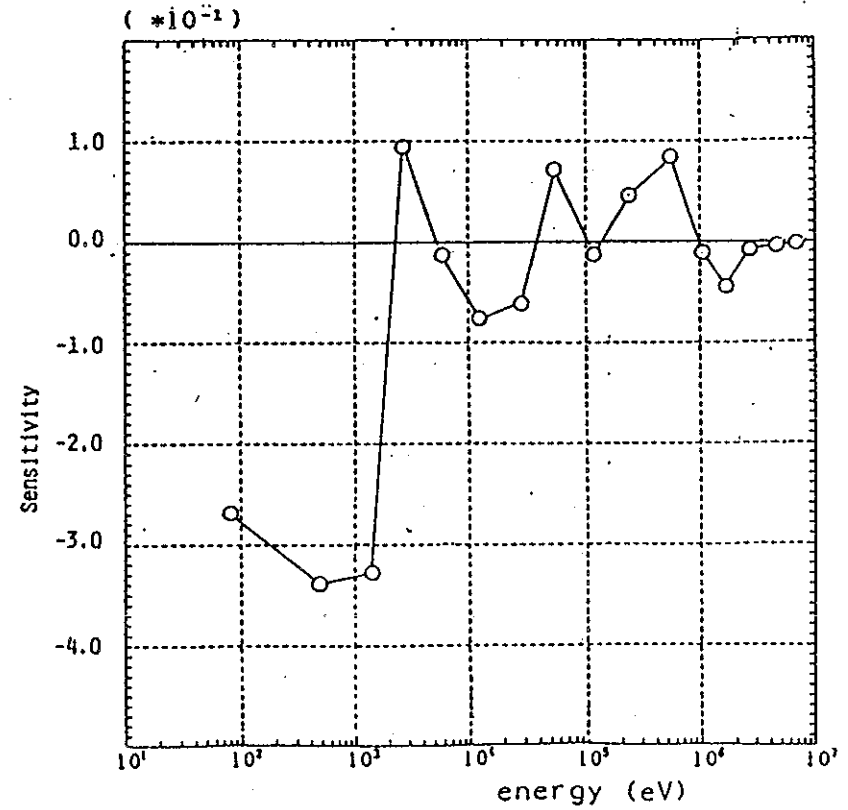
Reaction	$k_{eff}$	CR.worth Center	CR.worth 3rd Ring	28C/49F
$^{8}\text{O}$ scattering	0.03	0.38	0.44	0.15
$^{26}\text{Fe}$ capture	0.15	0.37	0.35	0.05
$^{235}\text{U}$ fission	0.03	0.02	0.05	0.00
$^{238}\text{U}$ capture	1.83	1.90	2.14	6.33
$^{238}\text{U}$ fission	0.20	0.46	0.07	0.01
$^{238}\text{U}$ $\nu$ value	0.19	0.31	0.08	0.00
$^{240}\text{Pu}$ capture	0.10	0.04	0.04	0.05
$^{239}\text{Pu}$ capture	0.44	0.59	0.40	0.14
$^{239}\text{Pu}$ fission	1.07	1.80	1.18	1.98
$^{239}\text{Pu}$ $\nu$ value	0.51	0.28	0.14	0.00
Diff. *	0.49	4.46	4.12	0.11
$^{238}\text{U}$ scattering <sup>1)</sup>	1.01	4.49	4.48	3.91
$^{238}\text{U}$ scattering <sup>2)</sup>	0.50	0.41	1.75	1.16
$^{238}\text{U}$ scattering <sup>3)</sup>	0.86	0.29	2.22	1.64
$^{238}\text{U}$ scattering <sup>4)</sup>	0.79	0.65	1.99	0.90
total	2.82	7.29	7.64	8.01

\* :Diffusion coefficient

1)-4): $^{238}\text{U}$  inelastic scattering, 1st-4th group (TABLE VI)



Sensitivity Coefficient of Na-Void Worth with respect to U-238 Capture Cross Section in Pu core (ZPPR-9)



Sensitivity Coefficient of Na-Void Worth with respect to Pu-239 Fission Cross Section in Pu core (ZPPR-9)

Fig. 4 Sensitivity Coefficient of Sodium Void Worth

#### IV. PREDICTION UNCERTAINTY IN A LARGE LMFBR

Using the adjusted cross section set we estimate the prediction uncertainties of core parameters of a 1000MWe LMFBR. The uncertainties for  $k_{eff}$ ,  $^{28}C/^{49}F$ , reaction rate distribution and control rod worth were calculated. For comparison the prediction uncertainties were also estimated by the bias factor method and a combined method of the adjustment and the bias factor methods. In the combined method, cross sections are first adjusted using benchmark experiments, and the adjusted cross sections are utilized to a mockup experimental analysis to obtain bias factors to be used in the design of a target LMFBR. TABLE IV lists the method error and experimental error used to prediction uncertainties for  $k_{eff}$ , control rod worth and reaction rate distribution for the mockup critical and target FBR core. The method error is mainly caused by the approximations used in the data processing and the cell (or assembly) calculations.

TABLE XII lists the numerical results of the prediction uncertainty of  $k_{eff}$ , the control rod worth and the power distribution ( $^{239}Pu$  fission rate distribution) for the target 1000MWe homogeneous core for the three methods and for the case without any information of critical assemblies. Without any information of critical experiments, the estimated standard deviation of  $k_{eff}$  is 2.2%. The bias method, the adjustment method and the combined method decrease this error to 0.7, 0.6, and 0.6%, respectively. From TABLE XII it is seen that the main contribution of this error comes from the cross section uncertainty for the case without the experimented data, and the cross section uncertainty has comparable contributions to the method uncertainty for the three methods. The method uncertainty component of 0.44% for the bias factor method and the combined method corresponds to the statistical sum of individual method errors except the common errors for the mockup and target FBR core shown in TABLE IV.

For the control rod worth, the use of the combined method reduces the standard deviation from 6.2 to 4.0%. Thus the combined method is useful for the reduction of prediction uncertainty. The cross section component for the bias method and the combined method is very small compared to the adjustment method. In the two methods, however, the bias factor is utilized, and the  $\beta_{eff}$  uncertainty has to be considered. Though the  $\beta_{eff}$  uncertainty is 4.0% for the bias method, it reduces to 1.8% for the combined method. This is because the  $\beta_{eff}$  is included in the adjustment.

For the  $^{239}Pu$  fission rate at the core edge, the uncertainty of 3.6% for the case without any experimental data is remarkably improved to about 2.4% by the three methods. This remaining error is mainly due to the method error.

TABLE XII

Prediction Uncertainty of Core Performance Parameters  
of a Target 1000MWe FBR

Component	Method			
	Without data	Bias	Adjust.	Adjust+bias
$k_{eff}$				
total	2.2*	0.7*	0.6*	0.6*
experimental error	---	0.04	---	0.04
method error	0.4	0.44	0.4	0.44
cross section error	2.2	0.5	0.5	0.4
Control Rod Worth (Central Rod)				
total	6.2	5.4	4.8	4.0
experimental error	---	1.6	---	1.6
method error	3.6	3.1	3.6	3.1
cross section error	5.0	0.8	3.2	0.7
$\beta_{eff}$ error	---	4.0	---	1.8
Control Rod Worth (3rd Ring)**				
total	6.2	3.3	3.9	3.3
experimental error	---	0.8	---	0.8
method error	3.6	3.1	3.6	3.1
cross section error	5.0	0.9	1.6	0.6
$^{239}\text{Pu}$ Fission Rate at Core Edge***				
total	3.6	2.5	2.3	2.4
experimental error	---	1.0	---	1.0
method error	2.2	2.2	2.2	2.2
cross section error	2.8	0.8	0.8	0.4

\* : Standard deviation in %

\*\* : Normalized by worth of central rod

\*\*\*: Normalized by  $^{239}\text{Pu}$  fission rate at core center

#### V. CONCLUDING REMARKS

We have adjusted a 16-group cross section set produced from JENDL-2 using the JUPITER integral data. The C/E spatial discrepancy of control rod worth was remarkably improved mainly by the diffusion coefficient, the  $^{238}\text{U}$  capture and the  $^{239}\text{Pu}$  fission cross sections. The  $^{238}\text{U}$  inelastic cross section has different sensitivities for individual excitation levels, and these levels were divided into four groups for adjustment. The change of these cross sections had significant contributions to  $k_{eff}$ , 28F/49F, and sodium void worth.

The three methods, the bias method, the adjustment method and the combined method have been utilized to calculate the prediction uncertainty. They have been applied to a 1000MWe homogeneous FBR core, and the prediction uncertainties for  $k_{eff}$ , control rod worth, and power distribution have been estimated. For all of these core parameters, the three methods were effective to reduce the uncertainty. Particularly the combined method was effective to reduce the control rod uncertainty.

#### REFERENCES

1. H. MITANI and H. KUROI, *J. Nucl. Sci. Technol.*, 9, 383 and 642 (1972).
2. M. YAMAMOTO et al., "Analysis of Large Conventional LMFBR Core critical Experiments and Their Implication to Design Methods," *Topical Meeting on Reactor Physics and Shielding*, September 17-19, 1984, Chicago, Illinois, USA.
3. H. TAKANO, A. HASEGAWA and K. KANEKO: "TIMS-PGG: A Code System for Producing Group Constants in Fast Neutron Energy Region", *JAERI-M 82-072* (1982).
4. T. TAKEDA et al., "Analysis of large LMFBR Critical Experiments by Improved Methods," *Proceeding of International Topical Meeting on Advances in Reactor Physics, Mathematics and Computation*, April 27-30, 1987, Paris, France.
5. K. SHIRAKATA et al., "International Conference on Nuclear Data for Science and Technology, May 30-June 3, 1988, Mito, Japan.
6. T. TAKEDA et al., "Thermal and Fast Reactor Benchmark Test of JENDL-3T," *International Reactor Physics Conference*, Sep. 18-22, 1980, Jackson Hole, Wyoming, USA.
7. A. HARA, T. TAKEDA and Y. KIKUCHI, "SAGEP: Two-Dimensional Sensitivity Analysis Code Based on Generalized Perturbation Theory," *JAERI-M 84-065* (1984).
8. J. P. DRISCHLER and C. R. WEISBIN, *ORNL-5318* (1977).
9. T. KAMEI and Y. KATO, *J. Nucl. Sci. Technol.*, 22, 1025 (1985).



UNCERTAINTY REDUCTION REQUIREMENTS  
IN  
CORES DESIGNED FOR PASSIVE REACTIVITY SHUTDOWN

D. C. Wade

ABSTRACT

The first purpose of this paper is to describe the changed focus of neutronics accuracy requirements existing in the current US advanced LMR development program where passive shutdown is a major design goal. The second purpose is to provide the background and rationale which supports the selection of a formal data fitting methodology as the means for the application of critical experiment measurements to meet these accuracy needs.

I. US ADVANCED LMR PROGRAM NEEDS FOR CRITICAL EXPERIMENTS

A) Passive Reactivity Shutdown Core Design Goal

A recent focus for advanced LMR design in the US has been on achieving passive reactivity shutdown in response to unprotected whole core accident initiators such as unprotected loss of flow (LOF), loss of heat sink (LOHS), rod runout transient overpower (TOP), and chilled inlet coolant. The coolant mixed mean outlet temperature reached asymptotically upon passive shutdown in each of these unprotected events is a useful figure of merit for assessing passive reactivity shutdown effectiveness. These asymptotic temperatures are found to depend on ratios of reactivity feedbacks and (for the TOP) on a ratio of burnup control swing to reactivity feedbacks.<sup>(1)</sup> The relevant reactivity feedbacks are identified in Table I. where also are shown the typical sizes of the reactivity coefficients in  $\phi/^\circ\text{C}$ .

One is struck by the small sizes of the numbers in Table I. In contrast to the multiple tens of dollars of shutdown reactivity vested in control rod scram, the passive shutdowns bring the core to zero power by balancing off reactivities in the range of cents or several tens of cents. As an example, Figure 1 shows the calculated results for passive shutdown of an unprotected LOHS accident in a 900 MW<sub>th</sub> metal-fueled modular LMR. As the core inlet temperature rises in response to the loss of heat sink, radial core expansion introduces a negative reactivity of several tens of cents, causing the power level to be reduced to near zero. The coolant temperature rise,  $\Delta T_c$ , collapses to a small value, and the final asymptotic state is achieved when the positive reactivity introduced by bringing power to zero, (A+B), is balanced by the negative reactivity introduced by raising the core average (nearly isothermal) temperature,  $\delta T_{in}$  C:

$$\delta T_{in} \text{ C} = (A+B) \quad (1)$$



Here C is the inlet temperature coefficient of reactivity ( $\phi/^\circ\text{C}$ ) and (A+B) is the decrement in reactivity, ( $\phi$ ) which occurs upon taking the core to full power and flow from isothermal at the normal coolant inlet temperature. The asymptotic core outlet temperature is equal, in the LOHS, to the asymptotic core inlet temperature, and its change relative to its normal full power value (of  $T_{in} + \Delta T_c$ ) is given by:

$$\Delta T_{out} \text{ (LOHS)} = - \left(1 - \frac{A+B}{CA T_c}\right) \Delta T_c \quad (2)$$

Table II summarizes the corresponding results -- in terms of ratios of reactivity parameters -- for the asymptotic core outlet temperature change resulting in each of the passively-shutdown ATWS events.

### B) Impact of Neutronics Uncertainties on Passive Shutdown Performance

The reactivities involved in passive shutdown are numerically extremely small -- i.e. several cents -- and moreover they derive not only from the traditionally-considered temperature dependencies of densities and of Doppler broadening but also from very subtle geometrical displacements. For example a  $10^\circ\text{C}$  temperature rise at the grid plate dilutes a 2 meter diameter core by only 4 millimeters and yet it comprises one of the important reactivity feedbacks for passive shutdown. In a generic way:

$$\begin{aligned} \Delta \rho = \Delta T * \left( \frac{\partial \rho}{\partial T} \right) & \quad \text{Na density} \\ & \quad \text{\& Doppler} \\ + \Delta T * \left( \frac{\Delta \text{ Position}}{\Delta \text{ Temperature}} \right) * \left( \frac{\partial \rho}{\partial \text{ Position}} \right) & \quad \text{radial and axial} \\ & \quad \text{expansion \& bowing} \end{aligned} \quad (3)$$

In view of the small sizes of the reactivities involved and of the subtleness of the thermo/structural processes on which major components of the reactivity feedbacks depend, one might anticipate that unavoidable uncertainties in the values of nuclear and thermo/structural properties present a hopeless situation as regards reliability of passive shutdown. That this is not so is one of the amazing aspects of the effort to design for passive shutdown. There are two principal features which mitigate the impact that uncertainties and variability of key neutronics, thermohydraulic, and structural properties impute to passive shutdown performance.

First, as summarized in Table II, the passive shutdown performance -- as characterized by asymptotic change in core outlet temperature -- depends not on individual reactivity coefficients but rather on groupings of feedbacks, A, B, C, which are measurable on the operating reactor. Thus, irrespective of the current level of uncertainty in individual reactivity coefficients, and irrespective of the core-to-core variability of manufactured equipment and of aging effects which change incore equipment, it will always be possible to monitor the actual values of the inlet temperature coefficient, C, the power reactivity decrement, (A+B), and the flow coefficient of reactivity, B, on any operating power reactor. Given the measured values of A, B, and C (and the measurement precision), one can ascertain from the formulas in Table II, whether or not the passive shutdown performance will be capable of maintaining the core in a safe condition. A "Tech Spec" requirement on the frequency of

measuring the integral parameters and on the allowed bands into which their values must fall will provide a means to assure that either the feedbacks do, in fact, provide for safety, or that the reactor must be shut down or derated until safety can be assured.

Second, the asymptotic core outlet temperature changes required to passively shut down ATWS events are insensitive to variations in the values of individual reactivity coefficients which comprise the overall integral parameters, A, B, and C defined in Table I. This gratifying result comes about because the same reactivity effects contribute both to the reactivity addition which accompanies power reduction and to the reactivity subtraction which accompanies core isothermal temperature rise; and these reactivities cancel by definition in passive shutdown. Consider, for example, core radial expansion coefficient in the LOHS accident. As the inlet temperature goes up, the grid plate dilates, causing a negative reactivity insertion from the radial expansion coefficient of reactivity. On the other hand, as the power is reduced, the coolant  $\Delta T$  rise across the core is reduced, the above core load pads cool causing the top of the core to contract relative to the bottom of the core, and this leads to a positive reactivity input from the radial expansion coefficient. Since the radial expansion coefficient of reactivity contributes to both the reactivity addition and the reactivity subtraction processes -- which asymptotically cancel -- uncertainties or variations in this reactivity coefficient tend to self cancel also. In a mathematical sense, the uncertainties in the components of the numerator and denominator of the formulas for  $\delta T_{out}$  in Table II are positively correlated, tending to reduce their impact on the variance of  $\delta T_{out}$ . This will happen not only for the neutronics reactivity coefficients, but also for the thermo/structural components (see Eq. 3) of the reactivity feedbacks comprising the global reactivity parameters A, B, and C.

This serendipitous partial self cancellation of individual reactivity coefficient uncertainties has two payoffs. First, the actual power reactor will experience less variation in its passive shutdown performance in response to unavoidable variations in composition and geometry which derive from manufacturing tolerances and aging effects. Thus, the Tech Spec monitoring will assure safety and the self cancellation property will enhance plant availability in the face of the Tech Spec, when the actual power reactor is in place. Second, during the design and licensing phase, when A, B, and C cannot be measured on the operating plant but must be calculated based on computed values of individual components and when design and licensing activities must rely on calculational prediction, then this insensitivity of passive shutdown performance to uncertainties in individual reactivity coefficients raises the confidence level ascribed to the calculations by designers and licensers alike.

### C) Specific Focus For Uncertainty Reduction Via Critical Experiments

There are two key places where the partial self cancellation of uncertainties as they affect passive shutdown consequences fail to take place. The first is for the TOP ATWS event where the uncertainties of the components comprising the BOEC hot, all-rods-out, reactivity excess are poorly correlated with those of the reactivity feedback coefficients. Here, the

initial\* core outlet temperature increase in response to an unprotected single rod runout is given by:

$$\delta T_{out} = \Delta T_c \left( \frac{\text{BOEC Excess}}{A+B} \right) \left( \frac{\text{First Rod Out Interaction Factor}}{\text{No of primary rods}} \right) \quad (4)$$

with

$$\begin{aligned} (\text{BOEC Excess}) &= (\text{Burnup Control Swing}) \\ &+ (\text{Excess to Cover Uncertainties}) \end{aligned} \quad (5)$$

Here the (Excess to Cover Uncertainties) is provided for by over-enrichment of the manufactured assemblies to cover contingencies such as:

$$(\text{Excess to Cover Uncertainties}) = \left\{ \begin{array}{l} (\text{uncertainty in burnup control swing})^2 \\ + (\text{uncertainty in cold to hot reactivity defect})^2 \\ + (\text{uncertainty in cold critical mass})^2 \\ + (\text{uncertainty due to fuel manufacturing tolerance})^2 \end{array} \right\}^{1/2}$$

It is evident that the uncertainties in Doppler, sodium density, and radial and axial expansion temperature coefficients of reactivity which comprise the (A+B) factor in the denominator of Eq. 4 are but loosely correlated with the uncertainties in the factors determining the burnup control swing in the numerator of Eq. 4. Thus, one does not expect a partial uncertainty self cancellation as was enjoyed for the other ATWS events. It must be noted that, in fact, the advanced LMR cores are designed to achieve a nominally zero burnup control swing so that -- to the degree that the design goal is achieved -- it is the (Excess to Cover Uncertainties) which controls the size of the (BOEC Excess) and of the TOP initiator. Nonetheless, the loose correlation between the contributors to uncertainty in the denominator and numerator of Eq. 4 persists with the exception of shared components in the cold to hot reactivity defect.

The second instance where uncertainties relevant to passive shutdown performance are poorly correlated with those of the reactivity feedback coefficients is for the local power peaking factor which is a necessary factor for converting the global core mixed mean coolant outlet temperature rise to a local, hot channel, value required in an actual assessment of margin to core damage in response to the passive shutdown of ATWS events.

$$\delta T_{out} (\text{local}) = \delta T_{out} (\text{core mixed mean}) * \quad (7)$$

- \* [Local Peaking Factor (Burnup State, Rod Position)]
- \* [Local/Ave Flow Redistribution]

From the results of the above discussions it is seen that at our current state of knowledge prior to power reactor construction, in order to reduce the neutronics uncertainties which importantly impact calculational predictions of

-----  
\* If the initial power rise corresponding to Eq. 4 is large enough to boil dry the steam generator, then a loss of heat sink on top of the TOP will determine the asymptotic state.

passive shutdown performance we must address the criticals measurements to:

- the reactivity coefficient components of A, B, and C. i.e.
  - Doppler
  - Na density
  - Axial and radial expansion
  - Control rod differential worth
- the burnup control swing
- The components of the BOEC (Excess to cover Uncertainties)  
i.e.
  - cold critical mass
  - cold to hot reactivity defect
  - fuel worth

and

- local power peaking factor
  - vs rod position and burnup state

This list is seen to encompass not only the traditional focus of previous criticals measurements programs, but additional ones which are not amenable to direct measurement on a critical facility such as burnup control swing and cold to hot defect.

#### D) Institutional Environment

To summarize the discussions of the previous section, we find that in a regime of cores designed for passive shutdown, the need for criticals experiments to both correct calculational predictions of reactor quantities and to reduce their uncertainties encompasses all of the neutronics quantities stressed in prior programs and more as well. Particular stress in the current US program must be put on reduced uncertainty in burnup control swing because the rod runout TOP is unique among the ATWS events in that the uncertainty of the outcome of the event does not benefit from a partial self cancellation of the uncertainties in the underlying parameters which control the outcome.

Not only have the design goals shifted so as to modify the focus of the ZPPR criticals program, but the current US institutional environment imposes additional boundary conditions on how it is to be conducted. First, while the NRC staff has informally indicated a willingness to "give credit" for passive shutdown of Beyond Design Basis Events in the licensing of advanced LMR's, "receiving credit" will require the establishment with the licensing bodies of a high degree of credibility for the calculational predictions of passive shutdown effectiveness and for the provision of margins which will comfortably accommodate the current level of uncertainty. One might protest that the ATWS events which depend on passive shutdown are Beyond the Design Base and therefore their consequences are to be computed based on best-estimate values and that uncertainties are irrelevant. But such an objection ignores the reality of how human judgments concerning acceptable protection from risk are made in the face of uncertainty. Beyond Design Base or not, sensitivity studies of passive shutdown scenarios to quantify the dependence of consequences on input variations and the establishment of large margins between nominal consequence and initiation of massive core disruption are a prerequisite to the use of passive shutdown features in licensing. Since the

licensing interactions are based in part on calculated performance, this implies the needs to:

- a)- validate the calculational predictions of core response to ATWS events
- b)- place realistic and defensible bounds on the ATWS event consequences when uncertainties in the underlying parameters are propagated

and beyond that, to

- c)- provide substantial additional margins to cover the undefined phenomena and/or scenarios unaccounted for in the calculations.

Recent sessions of the U.S. Congress have reflected both the general public's disenchantment with nuclear power and it's concern over the federal deficit by allocating funding for but a small and at best non-expanding advanced reactor program. Since public perceptions comprise a significant factor in influencing public policy and public spending, notwithstanding the NRC staff's encouragement regarding acceptability of passive shutdown as a component of licensing, it is essential to establish a widespread perception that passive shutdown has technical credibility and that, as a result, an R&D program to pursue its potential is in the public interest. This institutional need imposes both a timeliness and a low-cost boundary condition on the measurements program to reduce uncertainties. Results are needed early to favorably influence funding of a continuing R&D program while at the same time these measurements must be conducted under the existing level of funding.

Thus, in view of the institutional boundary conditions:

- d)- the establishment of a widespread perception of credibility for passive shutdown must occur early in the program in order to favorably influence the continuing flow of development funds,
- e)- this requires not only demonstrating acceptable performance on a best estimate basis but also requires that a defensible quantification of the uncertainty levels be provided
- f)- and that the entire process be "explainable" to a general audience who are not technical specialists in critical experiments or in uncertainty propagation,

and finally,

- g)- the program to achieve these goals cannot depend upon massively expensive testing programs.

## II. APPROACH TO APPLYING ZPPR CRITICALS TO DESIGN

### A) Traditional Methodology

The technical and institutional requirements discussed above for the application of critical experiments to the US Advanced LMR Program present a dilemma for the ZPPR critical experiments program in that the past 15 year's worth of high quality criticals measurements data from ZPPR have been focused on the oxide fuel form, whereas the metal fuel form is now the centerpiece of the US LMR program because, among others, of properties advantageous for passive shutdown. Moreover, some of the key parameters influencing passive shutdown performance are not amenable to direct measurement in a critical experiment. And finally, with a heightened focus not only on the nominal calculated value but also on the uncertainty of the calculated prediction, a means to address ZPPR critical experiments to not only the traditional best estimate value, but also to a defensible quantification of its uncertainty is needed.

In previous US LMFBR programs the critical experiments have been applied to the design process through the use of bias factors. At a relatively late stage of the reactor design process (which is conducted using the evaluated ENDF data library) an Engineering Mockup Critical (EMC) is assembled, and as many design-related quantities as feasible are measured. The reactor design team models this EMC using their design-level modeling rules and codes to establish the calculated to experimentally measured C/E ratio for the quantities of design interest which are measurable. Then, the best estimate power reactor prediction is determined by:

$$(C')_{\text{power}} = (C)_{\text{power}} * \left(\frac{1}{C/E}\right)_{\text{ZPPR}} \quad (8)$$

for those quantities which are measurable on the critical. For those quantities which are not measurable, ad hoc corrections are made. Finally, uncertainties are estimated based on historical trends of variation of C/E's for similar EMC's.

But vis-a-vis the current US advanced LMR program's set of technical requirements and institutional boundary conditions this traditional bias factor approach is inadequate in a number of its facets:

- First, it produces licensing-related results rather late in the project's life cycle as a result of resting on measurements from an EMC; but the current need is to establish credibility of the veracity of passive shutdown early in the program to favorably influence R&D funding.
- Second, it is not possible to develop other than an ad hoc estimate for the uncertainties in the calculational predictions based on bias factors from an EMC program; but the current need is for a quantitative bound on the impact of uncertainties -- which is defensible in a licensing arena considering, for the first time, whether to give credit for passive shutdown.
- Third, some of the key reactor performance quantities important to passive shutdown are not amenable to direct

measurement in a critical experiment; an example is the burnup control swing which strongly influences the feasibility of passive shutdown of a rod runout TOP.

## B) Formal Data Fitting Methodology

In confronting the disparity between the capabilities of the traditional bias factor methodology for applying ZPPR critical experiments results to design and the US LMR Program's current needs in an regime of metallic fuel, design focus on passive shutdown, funding uncertainty, and need for timely, inexpensive, and credible reduction and quantification of neutronics uncertainties, the formal data fitting methodology appears to offer a number of advantages. As extensively developed in the 1970's this methodology updates a multigroup cross section vector,  $\underline{T}$ , having covariance matrix,  $\underline{M}$ , to a revised set,  $\underline{T}'$  and  $\underline{M}'$ , by using least squares fitting to find that set of cross section revisions ( $\underline{T}' - \underline{T}$ ) which minimizes the square of the deviation between an ensemble of criticals measurements,  $\underline{R}$ , and calculations of those measurements,  $\underline{C}(\underline{T})$ , based on the original cross sections,  $\underline{T}$ . The formal results are given by:

$$\underline{T}' - \underline{T} = \underline{M}\underline{G}^T \underline{W} (\underline{C} - \underline{R}) \quad (9)$$

$$\underline{M}' = \underline{M} - \underline{A}\underline{W}\underline{A}^T \quad (10)$$

where

$$\underline{W} = [\underline{M}\underline{G}^T + \underline{V}]^{-1} \quad (11)$$

$$\underline{A} = \underline{M}\underline{G}^T \quad (12)$$

and

$\underline{M}$  = covariance matrix for the cross section,  $\underline{T}$

$\underline{V}$  = covariance matrix for the criticals measurements,  $\underline{R}$

$\underline{G}$  = matrix of sensitivity coefficients =  $\frac{\% \text{ change in } R}{\% \text{ change in } \sigma}$

(computed using unadjusted cross sections,  $\underline{T}$ ).

The strength of the data fitting methodology is its ability to both improve the calculational predictions of the critical experiment results to which the fitting is done

$$\underline{C}' = \underline{C}(\underline{T}) + \underline{G}^T(\underline{T}' - \underline{T}) \quad (13)$$

and to reduce their variance to a value which is near that of the criticals measurements -- which are generally of a higher precision than can be calculated:

$$\begin{aligned} \overline{(\underline{C}')^2} - \overline{(\underline{C}')^2} &= \underline{G} \underline{M}' \underline{G}^T \\ &= \underline{G}\underline{M}\underline{G}^T - (\underline{G}\underline{M}\underline{G}^T)^T \underline{W} (\underline{G}^T \underline{M}\underline{G}) \end{aligned} \quad (14)$$

$$= \underline{GMG}^T \{ \underline{I} - \underline{I} + (\underline{GMG}^T + \underline{V})^{-1} \underline{V} \}$$

$$\approx \underline{V}$$

if  $\underline{V} \ll \underline{G}^T \underline{MG}$ .

It is noted that the cross sections per se are not necessarily improved either by a movement of their values closer to physical truth or by a reduction of their uncertainties. It is the design predictions as calculated using a specified modeling and computer code set which improve.

Moreover, if the dependences on cross sections of the power reactor are "the same" as those of the ensemble of critical experiments, these advantages carry over to the power reactor as well. For example, for a power reactor having a sensitivity matrix,  $\underline{S}$ , relating quantities of interest to cross sections, the adjusted cross sections yield corrected power reactor calculational predictions:

$$\underline{C}'_{\text{power}} = \underline{C}'_{\text{power}}(\underline{T}) + \underline{S}^T(\underline{T}' - \underline{T}) \quad (15)$$

and revised uncertainty levels:

$$\left( \overline{C'^2}_{\text{power}} - \underline{C}'^2_{\text{power}} \right) = \underline{S}^T \underline{M}' \underline{S} \quad (16)$$

$$= \underline{S}^T \underline{MS} - (\underline{GM}^T \underline{S})^T \underline{W} (\underline{GM}^T \underline{S})$$

If the projection of  $\underline{G}$  on  $\underline{S}$  is large, the data fitting will lead to a reduction in uncertainty of power reactor quantities -- even for quantities which cannot be directly measured in the critical experiments.

Finally, among the potential institutional-related advantages of this approach are first, that use of the method allows us to benefit from the very substantial historical accumulation of high-quality criticals measurements on a variety of fast spectrum cores (albeit not metal-fueled EMC's) and to thereby produce results for the metal-fueled conceptual core designs prior to the buildup of a comparable multi-year data base for design-specific metal-fueled EMC's. This property of the data fitting methodology facilitates the effort to establish a credibility for passive shutdown early in the program and at low cost.

Second, use of the method permits us to establish a formal, mathematically-well-founded procedure for quantifying the uncertainties in key neutronics quantities important to passive shutdown performance. For a power reactor having sensitivity matrix,  $\underline{S}$ , whereas the original uncertainties in calculationally-predicted quantities are

$$\underline{S}^T \underline{MS}$$

after data adjustment they are reduced to

$$\underline{S}^T \underline{M}' \underline{S} = \underline{S}^T \underline{MS} - (\underline{GM}^T \underline{S})^T \underline{W} (\underline{GM}^T \underline{S}).$$



This property of the data fitting methodology to replace the ad hoc uncertainty estimates of the bias factor method with estimates which are rigorously founded in the mathematics of least squares fitting is uniquely important in a licensing regime where, for the first time the petitioner will ask that credit be given for passive shutdown properties.

Third, the formal data fitting methodology permits us to reduce uncertainties on even those reactor performance quantities which are not directly measurable on a critical experiment. To the degree that the projection of the power reactor's sensitivity vectors,  $\underline{S}$ , onto those of the critical,  $\underline{G}$ , is large, the criticals help to reduce uncertainty in unmeasurable quantities. The salient example here is burnup control swing. Even though a burnup control swing does not occur and therefore cannot be measured on a critical assembly, the uncertainty in its value can be reduced by measurements such as  $c^{28}/f^{49}$ ,  $(1 + \alpha^{49})$ , and small sample worth,  $\rho^{28}/\rho^{49}$ , measurements on a critical.

And last, once the computational and data management machinery is set in place to implement the formal data fitting methodology, all future relevant experimentation can be added to the cumulative integral data base and will influence an evolutionary, monotonic improvement of design predictions. Not only critical experiments can be brought to bear on design in the existing framework, but so also can operating power reactor data which addresses those phenomena such as fission product poisoning, temperature coefficients and burnout which are not amenable to direct study in a critical assembly.

#### D) Interface Between ZPPR Criticals and Core Designers

The formal data fitting methodology possesses a number of features which meet the needs of the current US advanced LMR program. However, unlike the situation in European programs where a uniform methodology is employed nationwide -- permitting the use of a National adjusted cross section set -- the US program must accommodate to the presence of a plethora of modeling rules, unit cell codes, and full-core analysis codes in use among the various industrial contractors and government laboratories. Since the formal data fitting methodology improves the predictions and reduces the uncertainties of reactor integral quantities as calculated using a specified set of modeling rules and computer codes, but does not necessarily improve the cross sections, per se, the production of an adjusted cross section set for widespread use is not appropriate to the US situation of nonuniform design codes and modeling rules.

We do not produce an adjusted cross section set. Instead, the interface between the design team and the ZPPR criticals staff is placed beyond the EMC and beyond the data set,  $\underline{T}$ , onto a design-specific calculational "Secondary Standard" which has the properties that:

- it is relevant to the reactor designer's design activity (it is probably a conceptual design which will be refined later)
- its performance quantities of specific design interest are identified and are calculated by the designer using his normal, design-level methods with the unadjusted ENDF cross sections.

Then

- The ZPPR staff calculates the sensitivity coefficients,  $S$ , for this Secondary Standard, using ENDF data and the ZPPR modeling rules and computer codes,
- selects the relevant critical experiments data base,
- performs the formal cross section adjustment for this data base to determine  $(\underline{T}'-\underline{T})$  and  $\underline{M}'$ , using the formal data adjustment methodology, ZPPR modeling rules, and ZPPR calculational codes and methods which correct for those higher order effects which are not well treated by design-level methods.
- and at the same time generates the best-estimate prediction of the Secondary Standard physical performance for the quantities of interest

$$\underline{C}' = \underline{C}(\underline{T}) + \underline{S}^T(\underline{T}'-\underline{T})$$

- The ZPPR staff also produces the quantified uncertainty estimates

$$(\overline{C'^2} - \overline{C^2}) = \underline{S}^T \underline{M}' \underline{S}$$

for these design quantities.

The designer can then note the difference between his design-level predictions of this Secondary Standard and the ZPPR staff's "best estimate" of its actual properties and their current level of uncertainties which resulted from the formal data fitting methodology and can use this information in his design activities in any way that is convenient.

As the project progresses, an EMC critical configuration will be specified based in part on an evaluation of its potential to further reduce uncertainties -- as indicated by an evaluation of the projection of the EMC's sensitivity vectors on those of the power reactor. The Secondary Standard procedure can then be repeated based on the final power reactor design and an extended integral data base which includes the new EMC measurement data.

### III. STATUS AND THE FUTURE

In the US advanced LMR program, the passive reactivity shutdown goal has been added to the traditional core neutronics design goals, and the previous focus on breeding performance has been replaced by a focus on high internal conversion ratio to minimize burnup control swing and thence TOP initiator. These design goals have placed increased focus upon use of ZPPR criticals for reduction of the current level of calculational uncertainties in reactivity coefficients and in burnup control swing as compared with earlier US designs where reactivity shutdown relied on control rod scram with rod banks possessing substantial shutdown margin to cover uncertainties, and Beyond Design Basis accidents consequences were mitigated by traditional containment

structures. Institutional boundary conditions imposed on the use of the critical experiments in design include quantification and reduction of uncertainties in a timely low-cost way as a means to help establish the credibility of passive shutdown. The traditional methods of applying ZPPR criticals data to design via bias factors from an EMC are ill-suited to the new set of technical and institutional needs.

The formal data fitting methodology has been implemented over the past four years at ANL as a means to bring the ZPPR criticals experiments to bear on neutronics design issues in the US advanced LMR program -- with a stress on uncertainty reduction in calculations of passive shutdown performance. The paper by Collins, et al. describes the criticals data base which has been assembled and regularized. The paper by Poenitz and Collins describes the specifics of the methodology, validation of the data base for internal consistency, and displays a number of relevant examples of the methodology's effaciousness.

In the near term, the application of the methodology to the FFTF metal core reload design and concomitant FSAR revision will provide its first full scale utilization in the US. The Poenitz and Collins paper addresses FFTF design quantities which are measurable on a critical, while the paper by Khalil and Downar addresses the methodology to the reduction of uncertainty in burnup control swing. The formal data fitting methodology will also be applied in support of the industrial sector's advanced LMR licensing interactions with the NRC over the next several years, and in support of the SP-100 space reactor ground test design, fabrication and test programs.

As for the continuing refinement of the methodology and extension of its applications, the paper by Hwang addresses interpretive methodologies for relating the power reactor's dependence on cross sections to that of the ensemble of critical assemblies and also discusses work in progress to incorporate a rigorous treatment of the differences in space and energy shelf shielding which exist in the criticals vis-a-vis the power reactor. The paper by Orechwa initiates a broader view of the advanced LMR design accuracy requirements than has been taken in the present work where the focus was on uncertainty reduction in passive shutdown performance; the closed, fissile self sufficient fuel cycle employed in the US advanced LMR program brings depletion dependences and nuclear properties of minor actinides, fission products, and waste streams into stronger focus than in past US LMFBR cycles. Over the next five years, burnup measurements data from EBR-II will be added to the data base as a part of the program to address these depletion-dependent issues.

## REFERENCES

1. D. C. WADE and Y. I. CHANG, "The Integral Fast Reactor (IFR) Concept: Physics of Operation and Safety," Proc.Int'l. Topical Meeting on Advances in Reactor physics Mathematics and Computation, Paris, Vol. 1, p. 311, April 1987.
2. P. J. COLLINS, C. ATKINSON, W. P. POENITZ, R. M. LELL, R. W. SCHAEFER, and J. J. R. LIAW, "A Data Base for the Adjustment and Uncertainty Evaluation of Reactor Design Quantities," (this conference).
3. W. P. POENITZ and P. J. COLLINS, "Utilization of Integral Experimental Data for the Adjustment and Uncertainty Evaluation of Reactor Design Quantities," (this conference).
4. H. S. KHALIL, T. DOWNAR, "Uncertainty in the Burnup Reactivity Swing of Fast Reactors," (this conference).
5. R. N. HWANG, "Topics in Data Adjustment Theory and Applications," (this conference).
6. Y. ORECHWA, "Target Accuracy Considerations for U.S. Advanced LMR Core Designs," (this conference.)

Table 1. Components of Power and Power/Flow Reactivity Decrements and of  $T_{inlet}$  Coefficient of Reactivity

$A (\phi) =$	$\left\{ \begin{array}{l} \alpha_D \end{array} \right.$	$\left[ \begin{array}{l} 0 \text{ bounded to clad} \\ \alpha_f \text{ free of clad} \end{array} \right.$			$\left. \right\} * \frac{\Delta T_f}{2}$ (ave. fuel - ave. coolant) temperature
$B (\phi) =$	$\left\{ \begin{array}{l} \alpha_D \end{array} \right.$	$\alpha_f$	$+ \alpha_{Na}$	$+ 2\alpha_R$	$\left. \right\} * \frac{\Delta T_c}{2}$ (ave. coolant - $T_{inlet}$ ) temperature
$C (\phi/^\circ C) =$	$\left\{ \begin{array}{l} \alpha_D \end{array} \right.$	$\alpha_f$	$+ \alpha_{Na}$	$+ \alpha_R$	$\left. \right\}$
	Doppler	Fuel axial expansion	Na density	Radial expansion	
Typical Size $\phi/^\circ C$	-0.05 to -0.1	-0.1	+0.15 to 0.2	-0.2 to 0.3	
	Associated with fuel temperature	?	Associated with coolant temperature		

Table 2. Quasi Static Reactivity Balance Results for Unprotected Accidents

	Asymptotic State				Intermediate State	Indicated Trend for Inherent Shutdown*
	P	F	$\Delta T_{in}$	$\Delta T_{out}$		
LOHS	-0	1	$\frac{A-B}{C}$	$\left( \frac{1+A/B}{C\Delta T_c} - 1 \right) \Delta T_c$	Monotonic transition to asymptotic	<ul style="list-style-type: none"> <li>• A+B small</li> <li>• C large</li> </ul>
TOP	-1 (after rise in $T_{in}$ due to BOP heat removal limit)	1	$\frac{\Delta\theta_{TOP}}{-C}$	$\Delta T_{out} = \Delta T_{in}$ $= \left( \frac{\Delta\theta_{TOP}/B}{-C\Delta T_c/B} \right) \Delta T_c$	Initial rise at constant $T_{in}$ $P = 1 + \frac{-\Delta\theta_{TOP}/B}{1 + A/B}$ $\Delta T_{out} = \left( \frac{-\Delta\theta_{TOP}/B}{1 + A/B} \right) \Delta T_c$	<ul style="list-style-type: none"> <li>• A-B large</li> <li>• C large</li> <li>• <math>\Delta\theta_{TOP}</math> small</li> </ul>
LOF	-0	Natural Circulation	0	$(A/B)\Delta T_c$	overshoot relative to delayed neutron hold-back of power decay minimized if $\lambda\tau(1-A/B)^2 B  \gg 1$	<ul style="list-style-type: none"> <li>• A small</li> <li>• B large</li> <li>• <math>\tau</math> long</li> </ul>
Chilled Inlet	$1 - \frac{C\Delta T_{in}}{A-B}$	1	$ \Delta T_{in}  \leq (T_{inlet} - T_{Na freeze})$ $= 1.5 \Delta T_c$	$\left( \frac{C\Delta T_c/B}{1 + A/B} - 1 \right) (-\Delta T_{in})$	monotonic transition	<ul style="list-style-type: none"> <li>• C small</li> <li>• A+B large</li> </ul>
Pump Overspeed	$\frac{1 + A/B}{1/F + A/B}$ (always > 1)	F > 1	0	$\left( \frac{1}{1 + \frac{A/B}{1 + A/B} (F-1)} \right) \Delta T_c$ (always < 0)	monotonic transition	<ul style="list-style-type: none"> <li>• A negative</li> <li>• B negative</li> </ul>

\*Conflicts are seen to exist between desirable trends for different ATWS events. Resolution of these conflicts is discussed in the text.

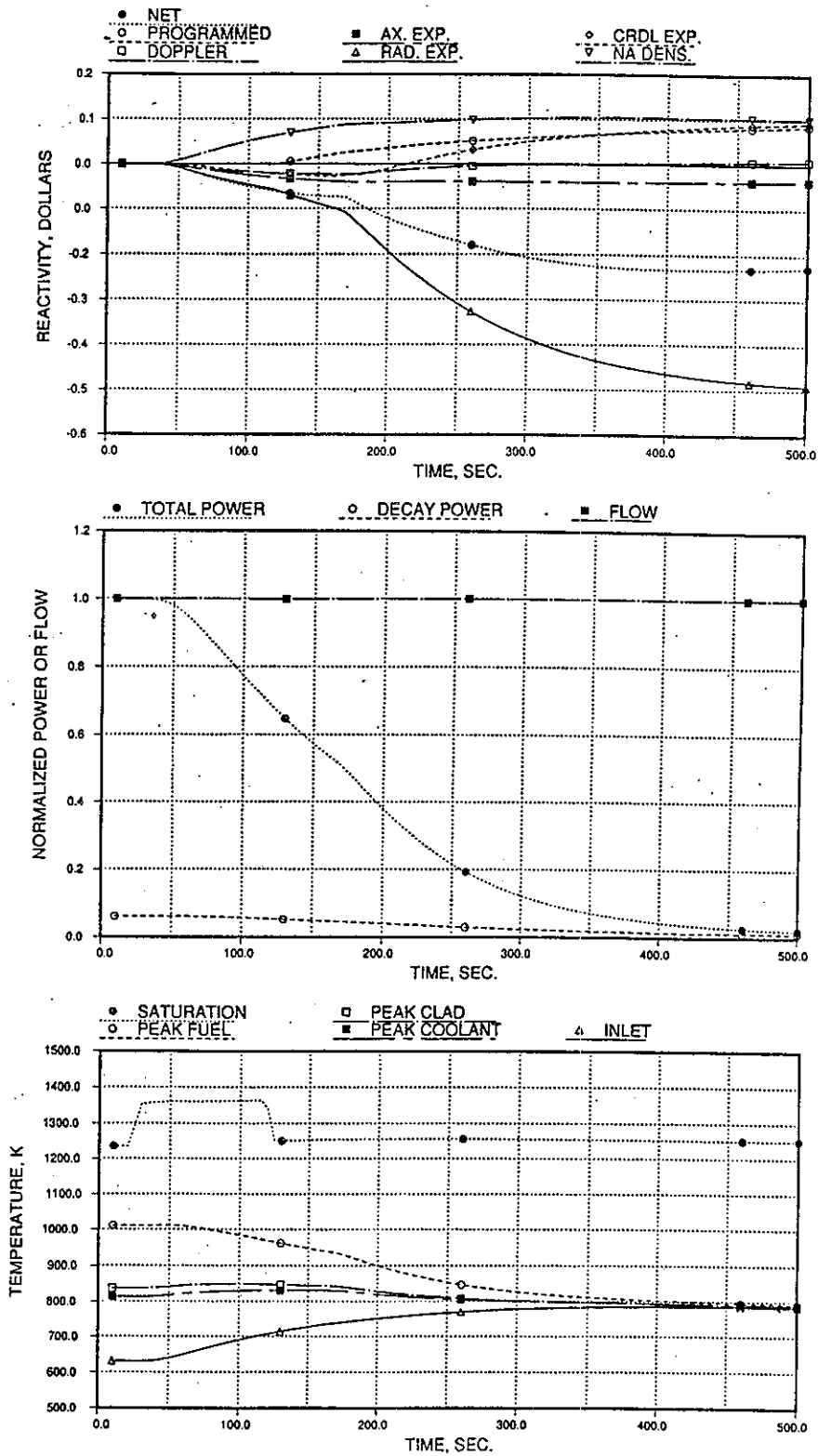


Fig. 1. Passive Shutdown of Loss of Heat Sink ATWS Event in a 900 MW<sub>th</sub> metal-fueled LMR ("Programmed" reactivity denotes vessel axial expansion)

**SESSION II**

**September 23, 1988**

**Chairman: Y. Orechwa (ANL, U.S.A.)**

**Rapporteur: T. Takeda (Osaka Univ., Japan)**





A Data Base for the Adjustment and Uncertainty  
Evaluation of Reactor Design Quantities

P. J. Collins, C. A. Atkinson, W. P. Poenitz, R. M. Lell,  
R. W. Schaefer and J. R. Liaw

Argonne National Laboratory - West  
Idaho Falls, ID 83403-2528, U.S.A

ABSTRACT

The requirement to provide best estimates and to evaluate and reduce uncertainties for LMR design quantities have led at Argonne National Laboratory, to a program of utilizing experimental integral data from past critical assemblies. Generalized-least-squares fitting is being used and the establishment of the best possible integral data base has been a first priority. The selection of critical assemblies and types of data included in the data base was guided by the need to cover wide spectral and compositional ranges, as well as to provide for the assessment of the predictability of typical reactor design parameters such as enrichments, breeding ratios, sodium void, power distributions, control rod worths, and material worths.

Experimental data have been revised and updated to latest reference data, where necessary, and uncertainty information has been included in order to permit the construction of a covariance matrix. Calculated values have been obtained consistently based on ENDF/B-V.2 and with the best methods feasible. Sensitivity vectors were obtained, as far as possible, with models consistent with the reference calculations. The covariance matrices of the basic parameters (cross sections, etc.) were obtained from ENDF/B-V.2 but improved and extended to cover the range of the parameters involved in the calculations.

INTRODUCTION

Integral data measured in critical assemblies are of interest and importance for the improvements and uncertainty reductions of values calculated for a reactor design. A program has been initiated at the Applied Physics Division of ANL to utilize, for this purpose, some of the substantial data base accumulated over the years from critical assembly experiments. Of current interest are applications to the metallic-fueled cores related to the IFR program. Possible future applications may be for space-reactor designs. The data-adjustment methodology is being used as the tool to obtain adjustments for the calculated quantities and to perform uncertainty evaluation. This method is based on data evaluation by generalized least-squares. It requires the covariance matrix,  $\underline{C}_p$ , of the prior evaluated parameters (e.g., the group cross sections derived from an evaluated nuclear data file), the experimental integral data,  $\bar{E}$ , and their covariance,  $\underline{C}_E$ , and correspondingly calculated values,  $\bar{C}$ , and their covariance,  $\underline{C}_C$ . Also required are the sensitivities of the calculated quantities to the parameters,  $\underline{S}$ .

The assessment of the suitability of the data adjustment methodology and the application of the method to the FFTF core conversion design will be presented elsewhere.<sup>1</sup> The purpose of the present paper is to describe the data base which has been assembled for this purpose. The selection of cores and types of integral data was based on a number of considerations:

- a) A wide range of spectra was considered desirable for the present and future applications, but limited to fast reactors.
- b) A wide range of compositions was desirable to include data for typical materials considered in reactor designs.
- c) Data not only from benchmark-type assemblies but also from diagnostic cores and generic mockups were included in order to make the assessment of adjustments of various quantities of designs for real reactors possible.
- d) Not only the traditional types of data, as  $k_{eff}$  and central reaction-rate ratios, but also material worth, control rod worth spatial reaction-rate distributions, flux ratios, and sodium void were included to make the assessment of the predictability of quantities beyond enrichment and breeding ratio possible.
- e) Data for which the calculated vs. experimental value ratios (C/E) were  $\sim 1$  were included, as well as those for which they were  $\neq 1$  (C/E discrepancies) in order to restrain the resolution of discrepancies at the cost of creating new ones.
- f) Data from different experimental programs were included in order to randomize the data base as much as possible, i.e., in order to avoid the biases of the experiments from one program to be transferred to biases for the reactor design.
- g) Data from similar critical assemblies were included in order to facilitate consistency checks.

#### DATA BASE

An overview of the data base is given in Tables I and II. About 260 calculated values were included so far. For some quantities, several measurements are available and  $\sim 300$  experimental data for the  $\sim 260$  quantities are in the data base. The data base ranges from the hard spectra Jezebel and Godiva to the soft spectra Zebra-8A and -8F, and from the 6 kg fissile loading of Flattop-Pu to the 2491 kg of ZPPR-13C. It includes the homogeneous assemblies Godiva, Jezebel, Jezebel-Pu, as well as such heterogeneous cores as ZPPR-13C and ZPPR-17A. Systems with few materials are represented, as well as typical LMR compositions. Assemblies with and without blankets and/or reflectors are present in the data base.

The integral quantities included in the data base are  $k_{eff}$  or  $k_{\infty}$  and central reaction rate ratios between F25, F49, F28 and C28 for most cores. A number of results for F40/F25, F41/F25 and for  ${}^1_0\text{B}(n,\alpha)$  (Helium production) relative to F25 are included as well. Material worths (derived from small sample worth data) for fissile and fertile isotopes and  ${}^1_0\text{B}$ ,

TABLE I

The Data Base -- Pu-fueled Assemblies

Assembly	Fissile Mass, kg	Median Energy, MeV	Core Characteristics <sup>a</sup>	Blanket/Reflector <sup>a</sup>	Quantities/Data <sup>b</sup>
Jezebel	16	1.314	Homogeneous Sphere, 95% Enrichment	None	$k_{eff}$ , F28/F25, F49/F25
Jezebel-Pu	15	1.254	Homogeneous Sphere, 20% <sup>240</sup> Pu	None	$k_{eff}$ , F28/F25
Flattop-Pu	6	0.896	Homogeneous Sphere, 95% Enrichment	19.6 cm thick Spherical Shell, NU	$k_{eff}$ , F28/F25
ZPPR-12V	272	0.251	Pu/Mo/U, Fe O <sub>2</sub> , Heterogeneous <sup>3</sup> Cell	U O <sub>2</sub> -Radial Blanket SS-Reflector	$k_{eff}$ , F28/F49, F25/F49 C28/F49, Radial Ratios -F49, -F25, -F28, -C28
ZPPR-12	249	0.217	Same as -12V but Na in Core	Same as -12V	Same as -12V plus Flux Ratios Groups 5-15, Small Sample Worth of <sup>235</sup> U, <sup>238</sup> U, <sup>239</sup> Pu
ZPPR-15A	1187	0.196	Pu/Mo/U, SS, Na, DU Heterogeneous Cell, Inner Core/Outer Core	DU, SS, Na-Radial Blanket, SS-Reflector	$k_{eff}$ , F28/F49, F25/F49 C28/F49, Small Sample Worth of <sup>235</sup> U, <sup>238</sup> U, <sup>239</sup> Pu, <sup>240</sup> Pu, <sup>241</sup> Pu, <sup>10</sup> B, Sodium Void, Control Rod Worth

TABLE I (cont'd)

Assembly	Fissile Mass, kg	Median Energy, MeV	Core Characteristics <sup>a</sup>	Blanket/Reflector <sup>a</sup>	Quantities/Data <sup>b</sup>
ZPPR-15B	1187	0.196	Same as -15A, Some SS replaced by Zr	Same as -15A	Same as -15A, plus IC/OC ratios for F49, F25, F28, C28. No small Sample Worth of <sup>241</sup> Pu.
Zebra-8B	---	0.174	Pu/Ga, NU, C Heterogeneous Cell, Infinite Medium	(Driver + Reflector)	k <sub>∞</sub> , F28/F25, F25/F49, C28/F49, F40/F25, F41/F25
ZPR-3/56B	333	0.172	Pu/U/Mo, U <sub>3</sub> O <sub>8</sub> , Na Fe <sub>2</sub> O <sub>3</sub> , Na <sub>2</sub> CO <sub>3</sub> Heterogeneous Cell	Ni, Na-Reflector	k <sub>eff</sub> , Radial Ratios Center/Edge -F49, -F28, -A10, Center/Reflector -F49, -A10, Worth of Replacing Central Fuel with B <sub>4</sub> C/Na and Ni/Na
Zebra-8E	---	0.167	Pu/Ga, NU, Na Infinite Medium Heterogeneous Cell	(Driver + Reflector)	k <sub>∞</sub> , F28/F25, F25/F49, C28/F49, F40/F25, F41/F25
ZPPR-13C	2491	0.161	Pu/U/Mo, U <sub>3</sub> O <sub>8</sub> , Na, Fe <sub>2</sub> O <sub>3</sub> , Heterogeneous Cell, Three Internal Blankets, Three Core Zones	DU, U <sub>3</sub> O <sub>8</sub> , Na- Radial Blanket, SS-Reflector	k <sub>eff</sub> , Radial Ratios - C/X F25, C/Y F25, Helium Production of <sup>10</sup> B/F25, Control Rod Worth of Ring 1, Ring 2 Ring 3, X, Y
Zebra-8D	---	0.146	Pu/Ga, NU, Na, C, Infinite Medium, Heterogeneous Cell	(Driver + Reflector)	k <sub>∞</sub> , F25/F49, F28/F49 C28/F49, F40/F25, F41/F25
ZPPR-17A	2300	0.138	Pu/U/Mo, Fe <sub>2</sub> O <sub>3</sub> , U <sub>3</sub> O <sub>8</sub> , Na, Na <sub>2</sub> CO <sub>3</sub> Heterogeneous Cell, Internal Blanket	DU, U <sub>3</sub> O <sub>8</sub> , Na Radial/Axial Blanket	k <sub>eff</sub> , F25/F49, F28/F49 C28/F49, Radial Ratios -F49, -F28, -C28, Control Rod Worth

08

94050089

TABLE I (cont'd)

Assembly	Fissile Mass, kg	Median Energy, MeV	Core Characteristics <sup>a</sup>	Blanket/Reflector <sup>a</sup>	Quantities/Data <sup>b</sup>
Zebra-8C	---	0.136	Pu/Ga, SS, C, NU Heterogeneous Cell Infinite Medium	(Driver + Reflector)	$k_{\infty}$ , F28/F25, F25/F49, C28/F49, F40/F25, F41/F25
ZPR-6/7	1134	0.132	Pu/U/Mo, Na, Fe <sub>2</sub> O <sub>3</sub> , U <sub>3</sub> O <sub>8</sub> Heterogeneous Cell	DU Blanket	$k_{eff}$ , F28/F49, F25/F49, C28/F49, Radial Ratio -F49
Zebra-8A	---	0.090	Pu/Ga, NU, C Heterogeneous Cell Infinite Medium	(Driver + Reflector)	$k_{\infty}$ , F28/F25, F25/F49, C28/F49, F40/F25, F41/F25
Zebra-8F	---	0.080	PuO <sub>2</sub> , UO <sub>2</sub> , C Heterogeneous Cell, Infinite Medium	(Driver + Reflector)	$k_{\infty}$ , F28/F25, F25/F49, C28/F49, F40/F25

<sup>a</sup>EU = enriched uranium, DU = depleted uranium, NU = natural uranium, SS = stainless steel.

<sup>b</sup>F28/F25, etc. = reaction rate ratios in core center.

TABLE II

The Data Base -- U-fueled Assemblies

Assembly	Fissile Mass, kg	Median Energy, MeV	Core Characteristics <sup>a</sup>	Blanket/Reflector <sup>a</sup>	Quantities/Data <sup>b</sup>
Godiva	49	1.085	Homogeneous Sphere 93% Enrichment	None	$k_{eff}$ , F28/F25, F49/F25
Flattop-25	17	0.801	Homogeneous Sphere 93% Enrichment	18cm thick Spherical Shell of NU	$k_{eff}$ , F28/F25, F49/F25
Jemima (53)	87	0.792	Heterogeneous Cylinder Alternating EU/NU Discs	None	$k_{eff}$
Jemima (37)	100	0.655	Same as (53)	None	$k_{eff}$
Jemima (12) <sup>c</sup>	312	0.367	Same as (53)	None	$k_{eff}$
Big-10	236	0.314	Cylinder, Homogeneous Core Heterogeneous Outer Core	DU Reflector	$k_{eff}$ , $\beta_{eff}$ , F28/F25, F49/F25, C28/F25, Small Sample Worth of $^{235}\text{U}$ , $^{239}\text{Pu}$ , $^{238}\text{U}$ , $^{10}\text{B}$ , Helium Production of $^{10}\text{B}/\text{F25}$
ZPR-9/36 (U9)	548	0.281	EU, DU Heterogeneous Cell	DU Reflector	$k_{eff}$ , $\beta_{eff}$ , F28/F25, F49/F25 C28/F25, F40/F25, F41/F25 Radial and Axial Ratios -F25, -F28, -C28, Small Sample Worth $^{235}\text{U}$ , $^{239}\text{Pu}$ , $^{238}\text{U}$ , $^{10}\text{B}$ , Flux Ratios
Scherzo <sup>d</sup>	---	0.243	EU, DU, NU Infinite Medium Heterogeneous Cell	(Driver)	$k_{\infty}$ , F28/F25, C28/F25
Zebra-8H	---	0.240	EU, NU Infinite Medium, Heterogeneous Cell	(Driver + Reflector)	$k_{\infty}$ , F28/F49, F25/F49
ZPPR-15D	1659	0.217	EU, DU, Na SS, Zr, 10% Pu/U/Mo Heterogeneous Cell	DU Radial Blanket, SS Reflector	$k_{eff}$ , F28/F49, F25/F49 C28/F49, IC/OC Ratios -F49, -F25, -F28, -C28, Small Sample Worth of $^{235}\text{U}$ , $^{239}\text{Pu}$ , $^{238}\text{U}$ , $^{10}\text{B}$ ; Na Void, Flux Ratios, Control Rod Worth of -Central, -Primary, -Total; Worth of Replacing Central Fuel with Na
ZPR-6/6A	1784	0.144	EU, Na, SS DU, $\text{U}_2\text{O}_8$ , $\text{Fe}_2\text{O}_3$ , Heterogeneous Cell	DU Reflector	$k_{eff}$ , F28/F25, C28/F25, Radial Ratio -F25

<sup>a</sup>EU = enriched uranium, DU = depleted uranium, NU = natural uranium, SS = stainless steel.<sup>b</sup>F28/F25, etc. = reaction rate ratios in core center.<sup>c</sup>Originally not named Jemima.<sup>d</sup>Originally named Scherzo-556 and included data from Zebra-8H. The Zebra data has been excluded here.

center core sodium void reactivities, control rod worths, and reaction rate distributions were included for some assemblies. Inclusion of spatial variations of reaction rate and control rod worths was considered important because these measurements have implications for power distributions and the experimental values are quite precise. Two values of  $\beta_{eff}$  were also included. Ratios of neutron fluxes from group 5 through group 15 to the sum of the flux group 5 to 15 were entered for 4 cores. Absolute cross sections for  $^{235}\text{U}(n,f)$ ,  $^{239}\text{Pu}(n,f)$  and  $^{238}\text{U}(n,f)$  averaged over the  $^{252}\text{Cf}$  fission neutron spectrum have not been used for the evaluation of ENDF/B-V, though they have been used for ENDF/B-VI. Reasonably accurate experimental data are available ( $\sim \pm 2\%$ ) and these have also been included in the data base.

#### Calculated Values

Some of the calculations have previously been reported in the context of ENDF/B-V.2 data testing<sup>2,3</sup> and only a summary is given here. All calculations were consistently based on ENDF/B-V.2.<sup>4</sup> Multigroup cross sections were processed for each core with 2082 - energy-group spectra calculations and reduced to 230-energy groups with MC<sup>2</sup>-II<sup>5</sup> for core, blanket and reflector regions. Cell heterogeneity processing was done with SDX<sup>6</sup> using one-dimensional cell models. Allowances were made for edge-region cells. Group-dependent buckling terms, obtained from a prior xyz calculation, were used in cell calculations for heterogeneous LMR cores, but not for other cases. The process led to the collapse into a 21-energy-group structure, favored by the core design group at ANL, using one-dimensional reactor models.

The integral transport calculation in SDX produced the values used for the infinite media Zebra-8 assemblies. These values were later confirmed through one-dimensional diffusion theory calculations.

Deterministic calculations were performed for the ZPR/ZPPR assemblies, using the three-dimensional nodal-transport option of DIF3D,<sup>7</sup> with complete geometric and compositional details represented in the models. The modeling of the benchmark assemblies was significantly improved in comparison with the CSEWG benchmark specification for the ZPR assemblies which date back some 20 years. Plate-cell streaming effects were included using anisotropic transport cross sections. The results indicate that improvements may still be required for the calculations of ZPPR-15D and ZPR-3/56B.

The smaller high-leakage cores from LANL were calculated with TWODANT<sup>8</sup> using higher order  $P_nS_n$ . Similar calculations were recently done at LANL<sup>9</sup> and the results are compared in Table III. The differences for the two Flattops are suspected to be caused by the angular distributions of the inelastic scattering which are not treated in the ANL cross section processing codes. Because of these problems, Monte Carlo calculations were performed with the VIM<sup>10</sup> code. Calculations with VIM were also performed for Zebra-8A, -8C and -8D, mainly because of strong heterogeneity effects. The results from the Monte Carlo calculations are also shown in Table III. The present Monte Carlo calculations were done with statistical uncertainties of  $\sim 0.1$  to  $0.2\%$  for  $k_{eff}$  and  $\sim 0.5$  to  $0.8\%$  for reaction rate



TABLE III

Comparison of Deterministic and Monte Carlo Calculations

Assembly/ Quantity	Deterministic		Monte Carlo		
	ANL	LANL <sup>y</sup>	ANL		LLNL <sup>11</sup>
Jezebel					
$k_{eff}$	0.9984	0.9982	0.9983	± 0.09%	
F28/F25	0.2031	0.2050	0.2060	± 0.67%	
F49/F25	1.4116	1.411	1.4132	± 0.61%	
Flattop-Pu					
$k_{eff}$	1.0124	1.0056	1.0071	± 0.11%	
F28/F49	0.1728	0.1750	0.1749	± 0.84%	
Godiva					
$k_{eff}$	0.9976	0.9901 <sup>a</sup>	0.9971	± 0.08%	0.995 ± 0.3%
F28/F25	0.1713	0.1704	0.1722	± 0.52%	
F49/F25	1.3963	1.393	1.3969	± 0.46%	
Flattop-25					
$k_{eff}$	1.0106	1.0062	1.0036	± 0.10%	1.003 ± 0.3%
F28/F25	0.1543	0.1541	0.1545	± 0.73%	
F49/F25	1.3725	1.370	1.3721	± 0.58%	
Jemima (53)					
$k_{eff}$	0.9938		0.9948	± 0.17%	
Jemima (37)					
$k_{eff}$	0.9978		0.9977	± 0.17%	
Jemima (12)					
$k_{eff}$	1.0055		1.0060	± 0.16%	
Zebra-8A					
$k_{\infty}$	0.9888		0.9780	± 0.20%	
F28/F25	0.01267		0.01347	± 0.60%	
C28/F49	0.1290		0.1267	± 0.60%	
F25/F49	1.2410		1.2334	± 0.60%	
Zebra-8C					
$k_{\infty}$	0.9544		0.9640	± 0.20%	
F28/F25	0.01076		0.01139	± 0.60%	
C28/F49	0.1309		0.1304	± 0.50%	
F25/F49	1.0849		1.0447	± 0.50%	
Zebra-8D					
$k_{\infty}$	0.9681		0.9742	± 0.20%	
F28/F25	0.01840		0.01874	± 0.50%	
C28/F49	0.1304		0.1297	± 0.50%	
F25/F49	1.0218		1.0141	± 0.50%	

<sup>a</sup>This result from Reference 9 appears to be in error. MacFarlane et al., (LA-10288-PR, p44, 1985) have a value 0.9990.

ratios. Some other Monte Carlo calculations with statistical uncertainties of ~ 0.3% for  $k_{eff}$  are shown in Table III as well.

Comparisons between Monte Carlo calculations and deterministic calculations for a larger number of more conventional cores<sup>12</sup> were used to estimate the uncertainties of the calculated  $k_{eff}$  values due to model and methods approximations for the remaining critical assemblies of the data base. This estimate was  $\pm 0.3\%$  of which a large part is due to cell heterogeneity and therefore assumed to be uncorrelated.

Small sample worths were calculated with first-order perturbation theory using the VARI3D code<sup>13</sup> and the flux and adjoint solutions from the xyz geometry finite difference diffusion theory calculations for the reference critical assemblies. Neutron streaming in the plate cells was accounted for with Benoist diffusion coefficients. Detector cross sections corresponding to a critically buckled, homogeneous cell were used. The  $\beta_{eff}$  values used to convert the measured values to the calculated  $\Delta k/k$  were corrected for the adjoint heterogeneity effect.<sup>14</sup> Corrections were also applied to account for the fission emission spectra of the perturbation samples. Corrections for sample size involving self-multiplication and self-shielding were calculated with the SARCASM code.<sup>15</sup> Cavity corrections were calculated and applied based on sample-independent one-group modeling which is known to underestimate the true cavity effect.<sup>16</sup>

Uncertainties of the calculated values for the radial-tube small-sample worths caused by model and methods approximations were estimated from differences observed between various methods of determining material worth in ZPPR-15A.<sup>17</sup> Uncertainties for global transport effects are so far unknown and have not been included.

The cross sections of  $^{235,238}\text{U}(n,f)$ , and  $^{239}\text{Pu}(n,f)$  averaged over the  $^{252}\text{Cf}$  spectrum have been calculated using a recent evaluation of the latter.<sup>18</sup> The contribution of the  $^{252}\text{Cf}$  spectrum to the uncertainties of the average cross sections is small for  $^{235}\text{U}(n,f)$  and  $^{239}\text{Pu}(n,f)$  (0.3%) but it is ~2.5% for  $^{238}\text{U}(n,f)$ .

#### The Experimental Integral Data

Information on the experimental integral data has been included in the data base following a previous recommendation.<sup>19</sup> The experimental values, their uncertainty components, and correlation information were entered on the data file, and the covariance matrix is constructed by the generalized least-squares fitting code GMADJ.<sup>20</sup>

All experimental values, specifically reaction rate ratios, have been updated to contain revised data and newer and consistent normalization factors (e.g. for thermal cross sections, fission yields, half-lives, sample masses). In some cases, corrections have been calculated and applied. Uncertainty components have been entered where given by the experimenters but have been also updated where data have been revised. Estimates of uncertainties have been made where such information was not available.

Several experimental values are available for the same integral quantities in some cases (e.g. the reaction rate ratios in Big-10 were measured by experimenters from several laboratories as part of the Interlaboratory Reaction Rate Program<sup>21</sup>). The separate experimental values were entered in the data base in order to account consistently for correlations.

The source of the data for the LANL critical assemblies was the updated CSEWG benchmark specifications<sup>22</sup> and several publications<sup>23</sup> and reports.<sup>24</sup> Newer revised data were found in Ref. 9 and ultimately used for the present data base. The data for the infinite media of the Zebra-8 series are based on a recent report<sup>25</sup> and private communications. The data for "Scherzo" are based on a French/German report<sup>26</sup> and explicitly exclude the data from Zebra-8H which have been entered into the data base separately. The data for the ZPR/ZPPR critical assemblies are from various internal Argonne National Laboratory reports. A detailed description of the data base and data modifications, where applicable, is given elsewhere.<sup>27</sup>

#### Covariance Matrix of the Parameters

Version V.2 of ENDF/B contains uncertainty and correlation information for a number of light, structural, and heavy nuclei. The given data have been expanded into 21 group covariance matrices with the NJOY.ERRORR module<sup>28</sup> using a fast neutron spectrum (ZPR-6/7) for weighting.<sup>29</sup> The majority of the covariances obtained with this method proved to be singular or not positive definite, probably because the information on ENDF given for a few energy regions was expanded into 21 energy groups. The correlation matrices have been made positive definite and nonsingular based on  $\underline{C} + a\underline{I}$  being positive definite for some value of  $a$  if  $\underline{C}$  is not positive definite ( $\underline{I}$  is the unity matrix). This resulted in very minor changes for the correlation matrices of the light and structural materials, however, more substantial changes were required for the actinides. The latter might affect uncertainty analyses and improvements are being considered.

The error information on ENDF/B-V.2 is incomplete for some nuclei (e.g.  $^{10}\text{B}$ ) and overly optimistic or pessimistic for others. Some improvements have been made. Specifically, the  $\text{Ni}(n,n')$  cross section uncertainties have been increased based on recent investigations,<sup>30</sup> the uncertainties for  $^{10}\text{B}$  cross sections have been adjusted to reflect changes between ENDF/B-VI and V.2.<sup>31</sup> Measurements of  $\bar{\nu}$  are mostly based on measurements relative to  $\bar{\nu}$  of  $^{252}\text{Cf}$ , fission cross sections of most actinides have been measured almost exclusively relative to the fission cross section of  $^{235}\text{U}$ , and the capture cross sections of the fissile nuclei were derived from alpha (capture to fission) measurements. Therefore, cross correlations have been introduced for these three types of cross sections.

Uncertainty estimates have been made for a number of other cross sections for which uncertainty information is not available from ENDF/B-V.2. However, because of the lesser importance of these reactions, they have been assumed to be uncorrelated. An evaluation has been performed based on sensitivities and error propagation in order to obtain a

covariance matrix of the fission spectra parameters. The parameters for the  $^{235}\text{U}$  and  $^{239}\text{Pu}$  fission spectra turn out to be highly correlated because of a very accurate measurement<sup>32</sup> of the ratio of the average energies of the two spectra.

### Sensitivities

Twenty-one energy group sensitivity vectors have been generated for each integral quantity for all important cross sections. The sensitivities for the small LANL cores, with few isotopes involved, were obtained with the TWODANT code by direct variations of the cross sections. However, a two-dimensional transport-sensitivity option for the VARI3D code is being developed. Two-dimensional XY or RZ models and the VARI3D code were used for generating the sensitivities for the more complex cores. For the central control rod worth of ZPPR-15D, a comparison was made between the sensitivities obtained with an RZ and an XY model. Total sensitivities were found to differ for the larger sensitivities (e.g. to  $^{235}\text{U}(n,\gamma)$ ,  $^{235}\text{U}(\bar{\nu})$ ,  $^{238}\text{U}(n,f)$ ,  $^{238}\text{U}(\bar{\nu})$ ,  $\text{Fe}(n,n)$ ), by less than 5%. However, for  $^{238}\text{U}(n,\gamma)$ ,  $^{238}\text{U}(n,n)$  and  $^{10}\text{B}(n,\alpha)$  they differ by 15%, 25% and 10%, respectively.

Simplified models and direct recalculations were used to derive sensitivities to the fission spectra parameters (one to three). Sensitivities of all reactivity worths to the delayed neutron yields enter via  $\beta_{\text{eff}}$  and again involve few parameters. These have been obtained also by direct calculations. Direct variations of cross sections were used to obtain sensitivities for the  $^{252}\text{Cf}$  spectrum averaged cross sections.

In first order, sensitivities are expected to be invariant to specific evaluated cross section sets. The total sensitivities obtained for ENDF/B-V.2 in the present work for ZPR-6/6A and -6/7 are compared in Table IV with sensitivities obtained at ORNL<sup>33</sup> for ENDF/B-IV, and at JAERI<sup>34</sup> for Jendl-2. The values agree reasonably well for most of the sensitivities. Where larger differences are observed, they are due to the total sensitivities being sums of positive and negative terms. For some of these the total absolute sensitivities are indicated in brackets in the table.

### DISCUSSION OF THE DATA BASE

Typical ranges for the calculated vs. experimental value ratios are compared in Table V for various types of integral quantities with the associated uncertainties. The  $k_{\text{eff}}$  values have the highest weight in a data fitting procedure for quantities like enrichment and breeding ratio, and have a high weight for several other types of quantities because of the low uncertainties of the experiments and of the calculational methods. The observed C/E's  $\neq 1$  are mostly explained by nuclear data uncertainties. The C/E's for  $k_{\text{eff}}$  of the larger plutonium-fueled LMR-type critical assemblies (ZPR-6/7, ZPPR-13C, ZPPR-15A, -15B, and ZPPR-17A) are consistent with the C/E of 0.993 for the latest critical assembly ZPPR-18. Large deviations of C/E from one of 1.6 and 1.4% are found for the hard spectra uranium-fueled LANL Big-10 (10% enrichment) and the similar ANL ZPR-9/36 (U9) (9% enrichment). However, these C/E's fall into a systematic pattern vs. average

TABLE IV  
Comparisons of Sensitivities ( $10^{-2}$ )

	Present	JAERI	ORNL	Present	JAERI	ORNL	Present	JAERI	ORNL	Present	JAERI	ORNL	
<u>ZPR-6/6A</u>		$^{235}\text{U}(n,f)$			$^{235}\text{U}(n,\gamma)$			$^{235}\text{U}(n,\gamma)$			$^{235}\text{U}(n,f)$		
$k_{\text{eff}}$	55.3	53.7	53.7	-25.5	-26.2	-26.5	-9.4	-10.5	-10.0	7.9	7.6	7.5	
C28/F25	-105.1	---	-103.3	94.9	---	96.6	-1.5 (2.3)	---	-0.8	0.26 (0.29)	---	0.22	
F28/F25	-66.9	-64.2	-62.7	27.9	28.5	29.4	10.6	11.7	11.4	97.4	97.0	96.4	
		$\text{Fe}(n,\gamma)$			$^{235}\text{U}(n,\gamma)$			$^{239}\text{Pu}(n,\gamma)$			$^{235}\text{U}(n,f)$		
$k_{\text{eff}}$	-1.84	-2.21	-1.87	-0.20	-0.28	-0.27	-2.4	---	-1.7	2.6	---	2.9	
C28/F25	-0.27 (0.41)	---	-0.14	-0.01 (0.03)	---	-0.01	4.46	---	3.49	0.98 (3.1)	---	0.37	
F28/F25	2.06	2.06	2.12	0.22	0.25	0.31	-27.1	---	-28.0	-5.2	---	-5.6	
<u>ZPR-6/7</u>		$^{239}\text{Pu}(n,f)$			$^{235}\text{U}(n,\gamma)$			$^{239}\text{Pu}(n,\gamma)$			$^{235}\text{U}(n,f)$		
$k_{\text{eff}}$	58.9	59.0	59.1	-23.4	-23.7	-23.9	-6.3	-7.3	-6.7	8.21	8.5	7.9	
C28/F49	-108.2	-107.1	-107.3	88.6	89.8	89.6	-2.54 (2.79)	-2.60	-2.02	0.51	0.31	0.52	
F28/F49	-76.8	---	-76.1	26.0	---	27.1	7.3	---	7.9	96.8	---	96.0	
		$\text{Fe}(n,\gamma)$			$\text{Na}(n,\gamma)$			$^{235}\text{U}(n,n')^a$			$\text{Fe}(n,n)^a$		
$k_{\text{eff}}$	-1.7	-2.0	-2.0	-0.19	-0.26	-0.25	-4.5	---	-4.2	1.9	---	1.9	
C28/F49	0.70	0.73	0.65	-0.07	-0.09	-0.09	7.3	---	6.8	2.4	---	2.4	
F28/F49	2.0	---	2.4	0.22	---	0.30	-25.5	---	-24.8	-4.3	---	-4.4	

<sup>a</sup>Data given in Ref. 34 for "scattering" are apparently for the sum of elastic and inelastic scattering and therefore are not quoted here.

TABLE V

## Ranges of C/E's and Sources of Uncertainties

Quantity	Range of C/E-1, %	Measurement Uncertainty, % <sup>a</sup>	Calculation + Model Uncertainty, %	Nuclear Data Uncertainty
$k_{eff}$	-1.2 to +1.6	<0.1 to 0.2	0.1 - 0.5	1.1 - 2.2
$k_{\infty}$	-2.2 to +1.0	0.3 to 0.7	0.1 - 0.5	1.6 - 3.4
Reaction Rate Ratios				
C28/F	-0.7 to +6.7	$\geq 1$ (r), 2 (c)	2	3
F28/F	-5.2 to +10.3	$\geq 1$ (r), 2 (c)	2	3.3 - 10.9
Spatial Reaction Rates				
F49, F25	-1.1 to +3.3 (-5.9 to +4.6) (17A, 13C) (+7.2) (3/56B)	1 to 2 (r)	1 to 2	0.8 - 2.1 3.1 (13C)
F28	-2.7 to +2.9 (-6.3) (17A)	1 to 2 (r)	1 to 2	1.0 - 1.9 (9) (17A)
Control Rod Worth	-10.9 to +3.7 [-11 (15D)]	< 1 (r), ~ 1 (c)	2	2.5 - 5.1
Control Rod Worth Distribution	+1 to +9	1 (r)	2	2.5 - 5.1
Material Worths				
Fissile	-3.1 to +4.2	1 to 5	3	2.5 - 7.9
Fertile	-3.3 to +2.3	1 to 5	3	4.9 - 14
Boron	-10.3 to -5.3	1 to 5	2	3.7 - 7.9
Central Sodium Void	+6 to +48	1 - 3 (r), ~ 1 (c)	5	6 - 15
Neutron Flux Ratios	-2 to +20	1 - 5 (r) 2 - 15 (c)	1 - 4	1 - 5

<sup>a</sup>r = random, c = correlated

energies of the critical assemblies which exists for all uranium fueled cores.<sup>1</sup>

A general bias of several percent between the C's and the E's of C28/F25 or C28/F49 is observed for the present improved calculations and revised experimental values which continues the historical "discrepancy" for capture in  $^{238}\text{U}$  vs. fission in  $^{235}\text{U}$  or  $^{239}\text{Pu}$ . The "discrepancy", however, is in most cases explained by parameter uncertainties. The bias for C28/F is also consistent with (inverse) deviations from one of the C/E's of the  $k_{\text{eff}}$ 's. The observed C/E's appear to be consistently ~1-2% larger for the ZPPR LMR cores than for the infinite media of Zebra. This difference has been noted before<sup>35</sup> but appears to be reversed in the recent IRMA reaction rate intercomparison.<sup>36</sup>

Large differences of the C's and the E's for F28/F25 or F28/F49 (up to 10%) tend to go in opposite directions for plutonium-fueled and uranium-fueled assemblies. For Godiva and Jezebel, these trends are confirmed by leakage spectra measurements. Changes of the inelastic scattering cross sections of  $^{239}\text{Pu}$  for Revision 2 of ENDF/B-V have not resolved the problem.

Several values for F40/F25 and F41/F25 from the Zebra-8 series and ZPR-9/36 are included in the data base. These values were obtained with fission chambers. Comparisons between such fission chamber measurements and the now conventional foil technique for F28/F25 in Zebra-8 showed differences of ~ 10% between the two measurement techniques. The C/E's for F40/F25 in Zebra-8 show discrepancies which are up to a factor 3 larger. These C/E's show no physical correlation with the average energy of the infinite media but appear to decline steadily through the series from 8A to 8F. The C/E's of the F40/F25 are consistent with the C/E's for the worth of  $^{240}\text{Pu}$  in ZPPR-15A and -15B in as far as a lower fission cross section of  $^{240}\text{Pu}$  would resolve or reduce the discrepancies. However, this is contradicted by the C/E of the  $k_{\text{eff}}$  for Jezebel-Pu containing 20%  $^{240}\text{Pu}$ .

Reaction rate distributions are well calculated in tightly coupled cores (C/E close to one) but discrepancies are observed between the C's and the E's for the loosely coupled cores of ZPPR-13C and ZPPR-17A. The C/E's for ZPPR-13C are clearly correlated with similar trends for the control rod worth distributions. Similar trends have been found in ZPPR-17A. The C/E's of the spatial reaction rates are also qualitatively consistent with measurements and calculations of the material worth distributions.

Central-core control rod worth is consistently calculated too low compared with experimental values, which are quite accurate (~ 1% uncertainty). This appears consistent with the small sample worth of  $^{10}\text{B}$  and suggests required increases of the  $^{10}\text{B}(n,\alpha)$  cross section. However, such a conclusion is premature; as it turns out, the C/E discrepancies for the central-core control rod worths and the  $^{10}\text{B}$  small sample worths can be resolved without adjusting the  $^{10}\text{B}(n,\alpha)$  cross sections.<sup>1</sup>

Substantial progress has been made in calculating material worth in recent years. However, now that more sensible C/E's are achieved, it appears desirable that some smaller effects at the few percent level should be resolved. This concerns specifically the cavity effect on the measured values and global transport effects on the calculated values. The C/E's

for the fissile and fertile material worth can be mostly explained by parameter uncertainties. However, discrepancies exist for the  $^{10}\text{B}$  worths and the  $^{240}\text{Pu}$  worths. A bias between the C/E's of Big-10 and ZPR-9/36, in spite of the similarities of the two assemblies, cannot be understood at present.

Finally, the present data for sodium-void which have been analyzed with ENDF/B-V.2 are limited to central zones of ZPPR-15 and the totally voided ZPPR-12 (-12V). Only values for 15A, 15B and 15D of ZPPR-15 have been entered into the data base at present. The C/E's for these range from 6 to 48%. However, the C-E's are rather similar and consistent with a result for the high-Zr zone of ZPPR-15 and with ZPPR-15C which had a 50/50 uranium/plutonium fuel loading. This can be seen in Table VI. Consistently, the sodium void reactivity is calculated too high for all these cases.

#### SUMMARY

An integral data base has been assembled with the objective of improving predictions for LMR-type reactor designs and to evaluate and reduce the uncertainties of such predictions. The selection of data to be entered into the data base was guided by the desirability of a wide range of applications, i.e., going beyond enrichment and breeding ratio. Providing a base for the assessment of our current capability to predict reactor quantities related to operation and safety was considered of paramount importance.

The present data base ranges from the small, homogeneous, hard spectra cores from LANL through the infinite media with specific material insertions to the large LMR-type cores of ANL with many materials involved. Several extensions of the data base appear desirable. The inclusion of experiments from different laboratories would help to guard further against systematic biases. Additional data on control rod worth distributions and sodium void, specifically in uranium fueled assemblies, is desirable because of the scarcity of such data in the present data base.

A survey of available experimental data suggests additional measurements on quantities related to the higher actinides, mainly because of the inconsistencies indicated for the data presently available. From the point of view of the data adjustment methodology, the Zebra-8 series experiments are potentially the most valuable as they permit the separation of effects of various materials and permit simple calculation models. Unfortunately, these experiments were performed some 20 years ago and reflect experimental techniques of that time. Cell heterogeneity of these experiments has an unduly large effect on their interpretation and corrections required for the effect of the driver could be reduced in more modern experiments. Further experiments of this type would be very desirable with corresponding variations in energy ranges and compositions.

#### ACKNOWLEDGEMENTS

This work was supported by the U.S. Department of Energy, Nuclear Energy Programs, under Contract W-31-109-Eng-38.



TABLE VI

Central Sodium Void Measurements in ZPPR-15

Core	Fuel	Measured Reactivity $\phi/\text{kg}(\text{Na})$	Uncertainty $1\sigma$	C-E $\phi/\text{kg}(\text{Na})$
15A	Pu/U	1.95	0.02	0.22
15B	Pu/U/Zr	2.08	0.02	0.15
High-Zr	Pu/U/Zr	1.74	0.03	0.29
15C	50% Pu/U/Zr 50% U/Zr	0.77	0.01	0.13
15D	10% Pu/U/Zr 90% U/Zr	0.23	0.01	0.12

## REFERENCES

1. W. P. Poenitz and P. J. Collins, "Utilization of Experimental Integral Data for the Adjustment and Uncertainty Evaluation of Reactor Design Quantities (Application to the FFTF Core Conversion Design), this meeting (1988).
2. C. A. Atkinson, "Data Testing of ENDF/B-V.2 Nuclear Data for Fast Reactor Calculation," Thesis presented to Idaho State University, Pocatello, Idaho, 1987, in partial fulfillment of the requirements for the degree of Master of Science in Nuclear Science and Engineering.
3. C. A. Atkinson and P. J. Collins, "The Performance of ENDF/B-V.2 Nuclear Data for Fast Reactor Calculations," Proc. Conf. Topical Meeting on Advances in Reactor Physics, Mathematics and Computations, p 963, Paris (1987).
4. Evaluated Nuclear Data File, ENDF/B-V, Version 2. For more information contact S. Pearlstein, National Nuclear Data Center, Brookhaven National Laboratory.
5. H. Henryson II., B. J. Toppel and C. G. Stenberg, "MC<sup>2</sup>-II, A Code to Calculate Fast Neutron Spectra and Multigroup Cross Sections," Argonne National Laboratory Report, ANL-8144 (ENDF 239), (1976).
6. W. M. Stacey et al., "A New Space-Dependent Fast-Neutron Multigroup Cross Section Preparation Capability," Trans. Am. Nucl. Soc., 15, p 292 (1972). See also:  
  
D. C. Wade, "Monte Carlo based Validation of ENDF/MC<sup>2</sup>-II/SDX Cell Homogenization Path," Argonne National Laboratory Report ANL-79-5 (1979).
7. Lawrence, R. D., "Three-Dimensional Nodal Diffusion and Transport Methods for the Analysis of Fast Reactor Critical Experiments," Proc. Topical Meeting on Reactor Physics and Shielding, Chicago, IL (1984).
8. R. E. Alcouffe et al., "User's Guide for TWODANT: A Code Package for Two-dimensional, Diffusion Accelerated, Neutral-particle Transport," Los Alamos National Laboratory Report LA-100490M (1984).
9. D. W. Muir, "Analysis of Central Worth and Other Integral Data from the Los Alamos Benchmark Assemblies," Los Alamos National Laboratory Report, LA-10230-MS (ENDF-340) (1984).
10. R. N. Blomquist, R. M. Lell, and E. M. Gelbard, "VIM - A Continuous Energy Monte Carlo Code at ANL," A Review of the Theory and Application of Monte Carlo Methods - Proceedings of a Seminar Workshop, Oak Ridge, TN, April 21-23 (1980).
11. R. J. Howerton, "Data Testing Results for the ENDF/B-V Evaluated Neutron Data File," Lawrence Livermore Laboratory Report UCID-18731 (1980).

12. R. D. McKnight and P. J. Collins, "Whole-Assembly Calculations with Monte Carlo," Report NEACRP-A-664 (1984).
  13. C. H. Adams, Argonne National Laboratory private communication.
  14. K. S. Smith, "The Effect of Intracell Adjoint Flux Heterogeneity on First-Order Perturbation Reactivity Calculations," Nucl. Sci. Eng., 81, p 451 (1982).
  15. P. J. Collins and R. G. Palmer, "Calculated Sample-Size Effects for Reactivity Perturbation Samples in ZPPR," Argonne National Laboratory Report ANL-7910, p 247 (1971).
  16. R. W. Schaefer and R. G. Bucher, unpublished information (1982).
  17. R. W. Schaefer, unpublished information (1986).
  18. W. Mannhart, "Evaluation of the  $^{252}\text{Cf}$  fission neutron spectrum between 0 MeV and 20 MeV," Leningrad, Proc. Conf. on Properties of Neutron Sources, International Atomic Energy Agency Report IAEA-TECDOC-410 (1987).
  19. W. P. Poenitz, "The Simultaneous Evaluation of Interrelated Cross-Sections by Generalized Least-Squares and Related Data File Requirements," Proc. Advisory Group Meeting on Nuclear Standard Reference Data, Geel, 1984, International Atomic Energy Agency Technical Document IAEA-TECDOC-335 (1984).
  20. W. P. Poenitz, unpublished information (1987).
  21. W. N. McElroy, "Interlaboratory Reaction Rate Program Progress Report," Hanford Engineering Development Laboratory Reports HEDL-TME 75-130, -77-34, -79-58 (1975 through 1979).
  22. Cross Section Evaluation Working Group Benchmark Specifications, Brookhaven National Laboratory Report BNL 19302 (ENDF-202), and Revisions (1974).
  23. G. E. Hansen and H. C. Paxton, "A Critical Assenbly of Uranium Enriched to 10% un Uranium-235," Nucl. Sci. Eng., 72, p 230 (1979).
- See also:
- C. G. Cherem and E. J. Lozito, "Investigation of the Criticality of Low-Enrichment Uranium Cylinders," Nucl. Sci. Eng., 33, p 139 (1968).
  24. G. E. Hanson and H. C. Paxton, "Reevaluated Critical Specifications of Some Los Alamos Fast-Neutron Systems," Los Alamos Scientific Laboratory Report LS-4208 (1969).
  25. D. Hanlon, B. M. Franklin, and J. M. Stevenson, "Calculations for the Intermediate-Spectrum Cells of Zebra-8 Using the MONK Monte Carlo Code," United Kingdom Atomic Energy Authority Report AEEW-R 2245 (1987).

26. J. P. Chandat et al., "Experiments in Pure Uranium Lattices with Unit  $k_{\infty}$ ," Karlsruhe Nuclear Research Center Report KFK 1865 (CEA-R-4552) (1974).
27. W. P. Poenitz et al., "A Data Base for the Adjustment of Calculated Reactor Quantities Based upon Experimental Integral Data," Argonne National Laboratory, to be published (1988).
28. D. W. Muir and R. E. MacFarlane, "The NJOY Nuclear Data Processing System, Vol. IV: The ERRORR and COVR Modules," Los Alamos National Laboratory Report LA-9303-M (ENDF-324) (1985).
29. J. R. Liaw and R. R. Schmidt, unpublished information (1987).
30. C Budtz-Jørgensen et al., "Fast-Neutron Total and Scattering Cross Sections of  $^{59}\text{Ni}$ ," Argonne National Laboratory Report ANL/NDM-61 (1981).
31. A. D. Carlson et al., "The Neutron Cross Section Standards Evaluations for ENDF/B-VI," Proc. Conf. on Nuclear Data for Basic and Applied Science, Santa Fe, Vol. 2, p 1429 (1985).
32. M. Sugimoto et al., "Ratio of the Prompt-Fission-Neutron Spectrum of Plutonium-239 to that of Uranium-235," Argonne National Laboratory Report ANL/NDM-96 (1986).
33. J. H. Marable et al., "Compilation of Sensitivity Profiles for Several CSEWG Fast Reactor Benchmarks," Oak Ridge National Laboratory Report ORNL-5262 (ENDF-234) (1977).
34. T. Aoyama et al., "Sensitivity Coefficients of Reactor Parameters in Fast Critical Assemblies and Uncertainty Analysis," Japanese Nuclear Data Committee Report, JAERI-M 86-004 (1986).
35. D. W. Maddison and G. Ingram, "ANL/AEEW Comparison of Reaction Rate Ratio Techniques in ZEBRA," 26th NEACRP-A-542 (1983).
36. W. Scholtyssek, "IRMA: Interlaboratory Comparison of Fission and Capture Rate Measurement Techniques at MASURCA," Proc. International Reactor Physics Conference, Jackson, WY (1988).



Utilization of Experimental Integral Data for the Adjustment  
and Uncertainty Evaluation of Reactor Design Quantities

(Application to the FFTF Core Conversion Design)

W. P. Poenitz and P. J. Collins  
Argonne National Laboratory - West  
Idaho Falls, ID 83403-2528, U.S.A.

ABSTRACT

Biases and uncertainties of calculated reactor design quantities caused by errors and uncertainties of basic parameters, such as neutron cross sections, fission spectra parameters, and prompt and delayed neutron yields, are large, and in most cases, exceed reactor design requirements. Errors and uncertainties due to models and methods approximations contribute as well. An extensive data base, with presently ~300 experimental integral values from 28 critical assemblies, has been assembled at Argonne National Laboratory in order to provide improvements and to investigate both sources of uncertainties. Generalized-least-squares fitting is being used. The available large data base permitted the investigation of the influence of specific input data, the constraints of the covariance information, the selection of parameters, and the reliability of the predictions. It is shown that reliable improvements of calculated quantities like enrichment, breeding ratio, sodium void, control rod worth, power distribution, and material worth can be made. Substantial reductions of the uncertainties of these quantities, which are caused by the uncertainties of the basic parameters, are obtained in most cases. The FFTF uranium-metal-core conversion is the first application of the present effort.

INTRODUCTION

The calculations of quantities of importance for the operation and safety of a reactor design are biased due to the errors of the parameters (e.g. group cross sections, fission spectra parameters, prompt and delayed neutron yields, etc.), used in their calculations, and due to the models and methods approximations. The uncertainties of the calculated quantities are substantial<sup>1</sup> and in most cases exceed reactor design requirements.<sup>2</sup> Biases for reactor design quantities in general are unknown, but ratios of calculated vs. experimental values (C/E) for critical assembly data indicate that they often exceed uncertainties.

The traditional approach in the US has been to build an engineering mockup critical assembly (EMC) of the reactor design in order to reduce biases and uncertainties. Calculations of quantities measured in the EMC then provided calibration factors for corresponding quantities calculated for the reactor design. This "bias method," unfortunately, replaced the biases of the calculated reactor design quantities, which are due to the errors of the basic parameters and, to some extent, due to the model and

methods approximations, with the biases of the experimental values. It also completely ignores the information content of the calculated values which is due to the a priori parameters. Further disadvantages of the bias method are that it can be applied directly only to those quantities which could be measured for the EMC, and that the estimation of the uncertainties for the biased quantities is often subjective.

The accumulation of a substantial data base from experiments in critical assemblies suggests another approach for reducing biases and uncertainties of calculated reactor design quantities. This approach is known as "data adjustment" and has been discussed by a large number of investigators (see for example Refs. 3-14). The present paper describes the use of the data adjustment methodology for the utilization of experimental integral data from critical assemblies for the reduction of biases and uncertainties of calculated reactor design quantities beyond what can be achieved with the bias method. A large data base has been assembled for this purpose at Argonne National Laboratory.<sup>15</sup> The first application is for improving predictions and reducing uncertainties of the FFTF uranium-metal-core conversion design (FFTF-CC). An EMC is not available for this design and the question of whether the information contained in the prior parameters and in the past experimental integral data is sufficient for adequate predictions is examined.

Most of the present investigations are based on considerations of the ratios of the originally calculated values vs. the experimental values (C/E), the adjusted vs. the experimental values (A/E), and the predicted vs. the experimental values (P/E) (i.e., the prediction has been obtained by eliminating the specific data from the fit.) Variations of these values must be seen in terms of the associated uncertainties, i.e., the uncertainties of the experimental data and the models and methods approximations ( $\sigma(E,M)$ ), the uncertainties of the calculated values due to the parameter uncertainties before ( $\sigma(C)$ ) and after ( $\sigma(A)$ ) adjustments have been made, and the uncertainties of the predicted values ( $\sigma(P)$ ).

#### ADJUSTMENT METHODOLOGY, UNCERTAINTY ANALYSIS AND DATA BASE

Parameter adjustment based on least-squares is due to Gauss<sup>16</sup> and modifications of the least-squares method in order to account for correlations as derived by Aitken<sup>17</sup> have been taken into account in recent work (e.g. Ref. 12). The present brief account is based on the summary given in Ref. 18. Other approaches, e.g. based on Bayes' theorem, lead to the same formulation as the generalized least-squares method (GLS) which is used here. Uncertainty analysis is considered in detail, e.g., in Ref. 19.

We consider the vector of  $m$  calculated quantities,  $\vec{Q} = (Q_1, Q_2, \dots, Q_m)$ , which contains components from critical assemblies, as well as reactor designs. The calculations are based upon  $n$  prior evaluated parameters,  $\vec{p} = (p_1, p_2, \dots, p_n)$ , with covariance  $\underline{C}_p$ . The covariance of the calculated quantities due to the parameter covariance then follows from error propagation, i.e.,

$$\underline{C}_Q = \underline{S} \underline{C}_p \underline{S}^T \quad (1)$$

where  $\underline{S}$  is the  $m \times n$  sensitivity matrix with components

$$S_{ij} = \frac{p_j}{Q_i} \frac{\partial Q_i}{\partial p_j} \quad (2)$$

which are the percent changes of the  $Q_i$ 's per percent changes of the parameters  $p_j$ .

It is assumed that the prior evaluation of the  $n$  parameters was based upon  $l$  (differential) experimental data ( $l > n$ ) and that  $k$  additional (integral) experimental data are available which are uncorrelated with the  $l$  values. Utilization of the additional  $k$  experimental data leads to adjustments on the prior evaluated parameters with the adjustment vector given by

$$\vec{\delta} = \underline{C}_p^{-1} \underline{S}^T \underline{W}^{-1} \vec{E} \quad (3)$$

$$\underline{W} = \underline{S} \underline{C}_p^{-1} \underline{S}^T + \underline{C}_E = \underline{C}_Q + \underline{C}_E \quad (4)$$

where  $\vec{E}$  is the reduced measurement vector with covariance  $\underline{C}_E$ . It is with the weight matrix,  $\underline{W}^{-1}$ , that the relative importance of the prior information, contained in the preevaluated parameters, and the additional information, contained in the  $k$  experimental values, is properly taken into account. The covariance matrix of the adjusted parameters is given by

$$\underline{C}_p' = \underline{C}_p - \underline{C}_p \underline{S}^T \underline{W}^{-1} \underline{S} \underline{C}_p \quad (5)$$

and is inserted in Eq. (1) in order to evaluate the uncertainties and correlations of the calculated quantities based upon the adjusted parameters. The latter can be obtained by recalculating  $\vec{Q}$  with the adjusted parameters, or, alternatively, by directly adjusting the calculated quantities with

$$\vec{Q}' = \vec{Q} (\vec{I} + \underline{S} \vec{\delta}), \quad (6)$$

where  $\vec{I}$  is the unit vector.

For the present considerations, the prior evaluated parameters are the cross sections and other parameters obtained from the evaluated nuclear data file, ENDF/B-V.2, which are reduced to group cross sections with a 21 energy-group structure. The additional experimental data are the data obtained from critical assembly experiments. The corresponding quantities are functions of the parameters which require linearization which are obtained from the Taylor series expansion, broken off with its first-order term:

$$Q_i = Q_{i0} + \sum_j \frac{\partial Q_i}{\partial p_j} (p_j - p_{j0}). \quad (7)$$

The neglect of the higher order terms in the Taylor series expansion leads to errors of the adjusted parameters which propagate to errors of the reactor quantities. However, if the adjustments are made on the calculated



quantities based on the same linear Taylor Series expansion, instead of recalculating the quantities with adjusted parameters, one would expect a partial compensation of the errors made. This can be shown to be the case for the simple example of a ratio of two parameters for  $C/E > 1$ . For the more complex case of calculated reactor quantities the effect has been considered by comparing the quantities of ZPPR-15B obtained from adjustments with Eq. 6 with those obtained by recalculation with the adjusted parameters. The comparison is given in Table I.

Some of the parameters are group cross sections and adjustments on infinite dilute cross sections are implied. However, the adjustments ought to be made on the underlying parameters, e.g. resolved resonance parameters, unresolved resonance parameters, pointwise cross sections, etc., labeled  $g$ . The linear term of the Taylor series expansion should therefore read

$$\sum_1 \frac{g_1}{Q_i} \frac{\partial Q_i}{\partial g_1} \frac{g_1 - g_{01}}{g_{01}} \quad (8)$$

Using the chain rule one obtains

$$\sum_1 \delta_1 \sum_j \frac{p_j}{Q_i} \frac{\partial Q_i}{\partial p_j} \frac{g_1}{p_j} \frac{\partial p_j}{\partial g_1} = \sum_1 \delta_1 \sum_j S_{ij} D_{j1} \quad (9)$$

where the  $\delta_1$  are the adjustments on the underlying parameters and the transformation matrix  $D$  contains the sensitivities of the group cross sections to the underlying parameters. This has been discussed in the context of higher order effects in sensitivity analysis by Greenspan et al.<sup>20</sup> As long as adjustments to the calculated quantities are small compared to one, uncertainties due to these effects should be small. Therefore, at present, they have been neglected, though efforts are underway to derive the transformation matrix  $D$ .<sup>21</sup>

The Taylor series expansion should involve all parameters, including those relating to the reactor model and methods approximation. The latter would be expressed as corrections<sup>1\*</sup> (for example for cell heterogeneity). However, most features involved in the models and most methods approximations are difficult to quantify and corresponding parameters are ignored. It is generally assumed that the model and methods approximations are fit into parameter adjustments. The uncertainties of the neglected parameters has been accounted for by replacing the covariance matrix of the experimental data  $C_E$ , with  $C_E + C_M$ . It is interesting to note that the generalized  $\chi^2$  of the fit<sup>8</sup>

$$(\vec{Q}' - \vec{E}) \underline{W}^{-1} (\vec{Q}' - \vec{E})^T \quad (10)$$

increases by about a factor of 10 if the model and methods uncertainties are not included in the covariance matrix for the reduced measurement vector  $(\vec{E} - \vec{Q})$ . This indicates that the model and methods approximations cannot be fit into parameter adjustments if such parameters are not provided for. Including the model and methods uncertainties, or not, with

TABLE I

Comparison between the Adjusted and the  
Recalculated Quantities for ZPPR-15B

Quantity	$Q_{AJD}/E-1, \%$	$Q_{REC}/E-1, \%$	$\sigma(A), \%$	Difference
$k_{eff}$	0.06	0.15	0.14	$2/3 \sigma$
Reaction Rate Ratios				
C28/F49	-0.82	-0.81	0.54	} negl.
F25/F49	-0.68	-0.66	0.46	
F28/f49	-2.42	-2.37	0.87	
IC/OC Ratios <sup>a</sup>				
F49	1.92	1.82	0.31	} $1/3 \sigma$
F25	2.40	2.31	0.31	
F28	0.87	0.78	0.32	
F28	0.86	0.72	0.49	
Material Worth				
$^{10}B$	-0.34	-0.41	1.24	negl.
$^{235}U$	0.91	1.20	0.92	$1/3 \sigma$
$^{239}Pu$	2.63	2.37	0.77	$1/3 \sigma$
$^{238}U$	-1.18	-1.40	0.97	$1/4 \sigma$
Sodium Void	-4.65	-4.53	1.80	negl.
Control Rod Worth	-0.98	-1.10	0.95	negl.

<sup>a</sup>Inner core to outer core.

the uncertainties of the experimental data has only minor effects on the adjusted quantities.

#### SELECTION OF PARAMETER SPACE AND DATA BASE

All important parameters which are involved in the calculations of any of the critical assemblies and reactor design quantities ought to be included in the adjustment procedure and the uncertainty evaluation in order to properly represent the physical reality. Fission, capture, elastic and inelastic scattering, and  $(n,\alpha)$  cross sections, prompt and delayed neutron yields, and fission spectra parameters were considered as parameters for  $^{235}\text{U}$ ,  $^{238}\text{U}$ ,  $^{239}\text{Pu}$ ,  $^{240}\text{Pu}$ ,  $^{241}\text{Pu}$ ,  $^{242}\text{Pu}$ , Fe, Cr, Ni, Na,  $^{10}\text{B}$ ,  $^{11}\text{B}$ , C, O, Mo, Zr, Mn, Ga, lumped fission products, and  $^{236}\text{U}$ . The subthreshold fission for the fissionable nuclei was ignored. Inelastic scattering is presently represented by total inelastic scattering cross sections, however, efforts are underway to replace these, at least for  $^{238}\text{U}$ , by cross sections for groups of discrete levels and the continuum. Delayed neutron parameters were included as one-energy-group parameters and fission spectra were represented by one (Maxwellian), two (Watt), or three (Madland-Nix) parameters. Angular distribution parameters were ignored. The above adds up to a possible parameter space of ~1000. However, the  $C(n,n)$  cross section is very well known and adjustments proved to be negligible, thus it was eliminated from the process. Also negligible adjustments were observed for the  $^{11}\text{B}$ ,  $^{10}\text{B}(n,n)$ , and Ga cross sections, mainly because of low sensitivities. Not enough items in the data base relate to the  $^{241}\text{Pu}$ ,  $^{242}\text{Pu}$  cross sections and these were, with the exception of  $^{241}\text{Pu}(n,f)$ , also eliminated as parameters. This left a parameter vector of ~700.

During a large number of tests it was observed that the adjustments on some cross sections were rather stable but adjustments on some other cross sections varied and depended on specific input data. Adjustments on some parameters were, at least qualitatively, similar to those from recent evaluations for ENDF/B-VI ( $^{235}\text{U}(n,f)$ ,  $^{238}\text{U}(n,\gamma)$ ,  $^{240}\text{Pu}(n,n)$ ) and recent measurements of  $^{235}\text{U}(n,\gamma)$ . However, other cross section adjustments, though restrained by their a priori uncertainties, appeared contradicted by more recent measurements ( $^{238}\text{U}(n,n)$ ,  $\text{Zr}(n,\gamma)$ ). A case in which adjustments were made on 754 parameters was compared with a case in which adjustments were made on 522 parameters in order to investigate the effect of such contradictory and questionable parameter adjustments on the adjustments of the derived quantities. The change of the bias after adjustments have been made and the average change of the adjustments are shown in Table II for the 522 parameters vs. 754 parameters cases. These changes are smaller, and in most cases small compared to the uncertainties of the adjusted values, thus parameter-adjustment variations have a much lesser (and negligible) effect on the adjusted integral quantities.

Probably the most uncertain data involved in the adjustment process are the a priori correlations of the parameters. In order to see how these correlations affect the adjustments of the integral quantities, a reference case in which the correlations as contained in the data base were taken into account was compared with a case in which the parameters were assumed to be a priori uncorrelated. As shown in Table II, the differences of the adjustments between these cases, as well as the differences of the biases after adjustments have been made, are again small compared with the

TABLE II

Effects Related to the Parameters and Data Base Selection

Type of Quantity	Reference Uncertainties after Adjustments	522 vs. 754 Parameters		Uncorrelated vs. Correlated Parameters		Bad Data Exclusion		Uncorrelated vs. Correlated Data	
		Average Changes, % Biases	Adjustments	Average Changes, % Biases	Adjustments	Average Changes, % Biases	Adjustments	Average Changes, % Biases	Adjustments
$k_{eff}$									
Uranium fueled	0.17	+0.01	-0.01	-0.01	-0.04	+0.08	+0.01	0.00	+0.03
Plutonium fueled	0.19	-0.03	-0.02	-0.02	-0.05	-0.03	+0.02	+0.05	+0.01
Reaction Rate Ratios									
C28/F	0.6	+0.1	-0.06	0.0	-0.04	+0.1	+0.00	+0.1	+0.07
F28/f	0.9	-0.1	-0.04	0.0	-0.04	-0.1	+0.01	+0.1	+0.01
Spatial Ratios									
F25, F49	0.4	+0.1	-0.10	+0.1	-0.16	0.0	0.00	+0.1	+0.03
C28	0.3	0.0	+0.02	+0.2	+0.03	+0.3	-0.09	0.0	+0.01
F28	0.5	-0.1	-0.09	-0.1	-0.11	+0.2	+0.03	-0.4	+0.02
Material Worth									
$^{235}\text{U}$ , $^{239}\text{Pu}$	1.0	+0.2	+0.17	-0.2	-0.01	-0.8	0.00	+0.2	+0.11
$^{10}\text{B}$	1.4	+0.3	+0.05	-0.6	+0.15	-0.7	+0.24	-0.7	+0.10
$^{238}\text{U}$	1.1	+0.2	+0.14	+0.4	+0.18	+0.3	-0.06	+0.1	+0.04
Control Rod Worth	0.9	-0.1	-0.06	-0.5	-0.28	+0.1	-0.05	-0.2	+0.03
Sodium Void	1.9	0.0	0.00	+0.2	-0.03	-0.5	-0.16	+0.4	-0.17

uncertainties of the adjusted quantities. The changes of the adjustments on the parameters, however, are again larger and very substantial for some cross sections, e.g. for the inelastic scattering. A very accurate measurement of the ratio of the average energies of the fission spectra of  $^{235}\text{U}$  and  $^{239}\text{Pu}$  causes the parameters of these spectra to be highly correlated. Consequently, errors of the calculated spectral differences between uranium and plutonium fueled critical assemblies are mainly removed by adjustments on the inelastic cross sections of  $^{235}\text{U}$  and  $^{239}\text{Pu}$ . Removal of the correlations eliminate the constraint for adjustments on the fission spectra parameters in opposite direction and much reduced adjustments on the inelastic cross sections are required. Though the changes of the parameter adjustments are substantial for some parameters if they are assumed to be uncorrelated, the change of the adjustment on  $k_{\text{eff}}$  of FFTF-CC is only 0.1%.

About 300 experimental values for ~260 integral quantities are in the data base. The availability of such a large data base facilitated the search for "bad" data which were indicated by a high  $\chi^2$  of 7.5 when all data were included in the adjustment fit. Data for which the A/E's were outside one or two  $\sigma(E,M)$ 's and for which the fit resulted in A/E's substantially worse than the original C/E's were reconsidered. For some of these data, specific problems could be identified and they were excluded from the adjustments, except for some tests. Some other data showed inconsistencies and persistently large A/E's in terms of the  $\sigma(E,M)$ 's. Sufficient justification could not be found for the exclusion of the latter because of the statistical nature of the data. The effect of excluding a total of 28 values from the fit has been considered by comparing with a fit of all data. The selection of some of the 28 values has been, by necessity, subjective, and some of the problems are discussed below. Table II shows that the changes for the biases and the adjustments on the remaining data are unimportant and represent only a slight improvement. The major benefit of eliminating some of the questionable data is in a reduction of  $\chi^2$  to closer to one.

Correlations between experimental data are due to common uncertainty components in various measurements. Because the data are from several laboratories and various types of measurements are uncorrelated, there are few correlations remaining. The extreme case of neglecting the correlations between the experimental data has been compared with the case in which the correlations were taken into account, in order to consider the effect of possible errors of the correlations. The observed effects (see Table II) are suitably small, thus errors of the correlations between the data are of no concern. The latter requires some reservations: the experimental control rod worths have low uncertainties and are highly correlated for any one critical assembly. The uncertainties for the model and methods approximations have been assumed to be uncorrelated. However, within one assembly they might be highly correlated as well. Proper inclusion of such correlations might have resulted in some changes (at present only for ZPPR-13C and ZPPR-15D).

PREDICTABILITY OF VARIOUS TYPES OF QUANTITIES  
AND QUANTITIES OF SPECIFIC REACTORS

The predictability of a given type of quantity in various assemblies, or of various quantities of different kinds in a given assembly, as well as the overall consistency of the data base, has been tested by excluding corresponding subsets of experimental data from the adjustment fits. The predicted values could then be compared with the adjusted values and the differences in terms of the associated uncertainties indicate if a certain type of quantity is consistent with the rest of the data base. Corresponding comparisons can show if data from one specific assembly have unduly high weight for the adjustment of a reactor design quantity. Comparison between the predicted values and the experimental data show the usefulness of the data base for obtaining adjustments for a reactor design. The following tables usually contain data for the originally calculated values, C/E (i.e., without fitting to the experimental integral data), the adjusted values, A/E (i.e., with utilization of the experimental integral data base, including the experimental values for the quantities listed in the tables), and the predicted values, P/E, for which the experimental data for all quantities listed in the specific table were removed from the adjustment fit.

Adjustments and Predictions of Various Types of Data

Table III shows the adjusted and the predicted values of  $k_{eff}$  for the plutonium and the uranium fueled critical assemblies ordered by the average energy of their flux spectra. The uncertainties of the adjusted  $k_{eff}$  values are typically reduced by a factor of 10 compared to the uncertainties of the originally calculated values. The original average biases of the calculated values of -0.5% for the plutonium fueled assemblies and of +0.3% for the uranium fueled assemblies are reduced by the fit to negligible values. Six of the adjusted values differ from the experimental values by more than the combined uncertainties of the adjusted values  $\sigma(A)$ , the experimental values and the uncertainties of the model and methods approximations,  $\sigma(E,M)$ . This is close enough to expectation not to be a concern. Various tests involving the exclusion of these data did result in some improvements which were not statistically significant enough to justify the removal of any of the  $k_{eff}$  values.

The  $k_{eff}$  data are the most accurate values in the data base, thus they are expected to strongly influence their own adjustments and the uncertainties of the adjusted  $k_{eff}$  values. The  $\sigma(P)$  given in Table III show that the reduction of the uncertainties of the  $k_{eff}$  values by utilizing all other experimental integral data from the critical assemblies but excluding the  $k_{eff}$  values is only about a factor of two compared with a factor of 10 if the  $k_{eff}$  data are included in the adjustment fit. The differences between the adjusted and the predicted values are less than the combined uncertainties  $\sigma(A)$  and  $\sigma(P)$  in all but six cases for which they are marginally larger. This indicates that the rest of the data base is overall consistent with the  $k_{eff}$  values of the critical assemblies.

The biases of the predicted values of  $k_{eff}$  are rather similar for the plutonium fueled and the uranium fueled critical assemblies, thus the bias

TABLE III

Adjustments and Predictions of  $k_{eff}$  and  $k_{\infty}$ 

Assembly	C/E-1, %	$\sigma(C)$ , %	$\sigma(E,M)$ , %	A/E-1, %	$\sigma(A)$ , %	P/E-1, %	$\sigma(P)$ , %
<u>Pu-fueled</u>							
Jezebel	-0.2	1.8	0.2	-0.1	0.18	0.0	1.1
Jezebel-Pu	-0.8	1.6	0.3	-0.7	0.20	-1.1	0.9
Flattop-Pu	0.7	1.6	0.2	0.4	0.14	1.3	0.8
ZPPR-12V	0.1	1.4	0.3	-0.1	0.14	0.3	0.6
ZPPR-12	-0.1	1.4	0.3	-0.2	0.12	0.1	0.6
ZPPR-15A	-0.5	1.6	0.3	0.2	0.14	0.4	0.6
ZPPR-15B	-0.5	1.7	0.3	0.1	0.14	0.3	0.6
Zebra-8B	1.0	3.2	0.4	0.7	0.25	1.5	0.6
ZPR-3/56B	-1.0	1.5	0.3	-0.5	0.16	-0.2	0.6
Zebra-8E	-1.6	2.7	0.4	-0.7	0.21	-0.4	0.6
ZPPR-13C	-0.7	1.6	0.3	0.0	0.12	0.3	0.6
Zebra-8D	0.1	2.6	0.5	0.7	0.20	1.4	0.6
ZPPR-17A	-0.7	1.6	0.3	0.0	0.12	0.4	0.6
Zebra-8C	-2.2	1.9	0.5	-0.4	0.27	0.1	0.8
ZPR-6/7	-0.8	1.6	0.3	-0.1	0.13	0.4	0.6
Zebra-8A	-1.4	2.0	0.7	-0.8	0.33	0.5	0.7
Zebra-8F	-0.3	1.9	0.5	0.5	0.33	1.8	0.7
Average	-0.5			-0.06		0.42	
<u>U-fueled</u>							
Godiva	-0.3	1.6	0.1	0.0	0.13	0.0	0.8
Flattop-25	0.4	1.2	0.1	-0.1	0.12	0.4	0.7
Big-10	1.6	2.0	0.3	0.1	0.17	0.9	0.7
ZPR-9/36	1.4	2.2	0.3	0.3	0.14	0.9	0.6
Scherzo	0.9	3.4	0.4	0.1	0.26	0.1	0.7
Zebra-8H	0.3	3.1	0.4	-0.4	0.20	0.0	0.6
ZPPR-15D	-0.7	1.1	0.3	-0.1	0.18	-0.1	0.6
ZPR-6/6A	-1.2	1.2	0.3	-0.1	0.19	0.0	0.6
Average	0.3			-0.03		0.28	

difference seen for the calculated values between these is removed. The highest correlations of the  $k_{\text{eff}}$  values are with C28/F25 or C28/F49 and the worth of the fertile and fissile materials. The positive bias of the predicted  $k_{\text{eff}}$  values of  $-0.3 - 0.4\%$  seems to be the result of larger downward adjustments on the  $^{238}\text{U}(n,\gamma)$  cross sections (by  $\sim 1\%$ ) due to the C28/F data. The effect of not using the  $k_{\text{eff}}$  data in the adjustment on other types of data is mostly within uncertainties. For example, the adjusted values for control rod worth change only by an average of  $\sim 0.1\%$ . The adjustment on  $k_{\text{eff}}$  of the reactor design (FFTF-CC) changes by  $0.2\%$  if the  $k_{\text{eff}}$  values of the critical assemblies are not included in the fit which is consistent with the prediction uncertainties of  $-0.3\%$  and  $\pm 0.7\%$  for  $k_{\text{eff}}$  data used or not used, respectively.

Adjustments and predictions for C28/F25 or C28/F49 are closely linked with  $k_{\text{eff}}$ , because of large anticorrelations between these quantities. The predicted values differ by only small amounts from the adjusted values compared with the combined uncertainties of  $\sigma(P)$  and  $\sigma(A)$  due to the consistency between the C/E's of the C28/F and  $k_{\text{eff}}$ . For the same reason the C/E "discrepancies", persisting for the last 20 years for capture vs. fission, are reduced to an unimportant amount of  $\sim 0.4\%$  not only for the adjusted but also for the predicted values. The uncertainties of the adjusted values are typically reduced by a factor of  $\sim 5$  compared with the uncertainties of the calculated values. The uncertainties of the C28/F are only slightly higher for the predicted than for the adjusted values.

Only three of the 23 adjusted values for material worth were found outside the combined uncertainties of  $\sigma(E,M)$  and  $\sigma(A)$ , and the differences between the predicted and the adjusted values exceed the combined  $\sigma(P)$  and  $\sigma(A)$  for only two. The latter are the  $^{240}\text{Pu}$  worths in ZPPR-15A and -15B. The large C/E difference of  $\sim 15\%$  between these two values is presently not understood. This difference is only slightly reduced in the fit and persists if the Jezebel-Pu data are removed, thus it is unlikely that it is caused by cross section errors. An inconsistency appears also to exist between the  $^{10}\text{B}$  worths in Big-10 and ZPR-9/36. Excluding these three values, the bias of the adjusted values of the material worth is small ( $\sim 0.7\%$ ) but increases by  $\pm 1\%$  for the predicted values. Uncertainties are reduced by factors of 3-9 for the fissile material which is in the core and by factors of 5-11 for the fertile material.

Spatial reaction rate ratios have low correlations with  $k_{\text{eff}}$  in some cores (e.g. ZPPR-12), and high correlations with  $k_{\text{eff}}$  in other cores (e.g. ZPR-9/36). However, for most assemblies the correlations with  $k_{\text{eff}}$  are only of medium size (e.g. ZPPR-15, ZPPR-13C, ZPPR-17A) but the correlations with control rod worth are substantially higher in most cases. Because of a high degree of error compensation, C/E's of spatial reaction rate ratios are usually near unity in tightly coupled cores and the uncertainties of the calculated values are low ( $\sim 1 - 2\%$ ). However, this is not the case for loosely coupled cores and an  $\sim 9\%$  C/E discrepancy exists between a radial and an azimuthal reaction rate ratio in ZPPR-13C, and several C/E's in ZPPR-17A differ from one by more than two standard deviations. There are also exceptions: the center to radial reflector reaction rate ratios in ZPR-3/56B C/E's differ from one by more than  $15\%$ . These discrepancies are not only removed in the adjustment fit but also substantially reduced in the predictions, thus they are due to parameter errors, which is consistent



with the remainder of the data base. For ZPPR-13C and ZPPR-17A the C/E-1, A/E-1, P/E-1, and  $\sigma(E,M)$  are shown in Figs. 1a and 1b. The uncertainties of the predicted spatial reaction rate ratios are reduced by typically a factor of ~4 compared to the uncertainties of the calculated values. Exceptions are the values for ZPR-3/56B for which the uncertainties of the predicted values depend very much on the use of these data in the adjustment fit.

The adjustments and predictions for the control rod worths are given in Table IV. The uncertainties of the adjusted values are reduced by factors of ~3 to 5 compared with the uncertainties of the originally computed values. The computed values are adjusted very well for the plutonium-fueled assemblies and the predicted values are very close to the adjusted values which indicates consistency with the rest of the data base. However, parameter adjustments cannot resolve the C/E discrepancies for the uranium fueled ZPPR-15D control rod worth data. This is probably unrelated to the fuel type but more likely due to problems in treating the specific cell structure of ZPPR-15D.

Sodium void data are so far included for only three assemblies, ZPPR-15A, -15B, and -15D. However, there are some moderate correlations between the sodium void and the reaction rate ratios and spatial reaction rates of ZPPR-12 and its totally sodium voided version ZPPR-12V. Therefore, additional predictions have been made by excluding all data from ZPPR-12V from the fit. The results are shown in Table V. The uncertainties of the adjusted values are reduced by factors of ~3 to 7 compared with the uncertainties of the originally calculated values, but only by a factor of 2 for the predicted values. The differences between the adjusted and the experimental values are, with the exception of the values for ZPPR-15B, within the combined  $\sigma(E,M)$  and  $\sigma(A)$ , and the differences between the adjusted and predicted values are close to the combined  $\sigma(A)$  and  $\sigma(P)$ . The difference between the original C/E's for sodium void of ZPPR-15A and -15B cannot be resolved by parameter adjustments. The sodium void information contained in the data of the ZPPR-12 and ZPPR-12V pair only slightly affects the central sodium void predictions for ZPPR-15.

The two  $\beta_{eff}$  values (for Big-10 and ZPR-9/36) are adjusted well and appear consistent with all other worth data. The related adjustments on the delayed neutron parameters are +2.4% for  $^{233}\text{U}$ , +0.3% for  $^{235}\text{U}$  and +1.6% for  $^{239}\text{Pu}$ .

The overall fit of the F28/F25 or F28/F49 looks quite good and several outstanding C/E discrepancies are resolved (e.g. for Godiva, Flattop-25, Big-10, ZPR-9/36, Scherzo and Zebra-8H with C/E's >1, and for Jezebel, Jezebel-Pu, Flattop-Pu, and ZPPR-12 with C/E <1). However, some discrepancies cannot be resolved by parameter adjustments or new discrepancies are created (e.g. for Zebra-8C, -8D, -8F and ZPPR-12V). Excluding the statistically poor data from the radial blanket of ZPPR-17A, the residual bias after the fit is -0.4%, and the uncertainties are reduced by more than a factor of 5. The predictions for F28/F are poor: there is a general negative bias, too many values have P/E's which are worse than the C/E's, and for too many values the differences between the adjusted and predicted values are larger than the combined  $\sigma(A)$  and  $\sigma(P)$ . The probable

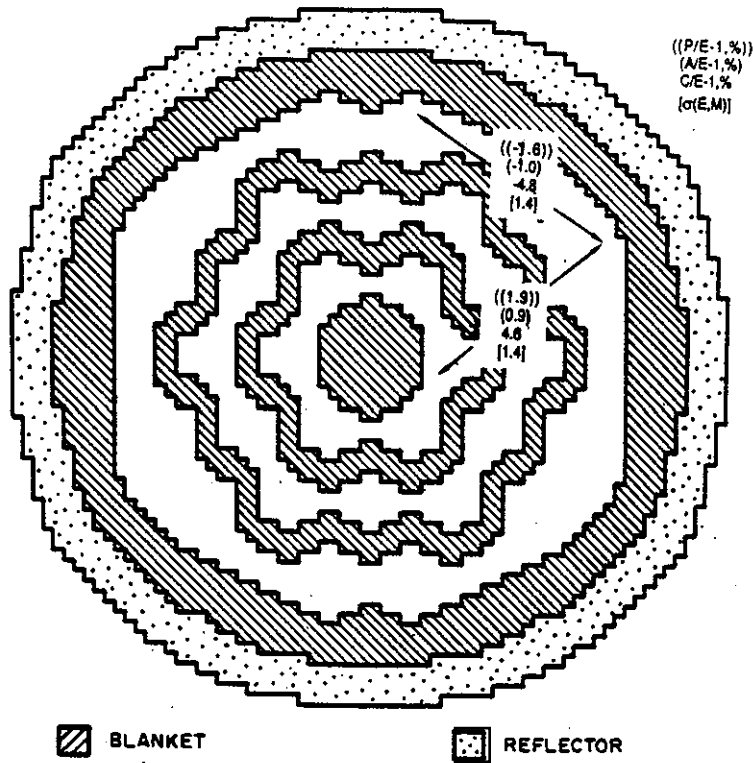


Fig. 1a) Spatial reaction rate ratios for F25 in ZPPR-13C

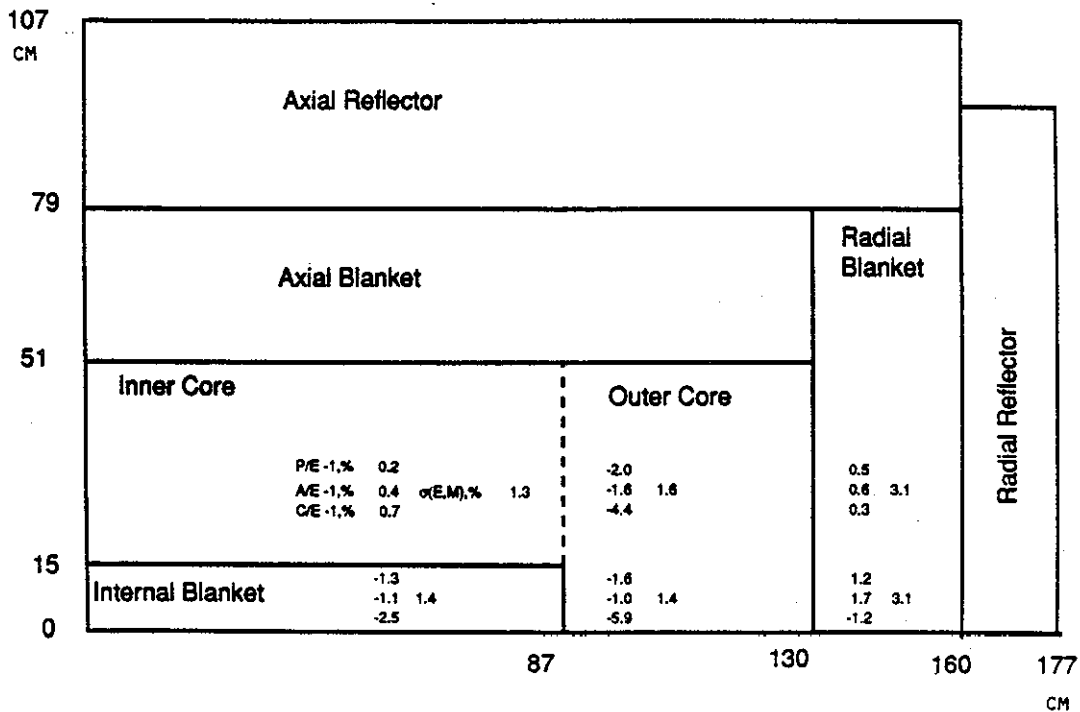


Fig. 1b) Spatial reaction rate ratios for F49 in ZPPR-17A

TABLE IV

## Adjustments and Predictions for Control Rod Worth

Assembly/ Quantity	C/E-1, %	$\sigma(C)$ , %	$\sigma(E,M)$ , %	A/E-1, %	$\sigma(A)$ , %	P/E-1, %	$\sigma(P)$ , %
ZPPR-13C							
Ring 1	-5.4	5.1	3.1	0.2	1.0	0.2	1.3
Ring 2	-2.1	3.6	3.2	1.6	0.8	1.4	1.0
Ring 3	0.7	3.7	3.1	-2.0	0.8	-2.1	0.9
X	3.7	4.0	3.1	0.6	0.8	0.4	0.9
Y	-4.4	4.2	3.2	0.0	0.9	-0.1	1.2
ZPPR-15A							
Center	-5.4	3.1	3.1	-0.9	1.0	-1.2	1.2
ZPPR-15B							
Center	-4.7	2.9	3.1	-1.1	0.9	-1.5	1.1
ZPPR-15D							
Center	-9.9	2.7	3.2	-3.6	1.0	-4.1	1.1
Primary	-10.6	2.5	3.2	-6.3	0.9	-6.9	1.0
Total	-10.9	2.5	3.2	-6.8	0.9	-7.4	1.0
ZPPR-17A							
Center	-7.8	3.9	3.1	-2.2	1.1	-2.1	1.3

TABLE V

## Adjustments and Predictions for Sodium Void

Assembly	C/E-1, %	$\sigma(C)$ , %	$\sigma(E,M)$ , %	A/E-1, %	$\sigma(A)$ , %	P/E-1, %	$\sigma(P)$ , %	Fits without ZPPR-12 P/E-1, %	$\sigma(P)$ , %
ZPPR-15A	10.6	5.9	3.1	0.7	1.7	-2.6	3.1	-3.6	3.2
-15B	6.2	6.7	3.1	-4.0	1.8	-7.5	3.4	-8.7	3.5
-15D	48.1	14.7	3.2	0.0	2.1	1.5	7.4	0.0	7.4

reason is that the F28/F causes mainly adjustments on the inelastic scattering cross sections and fission spectra, parameters which are less important for the adjustments of other quantities.

Neutron flux ratios have larger uncertainties and the C/E's often differ from one by the experimental uncertainties or more. The C/E's improve only by minor amounts in the adjustment fit.

It is expected that a more detailed representation of the inelastic scattering cross sections will improve the adjustments on the F28/F and the flux ratios.

#### Adjustments and Predictions for Various Critical Assemblies

The predictability of quantities of a specific reactor design has been investigated by considerations of the predictability of critical assemblies of specific material compositions and spectral ranges. The latter has been done by excluding the data from one, two or three of the assemblies from the adjustment fit and comparison of the A/E's and P/E's in terms of corresponding uncertainties. It was generally found that the adjustments on the data remaining in the fit were very little changed compared with the reference case in which all data were used.

Table VI shows the adjustments and predictions for ZPR-6/6A and -6/7. Both are LMR benchmark cores, uranium and plutonium fueled, respectively. The differences between the predictions and the adjusted values are for all quantities smaller than the combined uncertainties of  $\sigma(A)$  and  $\sigma(P)$ . The uncertainties of the predictions are reduced by factors of ~3 to 8 compared with the uncertainties of the originally calculated values. All P/E-1's are within the combined uncertainties of  $\sigma(E,M)$  and  $\sigma(P)$ . For the data of ZPR-6/6A, the predictions also test the use of the adjustment methodology as an extrapolation tool because this assembly has the lowest average energy of all uranium fueled assemblies in the data base. It apparently works very well though the relatively large uncertainties of the reaction rate ratios and the absence of other data (sodium void, control rod worth, material worth) limits the validity of this conclusion. Extrapolation to the low energy side of the spectral range for plutonium fueled assemblies has been tested by obtaining predictions for Zebra-8A and -8F. Extrapolation seems to work quite poorly in this case, i.e., four of the eight P/E-1's exceed the combined uncertainties of  $\sigma(E,M)$  and  $\sigma(P)$ . Extrapolation to the high energy side of the spectral range has been considered based on predictions of quantities for Godiva, Flattop-25, Jemima (53), Jemima (37), Jezebel, Jezebel-Pu, and Flattop-Pu. By testing the effects of exclusion of various sets of data or combinations of data sets, it was concluded that the  $k_{eff}$  values of the two Jemimas, Jezebel-Pu, and Flattop-Pu are inconsistent with the rest of the data base and among themselves. This conclusion is, of course, limited by the statistical nature of the data. Thus, though all four values are outside two standard deviations after adjustments ( $\sigma(E,M)$  and  $\sigma(A)$  combined), the  $k_{eff}$  values of the plutonium fueled assemblies were retained in the data base but they were excluded for the Jemimas, because the C/E's improve for the former but get worse for the latter in the adjustment fit.

TABLE VI

Adjustments and Predictions for ZPR-6/6A and ZPR-6/7

Assembly	C/E-1, %	$\sigma(C)$ , %	$\sigma(E,M)$ , %	A/E-1, %	$\sigma(A)$ , %	P/E-1, %	$\sigma(P)$ , %
<u>ZPR-6/6A</u>							
$k_{eff}$	-1.2	1.2	0.3	-0.1	0.2	-0.1	0.2
C28/F25	4.1	2.5	4.7	0.3	0.6	0.5	0.6
F28/F25	0.0	4.9	4.5	-2.8	1.0	-3.0	1.0
F25 Radial Reaction Rate Ratio	-1.1	0.8	2.3	-1.1	0.2	-1.2	0.3
<u>ZPR-6/7</u>							
$k_{eff}$	-0.8	1.6	0.3	-0.1	0.1	-0.1	0.2
C28/F49	6.5	2.9	3.9	1.6	0.6	2.0	0.6
F25/F49	0.9	2.5	4.0	0.5	0.5	0.5	0.6
F28/f49	-0.1	4.9	4.8	0.2	0.8	0.2	0.8
F49 Radial Reaction Rate Ratio	-1.0	1.6	2.3	-1.9	0.4	-2.0	0.5

However, very good predictions were observed for all other critical assembly data in which the adjustment methodology is used in an interpolation mode. The differences between the predicted and the adjusted values were found to be less or approximately equal to the combined uncertainties of  $\sigma(P)$  and  $\sigma(A)$ , and the P/E-1's were less or equal to the combined uncertainties of  $\sigma(E,M)$  and  $\sigma(P)$  for a large majority of data.

The adjustments and predictions for the two critical assemblies ZPPR-13C and ZPPR-17A are given in Table VII. These assemblies are generic mockups of radial and axial heterogeneous core designs. It is interesting (but not surprising based on the sensitivities) that much improved predictions are also obtained in this case though heterogeneous cores are not in the remainder of the data base which is used in the adjustment fit. Including the data of one of these critical assemblies (ZPPR-13C) in the fit further improves the predictions for the other assembly (ZPPR-17A) as shown in the last column of Table VII.

Finally, the two critical assemblies which bear directly on the present application, i.e. deriving adjustment factors for calculated values for the core-conversion design of FFTF, are ZPR-3/56B and ZPPR-15D. The critical assembly ZPR-3/56B was built as a physics benchmark for the original plutonium fueled FFTF. Data from this critical assembly would be potentially useful because of the nickel reflector for which information is not otherwise available in the data base. However, as the experiments were done ~20 years ago, experimental techniques were not as well developed and refined as they are today and resulted in substantial uncertainties of some of the data. Values for the worths of B C and Ni in the center of the core had to be abandoned because inconsistencies in the measurements were recalled. Measurements of radial reaction-rate distributions had been made with proportional counters in an open channel and corrections were applied for the present applications in order to account for streaming effects and inelastic scattering in the counters. These corrections were obtained by rough modeling, in part because of the lack of detailed information, and therefore are very uncertain. The adjustments and predictions for ZPR-3/56B are given in Table VIII. Because of the importance of this specific assembly for the application, the adjustments for some quantities of FFTF are also given for the cases where the ZPR-3/56B data were included in the fit and where they were not.

The differences between the adjusted and predicted values are well within the combined uncertainties of  $\sigma(A)$  and  $\sigma(P)$ . However, whereas the deviation from one of the P/E's appear acceptable for the radial reaction rate ratios when compared to the combined uncertainties of  $\sigma(E,M)$  and  $\sigma(P)$ , the value for  $k_{eff}$  indicates a problem. The latter might be due to the inability to recover the data of the core loading in such detail as they are recorded in more modern experiments, or to shortcomings of the modeling and methods approximations concerning the Ni reflector. The small change of the adjustments for  $k_{eff}$  of the FFTF design of ~0.15% provides only a partial reassurance because these values may well have been different if  $k_{eff}$  of ZPR-3/56B would have adjusted closer to the experimental value.

The adjustments and predictions for the generic metal-core-design benchmark assembly ZPPR-15D are given in Table IX. With the exception of the values for the Na void and the worth of replacing fuel in the center of

TABLE VII

Adjustments and Predictions for ZPPR-13C and ZPPR-17A

Assembly/ Quantity	C/E-1, %	$\sigma(C)$ , %	$\sigma(E,M)$ , %	A/E-1, %	$\sigma(A)$ , %	P/E-1, %	$\sigma(P)$ , %	A/E-1, %
<u>ZPPR-13C</u>								
$k_{eff}$	-0.7	1.6	0.3	0.0	0.1	0.2	0.2	-0.1
FR1/FR3F25 <sup>a</sup>	-4.8	3.1	1.4	-1.0	0.5	-2.0	0.7	-1.4
FR3-X/FR3Y F25	4.6	3.0	1.4	0.9	0.4	2.4	0.7	1.4
B10/F25 SC <sup>b</sup>	-6.2	1.8	2.4	-2.3	0.9	-2.3	1.0	-2.2
B10/F25 DC	-4.9	1.8	2.4	-0.8	0.9	-0.8	1.0	-0.7
Control Rod Worth								
Ring 1	-5.4	5.1	3.1	0.2	1.0	-2.0	1.5	-0.8
Ring 2	-2.1	3.6	3.2	1.6	0.8	0.0	1.1	1.0
Ring 3	0.7	3.7	3.1	-2.0	0.8	-1.5	0.9	-1.8
X	3.7	4.0	3.1	0.6	0.8	1.2	0.9	0.8
Y	-4.4	4.2	3.2	0.0	0.9	-2.0	1.3	-0.9
<u>ZPPR-17A</u>								
$k_{eff}$	-0.7	1.6	0.3	0.0	0.1	-0.1	0.2	0.0
Control Rod Worth	-7.8	3.9	3.1	-2.2	1.1	-4.2	1.5	-2.9
Radial Ratios								
IBC/IBE F49 <sup>c</sup>	-2.5	0.8	1.4	-1.1	0.2	-1.6	0.3	-1.3
z = 5cm F28	-6.3	0.6	5.0	-5.1	0.2	-5.5	0.2	-5.2
C28	-1.2	0.8	1.4	0.2	0.2	-0.3	0.3	0.0
IBC/OC F49	-5.9	2.9	1.4	-1.0	0.7	-2.1	0.9	-1.6
z = 5cm F28	-6.3	9.0	4.4	-4.6	1.4	-6.8	1.7	-5.9
C28	-3.6	2.6	2.1	1.0	0.5	-0.1	0.7	0.6
IBC/RB F49	-1.2	1.4	3.1	1.7	0.4	0.8	0.6	1.2
z = 5cm F28	-1.6	2.1	13.5	2.9	0.7	1.6	0.9	1.6
C28	-3.6	1.4	1.8	-1.0	0.3	-1.7	0.5	-1.3

TABLE VII (cont'd)

Assembly/ Quantity	C/E-1,%	$\sigma(C)$ ,%	$\sigma(E,M)$ ,%	A/E-1,%	$\sigma(A)$ ,%	P/E-1,%	$\sigma(P)$ ,%	P/E-1,%
ICC/ICE F49	-0.7	0.7	1.3	0.4	0.1	0.0	0.2	0.2
z = 18cm F28	-2.4	0.6	2.6	-1.4	0.1	-1.7	0.2	-1.5
C28	-1.9	0.7	1.9	-0.8	0.2	-1.2	0.2	-1.0
ICC/OC F49	-4.4	1.7	1.6	-1.6	0.4	-2.5	0.5	-2.0
z = 18cm F28	-4.8	1.5	2.8	-2.2	0.3	-3.0	0.5	-2.5
C28	-5.4	1.8	2.0	-2.6	0.4	-3.5	0.6	-2.9
ICC/RB F49	0.3	0.8	3.1	0.6	0.5	0.2	0.6	0.5
z = 18cm F28	2.7	6.7	17.4	8.4	1.0	8.2	1.1	8.4
Reaction Rate Ratios								
IB F25/F49	3.1	2.7	1.7	2.9	0.8	2.5	0.9	2.7
z = 5cm C28/F49	4.6	3.0	2.2	-0.4	0.7	0.3	0.8	0.1
F28/F49	1.4	10.2	4.9	-1.9	1.5	-2.6	1.7	-2.3
OC F25/F49	-0.2	2.4	1.7	-0.5	0.5	-0.3	0.6	-0.4
z = 5cm C28/f49	4.7	2.9	2.4	0.1	0.5	0.5	0.6	0.3
F28/F49	0.1	4.8	3.5	-0.1	0.8	-0.3	0.8	-0.2
RB C28/F49	9.2	3.0	3.6	4.0	0.6	4.9	0.7	4.6
z = 5cm F28/F49	-2.3	10.8	11.5	-7.5	1.3	-8.1	1.5	-8.9
IC F25/F49	-0.3	2.4	1.7	-0.6	0.5	-0.4	0.6	-0.4
z = 18cm C28/F49	4.6	3.2	2.1	-0.5	1.1	-0.5	1.4	-0.7
F28/F49	0.7	4.6	3.0	0.6	0.8	0.5	0.8	0.6
OC F25/F49	-0.6	2.4	1.7	-1.0	0.5	-0.7	0.6	-0.8
z = 18cm C28/F49	4.7	2.9	2.7	0.1	0.5	0.5	0.6	0.4
F28/F49	-0.8	4.7	3.6	-0.8	0.8	-1.0	0.8	-0.9
RB C28/F49	10.9	3.0	3.8	5.7	0.7	5.6	0.7	6.5
z = 18cm F28/F49	-2.4	10.8	15.5	-7.7	1.3	-8.2	1.4	-8.1

<sup>a</sup>FR = fuel ring

<sup>b</sup>SC - single column drawer, DC = double column drawer

<sup>c</sup>IBC - internal blanket center, IBE = internal blanket edge

OC = outer core, RB = radial blanket, IC = inner core



TABLE VIII

Adjustments and Predictions for ZPR-3/56B

Quantity	C/E-1, %	$\sigma(C)$ , %	$\sigma(E, M)$ %	A/E-1, %	$\sigma(A)$ , %	P/E-1, %	$\sigma(P)$ , %
$k_{eff}$	-1.0	1.5	0.3	-0.5	0.2	-0.7	0.3
Center/Edge Radial Ratios							
F49	7.2	2.1	3.5	4.3	0.6	5.4	1.8
F28	2.9	1.5	5.4	0.6	0.7	1.5	1.3
B10	0.5	5.0	4.8	-3.5	1.2	-1.7	4.5
Center/Ref1. Radial Ratios							
F49	14.8	13.6	3.6	-0.7	2.4	5.5	12.4
B10	15.9	16.7	5.8	0.3	3.0	7.7	15.3
Predictions for FFTF-CC				P/C-1, %	$\sigma(P)$ , %	P/C-1, %	$\sigma(P)$ , %
$k_{eff}$				0.45	0.24	0.30	0.31
Radial Power Fraction							
IC				-0.8	0.2	-0.5	0.5
OC				1.1	0.3	0.7	0.8
C28/F25 IC				-3.0	0.6	-3.0	0.6
Worth $^{235}U$							
IC				-2.7	1.0	-2.2	1.4
OC				-0.6	1.1	-0.7	1.1

TABLE IX

## Adjustments and Predictions for ZPPR-15D

Quantity	C/E-1,%	$\sigma(C),\%$	$\sigma(E,M)\%$	A/E-1,%	$\sigma(A),\%$	P/E-1,%	$\sigma(P),\%$
$k_{eff}$	-0.7	1.1	0.3	-0.1	0.2	-0.1	0.2
F28/F49	0.2	5.1	2.3	-2.4	1.0	-2.6	1.2
F25/F49	0.9	2.3	1.6	0.6	0.4	0.5	0.4
C28/F49	5.9	3.0	1.8	1.8	0.6	2.0	0.6
Radial Ratios							
IC/OC							
F28	-2.7	1.5	2.0	-1.3	0.5	-1.4	0.6
F25	-0.6	1.0	1.7	1.0	0.3	1.1	0.4
F49	0.2	1.0	2.3	1.7	0.3	1.8	0.4
C28	1.3	0.9	1.5	2.2	0.3	2.3	0.4
Material Worth							
$^{10}B$	-9.8	3.7	2.9	-0.4	1.3	-0.9	1.6
$^{235}U$	1.2	2.6	2.9	1.4	0.8	1.6	1.1
$^{239}Pu$	2.1	3.4	2.9	2.0	1.1	2.3	1.4
$^{238}U$	-1.5	4.9	3.7	-0.6	1.1	-0.8	1.4
Sodium Void	48.1	14.7	3.2	0.0	2.1	7.1	7.1
Center Core Worth							
Fuel	3.8	3.7	3.2	5.8	1.4	7.2	1.8
Control Rod	-9.9	2.7	3.2	-3.6	1.0	-3.2	1.3
Control Rod Worth							
Primary	-10.6	2.5	3.2	-6.3	0.9	-6.3	1.2
Total	-10.9	2.5	3.2	-6.8	0.9	-6.8	1.2
Predictions for FFTF-CC				P/C-1,%	$\sigma(P),\%$	P/C-1,%	$\sigma(P),\%$
$k_{eff}$				0.45	0.24	0.38	0.29
Radial Power Fraction							
IC				-0.8	0.2	-0.8	0.2
OC				1.1	0.3	1.1	0.3
C28/F25 IC				-3.0	0.6	-3.1	0.7
Worth of $^{235}U$							
IC				-2.7	1.0	-2.8	1.3
OC				-0.6	1.1	-0.5	1.4

the core with sodium, the predictions are very close to the adjusted values, i.e. their differences are small compared to the combined uncertainties  $\sigma(P)$  and  $\sigma(A)$ . Most differences of P/E from one are reasonable if compared with the combined uncertainties of  $\sigma(P)$  and  $\sigma(E,M)$ , however, the worth of replacing fuel in the center of the core with sodium and the primary and total control rod worths are not predicted well.

The effect of including or not including the data for ZPPR-15D on the adjustments for some quantities of FFTF-CC is also shown in Table IX. These effects are very small in part because of the consistency of the data base and in part because of low correlations between FFTF-CC and ZPPR-15D (e.g. for radial power fractions).

#### ADJUSTMENTS AND UNCERTAINTIES FOR THE FFTF METAL CORE CONVERSION DESIGN

The correlation coefficients derived from the covariance matrix of the calculated quantities provide a quantitative measure for the usefulness of the data base for improving the predictions and reducing the uncertainties of reactor design quantities. Large anticorrelations are as helpful as large correlations. An overview of the absolute values of the (anti)correlations is given in Table X. As expected, the largest correlations of FFTF-CC quantities are with quantities of a similar type for critical assemblies with the best spectral and compositional match. Though the  $k_{eff}$  data of the critical assemblies play an important role in the determination of adjustments and uncertainty reductions for a reactor design (because of their low uncertainties), it is clear that for some quantities (e.g. radial power fractions, all material worths) other data have higher or equal importance because of the larger number of them. The most desirable case is one for which a design reactor quantity is correlated similarly with a large number of integral data. In contrast, if a quantity is correlated strongly only with one or two experimental data, then the danger of carrying the bias of the experimental values over to the adjustment of the design reactor quantity is high. However, because of the complex involvement of correlations between the quantities and the weights of the data as determined by their uncertainties and correlations, this is best evaluated by successive exclusion of data from the adjustment fit as has been done in the previous section.

Examples of the effects of excluding the data from the two related assemblies ZPR-3/56B and ZPPR-15D on the uncertainties and adjustments of FFTF-CC quantities have been shown in Tables VIII and IX. Instead of listing the effects of the many cases which have been investigated individually, average values for the adjustments and the uncertainties have been obtained and are given in Table XI.  $\bar{A}$  and  $\bar{\sigma}(A)$  are the average adjustments and their uncertainties for up to 63 of the cases considered. Also given are the standard deviations for the adjustments and their uncertainties,  $s(A)$  and  $s(\sigma)$ . It should be emphasized that the results from the 63 cases used to investigate the effects due to exclusion of data, parameters, correlations etc., as described above, do not represent a statistical sample population, thus the standard deviation does not have its usual meaning. However, the  $s(A)$  if found to be one half or less of the average uncertainties for all but the worth of sodium, thus indicates that the average variations of the results due to variations of the data base, parameter space, or correlations are within the uncertainties of the

TABLE X

Overview of Correlations between FFTF-CC  
Quantities and the Experimental Integral Data Base

FFTF	Experimental Integral Data with the Largest (Anti)Correlations	Comments
$k_{\text{eff}}$ BOEC, EOEC	$k_{\text{eff}}$ of ZPPR-15D and ZPR-6/6A  0.91 and 0.85	All other $< 0.55$
Rad. Power Fraction	All Radial Reaction Rate Ratios of ZPR-3/56B (see Table VIII)	
IC	0.9 to 0.8	All others $< 0.15$
MC	0.7 to 0.6	Many others $\leq 0.3$
OC	-0.9 to -0.8	Many others $\leq 0.25$
C28/F25 IC, MC, OC	C28/F25 of Scherzo, Zebra-8H, Big-10 and ZPR-9/36  ~ 0.9	Anticorrelated with $k_{\text{eff}} > -0.7$  Many medium size
Worth of $^{235}\text{U}$ IC, MC, OC	Diverse ( $k_{\text{eff}}$ of Big-10, ZPR-9/36; Worth of $^{235}\text{U}$ and Control Rod Worth of ZPPR-15D)  ~ 0.9 to 0.6	All other $< 0.6$
Worth of $^{238}\text{U}$ IC, MC, OC	Diverse (worth of $^{238}\text{U}$ in ZPPR-15D Big-10, ZPR-9/36; Control Rod Worth in ZPPR-15D, Spatial Ratios F25, He-Production in Big-10)  ~ 0.9	Many others $> 0.8$
Worth of Na	Diverse (Na Void, Control Rod Worth, Worth of $^{10}\text{B}$ , Spatial Ratio F49 - all in ZPPR-15D, Spatial Ratio F25 in ZPPR-12, $k_{\text{eff}}$ of Flattop-25)  0.5 to 0.3	All others $< 0.3$

TABLE XI

Adjustments for Various Quantities of FFTF-CC

Quantity (all EOEC)	Average of 63 Cases							"Best Case"		$\sigma(C),\%$
	$\bar{A},\%$	$\bar{\sigma}(A),\%$	$s(A),\%$	$s(\sigma),\%$	$A_{max},\%$	$A_{min},\%$	$\sigma_{max},\%$	$A,\%$	$\sigma(A),\%$	
$k_{eff}$	0.43	0.25	0.12	0.06	0.71	0.15	0.66	0.45	0.26	1.0
FL1/FLT <sup>a</sup>	-0.6	0.4	0.2	0.0	-1.3	-0.3	0.4	-0.4	0.4	0.8
FL2/FLT	1.6	1.0	0.5	0.0	3.4	0.8	1.2	1.0	1.0	2.2
FL3/FLT	4.1	2.9	1.1	0.2	7.6	2.4	3.6	3.0	2.9	5.1
RPF <sup>b</sup> IC	-0.7	0.2	0.1	0.1	-1.0	-0.4	0.5	-0.8	0.2	0.6
MC	-0.3	0.1	0.1	0.0	-0.5	-0.2	0.2	-0.3	0.1	0.3
OC	1.0	0.3	0.1	0.1	1.4	0.7	0.7	1.1	0.3	0.8
C28/F25 IC	-2.9	0.6	0.2	0.1	-3.4	-2.7	1.0	-3.2	0.6	2.7
MC	-2.5	0.6	0.2	0.1	-3.0	-2.3	1.0	-2.8	0.6	2.7
OC	-2.6	0.6	0.2	0.1	-3.1	-2.4	1.0	-2.8	0.6	2.5
Wth25 <sup>c</sup> IC	-2.6	1.0	0.5	0.1	-4.9	-1.8	1.4	-2.8	1.1	2.7
MC	-2.0	1.0	0.5	0.1	-3.8	-1.2	1.3	-1.9	1.0	2.7
OC	-0.6	1.1	0.4	0.1	-2.1	0.3	1.4	-0.2	1.1	2.6
Wth28 IC	-4.0	1.7	0.9	0.1	-6.3	-2.9	2.1	-4.8	1.8	7.2
MC	-3.0	2.1	0.9	0.2	-6.1	-1.7	2.6	-3.5	2.2	8.8
OC	-1.1	2.0	0.9	0.4	-4.6	0.3	2.5	-1.2	2.0	7.0
WthNA IC	20.3	5.1	5.5	1.4	24.4	16.1	6.4	20.4	5.4	11.0
OC	11.0	4.0	3.2	1.1	14.5	7.3	4.6	10.6	4.2	7.1
MC	3.2	3.0	1.5	0.8	6.4	0.7	3.4	2.2	3.2	4.7

<sup>a</sup>Flux ratios<sup>b</sup>Radial power fractions<sup>c</sup>Worth of <sup>235</sup>U, <sup>238</sup>U and Na

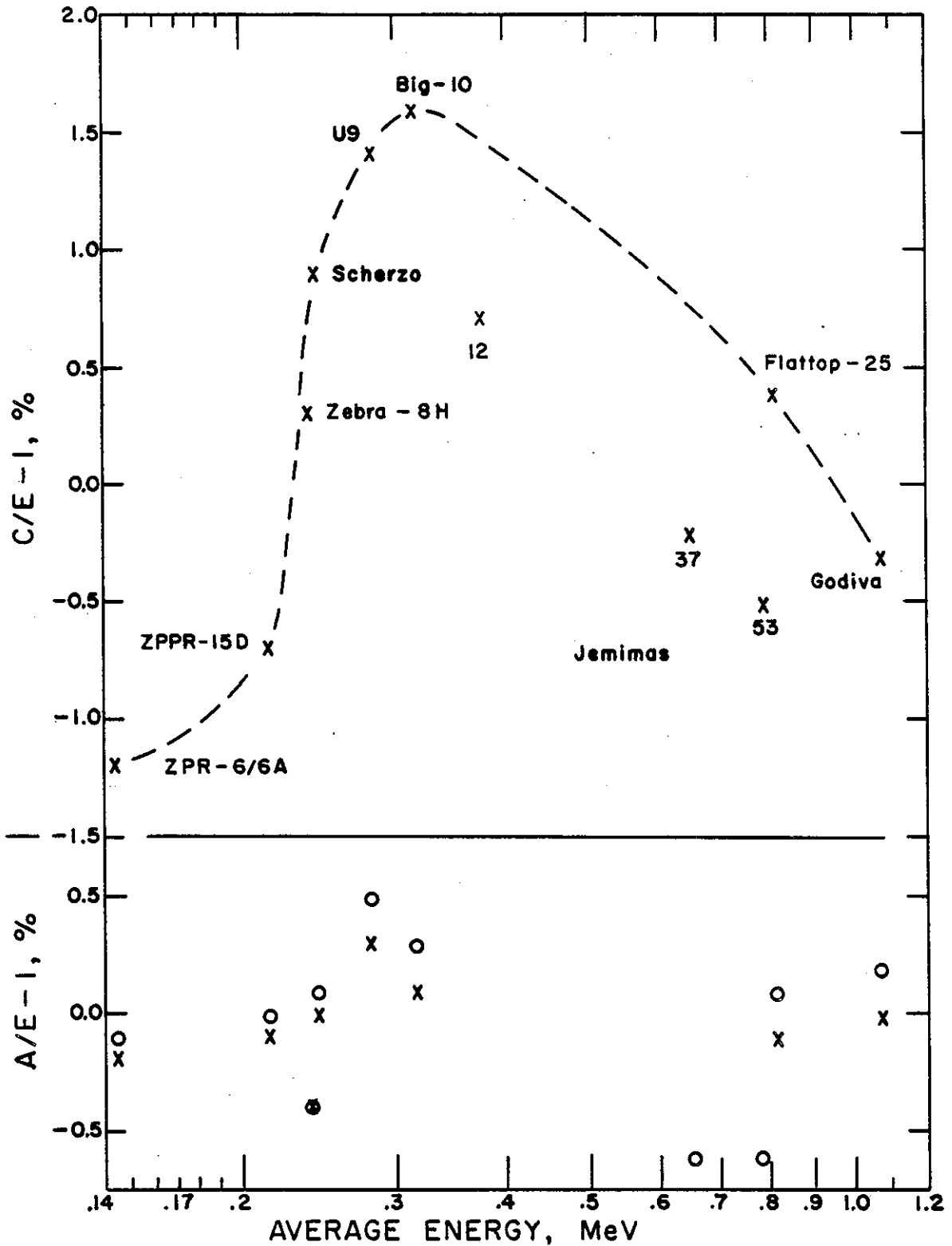


Fig. 2 Calculated vs. experimental ratios for  $k_{eff}$  of uranium-fueled assemblies and corresponding ratios for the adjusted values (X = adjusted without the Jemimas, O = with the Jemimas)

adjustments. The maximum and minimum adjustments for the 63 cases are also listed in Table XI and found around  $\bar{A} \pm \bar{\sigma}(A)$ .  $s(\sigma)$  is small compared to the average uncertainty and indicates a lesser sensitivity of the uncertainties to data base variations than the adjustments do.

#### SUMMARY AND CONCLUSIONS

A large data base has been used in order to investigate the usefulness of the data adjustment methodology for the improvement of predictions and reduction of uncertainties for operational and safety parameters of LMR-type reactor designs. The effects of parameter selections, of questionable data, and of the correlations between the parameters and between the data were found to be within the uncertainties of the predictions. Using data from specific critical assemblies with a wide variation in spectral range and compositions as test cases, it was found that substantially improved predictions can be obtained for design reactor oriented quantities like enrichment, breeding ratio, control rod worth, sodium void, material worth (of the major fissile and fertile materials), and power distributions. The resolution of C/E discrepancies of  $k_{\text{eff}}$  for uranium fueled assemblies can be seen in Fig. 2. The uncertainties of these predictions are reduced by typical factors of -2 to 8.

Some reservations must be made for the spatial distributions of control rod worth and sodium void in uranium fueled assemblies because of the scarcity of data and some inconsistencies. The same applies to predictions of structural material damage (related to F28/F) which one might want to make.

Doppler effect can at present not be predicted because appropriate parameters have not yet been included and poor adjustments for the neutron flux ratios are observed. Fuel cycle evaluations are not possible with the present data base because of inconsistencies between F40/F25 and  $^{240}\text{Pu}$  worth data on the one hand and  $k_{\text{eff}}$  data (mainly Jezebel-Pu) on the other hand, and the lack of data for any other higher actinides.

Adjustments have been derived for the calculated  $k_{\text{eff}}$ , flux ratios, radial power fractions, C28/F25 and the material worth of  $^{235}\text{U}$ ,  $^{238}\text{U}$  and Na of the core conversion design for FFTF. The variations of these adjustments for a large number of test cases involving parameter and data selections were within the predicted uncertainties. The latter were much reduced compared with the uncertainties of the originally computed values (factors of 2 to 4).

#### ACKNOWLEDGEMENTS

The data base used for the present investigation was assembled by the authors of Ref. 15. This work was supported by the U.S. Department of Energy, Nuclear Energy Programs, under Contract W-31-109-Eng-38.

#### REFERENCES

1. P. J. Collins, W. P. Poenitz and H. F. McFarlane, "Integral Data for Fast Reactors," Proc. International Conference on Nuclear Data for Science and Technology, Mito, Japan, May 1988, to be published.

2. J. L. Rowlands, "Nuclear Data for Reactor Design, Operations and Safety," Proc. International Conference on Neutron Physics and Nuclear Data for Reactor and other Applied Purposes, AERE, Harwell, p 7 (1978). See also:  
  
M. Salvatores and G. Palmiotti, "LMFBR Design Parameter Uncertainties and Target Accuracies," Ann. Nucl. Energy, Vol. 12, p 29 (1985).
3. G. Cecchini et al., "Analysis of Integral Data for Few Group Parameter Evaluation of Fast Reactors," Proc. International Conference on the Peaceful Uses of Atomic Energy, Geneva, Aug. 1964, Vol. 2, p 388 (1964).
4. P.C.E. Hemment and E. D. Pendlebury, "The Optimization of Neutron Cross-Section Data Adjustments to Give Agreement with Experimental Critical Size," Proc. International Conference on Fast Critical Experiments and Their Analysis, Argonne National Laboratory, Oct. 1966, ANL-7320, p 88 (1966).
5. J. L. Rowlands and J. D. Macdougall, "The Use of Integral Measurements to Adjust Cross Sections and Predict Reactor Properties," Proc. International Conference on the Physics of Fast Reactor Operations and Design, London, June 1969, The British Nuclear Energy Society, p 180 (1969).
6. A. Gandini and M. Salvatores, "Nuclear Data and Integral Measurement Correlations for Fast Reactors," CNEN Report RT/FI (74) (1974).
7. H. Mitani and H. Kuroi, "Adjustment of Group Cross Sections by Means of Integral Data," Nucl. Sci. and Tech., 9, p 383 (1972).
8. J. B. Dragt, J.W.M. Dekker and H. Gruppelaar, "Methods of Adjustment and Error Evaluation of Neutron Capture Cross Sections," Nucl. Sci. Eng., 55 p 280 (1974).
9. P. J. Collins, M. J. Lineberry and K. S. Smith, American Nuclear Society 1977 Winter Meeting, San Francisco, Nov. 1977, TANSO 27, p 884 (1977).
10. C. R. Weisbin et al., "Data Adjustment: A Cautiously Optimistic View for the Improvement of Design Performance Calculations and Data Assessment," American Nuclear Society Winter Meeting, San Francisco, Nov. 1977, TANSO 27, p 881 (1977).
11. L. N. Usachev et al., "Adjustment of Evaluated Microscopic Data on the Basis of Evaluated Integral Experiments," International Atomic Energy Agency Report, INDC(CCP)-109/U (1977).
12. F. Schmittroth, "Generalized Least-Squares for Data Analysis," Hanford Eng. Dev. Lab. Report HEDL-TME 77-51 UC-79d (1978).
13. T. Takeda and T. Umamo, "Burnup Sensitivity Analysis in a Fast Breeder Reactor," Nucl. Sci. Eng., 91, p 1 (1985).



14. W. P. Poenitz, unpublished information (1987).
15. W. P. Poenitz et al., unpublished information (1988).  
See also:  
  
P. J. Collins et al., this meeting (1988).
16. C. F. Gauss, "Methode der kleinsten Quadrate," Stankiewicz, Berlin (1887).
17. A. C. Aitken, "On Least-Squares and Linear Combinations of Observations," Proc. of the Royal Society Edinburgh A, 55, p 42 (1934).
18. W. P. Poenitz, "Covariances for Adjusted Derived Quantities," Proc. IAEA Specialists' Meeting on Covariance Methods and Practices in the Field of Nuclear Data, Rome, Italy, Nov. 1986, INDC(NDS)-192/L, p 111 (1986).
19. W. L. Zijp, "Treatment of Measurement Uncertainties," Netherlands Energy Research Foundation Report, ECW-194 (1987).
20. E. Greenspan, Y. Karni and D. Gilai, "High Order Effects in Cross Section Sensitivity Analysis," Proc. of a Seminar on the Theory and Application of Sensitivity and Uncertainty Analysis, Oak Ridge, Aug. 1978, ORNL/RSIC-42, p 231 (1978).
21. R. N. Hwang, Argonne National Laboratory, private communication (1987).

SPECIALIST'S MEETING ON THE  
APPLICATION OF CRITICAL EXPERIMENTS AND OPERATING DATA TO  
CORE DESIGN VIA FORMAL METHODS OF CROSS-SECTION DATA ADJUSTMENT  
JACKSON-HOLE, SEPTEMBER 23/24, 1988

USE OF SUPERPHENIX START-UP EXPERIMENT  
FOR DATA ADJUSTMENT  
A NEW APPROACH

J.C. CABRILLAT\* - G. PALMIOTTI\*\* - M. SALVATORES\*

\* CEA/CADARACHE

\*\* CISI/INGENIERIE

ABSTRACT

Analysis of SUPER PHENIX start-up experiment have emphasized the role of cross-sections uncertainties in the C/E discrepancies, once the method approximation being clarified.

An action is undertaken to enlarge the classical "clean core" integral experiment data base with the SUPER PHENIX experimental results, in order to perform a statistical re-adjustment of the CARNAVAL-IV data set,

A first attempt shows the feasibility of such a procedure.

## 1 - INTRODUCTION

Power reactor start-up experiments provide a unique source of experimental informations, which can be analyzed in terms of basic data uncertainties, once the method approximations have been clarified. These experiments can then be used to enlarge the experimental data base to validate and eventually to adjust basic data.

We have made a first attempt to use some SUPER PHENIX start-up experiments in an adjustment procedure, to verify their consistency, and, in general, the feasibility of that approach. However, for a realistic case, we have considered both "clean core" integral experiments / 1 /, and start-up experiments.

Among these last experiments, we have chosen several subcritical configurations of the working core of SUPER PHENIX, corresponding to different control rod patterns. It is known / 2 / that a detailed sensitivity analysis has indicated that some C/E discrepancy on the reactivity level, can be attributed to data uncertainties.

Moreover, the critical configurations of the minimum critical mass core (C1D) and of the working core (CMP) may be added, to provide the necessary conditions, which avoid the problem of "criticality reset" in the calculation of the sensitivity coefficients.

"Clean core" configurations have been added, to provide a realistic frame for the adjustment. These experiments are essentially those which have provided the basis for the CARNAVAL-IV development / 3 /.

2 - THE METHOD

The main specific feature of the present adjustment procedure, is represented by the use of subcritical counting rates, as integral parameters. To interpret the C-E values in terms of multigroup cross-section adjustments it is necessary to provide the appropriate sensitivity coefficients to correlate in the standard way the C-E to the  $\delta\sigma$ . These sensitivity coefficients have been derived using the EGPT (Equivalent Generalized Perturbation Theory) / 4 /.

The counting rate on detector j for the configuration K can be expressed as :

$$R_k^j = \langle \phi_K \Sigma_d^j \rangle$$

where  $\Sigma_d^j$  is the detector j cross-section,  $\phi_k$  is the solution of the subcritical equation with inherent source S :

$$M_k \phi_k = S$$

and  $\langle \rangle$  indicates energy and volume integration.

The ratio of the counting rate of the detector j in configuration k with respect to a reference configuration, k', is given by :

$$T_k^j = \frac{R_k^j}{R_{k'}^j} = \frac{\langle \phi_k \Sigma_d^j \rangle}{\langle \phi_{k'} \Sigma_d^j \rangle}$$

A variation of  $T_k^j$  due to a basic parameter variation (i.e. a variation of the Boltzman operator or the source term) can be expressed, at first order as :

$$\frac{\delta T_k^j}{T_k^j} = \frac{\delta R_k^j}{R_k^j} - \frac{\delta R_{k'}^j}{R_{k'}^j} \quad (1)$$

Each term on the left of equation (1) can be expressed using the GPT for subcritical systems :

$$\delta R_k^j = \langle \phi_k \delta M_k \psi_{kj}^+ \rangle + \langle \psi_{kj}^+ \delta S \rangle$$

$$\delta R_{k'}^j = \langle \phi_{k'} \delta M_{k'} \psi_{k'j}^+ \rangle + \langle \psi_{k'j}^+ \delta S \rangle$$

where  $\psi_{kj}^+$  and  $\psi_{k'j}^+$  are solutions of the following equations :

$$M_k^+ \psi_{kj}^+ = \Sigma_d^j / R_k^j$$

$$M_{k'}^+ \psi_{k'j}^+ = \Sigma_d^j / R_{k'}^j$$

Since  $M_k$  and  $M_{k'}$  differ only for the geometrical definition of the configuration (e.g. the rod configuration), if we consider variations of  $M_k$  and  $M_{k'}$ , due to microscopic cross-sections, we have  $\delta M_k = \delta M_{k'}$  (apart from an eventual direct effect, e.g. of a rod on itself). We have then for  $\delta T_k^j / T_k^j$  and for an element  $\delta m$  of the matrix  $\delta M_k$  and for an element  $\delta s$  of the vector  $\delta S$  :

$$\delta T_k^j / T_k^j = \left\{ \frac{1}{R_k^j} \langle \phi_k \psi_{kj}^+ \rangle - \frac{1}{R_{k'}^j} \langle \phi_{k'} \psi_{k'j}^+ \rangle \right\} \delta m +$$

$$+ \left\{ \frac{\psi_{kj}^+}{R_k^j} - \frac{\psi_{k'j}^+}{R_{k'}^j} \right\} \delta s$$

This expression allows the calculation of the needed sensitivity coefficients. It is to be noted that we have made the choice, based on the experimental values available, to correlate subcritical counting rate, normalized to a reference situation, to basic data. This procedure has the obvious advantage to be free from detector data from one side, and to be directly related to the actual experimental values used to assess subcritical reactivities.

In the case of "clean core" experiments, no new developments were needed. Standard GPT formulations were used to assess the sensitivity coefficients. The CCRR code system allows to calculate both standard sensitivities and the new ones, defined above, in a consistent way. Finally, we used the statistical adjustment technique / 5 / and the AMARA code / 6 / for the practical resolution with the Lagrange multipliers method.

## 2 - EXPERIMENTAL DATA BASE AND CORRESPONDING CALCULATED VALUES

The set of experiments to be used to adjust the CARNAVAL-IV formulaire is made from both a selected set of results issued from the start-up of the reactor and typical "clean core" experiments performed at MASURCA and ERMINE facilities in the past years for this purpose.

The calculation are performed using, as far as possible the most refined methods of the moment, as it is detailed in reference / 7 /. Obviously in the case of SUPER PHENIX experiments any bias factors previously issued from C/E comparison and associated to CARNAVAL-IV have been eliminated.

### 2.1 - SUPER PHENIX

The core parameters taken into account are those having the greatest importance from the designer point of view : critical mass, rod worth, flux distributions.

#### a) Critical mass

The so called critical mass of SUPER PHENIX is represented by the minimal number of S/A required to obtain criticality with control rods out of the core. The core configuration which approaches these conditions is the C1D core (first criticality core), which is shown in figure / 1 /. The main control system is only 8 cm inserted in the core and so its influence may be considered as negligible.

This kind of experimental data could eventually be completed by some other typical critical configurations as the critical working core (CMP) / Fig. 2 /.

In this case, the physical information is more complex, because of the important control rod insertion.

The C/E comparison established in Réf. / 7 / is recalled in table / 1 / excluding any "formulaire" correction (bias factor) (260 pcm), for the C1D core.

Such calculations take carefully into account heterogeneity and transport effects due to the presence of different kinds of S/A (dummy, diluent, fuel S/A, control rods and control rods followers).

! Configuration !	E-C (pcm)
! C1D core !	0.00190 ± 0.00340 !

Table 1

b) Control rods

Numerous control rod configurations have been measured in the first criticality (C1D) and in the final working core (CMP). A sample of configurations has been chosen, taking into account the conclusions of a previous detailed analysis, which showed the role of data uncertainties in the remaining E/C values and inconsistencies among them. In particular, it has been shown that the influence of cross-sections can be fairly dependent on the rod configurations. For example the effect of an increase in U-238 capture cross-sections are of opposite sign on the internal and on the external rod ring rod worth.

As previously emphasized, we preferred to use counting rates associated to subcritical configurations rather than antireactivity of rods. A set of representative configurations is the following (CMP core).

- 1 - SCP\* at critical level and SAC\* down (fully inserted) (reference situation).
- 2 - SCP and SAC down.
- 3 - SCP down SAC up (fully withdrawn).
- 4 - { Internal ring of SCP up  
External ring of SCP down
- 5 - { Internal ring of SCP down  
External ring of SCP up
- 6 - { SCP down - SAC up  
One rod of SCP withdrawn (simulating handling error).

Counting rates calculations of such cases are issued from 3D 25 energy groups calculations using "equivalent" cross-sections for the rods, taking into account transport, finite mesh, and heterogeneity effects / 8 /.

c) Flux distributions

The flux (power) distributions have been experimentally measured by means of two detectors irradiations at very low power level, along a core radius and for approximately the whole height of the fuel pin.

---

\* SCP : main control system

\* SAC : complementary shutdown system (see fig. / 1 / or / 2 /.



The first E/C comparison / 7 / did show a general good agreement if heterogeneity, transport and finite mesh effects related to control rods are well taken into account by means for example, of equivalent cross-sections / 8 /. Nevertheless it seems that such calculations (3D 25 energy groups) overestimate, slightly, the radial flux gradient, particularly in the external core. Basic data may have a role in such an effect, and analysis in that direction is being undertaken. The experimental parameter tested should be the ratio of fluxes at core center and at the periphery of internal or external cores.

## 2.2 - "Clean core" experiments

"Clean core" experiments are part of those used to assess the CARNAVAL-IV data set / 1,3 /. The choice concerns experiments which give informations on the different components of LMFBRs, such as :

- plutonium and U-238 (ZONA1, ZONA2, ZONA3),
- uranium isotopes (R1),
- iron (OA10),
- nickel (ON10).

These experiments were performed both at MASURCA (ZONA1, ZONA2, ZONA3, R1) and at ERMINE (OA10, ON10) facilities.

The integral parameters used for the adjustment are :

- material buckling obtained from fission rate distributions with fission chamber, radially and axially,
- reaction rate ratios (F8/F5, C8/F5, F9/F5, measured with activation foils and fission chambers),
- $K_{\infty}$  obtained from cell reactivity worth measurement,
- critical mass.

If necessary, corrections have been applied to such parameters to produce the "cell averaged" values in fundamental mode (i.e., for exemple elimination of harmonics related to finite size of assembly).

Calculations are performed using the cell code HETAIRE / 1,3 / (fundamental mode parameters) and 2D (RZ geometry) in diffusion approximation corrected from transport, heterogeneity, streaming, edge effects... ( $K_{eff}$  values).

### 2.3 - Uncertainties

Experimental uncertainties have been assessed both for critical facilities and power reactor experiments and we have used these uncertainties, without correlations among them, at least in this first stage. We have also considered that part of the uncertainties, attached to E/C values, is due to core modelisations, and methods used to correct basic calculations (3D 25 energy groups for SPX1).

## 3 - CROSS-SECTIONS

The CARNAVAL-IV formulaire includes cross-sections, adjusted mainly by means of integral experiments related to the study of neutron balance. Actually the good performance of the formulaire to predict the critical mass of SUPER PHENIX has been emphasized.

Nevertheless, discrepancies on rod worth and related sensitivities studies / 7 /, tend to emphasize that calculated control rod reactivities are sensitive to basic data changes which are not of importance for critical mass determination or the effects of which have compensating effects on  $K_{eff}$ .

An example is the simultaneous increase of the iron transport cross-section (above  $\sim 10$  keV) and of the capture cross-section (below  $\sim 100$  keV).

Such considerations, completed by the trends revealed by recent evaluations / 2,7 /, suggest to perform an adjustment of the following cross-sections, within the associated estimated uncertainties (table 2) :

Isotope	Cross-section	Energy range	Uncertainties (1 $\sigma$ ) %
Iron	Capture	E < 1 MeV	+ 50
	Transport	E > 10 keV	+ 10
	Inelastic	All the range	+ 20
	Elastic	E > 10 keV	+ 10
Nickel	Capture	E < 1 MeV	+ 50
	Transport	E > 10 keV	+ 10
	Inelastic	All range	+ 30
	Elastic	E > 10 keV	+ 10
Pu239	Fission	1 MeV > E > 500 eV	+ 5 %
	Capture	Same	+ 10 %
U238	Fission	All range	+ 10 %
	Transport	500 eV > E < 500 keV	+ 10 %
	Inelastic	All range	+ 20 %
Oxygen	Transport	E > 10 keV	+ 10 %
	Elastic	Same	+ 10 %

Table 2

For a statistical adjustment procedure, cross-section uncertainties and correlations are needed. At present, no major datafile provides complete informations on these data. For the CARNAVAL-IV system, a set of uncertainties and correlations have been associated to the data, as a result of the previous adjustment. However, for our first attempt, we did use

uncertainties (see table 2) which take into account also further informations coming from more recent evaluations. No correlations have been considered in the first step presented in the paper. Their assessment and use is however foreseen for eventual next steps.

#### 4 - SENSITIVITY CALCULATIONS AND VALUES

##### 4.1 - SUPER PHENIX

For the reactivity counting rate ratios and flux ratios, the sensitivity coefficients are calculated by the means of 2D geometry models (hexagonal - 25 energy groups), using if necessary, the simulation of partial rod insertions by an equivalent "dilution" of boron.

The CCRR code system / 9 / provides the modules calculating sensitivities according to the formalisms described above.

Sensitivities both for counting rates and reactivities are proportionnal to the reactivity level of the core configuration. This simple property (well verified in our case) has been used to correct the sensitivities values for the discrepancies introduced by the simplified 2D modelisations.

##### 4.2 - Clean core experiments

Sensitivities are provided by infinite cell calculation (XY geometry).

##### 4.3 - Sensitivities - Some examples

A reasonable performance of such adjustment can be obtained if the sensitivities energy profiles and magnitudes are different ("orthogonal").

A limited sample of sensitivities values is displayed on figure / 3 / and / 4 / corresponding to the variation of + 100 % of  $\sigma_{\text{capture}}^{\text{U238}}$  and + 100 % of  $\sigma_{\text{transport}}^{\text{Fe}}$ .

The concerned experiment are : ClD core reactivity, counting rate ratios relative to SPX1, OA10 (C8/F5), ZONA2 (B<sup>2</sup> and critical mass).

We can make the following comments :

a) The SPX core sensitivities have the highest magnitude as expected. Since the agreement between experience and calculation is good, this point corresponds to a strong constraint on further data adjustment.

b) Profiles related to some SPX1 experiments are rather different from those related to clean core experiments and this confirms their original contribution to the formulaire adjustment.

#### 5 - A FIRST ADJUSTMENT ATTEMPT

At this stage a very simple attempt has been made namely :

a) A limited number of cross-section to be adjusted have been considered :

- Pu 239 fission and capture,
- U 238 fission and capture,
- oxygen transport,
- iron transport and capture.

No correlations have been taken into account.

b) A limited number of experiments have been chosen among those proposed above :

- one critical configuration (C1D),
- two counting rate ratio (given in table 3),
- OA10 experiments,
- ZONA1, ZONA2, ZONA3 experiments.

Table / 3 / resumes the input experimental data of the AMARA code, which has been used for the statistical adjustment.

AMARA INPUT RELATED TO INTEGRAL PARAMETERS

TABLE / 3 /

Type of experiment	Parameter	E-C/C	Standard deviation
<u>SUPER PHENIX</u>			
C1D core	Reactivity	0.00190	+ 0.00340
Reference :			
{ SCP at critical level	} counting rates ratio	- 0.10	+ 0.04
{ SAC down			
{ SCP down			
{ SAC down			
{ SCP down		- 0.05	+ 0.04
{ SAC up			
<u>ERMINE</u>			
OA10	F8/F5	0.10	+ 0.014
	C8/F5	- 0.005	+ 0.015
	F9/F5	- 0.015	+ 0.01
	K*	0.0105	+ 0.00145
<u>MASURCA</u>			
ZONA 1	Core reactivity	0.00584	+ 0.0011
	F8/F5	- 0.004	0.0017
	C8/F5	0.012	0.023
	F9/F5	- 0.01	0.016
	B <sup>2</sup>	- 0.0120	0.0008
ZONA 2	Core reactivity	0.00575	+ 0.00115
	F8/F5	- 0.012	0.002
	C8/F5	- 0.008	0.024
	F9/F5	- 0.04	0.015
	B <sup>2</sup>	0.008	0.008
ZONA 3	Core reactivity	0.00566	+ 0.00130
	F8/F5	0.053	0.014
	C8/F5	- 0.017	0.023
	F9/F5	0.024	0.015
	B <sup>2</sup>	0.035	0.015

## RESULTS

The main features of this first attempt is that the feasibility of the process seems proved (i.e., no conflicting results have been detected).

The main trends that seemed reasonable from our past "qualitative" studies are roughly respected.

For exemple the most significantly results are :

- an increase of transport cross-section of iron (above 100 keV, 20 %, as expected),

- an increase of fission cross-section of Pu-239 (1 keV < E < 100 keV),

- an increase of the capture cross-section of iron, above 100 keV (+ 5 ÷ 8 %, even if lower than expected, 20 - 40 %).

## 6 - CONCLUSIONS

The first analysis of SUPER PHENIX start-up experiment emphasize the role of basic data uncertainties to explain the remaining C/E values for parameter like control rod worths.

To include such informations in the CARNAVAL-IV formulaire by the mean of an adjustment of cross-sections, we have enlarged the traditionnal set of integral parameters ("clean core" experiments) with those issued from the experiment performed during the SUPER PHENIX start-up.

For that purpose :

- a) A method has been developped to calculate sensitivities of counting rater ratios (preferred to rod antireactivity) to cross-sections.



b) An experimental data set has been defined :

- critical mass of SUPER PHENIX,
- counting rate ratios associated to different subcritical configurations,
- flux gradient (still to be used),
- "clean core" experiments in critical assemblies.

c) A cross-section set has been chosen for adjustment, with associated uncertainties.

d) A first attempt has been performed using a limited number of experiments and data. The feasibility of such a process, i.e. to modify the CARNAVAL-IV data, before making a new formulaire, starting from JEF data, has been indicated.

This action will be continued using the complete integral data base, more cross-section parameters and correlations (in energy and among data), to give to the designer a better tool to perform the follow-up of SUPER PHENIX.

## REFERENCES

- / 1 / J.Y. BARRE et al. Proc. Int. Conf.  
Physics of Fast Reactors, Tokyo (1973), p. 396.
  
- / 2 / M. SALVATORES et al.  
Proc. ANS Topical Meeting, Paris (1987) p. 907.
  
- / 3 / J.P. CHAUDAT et al.  
Trans. Am. Nucl. Soc. 27, 877 (1977).
  
- / 4 / A. GANDINI, G. PALMIOTTI, M. SALVATORES.  
Annals of Nucl. En. 13, 109 (1986).
  
- / 5 / A. GANDINI, CNEN Report RT/FI(73)22
  
- / 6 / A. GANDINI, M. PETILLI.  
CNEN Report RT/FI(73)29
  
- / 7 / J.C. CABRILLAT et al.  
Methods and data from the SUPER PHENIX start-up  
experiments analysis. ANS meeting. Jackson-Hole (USA)  
September 88.
  
- / 8 / G. PALMIOTTI et al.  
Control heterogeneity effect in LMFBR : a method  
development and experimental validation.  
Proc. Int. Conf. on Advances in Reactor Physics  
Mathematics and Computation.  
PARIS 27-30 April 1987.
  
- / 9 / C. GIACOMETTI et al.  
CCRR - Calculation code for fast reactors.  
Proc. of the ANS topical meeting on advances in nuclear  
engineering computational method. KNOX VILE, April 1985.
  
- / 10 / M. SALVATORES, C. NORDBORD, Proc. 1988 Int. Conf. on  
Reactor Physics, Jackson Hole (1988).

Fig.1 - SUPER PHENIX 1-C1D CORE

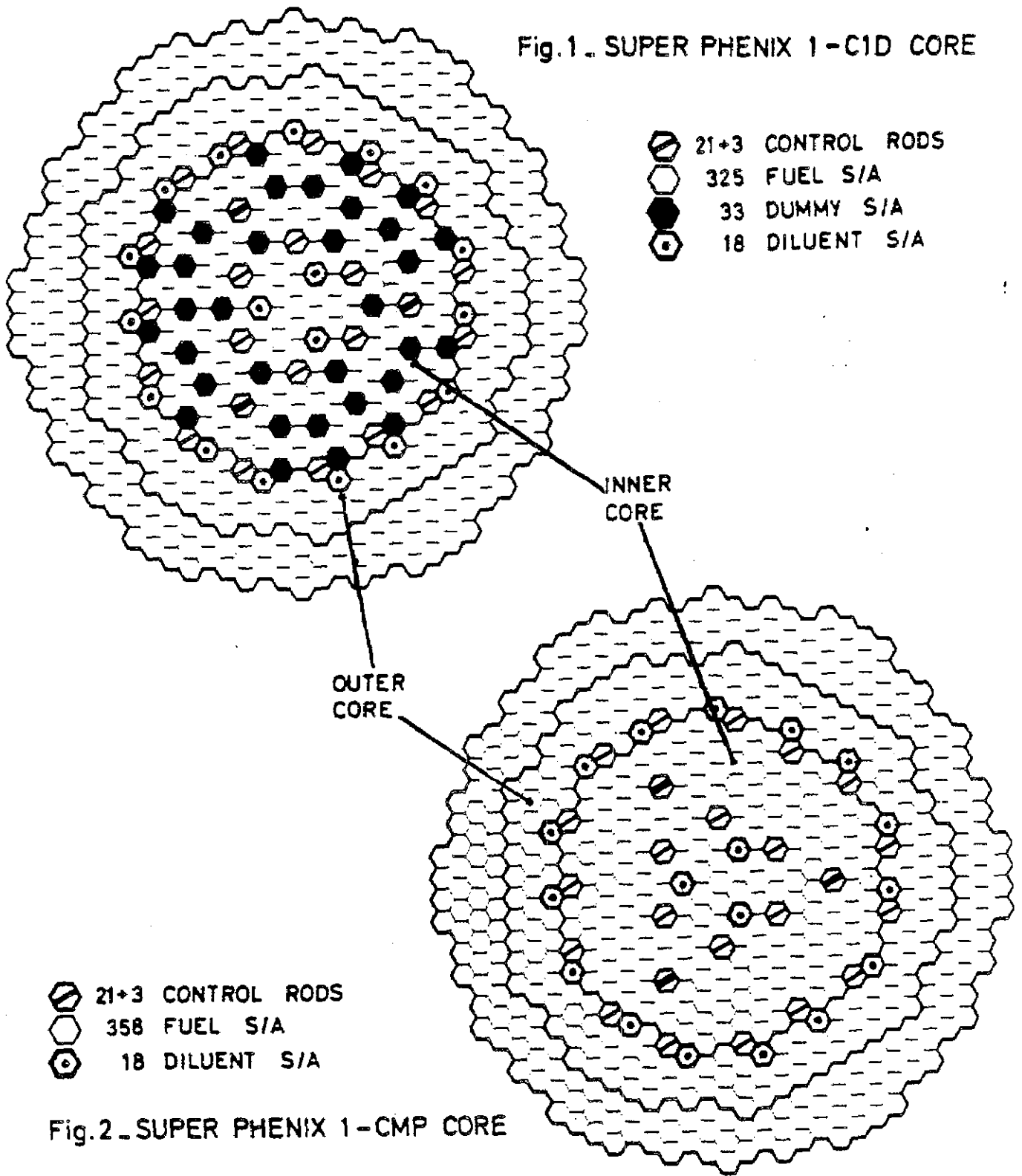


Fig.2 - SUPER PHENIX 1-CMP CORE

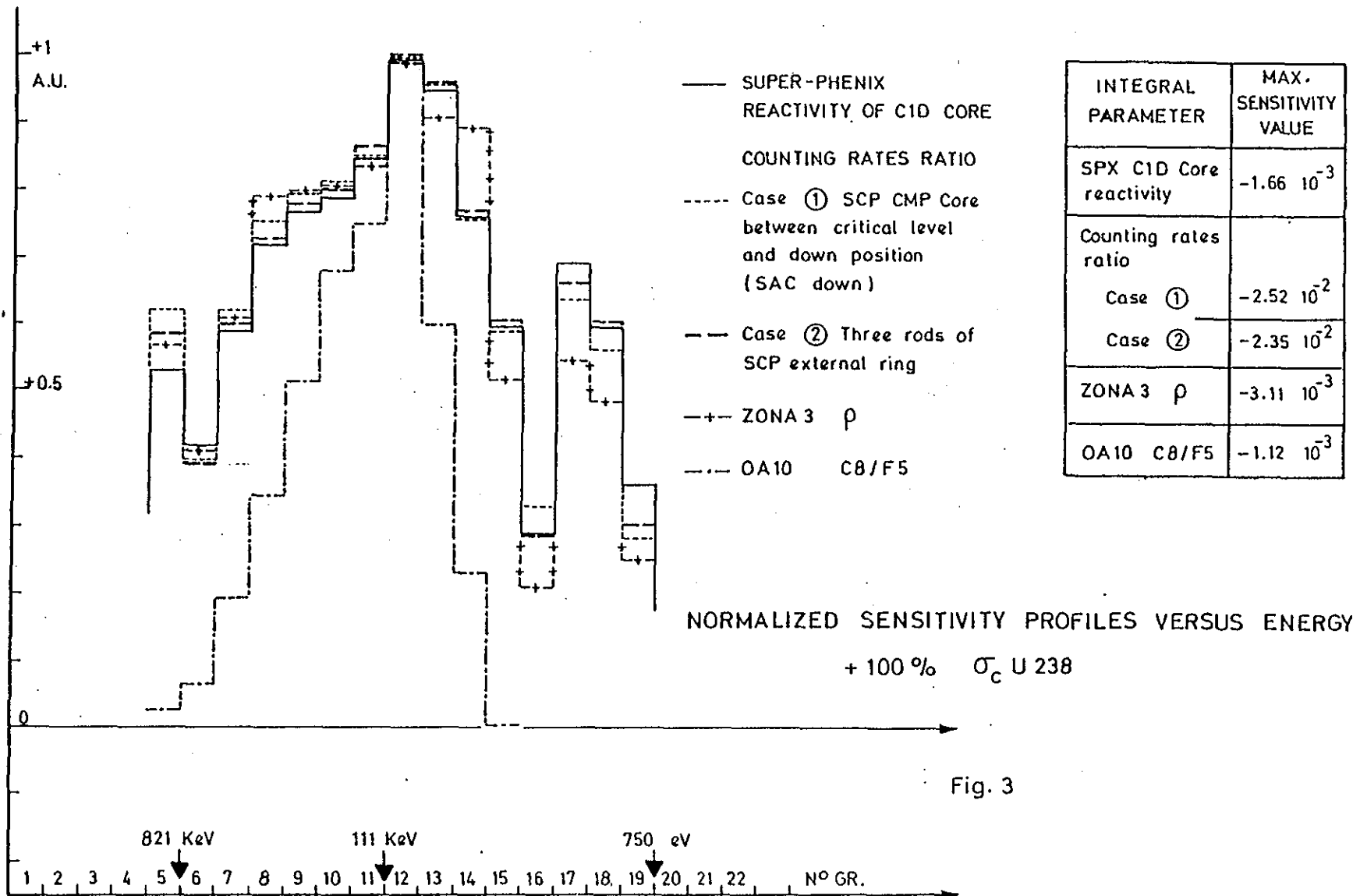
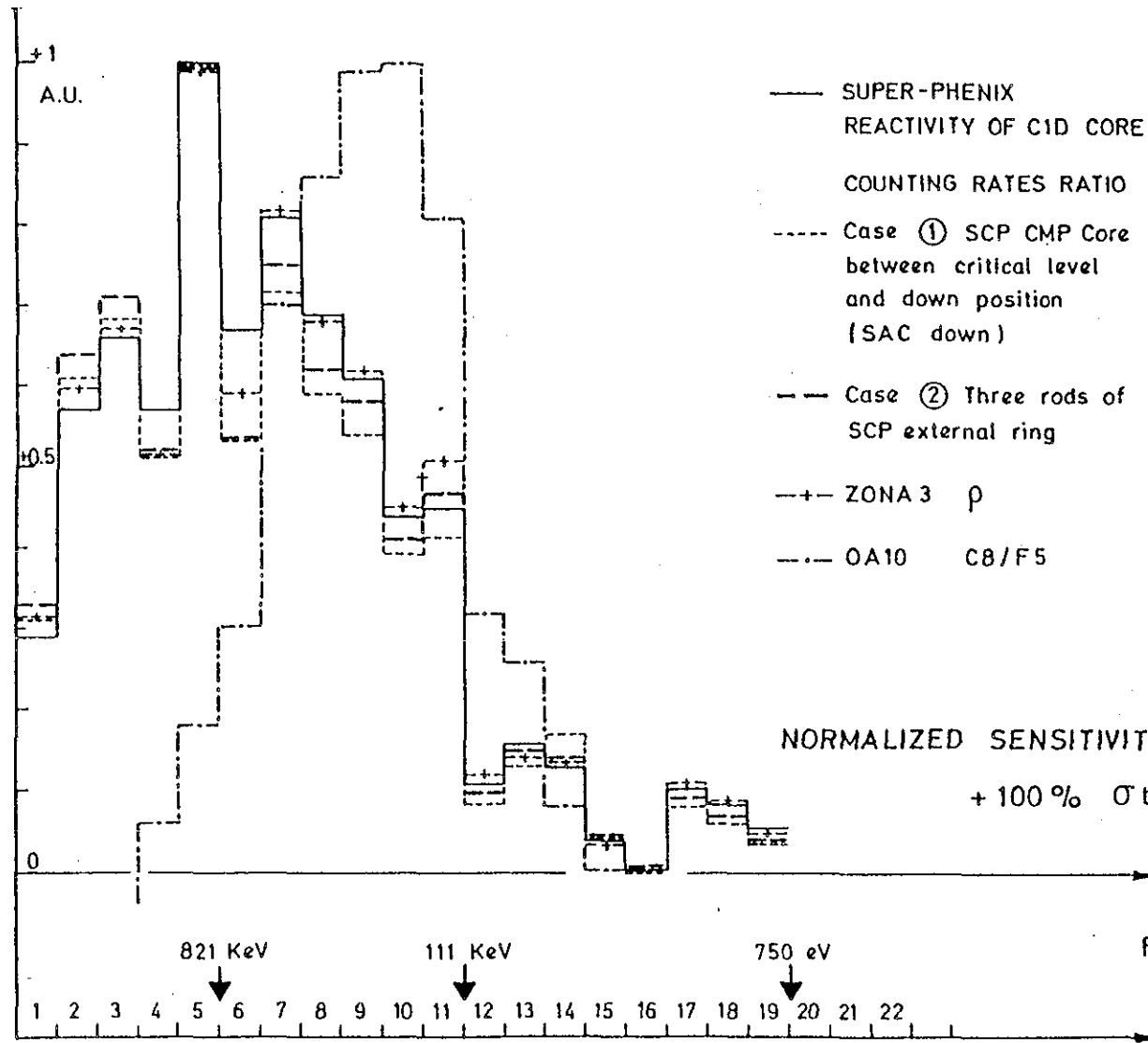


Fig. 3



— SUPER-PHENIX  
REACTIVITY OF C1D CORE

..... COUNTING RATES RATIO

- - - Case ① SCP CMP Core  
between critical level  
and down position  
(SAC down)

- · - Case ② Three rods of  
SCP external ring

- · · ZONA 3  $\rho$

- - - OA10 C8/F5

INTEGRAL PARAMETER	MAX. SENSITIVITY VALUE
SPX C1D Core reactivity	$2.7 \cdot 10^{-3}$
Counting rates ratio	
Case ①	$3.49 \cdot 10^{-2}$
Case ②	$3.27 \cdot 10^{-2}$
ZONA 3 $\rho$	$1.12 \cdot 10^{-2}$
OA10 C8/F5	$2.08 \cdot 10^{-4}$

NORMALIZED SENSITIVITY PROFILES VERSUS ENERGY  
+ 100%  $\sigma$  transport Iron

Fig. 4

Prediction Uncertainty Analysis by use of Sensitivity-based Methodology  
in the Nuclear Designing of a Large Fast Breeder Reactor

T. KAMEI

Nippon Atomic Industry Group Company, Ltd.,  
NAIG Nuclear Research Laboratory  
4-1, Ukishima-cho, Kawasaki-ku, 210 Kawasaki-shi, JAPAN

T. TAKEDA

Osaka University, Faculty of Engineering,  
Nuclear Engineering  
Yamada-oka, Suita-shi, 565 Osaka, JAPAN

K. SHIRAKATA

Power Reactor and Nuclear Fuel Development Corporation  
9-13, 1-chome, Akasaka, Minato-ku, 107 Tokyo, JAPAN

Abstract

The prediction accuracies of key neutronics parameters including burnup property are evaluated with the use of the sensitivity-based methodology for a large liquid-metal fast breeder reactor (LMFBR). The evaluation is performed by the use of the bias-factor method, the cross section adjustment method, and the combined method and the results are compared. The large C/E space dependence of the control rod worth in the ZPPR-10A and -10D are investigated and a new recipe of the cross section adjustment method is proposed. The recipe is useful when the combined method is applied. Error from the misprediction of the space dependence of the control rod in a large-sized reactor is also taken into account in the evaluation of the total prediction uncertainty.

The prediction uncertainties were predicted to be 0.6 % for  $k_{\text{eff}}$ , 4.3 -5.5 % for the control rod worth depending on how precisely bias factor is selected, 2.5 % for the  $^{239}\text{Pu}$  fission rate distribution, 18% for burnup reactivity loss, and 2.5% for breeding ratio.

I. INTRODUCTION

Efforts are made to decrease the prediction uncertainties of reactor performance parameters so that the prediction uncertainties in reactor designing might not necessitate excessive and expensive design margins. In order to decrease the prediction uncertainties of the key neutronics parameters such as criticality, control rod worth, and power distribution, we heavily rely on useful experimental information from mockup criticals.

94050154

The experimental information is utilized into our analysis in two ways. They are (i) the bias factor method<sup>(1)</sup> and (ii) the cross section adjustment method<sup>(2,3)</sup>.

The bias factor method introduces so-called bias factors to correct the difference between integral experimental results and calculated results in mockup criticals. The bias factor is applied directly to the calculated nuclear performance of our reactor of concern. This method is very useful when the nuclear performance of the experimental system is quite similar to that of our specific reactor. However, in reality, even in the case where the mockup system simulates the target system precisely, there still exist certain differences between the two, as in the geometry of the fuels and the plutonium isotopic ratio of their fuels.

The cross section adjustment method is an approach, in which cross sections are adjusted so that the calculation may reproduce the experimental results. With this method, experimental information is incorporated into adjusted group cross sections. The deviations between calculated and experimental results are expected to be narrowed with the use of the adjusted cross sections.

Either method described above can be applied to decrease the prediction uncertainties in nuclear designing of large LMFBR. In the followings, we describe how the prediction uncertainties are decreased when the bias factor method and the cross section adjustment method are applied. The application example of the cross section adjustment method to decrease the C/E space dependence of control rod worth are also described together with the application example to the burnup characteristics.

## II. EVALUATION MODEL OF PREDICTION UNCERTAINTIES OF KEY NEUTRONICS PARAMETERS

In the present section, we describe analytical formulae of the prediction uncertainties of key neutronics parameters when we apply the bias factor method and the cross section adjustment method. The formulae of the prediction uncertainties are given at first for the cases in which the experimental error and the method error in the analysis are neglected. In the latter part of this section, these errors are included and the comparative study of the prediction uncertainties are discussed.

Consider a set of  $n$  microscopic cross sections  $T$  with a covariance matrix  $M$  of order  $(n \times n)$ , where  $n$  is the product of the number of nuclides, the number of groups and the number of reactions. Let there be  $m$  measured integral quantities  $I(m \times 1)$ . The  $I$  may be the effective multiplication factor, control rod worth, or reaction rate distribution, etc. The dependence of  $I$  on a partial change of  $T$  is expressed as the sensitivity matrix  $G(m \times n)$ ;

$$G_{ij} = (\delta I_i / I_i) / (\delta T_j / T_j) \quad (i=1,2, \dots, m; j=1,2, \dots, n) \quad (1)$$

The integral quantities calculated with a reference cross section set  $T_0$  are denoted by  $I_0$ . The integral quantities  $I$  calculated with a cross section set  $T$ , which deviates by  $\delta T$  from  $T_0$ , have the following relation with  $I_0$ :

$$I = I_0(1 + G \cdot \delta T) \quad (2)$$

The covariance of  $(I/I_0)$  is given by

$$\begin{aligned} V &= (GT - GT_0)(GT - GT_0)^t \\ &= G(T - T_0)(T - T_0)^t G^t \\ &= G\delta T \delta T^t G^t \end{aligned} \quad (3)$$

where  $t$  stands for the transpose of the matrix. By Eq.(3), we can evaluate the prediction uncertainties of neutronics parameters when the sensitivity coefficient  $G$  is given. The square root of the diagonal term  $V_{ii}$  of  $V$  is the standard deviation in the integral quantity  $I_i$ . The nondiagonal term  $V_{ij}$  ( $i \neq j$ ) yields the degree of correlation between the errors of  $I_i$  and  $I_j$ . The element  $r_{ij}$  of the correlation matrix is obtained by dividing the element  $V_{ij}$  by the products of standard deviation  $V_{ii}$  and  $V_{jj}$ .

$$r_{ij} = \frac{V_{ij}}{V_{ii}^{1/2} V_{jj}^{1/2}} \quad (4)$$

The above prediction error is for the case when no experimental information is available. When experimental information is available, the prediction uncertainties are decreased by introducing the bias factor method or the cross section adjustment method.

In the bias-factor method, the core performance parameters of a design system are predicted by correcting the calculated value with a ratio of experiment-to-calculated (E/C) values obtained on an experimental system. This method is rather intuitive approach and only a few study has been performed on the evaluation of the prediction uncertainties which still exist after the application of the bias factors<sup>(4)</sup>. The prediction uncertainties are evaluated as is described below.

Let us denote the integral quantities of the experimental system and target system as  $I^{(1)}$  and  $I^{(2)}$ , respectively. The predicted integral quantities  $\tilde{I}^{(2)}$  is obtained as follows,

$$\tilde{I}^{(2)} = I_c^{(2)} \times (E/C) = I_c^{(2)} \times [I_e^{(1)} / I_c^{(1)}], \quad (5)$$



Using Eq.(2) for I, we obtain

$$\tilde{I}^{(2)} = I_0^{(2)} \times [1 + G^{(2)} \delta T] / [1 + G^{(1)} \delta T].$$

Since  $(G\delta T) \ll 1$  in general,  $\tilde{I}^{(2)}$  can be written as

$$\begin{aligned} \tilde{I}^{(2)} &= I_0^{(2)} \{ [1 + G^{(2)} \delta T] \cdot [1 - G^{(1)} \delta T] + O[(\delta T)^2] \} \\ &= I_0^{(2)} \{ 1 + [(G^{(2)} - G^{(1)}) \delta T] + O[(\delta T)^2] \}. \end{aligned}$$

The predicted integral quantity  $\tilde{I}^{(2)}$  for system 2 (target system) scatters around  $I_0^{(2)}$  with covariance matrix  $V$  as

$$V = [G^{(2)} - G^{(1)}] M [G^{(2)} - G^{(1)}]^t. \quad (6)$$

The benefit obtained by utilizing experimental information is evident when Eq.(6) is compared with Eq.(3). We expect that the variance of predicted integral quantities resulting from uncertainties in the cross section set is decreased to

$$[G^{(2)} - G^{(1)}] M [G^{(2)} - G^{(1)}]^t$$

from  $G^{(2)} M G^{(2)t}$ .

It is also possible to decrease the prediction error by using the adjusted cross section library, in which the cross section is corrected<sup>(3)</sup> to yield better agreement with experimental data obtained at critical facilities. The best-estimate cross section set  $T'$  and its covariance matrix  $M'$  can be obtained on the Bayes theorem. The adjusted vector  $T'$  is found as the vector that minimizes  $q^2$ ;

$$\begin{aligned} q^2 &= (T' - T)^t M^{-1} (T' - T) \\ &\quad + (I' - I_e)^t U^{-1} (I' - I_e) \end{aligned} \quad (7)$$

where  $I'$  is the integral quantity obtained by using cross section set  $T'$ ,  $I_e$  is the experimental value, and  $U$  is the uncertainty of C/E values or C-E values. The  $T'$  that minimized  $q^2$  of Eq.(7) and the covariance matrix  $M'$  of a new cross section set  $T'$  are given as

$$T' = T + M' G^t U^{-1} (I_e - I) \quad (8)$$

$$M' = (M^{-1} + G^t U^{-1} G)^{-1} \quad (9)$$

The prediction error in the case where an adjusted cross section library is employed is given by

$$V = G M' G^t \quad (10)$$

This expression is the same with Eq.(3) except that the covariance matrix  $M'$  appears instead of  $M$ . Usually,  $M'$  is much smaller than  $M$ .

Further, we can also apply the bias factor on the results obtained by the cross section adjustment method. We call this method as combined method.

Now we summarize the evaluation formulae of the prediction uncertainties of core performance parameters below. In the expression, the uncertainties from experimental error,  $V_e$ , and method errors,  $V_c^{(1)}$  and  $V_c^{(2)}$ , are also included, where  $V_c^{(1)}$  and  $V_c^{(2)}$  stand for the method errors in the analysis of the experimental mockup and the target system.

- (1) No experimental Information;  $V = GMG^t + V_c^{(2)}$
- (2) Bias Factor Method;  $V = \Delta GM\Delta G^t + \Delta V_c + V_e$ , where  $\Delta V_c$  stands for the standard deviation of the relative error of the calculated values in the mockup criticals and the target system.
- (3) Cross Section Adjustment Method;  $V = GM'G^t + V_c^{(2)}$ , where  $M'$  is the covariance matrix of adjusted cross section set given by Eq.(9).
- (4) Combined Method (Bias factor Method after Cross section Adjustment);  
 $V = \Delta GM\Delta G^t + \Delta V_c + V_e$

In Ref(5), we actually estimated method errors for key neutronics parameters and evaluated the prediction uncertainties of  $k_{eff}$ , control rod worth and power distribution ( $^{239}\text{Pu}$  fission rate distribution) of a 1000 MWe LMFBR. Table I shows the method error and experimental error, and Table II shows the prediction uncertainties for the four prediction methods described above. When no experimental information is given, the prediction uncertainty for  $k_{eff}$  is 2.2 %. The bias factor method, adjustment method and the combined method decrease this error to 0.7, 0.6, and 0.6 % respectively.

For the control rod worth, the use of the combined method reduces the standard deviation from 6.2 to 4.3 %. Thus, the combined method is useful for the reduction of prediction uncertainties. The cross section component for the bias method and the combined method is very small compared to that of the adjustment method. It is noteworthy that the  $\beta_{eff}$  uncertainty reduces to 1.8% in the combined method from 4.0% of the bias factor method. This is because the  $\beta_{eff}$  is included in the adjustment.

The uncertainty of the  $^{239}\text{Pu}$  fission distribution in the core is 3.6 % for the case without any experimental data. This uncertainty is reduced to 2.5 to 2.4 % for the cases No.2 to 4. The remaining error is mainly due to the method error.

The prediction uncertainties shown in Table II include only those associated with cross section uncertainties, experimental error, and analytical errors in the modeling. All these errors categorized above can be evaluated numerically in some way or another. However in some instances, we often encounter the situation in which C/E value largely

differs from unity and we do not understand the reason of the large difference. This situation occurred in the analysis of the control rod worth in ZPPR-10D. The C/E values of the control rod worth in the assembly have strong space dependence, namely the C/E value of the outermost ring is larger than that of the central control rod by about 10 %. The error may come from a modeling error in the analysis or cross section error, but the error source is not clear yet. Therefore, the prediction uncertainty from the C/E space dependence is not included in the table II, but it is discussed in detail in the next Section.

### III. New Application of the Cross Section Adjustment Method to decrease the Space Dependence of Bias Factors for Control Rod Worths and Reaction Rate Distributions in a Large LMFBR Core

A series of critical experiments under collaboration between the USA and Japan has been performed at the Zero Power Plutonium Reactor (ZPPR). The program is called JUPITER which is the acronym of Japan and United States Program of Integral Test and Experimental Research. The analysis was performed by several Japanese organizations of atomic industry under the sponsorship of Power Reactor and Nuclear Fuel Development Corporation (PNC) as well as by the USA organizations. The analysis results obtained in the USA and Japan were brought together and discussed in the JUPITER analysis meeting which was held by the two countries. We came across a problem that the C/E values of control rod worths increase with the distance of rod positions from the core center. Those of the reaction rate distribution also show the same tendency.<sup>(6),(7)</sup> For example in the ZPPR-10A and 10D assemblies, the C/E value of the outer ring control rod worth is 4 to 12 % higher than that of the core center. As for the  $^{239}\text{Pu}$  fission rate distribution, 4 to 5 % space dependence is observed in the C/E values. Such a large space dependence of C/E values brings about difficulty in the accurate prediction of control rod worths and power distribution of the large LMFBR. That pushed us for the endeavor to make the C/E space dependence small.<sup>(8)</sup>

#### III.A. Approach

As a method to investigate the cause of the C/E space dependence, we employed the cross section adjustment method. The adjusted cross section set  $T'$  and the associated covariance matrix  $M'$  are obtained as was described in Eqs.(8) and (9). Usual procedure in the cross section adjustment is to get a cross section set which minimizes the values (C/E - 1.0) of various integral parameters of concern with the weight of the inverse of the uncertainty of each parameter. We refer to this approach as Method 1.

Table III shows the measured and analysis uncertainties considered in the present cross section adjustment. As for the criticality factor prediction, most of the total uncertainty come from the analysis

uncertainties such as the heterogeneity effect prediction uncertainty and the transport effect prediction uncertainty. As for the control rod worth, the main part of the uncertainty in the prediction comes from the delayed neutron data ( $\beta_{eff}$ ) uncertainty. In the adjustment of cross sections, the same covariance matrix M was used as was reported in Ref.(4).

Table IV shows the C/E values before and after the cross section adjustment by Method 1. From the table, we can see that the C/E values for all the neutronics parameters except for the control rod worth becomes very close to unity, in other words good prediction is achieved except for the control rod worth. However, the control rod worth C/E values are not improved yet, and the C/E space dependence of the ZPPR-10D control rod worth still exists, being about 7 % even after the cross section adjustment. Such large space dependence of the control rod C/E values brings about difficult problem in the nuclear designing because the control rod worth is very important quantity in the nuclear designing and such large space dependence is too large to be corrected even by the bias factor method.

In order to improve the large C/E space dependence for the control rod worth, we tried a new application approach of cross section adjustment method. We refer to this method as Method 2. In this method, emphasis is placed on the minimization of the C/E space dependence of reaction rate and control rod worth, and not on the minimization of the (C/E-1.0) for the control rod worth. The merit of this approach exists in the point that the uncertainty of the relative control rod worth is smaller than that of the absolute worth. Table V shows the uncertainties of the calculated and measured values which were used in the cross section adjustment. The uncertainty in the control rod worth in Method 2 is smaller than that in Method 1 because the systematic error such as the uncertainty in the conversion factor from inhour reactivity to  $k_{eff}$  is eliminated in the Method 2. The uncertainty in the conversion factor mainly comes from the delayed neutron fraction uncertainty. We summarize the approach as follows;

Method 1 : The (C/E -1.0) of various integral quantities are minimized  
— conventional method

Method 2 : The space dependence of the C/E values for control rod worth and reaction rate distributions are minimized. As for the other quantities, the (C/E - 1.0) are minimized as in the Method 1  
— our proposed recipe

We apply the Method 2 in the cross section adjustment and show how this method works.

### III.B. Results and Discussion

Table VI shows the C/E values before and after the cross section adjustments. Figure 1 compares the space dependence of control rod worth

C/E values in the ZPPR-10D assembly for non-adjusted case and for the cases in which Methods 1 and 2 are employed. From the table and figure, we can see that the space dependence of C/E values for the control rod worth and reaction rate distribution has been reduced considerably in Method 2, though that of Method 1 is large in the ZPPR-10D control rod worth even after the cross section adjustment.

Table VII shows the amounts of cross section changes in Method 2 for important reactions in a large LMFBR neutronics calculations. It is interesting to see that the capture cross section of  $^{238}\text{U}$  is decreased by 6 to 10 % below 100 keV, the fission cross section of  $^{239}\text{Pu}$  is decreased by about 5 % between 800 to 100 keV and is decreased by about 2 % between 100 keV and 1 keV. These quantities of cross section changes seem to be acceptable level. Table VIII shows the cross section uncertainties after the cross section adjustment by Method 2. The uncertainties of the capture cross section of  $^{238}\text{U}$  and the fission cross section of  $^{239}\text{Pu}$  is remarkably decreased.

Here, we have to note that only the application of the Method 2 does not improve the prediction, because the Method 2 does not try to make the C/E unity. In order for the Method 2 to be useful, we have to apply the bias factor after the Method 2 adjustment - which we refer to as the combined method - or we have to adjust the delayed neutron data at the same time, because the delayed neutron data is a main contributor of the difference of the control rod worth C/E values from unity.

#### IV. REDUCTION OF PREDICTION ERROR OF BURNUP CORE PERFORMANCE PARAMETERS BY THE USE OF CROSS SECTION ADJUSTMENT METHOD

Prediction accuracy of neutronics parameters of a large liquid-metal fast breeder reactor (LMFBR) is now remarkably improving through the accumulation of nuclear data for cross section evaluation, experimental data from critical facilities, and the refinement of calculational model. However, the direct experimental data for the quantities which are connected with burnup property are not obtained at zero power facility. The burnup properties such as burnup reactivity loss, breeding ratio, fissile inventory, and the change of power distribution during burnup are very important in the design of large LMFBRs. Under these circumstances, P. Hammer proposed an international benchmark problem<sup>(9)</sup> for the burnup characteristics of a 3000 MW(thermal) FBR at 1980 Nuclear Energy Agency committee on Reactor Physics (NEACRP), and many organizations had participated. One of the results is shown in Table IX. As seen in the table, the burnup reactivity varies largely from 0.5 to 1.9%  $\Delta k/k$ . The fact that no direct experimental value can be obtained for these burnup characteristics makes the situation difficult. At the present stage, no one knows the true value for the benchmark problem.

Under these backgrounds, we performed a study to evaluate the

prediction error of the burnup characteristics of large LMFBRs.<sup>(10)</sup> We review the study below.

#### IV.A. Evaluation of Prediction Error of Burnup Characteristics of a 1000-MW(electric) LMFBR

We assumed a typical 1000-MWe LMFBR for the evaluation of prediction error of burnup characteristics. The thermal power of the reactor is 2480-MW and the burnup period is 292 equivalent full power days(EFPDs), which corresponds to the one year operation cycle with the availability factor of 80%. The sensitivity coefficients for the burnup properties were calculated by the use of the generalized perturbation method developed by T. Takeda et. al.<sup>(11)</sup>

First, we evaluate the prediction error of burnup properties when our cross section set is used in the prediction without any correction for the predicted value. The prediction error is calculated by Eq.(3). Table X shows the uncertainties for burnup reactivity loss, breeding ratio and fissile plutonium number densities.

The prediction error is about 30% for burnup reactivity loss, and about 5% for the breeding ratio. The prediction error for  $^{239}\text{Pu}$  atomic number density is 1-2% in the core and 2-3% in the blanket, and that for  $^{241}\text{Pu}$  atomic number density is 2-3% and about 15% in the core and blanket, respectively. These error values are larger than generally assumed in the design of a large LMFBR. Now, we evaluate how these error values can be decreased by utilizing experimental information.

Since there is no direct experimental information from critical facilities for burnup properties, we can not employ the bias factor method described in Sec. II. The cross section adjustment method is the best way to decrease the prediction error in this case. In the present study, the experimental data from ZPPR-9 shown in Table XI were employed in the adjustment of our cross section set. Table XI also includes the uncertainty of C/E value for each integral data. This uncertainty includes experimental error as well as the error encountered in the analysis.

The error in the case where an adjusted cross section is employed can be obtained by Eqs.(9) and (10). Here, we selected six cases as the pattern of the employment of experimental data as shown in Table XI. Table XII shows the predicted errors of burnup properties for the above six cases. We find by comparing the results of cases 1 and 3 that the reaction rate ratio of  $^{238}\text{U}(n,\gamma)$  to  $^{239}\text{Pu}(n,f)$  shows remarkable improvement in the prediction of burnup properties. Namely by the employment of the integral data, the prediction error is decreased from 29% to 20% for burnup reactivity loss and from 4.3% to 3.2% for breeding ratio. The error of  $^{239}\text{Pu}$  atomic number density is also decreased. The next large improvement is achieved by the employment of criticality data (case 2). The errors of burnup reactivity loss and breeding ratio are decreased by 4%, and 1.2%,

respectively. The employment of fission rate ratio of  $^{239}\text{Pu}$  to  $^{235}\text{U}$  and  $^{238}\text{U}$  to  $^{235}\text{U}$  show small improvement in the prediction of breeding ratio.

Case 6, in which all the five types of integral data are utilized, shows that the prediction errors are 18% for burnup reactivity loss and 2.2% for breeding ratio. These values are about a half that of the case where nonadjusted cross section set is employed. The prediction error for  $^{239}\text{Pu}$  atomic number density is also remarkably improved. On the other hand, that of  $^{241}\text{Pu}$  atomic number density does not show any improvement because the data which works for the refinement of  $^{241}\text{Pu}$  cross section are not included in the integral data shown in Table XI. Table XIII shows the one standard deviation of the adjusted library together with that of nonadjusted library (case 1). We can see that the errors of  $^{238}\text{U}(n,r)$ ,  $^{239}\text{Pu}(n,\gamma)$ , and  $^{239}\text{Pu}(n,f)$  of adjusted library (cases 2 through 6) are remarkably decreased compared to that of the nonadjusted library.

#### IV.B. Prediction Error of Power Distribution in a Burnt Core

The impact on the power distribution of the prediction error of fissile Pu atomic number densities were also studied. Table XIV shows the uncertainties of the  $^{239}\text{Pu}$  and  $^{241}\text{Pu}$  number densities of burnt core before and after cross section adjustment by case 6. These uncertainties inevitably introduce error in calculated power distribution after the burnup of a reactor. We evaluated these uncertainties by direct calculations and found that the error of the power distribution in a large LMFBRs was about 3 % in the non-adjusted case, but it was reduced to about 1.5% when the cross section set is adjusted by case 6.

### V. CONCLUDING REMARKS

An evaluation study has been performed to predict the present accuracy of neutronics properties of a 1000 MWe LMFBR. In Sec.II, the prediction accuracy of criticality, control rod worth, and reaction rate distribution was quantitatively evaluated by using an evaluation model based on the sensitivity analysis methodology. The evaluation in the Sec.II was focussed on the well defined error sources. In Sec.III, focus was placed on the most puzzling problem of the C/E space dependence of the control rod worth in the ZPPR-10A and -10D. As was discussed in Sec.III, the conventional cross section adjustment method did not show so much improvement in the prediction of the space dependence of the control rod worth. The application of bias factors after the cross section adjustment by Method 2 would be able to decrease the large uncertainty associated with the C/E space dependence of the control rod worth.

A quantitative discussion was also performed of the accuracy of the burnup properties in a large LMFBR. In Sec.IV, we discussed how the prediction error would be decreased when cross section set was adjusted by use of experimental data such as criticality and reaction rate ratios.

Table XV summarizes prediction uncertainties of key neutronics parameters including those of the burnup properties. As is seen in the table, the combined method (application of bias factors after the cross section adjustment) would be most suitable to decrease the prediction uncertainties. However, it is very important to make clear the cause of the puzzling large C/E space dependence of the control rod worth. We hope that effort will be made on this matter from experimental side and analysis side.

### References

- (1) For example, see S. IJIMA, A. SHIMIZU, and I. INOUE, "The analysis of FCA Critical Experiments and Its Application to 'JOYO' Nuclear Design, "Proc. Int. Symp. Physics of Fast Reactors, Tokyo, Japan, October 16-23, 1973, Vol.III, p.1334, International Atomic Energy Agency(1973)
- (2) M. HUMI, J.J. WAGSCHAL, and Y. YEIVIN, "Multigroup Constants from Integral Data", Proc. 3rd Int. Conf. Peaceful Uses Atomic Energy, 2, 398, United Nations, New York(1964)
- (3) J. B. DRAGT, et al., Nucl. Sci. Eng. 62, 117 (1977)
- (4) T. KAMEI, T. YOSHIDA, Nucl. Sci. Eng. 84,83 (1983)
- (5) T. TAKEDA, A. YOSHIMURA, T. KAMEI, K. SHIRAKATA, "Prediction Uncertainty Evaluation Methods of Core Performance Parameters in Large LMFBRs", Proc. the 1988 Int. Reactor Physics Conf., Sept 18-22, 1988, Jackson Hole, Wyoming, USA(1988)
- (6) S. CARPENTER, et al., "Experimental Studies of 6000-litre LMFBR Cores at ZPPR", Proc. of the Topical Meeting - 1980 Advances in Reactor Physics and Shielding, 521-534, Sept 14-17, 1980, Sun Valley, Idaho, USA (1980).
- (7) M. YAMAMOTO, et al., " Analysis of Large Conventional LMFBR Core Critical Experiments and Their Implication to Design Methods", Proc. of the Topical Meeting on Reactor Physics and Shielding, Volume II, 773-787, Sept 17-19, 1984, Chicago, Illinois, USA (1984)
- (8) T. KAMEI and Y. KATO, J. Nucl. Sci. Technol., 22[12],1025(1985)
- (9) P. HAMMER, "Proposal for Burnup Calculation Applied to the NEACRP Fast Breeder Benchmark", NEACRP-A\_439, Nuclear Energy Agency Committee on Reactor Physics(1980)
- (10) T. KAMEI, T. YOSHIDA, T. TAKEDA, T. UMANO, Nucl. Sci. Eng., 91,11(1985)
- (11) T. TAKEDA and T. UMANO, Nucl. Sci. Eng., 91, 1(1985)



Table I Uncertainty of Neutronics Parameters due to Method Error and Experimental Error ( in %, 1 $\sigma$  )

Error Item	Criticality		Control Rod Worth		Reaction Rate Distribution	
	A	B	A	B	A	B
Analysis Error						
Processing of Nuclear Data	0.3		3.0		1.0	
Cell(Assembly) Modeling	0.3	0.2	2.0	1.0	1.0	1.0
Neutron Streaming	0.2	0.1	1.0	1.0	1.0	1.0
Cell Interaction	0.1	0.0	2.0	1.0	1.0	0.0
Core Calculation	0.1		1.0		1.0	
Total	0.5	0.4	4.4	3.6	2.2	2.0
Experimental Error	0.04		4.3*		1.0	

A : Mockup Critical, B : Typical 1000 MWe LMFBR

\* :  $\beta_{eff}$  uncertainty of 4.0% included

Table II Prediction Uncertainty of Core Performance Parameters of a Target 1000 MWe FBR ( not include C/E space dependence of control rod worth and reaction rate distribution ) ( in %, 1 $\sigma$  )

Component	Integral Data	Method		
	Not-available	Bias Factor	Adjustment	Bias After Adjustment
$k_{eff}$				
Experimental Error	---	0.04	---	0.04
Method Error	0.4	0.44	0.4	0.44
Cross Section Error	2.2	0.5	0.5	0.4
Total	2.2	0.7	0.6	0.6
Control Rod Worth (Central Rod)				
Experimental Error	---	1.6	---	1.6
Method Error	3.6	3.5	3.6	3.5
Cross Section Error	5.0	0.8	3.2	0.7
$\beta_{eff}$ Error	---	4.0	---	1.8
Total	6.2	5.6	4.8	4.3
$^{239}\text{Pu}$ Fission Rate Distribution				
Experimental Error	---	1.0	---	1.0
Method Error	2.2	2.2	2.2	2.2
Cross Section Error	2.8	0.8	0.8	0.4
Total	3.6	2.5	2.3	2.4

Table III Uncertainties of the Measured and Calculated Integral Quantities in Method 1 ( %, 1  $\sigma$  )

Item	Criticality Factor	Control Rod Worth	<sup>239</sup> Pu(n,f) Rate Distribution	Reaction Rate Ratio C <sup>28</sup> /F <sup>49</sup>	Rate Ratio F <sup>28</sup> /F <sup>49</sup>
Measured	0.04	4.3*	1	2	3
Calculated	0.5	3	2	2	2
Total	0.5	5	2	3	4

Note \*) Include the uncertainty (4 %) of the conversion factor from inhour to  $k_{eff}$  associated with delayed neutron data,  $\beta_{eff}$  uncertainty

Table IV C/E Values Before and After Cross Section Adjustment for Various Integral Quantities (Method 1)

	Before Adjustment		After Adjustment Method 1	
	C/E	Space Dependence	C/E	Space Dependence
<b>Criticality Factor</b>				
ZPPR- 9	.9994		1.001	
ZPPR-10A	.9967		1.000	
ZPPR-10D	.9961		1.000	
<b>Reaction Rate Ratio</b>				
C <sup>28</sup> /F <sup>49</sup>	1.060		1.009	
F <sup>28</sup> /F <sup>49</sup>	.988		.998	
<b>Control Rod Worth</b>				
ZPPR-10A				
Central Rod	.951	1.000	.994	1.000
1st Ring Rods	.947	.996	.983	.989
2nd Ring Rods	.988	1.039	.989	.995
ZPPR-10D				
Central Rod	.943	1.000	.991	1.000
1st Ring Rods	.954	1.012	.997	1.005
2nd Ring Rods	1.003	1.064	1.025	1.034
3rd Ring Rods	1.064	1.128	1.061	1.071
<b><sup>239</sup>Pu(n,f) Rate Distribution</b>				
ZPPR-10A				
Core center	.981	1.000	.995	1.000
Mid Inner Core	.980	1.012	.990	.995
Outer Core	1.016	1.037	1.006	1.011
ZPPR-10D				
Core center	.986	1.000	1.002	1.000
Mid Inner Core	.977	1.018	.987	.985
Outer Core	1.008	1.047	.996	.993

Table V Uncertainties of the Measured and Calculated  
Integral Quantities (%, 1 $\sigma$ )

Method	Criticality Factor	Control Rod Worth	<sup>239</sup> Pu(n,f) Rate Distribution	Reaction Rate Ratio C <sup>28</sup> /F <sup>49</sup>	Reaction Rate Ratio F <sup>28</sup> /F <sup>49</sup>
1	0.5	5	2	3	4
2	0.5	2	2	3	4

Table VI C/E Values Before and After Cross Section Adjustment for Various  
Integral Quantities

	Before Adjustment		After Adjustment			
	C/E	Space Dependence	Method 1 C/E	Method 1 Space Dependence	Method 2 C/E	Method 2 Space Dependence
<b>Criticality Factor</b>						
ZPPR-9	.9994		1.001		1.002	
ZPPR-10A	.9967		1.000		1.000	
ZPPR-10D	.9961		1.000		1.000	
<b>Reaction Rate Ratio</b>						
C <sup>28</sup> /F <sup>49</sup>	1.060		1.009		1.019	
F <sup>28</sup> /F <sup>49</sup>	.988		.998		.992	
<b>Control Rod Worth</b>						
ZPPR-10A						
Central Rod	.951	1.000	.994	1.000	1.029	1.000
1st Ring Rods	.947	.996	.983	.989	1.012	.983
2nd Ring Rods	.988	1.039	.989	.995	.993	.965
ZPPR-10D						
Central Rod	.943	1.000	.991	1.000	1.034	1.000
1st Ring Rods	.954	1.012	.997	1.005	1.036	1.002
2nd Ring Rods	1.003	1.064	1.025	1.034	1.048	1.014
3rd Ring Rods	1.064	1.128	1.061	1.071	1.062	1.027
<b><sup>239</sup>Pu(n,f) Rate Distribution</b>						
ZPPR-10A						
Core center	.981	1.000	.995	1.000	1.002	1.000
Mid Inner Core	.980	1.012	.990	.995	1.009	1.007
Outer Core	1.016	1.037	1.006	1.011	1.002	1.000
ZPPR-10D						
Core center	.986	1.000	1.002	1.000	1.013	1.000
Mid Inner Core	.977	1.018	.987	.985	1.020	1.007
Outer Core	1.008	1.047	.996	.993	1.013	1.000

Table VII Cross Section Changes of Important Reactions  
( Method 2) (%)

Reaction	Group†	Cross section changes
$\sigma_f^{49}$	1	-2.4
	2	-5.1
	3	-2.2
	4	1.7
$\sigma_c^{49}$	1	2.8
	2	2.6
	3	-0.8
	4	-2.6
$\sigma_f^{28}$	1	-3.0
	1	-1.2
$\sigma_c^{28}$	2	-1.3
	3	-5.8
	4	-9.6
	4	-9.6
$\sigma_{in}^{28}$	1	-10.3
	2	-10.7

† Lower energy of each group: 800, 100, 1 keV and 0.025 eV

Table VIII Cross Section Uncertainties Before and After Cross Section Adjustment  
(Method 2) (% ,  $1\sigma$ )

Reaction	Group†	Cross section uncertainties	
		Before adjustment	After adjustment
$\sigma_f^{49}$	1	3.0	2.2
	2	5.0	2.8
	3	6.0	4.0
	4	6.0	5.1
$\sigma_c^{49}$	1	15.0	14.8
	2	15.0	14.4
	3	15.0	12.9
	4	15.0	12.5
$\sigma_f^{28}$	1	10.0	6.4
	1	15.0	13.2
$\sigma_c^{28}$	2	15.0	11.9
	3	10.0	6.8
	4	10.0	7.9
	4	10.0	7.9
$\sigma_{in}^{28}$	1	20.0	15.4
	2	20.0	16.7

† Lower energy of each group: 800, 100, 1 keV and 0.025 eV

**Table IX** Reactivity Loss of 365-Day Burnup for a 3000-MW(thermal) LMFBR – An International Benchmark for Burnup Calculation

Nuclear Data File	Reactivity Loss	Organization
JENDL-2 ENDF/B-IV	1.5% $\Delta k/k$ 0.5 to 0.7	Japan Atomic Energy Research Institute Swiss Federal Institute for Reactor Research, Comitato Nazionale per l'Energia Nucleare, Australian Atomic Energy Commission
ENDF/B-V	1.0	Argonne National Laboratory
KEDAK-3	1.9	Kernforschungszentrum Karlsruhe
CARNAVAL-IV	1.3	Commissariat à l'Energie Atomique

**Table X** Prediction Uncertainty of 1000-MW(electric) Core Burnup Characteristics (Nonadjusted Library) – Uncertainty for 292 EFPD Burnup

A. Burnup Reactivity and Breeding Ratio

Burnup Reactivity  $2.557 \times (1 \pm 0.290)\% \Delta K/K'$   
Breeding Ratio  $1.204 \times (1 \pm 0.043)$

B. Fissile Number Density [End of Equilibrium Cycle (EOEC)]

Region	$^{239}\text{Pu}$ ( $\times 10^{20}$ atom/cm <sup>3</sup> )	$^{241}\text{Pu}$ ( $\times 10^{20}$ atom/cm <sup>3</sup> )
Inner core	$8.435 \times (1 \pm 0.019)$	$1.271 \times (1 \pm 0.031)$
Outer core	$9.704 \times (1 \pm 0.012)$	$1.733 \times (1 \pm 0.021)$
Radial blanket-1	$1.874 \times (1 \pm 0.031)$	$0.001 \times (1 \pm 0.164)$
Radial blanket-2	$0.636 \times (1 \pm 0.016)$	$-0 \times (1 \pm 0.162)$
Axial blanket-1	$2.286 \times (1 \pm 0.027)$	$0.004 \times (1 \pm 0.142)$
Axial blanket-2	$1.373 \times (1 \pm 0.019)$	$-0 \times (1 \pm 0.146)$

Table XI Error for Each Integral Datum (1 $\sigma$ )

	Error (%)
$k_{eff}$	0.5
$C^{238}/F^{235}$	3
$F^{238}/F^{235}$	4
$F^{49}/F^{235}$	3
Doppler (UO <sub>2</sub> sample)	5

Table XII Prediction Uncertainty of 1000-MW(electric) Core Burnup Characteristics (Adjusted Library)\*

Case Number	Integral Data Employed	Burnup Reactivity	Breeding Ratio	<sup>239</sup> Pu Number Density at 292 EFPD Operation (%)			
				Inner Core	Outer Core	Radial Blanket (Core Side)	Axial Blanket (Core Side)
1	None	29.0	4.3	1.9	1.2	3.1	2.7
2	Only $k_{eff}$	25.4	3.1	1.4	1.0	1.6	1.6
3	Only $C^{238}/F^{235}$	19.8	3.2	1.4	0.9	2.1	1.8
4	$C^{238}/F^{235}$ , $F^{49}/F^{235}$ , $F^{238}/F^{235}$	19.1	2.6	1.1	0.8	1.5	1.4
5	$k_{eff}$ , $C^{238}/F^{235}$ , $F^{49}/F^{235}$ , $F^{238}/F^{235}$	19.1	2.5	1.1	0.8	1.2	1.2
6	$k_{eff}$ , $C^{238}/F^{235}$ , $F^{49}/F^{235}$ , $F^{238}/F^{235}$ , Doppler	17.9	2.2	1.0	0.6	1.1	1.1

\*The prediction uncertainty of the <sup>241</sup>Pu atomic number density was hardly changed from the figures shown in Table IX for cases 2 through 6.

Table XIII One Standard Deviation of Adjusted Library (%)

Reaction Group <sup>a</sup>	Case 1 (None)	Case 2 ( $k_{eff}$ )	Case 3 ( $C^{28}/F^{25}$ )	Case 4 ( $C^{28}, F^{28}, F^{49}$ Ratio to $F^{25}$ )	Case 5 (All Except for Doppler)	Case 6 (All)
1 <sup>235</sup> U CAP 3G	9.0	9.0	9.0	9.0	9.0	9.0
2 <sup>235</sup> U CAP 4G	7.0	7.0	7.0	7.0	7.0	7.0
3 <sup>235</sup> U FIS 2G	3.0	3.0	3.0	2.9	2.9	2.9
4 <sup>235</sup> U FIS 3G	3.0	3.0	2.9	2.8	2.7	2.7
5 <sup>235</sup> U FIS 4G	3.0	3.0	2.9	2.8	2.8	2.8
6 <sup>238</sup> U CAP 1G	5.6	5.1	4.3	4.2	4.2	4.2
7 <sup>238</sup> U CAP 2G	7.5	6.9	5.9	5.8	5.8	5.8
8 <sup>238</sup> U CAP 3G	7.6	6.5	3.9	3.9	3.7	3.7
9 <sup>238</sup> U CAP 4G	8.6	7.4	4.8	4.7	4.6	4.6
10 <sup>238</sup> U FIS 1G	5.0	4.9	5.0	4.4	4.4	4.4
11 <sup>238</sup> U TRA 1G	2.0	2.0	2.0	2.0	2.0	2.0
12 <sup>238</sup> U TRA 2G	2.0	2.0	2.0	2.0	2.0	2.0
13 <sup>238</sup> U TRA 3G	2.0	2.0	2.0	2.0	2.0	2.0
14 <sup>238</sup> U SLD 1G	20.0	19.2	19.9	12.4	12.4	12.4
15 <sup>238</sup> U SLD 2G	20.0	19.6	19.9	15.3	15.3	15.3
16 <sup>238</sup> U SLD 3G	20.0	19.9	20.0	18.2	18.2	18.2
17 <sup>239</sup> Pu CAP 1G	15.0	15.0	15.0	15.0	14.9	14.8
18 <sup>239</sup> Pu CAP 2G	15.0	14.9	15.0	15.0	14.5	14.3
19 <sup>239</sup> Pu CAP 3G	15.0	14.6	15.0	14.9	13.3	11.1
20 <sup>239</sup> Pu CAP 4G	15.0	14.6	15.0	14.9	13.2	9.4
21 <sup>239</sup> Pu FIS 1G	3.0	2.6	3.0	2.6	2.4	2.3
22 <sup>239</sup> Pu FIS 2G	5.0	4.0	5.0	3.9	3.4	2.9
23 <sup>239</sup> Pu FIS 3G	6.0	4.5	6.0	4.2	3.5	3.3
24 <sup>239</sup> Pu FIS 4G	6.0	5.3	6.0	5.1	4.9	4.8

<sup>a</sup>Here, CAP = capture, FIS = fission, TRA = transport, and SLD = slowing down.

Table XIV Uncertainties of the Number Densities  
After One-Cycle Burnup

Region	Item			
	Before Adjustment		After Adjustment	
	<sup>239</sup> Pu (%)	<sup>241</sup> Pu (%)	<sup>239</sup> Pu (%)	<sup>241</sup> Pu (%)
Inner core	±1.92	±3.06	±0.96	±3.04
Outer core	±1.23	±2.09	±0.64	±2.05

Table XV Summary of the Prediction Uncertainty of a 1000 MWe LMFBR  
(in %,  $1\sigma$ )

Parameter	Integral Data Not available	Bias Factor	Adjustment	Bias Factor After Adjustment
Keff	2.2	0.7	0.6	0.6
Control Rod Worth				
Average Rod	6.2	5.6	4.8	4.3
Space Dependence	6.4 <sup>a</sup>	<6.4 <sup>b,c</sup>	6.1 <sup>a</sup>	<3.5 <sup>b,c</sup>
Total	8.9	<8.5 <sup>b</sup>	7.8	<5.5 <sup>b</sup>
Reaction Rate Distribution <sup>d</sup>	3.9	<3.0 <sup>b</sup>	2.6	<2.5 <sup>b</sup>
Burnup Reactivity	30		18	
Breeding Ratio	5		2.5	
239Pu Inventory				
Core	2		1	
Blanket	3		1	
241Pu Inventory				
Core	3		3	
Blanket	15		15	
Power Peaking Factor in Core	3		1.5	

Note a) the largest deviation from unity of control rod worth C/E values of ZPPR-10A and -10D in Table VI

b) depend on how precisely bias factors are applied

c) the deviation from unity of the average of the maximum and the minimum of the control rod worth C/E values of ZPPR-10A and -10D in Table VI

d) include space dependence uncertainty



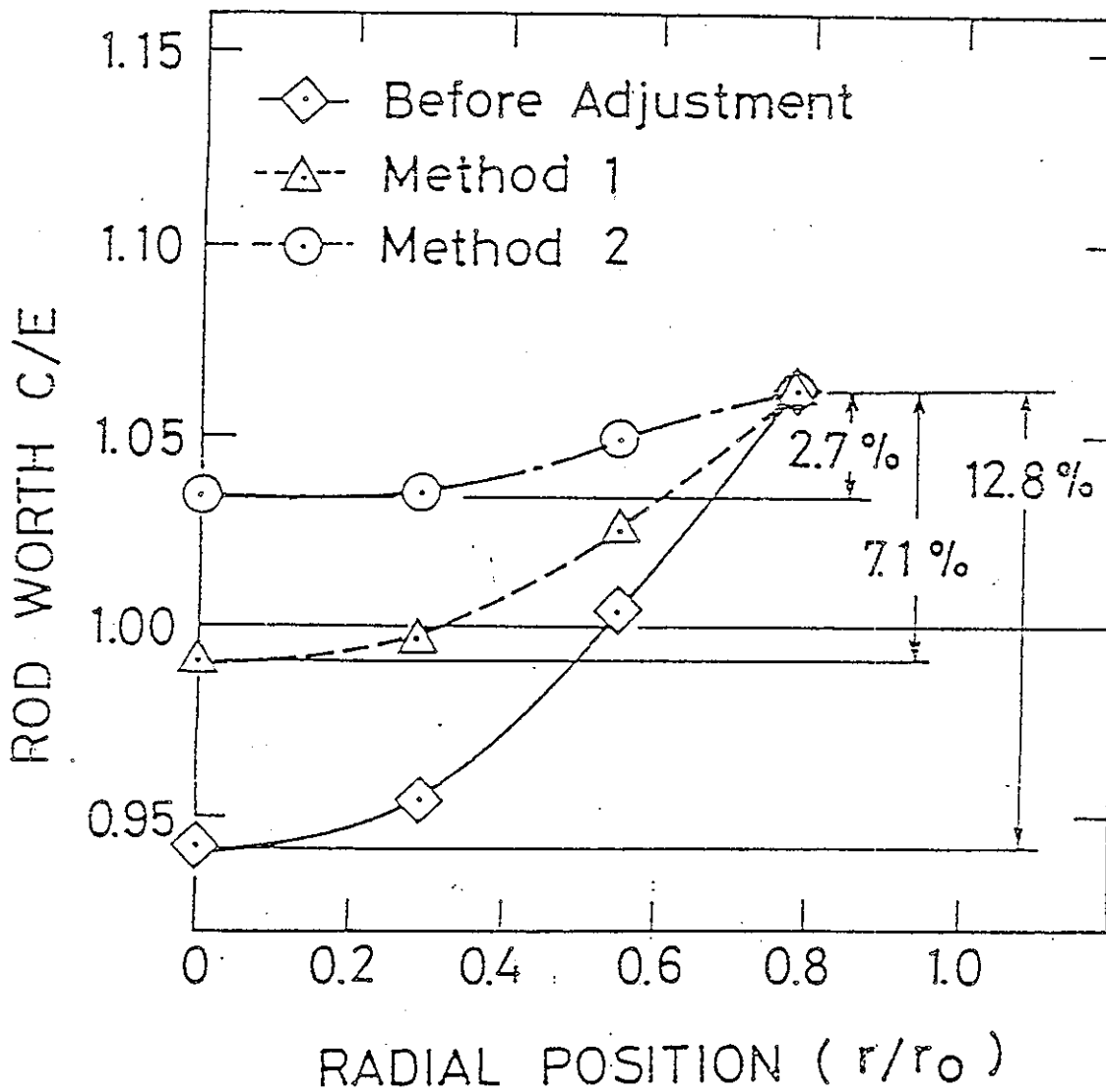


Fig. 1 Spatial Variation of Control Rod Worth C/E Values in the ZPPR 10D Assembly  
 — before and after adjustment —  
 $r$  : radius of bank rods inserted  
 $r_0$  : core radius

**SESSION III**

**September 24, 1988**

**Chairman: K. Sirakata (PNC, Japan)**

**Rapporteur: J. Rowlands (UKAEA AEE, U.K.)**



SPECIALIST'S MEETING ON THE  
APPLICATION OF CRITICAL EXPERIMENTS AND OPERATING DATA TO  
CORE DESIGN VIA FORMAL METHODS OF CROSS-SECTION DATA ADJUSTMENT  
JACKSON-HOLE, SEPTEMBER 23/24, 1988

RECENT INTEGRAL EXPERIMENTS DESIGNED TO IMPROVE  
HIGHER ACTINIDE DATA TO MEET DESIGN TARGET ACCURACIES

A. D'ANGELO\* - M. SALVATORES\*\*

\* ENEA-CASACCIA

\*\* CEA-IRDI/DEDR/DRP/SPRC CADARACHE

ABSTRACT :

Data adjustments are made to meet target accuracies on integral design parameters. A typical case is the reactivity loss per cycle. This parameter is of particular relevance for the optimization of future LMFBRs.

To meet a stringent target accuracy, it is necessary to improve data (and uncertainties) on both the heavy isotope and the fission products component of the reactivity effect.

For the heavy isotopes component, integral experiments have been performed on MASURCA, to obtain informations on the reactivity/atom of the Pu isotopes and of U-238. Moreover, extensive fuel pin and pure sample irradiation programs in PHENIX, have given complementary informations on these isotopes.

This paper describes :

- a) The adjustment procedure used to exploit these informations.
- b) The results obtained.
- c) The residual uncertainties on the reactivity loss per cycle, due to the heavy isotope component.

## 1 - INTRODUCTION

Integral experiments have an important role in the reduction of the uncertainties associated to the LMFBR's design parameters.

In the past the uncertainty on the calculated LMFBR's parameters has been reduced adjusting the CARNAVAL "formulaire" on a very large number of experimental results / 1 /.

In that paper we have indicated the general strategy that has been followed.

In practice, when a particular experiment type, used to perform cross-section adjustments, is related directly to a design parameter (e.g. the  $K_{eff}$ ), the recalculated E-C values are used to define bias factors (and uncertainties) on that integral parameter.

For other integral parameters (like control rod worths or reactivity loss per cycle), not directly used in the adjustment process, or not directly available in critical facilities, bias factors and uncertainties are deduced "independently", or "a posteriori" with respect to adjustments. In particular, estimated residual uncertainties on one-group cross-sections, have been used to deduce the uncertainty on the heavy isotope component of the reactivity loss / 1 /. This procedure can be penalizing and the resulting uncertainties are fairly large. Specific adjustment procedures can than be envisaged.

In this paper we will show how the reactivity loss per cycle uncertainty determination can be further improved using the high precision irradiation experiments performed in the PHENIX reactor and the "ad hoc" performed fuel replacement experiments in the MASURCA critical facility.

In the first part of this paper we will justify the choice of the experimental results and we will report the sensitivities of the calculated values to the heavy isotopes cross-sections. Afterwards, the adjustment results are presented. Finally we will verify both the consistency among the different experiment informations and the importance of the calculated reactivity loss per cycle improvement.

## 2 - EXPERIMENTAL RESULTS

Experimental results have been chosen in order to reduce the reactivity loss per cycle uncertainty.

For that reason we will shortly present them, stressing their role in the adjustment procedure. More detailed description of the experimental techniques and their uncertainties can be found in the appropriate references.

### 2.1 - BALZAC-HI - Experimental results

The "HI" (heavy isotopes) phase of the BALZAC experimental program in the MASURCA critical facility / 2, 3 / has been designed in order to give information on the reactivity/atom of the Pu isotopes and of U-238.

Starting from a critical "reference" configuration, three substitutions of the central fuel zone in a simple core configuration have been realised, leaving the same fuel enrichment and cell structure but using oxide fuel pins from different stocks, characterized by different Pu vectors.

As the fuel stock used for the reference configuration was the most reactive one, the three following configurations ("HI1", "HI2" and "HI3") were subcritical. The reactivity of these configurations has been obtained by MSM measurements, relative to a reference calibration reactivity.

A fourth configuration has been also realised in order to have information on the uranium oxide reactivity. In this configuration ("HI4") the plutonium fuel stock used was the same of the "HI2" configuration but the amount of  $UO_2$  has been increased.

With this procedure, the information about the heavy isotopes reactivity has been obtained with a very small perturbation of the flux (real and adjoint) which is found at the core center. We have verified the possibility of neglecting the effects of the isotopes other than the replaced ones (indirect effects), in the analysis of discrepancies between calculated and experimental values.

Table 1 shows the sensitivity coefficients of the calculated configuration reactivities to the average cross-sections of the heavy isotopes.

We can see that the sensitivity coefficients of the plutonium fission cross-section are generally higher than the sensitivities of the capture cross-sections. For that reason the BALZAC results should be completed, for the cross-section adjustment, by pure sample irradiation experimental results, which are mainly sensitive to capture cross-sections. Table 2 shows the discrepancies existing between experimental and calculated BALZAC-HI reactivity values, when the CARNAVAL-IV "formulaire" is used.

The same table shows both the uncertainties and their correlations obtained taking into account the different uncertainty sources :

- a) Experimental uncertainty.
- b) Fuel density uncertainty.
- c) Effective beta uncertainty.

A correlation matrix has been obtained from the simple correlations existing between the different uncertainty sources (B matrix), using the correlation matrix transformation law :

$$B_y = S^T B S$$

Where S is the sensitivity matrix of the integral measurement to the different measured and calculated parameters, which are sources of uncertainty.

## 2.2 - PROFIL irradiation experimental results

The PROFIL separate pure isotope irradiation experiments have been performed in the PHENIX reactor in two phases (PROFIL 1 and PROFIL 2) / 4, 5 /.

Separate isotopes were contained in small containers of stainless steel ; these containers were piled up in a standard clad. For each isotope, many containers were irradiated in order to test the consistency of the results and to validate the measurements.

After irradiation, each container was extracted out of the clad, put into solution and analysed by mass spectrometry.

For what concerns the cross-section adjustment, the pure separate isotope irradiation experimental information is quite "orthogonal" to the BALZAC-HI one. In fact the results concerning the sample composition before and after irradiation can be directly interpreted in terms of mean capture cross-section values / 4, 5 /.

For the reactivity loss per cycle uncertainty reduction, the most important results are those for Pu-239, Pu-240, Pu-241 and U-238 samples, interpreted in terms of the mean capture cross-section of these isotopes.

Table 3 shows the discrepancies existing between the experimental PROFIL mean cross-sections and the CARNAVAL-IV calculated ones.

The correlation between the uncertainties are mainly due to the interpretation of the original reaction rate ratio results ( $\sigma_f$  U-235 used as normalisation) as mean capture cross-sections.

### 2.3 - TRAPU experimental results

The TRAPU experiments consisted in a six cycles irradiation in the PHENIX reactor of mixed-oxide pins. These pins contained plutonium with different isotopic compositions.

The following table shows the relative compositions of the three types of plutonium which were used.

Experiment	% Pu isotope composition				
	Pu-238	Pu-239	PU-240	Pu-241	Pu-242
TRAPU 1	0.1	73.3	21.9	4.0	0.7
TRAPU 2	0.8	71.4	18.5	7.4	1.9
TRAPU 3	0.2	34.0	49.4	10.0	6.4

TRAPU FUEL PINS RELATIVE COMPOSITIONS



After irradiation, small samples were cut out of the experimental pins, put into solution, then analysed. Not irradiated pellets of each fabrication were also analysed for an accurate determination of the initial composition.

We have used nine TRAPU experimental results in our CARNAVAL-IV data adjustment. In particular the final (after irradiation) atom density ratios  $\frac{\text{Pu-239}}{\text{U-238}}$ ,  $\frac{\text{Pu-240}}{\text{U-238}}$ ,  $\frac{\text{Pu-241}}{\text{U-238}}$  of the three different irradiated fuels.

Table 4 shows the sensitivity coefficients of the calculated TRAPU results to the data to be adjusted.

We can see that the calculated TRAPU results are generally sensitive to both the capture (U-238) and the fission (Pu-239 and Pu-241) cross-sections.

Moreover their uncertainties (table 5) are relatively small.

Uncertainties and correlations reported in table 5, take into account two kinds of sources :

a) Experimental uncertainties (on Pu-239/U-238, PU-240/Pu-239 and on PU-241/Pu-239 measurements).

b) The total fluence (used in burn-up calculations) renormalisation to the quantity of Nd-148 fission product measured after the pin irradiation.

### 3 - ADJUSTMENT AND UNCERTAINTY ANALYSIS

The discrepancies (tables 2, 3 and 5) between experimental results and CARNAVAL-IV calculated results (generally lower than one standard deviation) show that the CARNAVAL-IV "formulaire" is well adjusted and this result is consistent with other performance studies / 1 /.

In principle we could not readjust the CARNAVAL-IV cross-section, because a very large number of anticorrelations (particularly in the energy slopes) have been certainly introduced by the global adjustment procedure, which was performed to obtain CARNAVAL-IV.

For that reason an adjustment of the recently evaluated JEF cross-section is considered an essential step for the next future developments.

The average one group data adjustment of this paper is a first test that we have made in order to check if the recent BALZAC, PROFIL and TRAPU experimental results allow to meet the design target accuracies.

Moreover the aim of this adjustment is also to check the consistency among the informations of the different experimental results. In this respect the average one group data adjustment is the correct procedure, since all the experimental results have been measured in the same spectrum conditions (1).

### 3.1 - Adjustment method and results

Experimental results and cross-section uncertainties have been assumed to be "normally" distributed.

Correlations on experimental data and some correlations (2) on cross-sections have been taken into account in a general least square method / 6 /.

In practice we used the AMARA code / 7 /, that solves the system of equations corresponding to the maximum of the likelihood function, using the Lagrange multiplier method.

---

(1) The MASURCA core composition during the BALZAC HI experimental phase is very similar to the PHENIX inner core composition.

(2) In particular, relative uncertainties on fission cross-sections and on fission yields have been considered fully anticorrelated.

Table 6 shows the average one group cross-section adjustment results.

Column A of this table shows the initial uncertainty associated to the CARNAVAL IV one group average data.

Column B shows the adjustment results obtained using only the five BALZAC-HI experimental results (see table 2). As we mentioned in the previous paragraph, capture cross-sections are practically not adjusted if one uses only the BALZAC-HI experimental data.

The column C of the same table shows the adjustment results obtained adding the PROFIL information on the capture cross-section to the BALZAC information on fission cross-sections and yields.

The corresponding capture cross-section uncertainty reduction is evident.

The adjustment obtained adding the TRAPU experimental results (table 5) to the BALZAC-HI and the PROFIL results, is shown in column D.

A particularly good  $\chi^2$  value (i.e. 15) is associated to this last adjustment, as the expected value is the number of experimental constraints (i.e. 18).

The strong uncertainty reduction obtained adding the TRAPU results (column D) to the BALZAC and PROFIL results (column C) and the very similar mean cross-sections adjustments confirm the general consistency among the different experimental informations.

In order to quantify the effect of the data uncertainty reduction, tables 7 and 8 show the different components of a LMFBR reactivity loss per cycle and the sensitivity coefficients related to the "heavy isotopes" component.

Table 9 shows the "heavy isotopes" component uncertainty contribution to the total reactivity loss uncertainty of a typical LMFBR.

In this table we can see the determinant role of the irradiation experiments (PROFIL and TRAPU) in order to reduce the uncertainty on the calculated LMFBR reactivity loss per cycle.

Finally, if we consider the modifications of the CARNAVAL IV mean cross-sections, all the different steps of the adjustment show the trend of increasing the fission cross-sections and decreasing the scattering cross-section of the U-238.

However, the U-238 capture cross-section increase indication has the most important effect on the calculated LMFBR reactivity loss per cycle. Using the sensitivity coefficients of table 8 and remembering the relative contribution ( $\sim 22\%$ ) of the heavy isotope component, we can easily obtain a 10 % relative decrease of the calculated reactivity loss.

#### CONCLUSIONS

The calculated reactivity loss per cycle uncertainty can be strongly reduced adjusting the basic data on specific integral experiments.

In particular the "heavy isotopes component" uncertainty can be reduced using the experimental information of both irradiation experiments and Pu reactivity measurements obtained in critical experiments.

A further important conclusion of this study, is the consistency and significance of all the integral experiments considered. For this reason, these experiments will play a key role in the future adjustment of the JEF-2 data.

SENSITIVITY TO THE MEAN CROSS-SECTIONS AND FISSION YIELDS															
ISOTOPE	U-238					Pu-239			Pu-240			Pu-241			
DATA	$\nu$	$\sigma_{fiss}$	$\sigma_{cap}$	$\sigma_{scatt}$	$\sigma_{trans}$	$\nu$	$\sigma_{fiss}$	$\sigma_{cap}$	$\nu$	$\sigma_{fiss}$	$\sigma_{cap}$	$\nu$	$\sigma_{fiss}$	cap	
HI 1	0.122	0.076	- 0.151	- 0.037	0.038	3.82	2.66	- 0.264	- 1.13	- 0.782	0.326	- 1.40	- 1.00	0.065	
HI 2	0.226	0.142	- 0.280	- 0.068	0.071	4.20	2.93	- 0.290	- 1.57	- 1.09	0.456	- 1.37	- 0.97	0.064	
HI 3	0.174	0.109	- 0.215	- 0.052	0.054	3.90	2.72	- 0.270	- 1.50	- 1.04	0.435	- 1.18	- 0.84	0.054	
HI 4 - HI 2	- 1.48	- 0.93	1.83	0.45	- 0.46	0.0	0.0	0.0	0.0	0.0	0.0	0.0	0.0	0.0	
REFERENCE CONFIGURATION CRITICALITY CONDITION	0.102	0.064	- 0.128	- 0.031	0.043	0.648	0.446	- 0.045	0.0302	0.0210	- 0.0088	0.0169	0.0120	0.0	

TABLE 1  
SENSITIVITIES OF THE DIFFERENT BALZAC CONFIGURATION REACTIVITIES TO THE BASIC DATA

DESCRIPTION	CARNAVAL IV (E-C)/C	UNCERTAINTY	n	UNCERTAINTY CORRELATIONS				
				1	2	3	4	5
$\Delta\rho$ BALZAC HI :	%	%	n	1	2	3	4	5
HI 1 reactivity	4.9	5.9	1	1.0				
HI 2 reactivity	1.0	7.1	2	0.83	1.0			
HI 3 reactivity	3.3	6.3	3	0.83	0.88	1.0		
HI 4 - HI 2 reactivity	- 3.3	8.3	4	0.37	0.18	0.35	1.0	
REFERENCE CONFIGURATION CRITICALITY CONDITION	0.00200	0.00100	5	0.0	0.0	0.0	0.0	1.0

TABLE 2

BALZAC-HI (E-C)/C VALUES, UNCERTAINTIES AND CORRELATIONS

DESCRIPTION	CARNAVAL IV (E-C)/C	UNCERTAINTY	n	UNCERTAINTY CORRELATIONS			
				1	2	3	4
PROFIL AVERAGE CAPTURE :	%	%					
U-238 AVERAGE CAPTURE	2.0	2.1	1	1.0			
Pu-239 AVERAGE CAPTURE	- 1.0	2.3	2	0.41	1.0		
Pu-240 AVERAGE CAPTURE	- 1.0	2.1	3	0.44	0.41	1.0	
Pu-241 AVERAGE CAPTURE	2.0	4.0	4	0.24	0.22	0.24	1.0

TABLE 3

PROFIL (E-C)/C VALUES, UNCERTAINTIES AND CORRELATIONS

SENSITIVITY TO THE AVERAGE CROSS-SECTIONS AND FISSION YIELDS									
ISOTOPE	U-238		Pu-239		Pu-240		Pu-241		
DATA	$\sigma_{fiss}$	$\sigma_{cap}$	$\sigma_{fiss}$	$\sigma_{cap}$	$\sigma_{fiss}$	$\sigma_{cap}$	$\sigma_{fiss}$	$\sigma_{cap}$	
TRAPU 1 $\frac{Pu-239}{U-238}$	0.0078	0.317	- 0.306	- 0.086	0.0	0.0	0.0	0.0	
TRAPU 2 $\frac{Pu-239}{U-238}$	0.0077	0.330	- 0.303	- 0.085	0.0	0.0	0.0	0.0	
TRAPU 3 $\frac{Pu-239}{U-238}$	0.0075	0.382	- 0.293	- 0.085	0.0	0.0	0.0	0.0	
TRAPU 1 $\frac{Pu-240}{U-238}$	0.0089	0.091	- 0.041	0.242	- 0.065	- 0.087	0.0	0.0	
TRAPU 2 $\frac{Pu-240}{U-238}$	0.0090	0.097	- 0.046	0.270	- 0.064	- 0.086	0.0	0.0	
TRAPU 3 $\frac{Pu-240}{U-238}$	0.0090	0.067	- 0.011	0.065	- 0.072	- 0.097	0.0	0.0	
TRAPU 1 $\frac{Pu-241}{U-238}$	0.0090	0.062	- 0.008	0.069	- 0.018	0.439	- 0.362	- 0.066	
TRAPU 2 $\frac{Pu-241}{U-238}$	0.0090	0.060	- 0.006	0.048	- 0.011	0.272	- 0.410	- 0.075	
TRAPU 3 $\frac{Pu-241}{U-238}$	0.0091	0.056	- 0.002	0.014	- 0.016	0.382	- 0.382	- 0.070	

TABLE 4  
SENSITIVITIES OF THE DIFFERENT TRAPU CALCULATED RESULTS TO THE BASIC DATA



DESCRIPTION	CARNAVAL IV (E-C)/C	UNCERTAINTY	n	UNCERTAINTY CORRELATIONS								
				1	2	3	4	5	6	7	8	9
TRAPU FINAL DENSITIES :	%	%	n	1	2	3	4	5	6	7	8	9
TRAPU 1 Pu-239/U-238	- 1.3	1.5	1	1.0								
TRAPU 2 Pu-239/U-238	0.2	0.8	2	0.08	1.0							
TRAPU 3 Pu-239/U-238	0.2	0.8	3	- 0.03	- 0.05	1.0						
TRAPU 1 Pu-240/U-238	- 2.1	1.7	4	0.76	- 0.15	0.06	1.0					
TRAPU 2 Pu-240/U-238	- 0.3	1.3	5	0.17	0.83	- 0.10	- 0.35	1.0				
TRAPU 3 Pu-240/U-238	- 0.4	0.8	6	0.05	0.07	0.91	- 0.09	0.16	1.0			
TRAPU 1 Pu-241/U-238	- 2.5	1.7	7	0.78	- 0.13	0.05	0.95	- 0.30	- 0.08	1.0		
TRAPU 2 Pu-241/U-238	0.0	1.0	8	0.13	0.94	- 0.08	- 0.25	0.93	0.12	- 0.22	1.0	
TRAPU 3 Pu-241/U-238	- 1.4	0.8	9	0.01	0.02	0.91	- 0.03	0.05	0.89	- 0.03	0.04	1.0

TABLE 5  
TRAPU (E-C)/C VALUES, UNCERTAINTIES AND CORRELATIONS

		A	B	C	D
BALZAC		NO	YES	YES	YES
PROFIL		NO	NO	YES	YES
TRAPU		NO	NO	NO	YES
NUMBER OF EXPER. RESULTS		ZERO	5	9	18
RESIDUAL $\chi^2$		ZERO	2	3	15
DATA ADJUSTMENT AND UNCERTAINTIES (%)					
U-238	$\nu$	$0.0 \pm 1$	$-0.3 \pm 0.8$	$-0.4 \pm 0.7$	$-0.4 \pm 0.6$
	$\sigma_f$	$0.0 \pm 10$	$+2.6 \pm 7.5$	$+3.6 \pm 7.2$	$+3.8 \pm 6.3$
	$\sigma_c$	$0.0 \pm 2$	$-0.2 \pm 1.9$	$+0.8 \pm 1.4$	$+1.7 \pm 1.1$
	$\sigma_s$	$0.0 \pm 10$	$-1.5 \pm 9.3$	$-2.1 \pm 9.2$	$-3.4 \pm 9.0$
	$\sigma_{tr}$	$0.0 \pm 5$	$+0.3 \pm 4.9$	$+0.5 \pm 4.8$	$+0.8 \pm 4.8$
Pu-239	$\nu$	$0.0 \pm 1$	$0.0 \pm 0.8$	$0.0 \pm 0.7$	$-0.2 \pm 0.5$
	$\sigma_f$	$0.0 \pm 2.5$	$0.0 \pm 2.0$	$0.0 \pm 1.8$	$+0.6 \pm 1.2$
	$\sigma_c$	$0.0 \pm 10$	$-0.2 \pm 8.3$	$-1.4 \pm 2.1$	$-0.5 \pm 1.9$
Pu-240	$\nu$	$0.0 \pm 1$	$0.0 \pm 0.3$	$+0.1 \pm 0.3$	$+0.1 \pm 0.2$
	$\sigma_f$	$0.0 \pm 25$	$-1.0 \pm 8.1$	$-1.7 \pm 6.5$	$-3.4 \pm 4.7$
	$\sigma_c$	$0.0 \pm 12$	$0.0 \pm 11.8$	$-1.5 \pm 2.0$	$-3.0 \pm 1.1$
Pu-241	$\nu$	$0.0 \pm 1$	$+0.4 \pm 0.8$	$+0.4 \pm 0.8$	$+0.2 \pm 0.2$
	$\sigma_f$	$0.0 \pm 7$	$-3.0 \pm 5.9$	$-3.1 \pm 5.8$	$-1.5 \pm 1.0$
	$\sigma_c$	$0.0 \pm 12$	$+0.7 \pm 12$	$-2.2 \pm 3.7$	$+0.2 \pm 2.8$

TABLE 6

ADJUSTMENTS AND UNCERTAINTIES USING DIFFERENT EXPERIMENTAL RESULTS

Component	Absolute contribution	Relative contribution
H.I.	~ - 650 pcm	22 %
F.P.	~ - 2350 pcm	88 %
TOTAL	~ 3000 pcm	100 %

H.I. stands for Heavy Isotope contribution.

F.P. stand for Fission Product contribution.

TABLE 7

AN EXAMPLE OF THE "HEAVY ISOTOPES CONTRIBUTION"  
TO THE TOTAL LMFBR REACTIVITY LOSS PER CYCLE

$\sigma$		$\frac{\delta \text{ H.I.}}{\text{H.I.}} / \frac{\delta \sigma}{\sigma}$
ISOTOPE	DATA	SENSITIVITY
U-238	$\nu$	+ 1.0
	$\sigma_f$	+ 0.7
	$\sigma_c$	- 29.
Pu-239	$\nu$	- 4.
	$\sigma_f$	+ 15.
	$\sigma_c$	+ 5.8
Pu-240	$\sigma_c$	- 3.4
Pu-241	$\nu$	+ 7.5
	$\sigma_f$	+ 11.
	$\sigma_c$	+ 0.7

TABLE 8

THE MOST IMPORTANT SENSITIVITY COEFFICIENTS OF THE CALCULATED LMFBR REACTIVITY LOSS "HEAVY ISOTOPES COMPONENT" TO THE BASIC DATA

	A	B	C	D
BALZAC	NO	YES	YES	YES
PROFIL	NO	NO	YES	YES
TRAPU	NO	NO	NO	YES
HEAVY ISOTOPES UNCERTAINTY CONTRIBUTION	~ 26 %	~ 23 %	~ 17 %	~ 9 %

TABLE 9

HEAVY ISOTOPES CONTRIBUTION TO THE LMFBR REACTIVITY  
LOSS PER CYCLE UNCERTAINTY

## REFERENCES

- / 1 / M. SALVATORES.  
"The CARNAVAL IV formulaire. Methods and performances", paper presented at this meeting.
- / 2 / R. SOULE et Al.  
"The experimental BALZAC program at MASURCA".  
Proceedings of the topical meeting on Reactor Physics and Safety, Saratoga springs, September 1986, NUREG CP - 0080 - Vol. 1.
- / 3 / R. SOULE et Al.  
"The BALZAC program on the MASURCA critical facility. Main results".  
88 International Reactor Physics Conference, JACKSON HOLE/USA, September 1988.
- / 4 / A. GIACOMETTI et Al.  
IAEA conference AIX-EN-PROVENCE. September 1979 ; IAEA-SM-244/22 pag 521, 540.
- / 5 / A. D'ANGELO et Al.  
"Calculation and experiment comparison for sample and fuel pin irradiation. Experiments in PHENIX".  
Proceedings of the topical meeting on Reactor Physics and safety, Saratoga Springs, September 1986 ; NUREG/CP-0080 - Vol. 1.
- / 6 / A. GANDINI.  
"Nuclear data and integral measurement correlations for fast reactors. Part 1 : statistical formulation".  
Technical note RT/FI (73)22, CNEN 1973.
- / 7 / A. GANDINI and M. PETILLI.  
"AMARA : A code using the Lagrange multipliers methods for nuclear data adjustment".  
Technical note RT/FI (73)39, CNEN 1973.



# UNCERTAINTY IN THE BURNUP REACTIVITY SWING OF FAST REACTORS

H. Khalil

Applied Physics Division  
Argonne National Laboratory  
Argonne, Ill.

T. J. Downar

School of Nuclear Engineering  
Purdue University  
West Lafayette, Ind.

## ABSTRACT

The uncertainty in the burnup reactivity swing attributable to nuclear data uncertainties is analyzed for current fast reactor core designs using depletion-dependent sensitivity coefficients. Two systems are analyzed: A non-breeding, uranium-fueled core simulating the Fast Flux Test Facility (FFTF) after completion of its planned conversion to metallic fuel and a 900 MWth, high-internal-conversion, plutonium-fueled design typical of current U.S. advanced liquid metal reactor (ALMR) designs. The burnup swing uncertainty is shown to be significantly larger for the latter system as a result of a greater sensitivity to nuclide field perturbations. The potential for reducing uncertainties by a factor of two to three by use of available integral experiment results is demonstrated.

## I. INTRODUCTION

The uncertainties in the performance and safety parameters of operating fast reactors tend to decrease with the accumulation of operating experience and the calibration of analysis methods to measurements. However, demonstration that new or conceptual designs satisfy safety and performance goals must be done by calculating reactor characteristics and determining their uncertainties. One of the most important performance characteristics of current fast reactor designs<sup>1,2,3</sup> is the burnup reactivity swing,  $\delta k$ , (the change in core multiplication over a burn cycle as a result of nuclide transmutations);  $\delta k$  is a key component of the required beginning-of-cycle (BOC) reactivity excess, which determines the required fissile enrichment and control rod worth, as well as the reactivity potentially available for transient over-power (TOP) initiation by accidental ejection of control rods. In particular, the passive accommodation of TOP events, currently a key goal in U.S. ALMR designs,<sup>4</sup> limits the tolerable excess reactivity and makes it imperative to minimize the uncertainty in  $\delta k$ .

An earlier study of the uncertainty in  $\delta k$  is reported by Kamei et al. in Ref. 5 where the relative uncertainty is estimated to be 30% for a 1000 MWe LMFBR configuration. This



estimate is derived from sensitivity coefficients computed by depletion-dependent perturbation theory<sup>6,7</sup> and four-group cross-section covariance data as described in Refs. 5 and 9. Reference 5 also illustrates a modest reduction of the uncertainty (to 20%) when some integral parameters measured on the ZPPR-9 critical assembly are utilized to adjust the cross sections.

In this work, we evaluate the uncertainties in  $\delta k$  attributable to data uncertainties for two metal-fueled core designs with rather different characteristics (described in Section II) and relate the observed difference in uncertainty to differences between the designs. We utilize a depletion-dependent adjoint sensitivity method recently developed to conform with core physics analysis methods used at ANL and cross section variance-covariance data based on the ENDF/B-V file and processed to 21 group structure. We also assess the reduction achievable in these uncertainties by using an extensive integral experiment data base (see Refs. 10-12) to derive nuclear data adjustments and adjusted covariance data. The core models and analysis methods are described in Section II. A brief overview of sensitivity theory and the uncertainty analysis methods are given in Section III. The results are presented in Section IV and concluding remarks in Section V.

## II. CORE MODELS AND ANALYSIS METHODS

The basic characteristics of the FFTF and ALMR core models are summarized in Table I. The FFTF model, depicted in Fig. 1, simulates an equilibrium cycle configuration attained after completion of the planned conversion of FFTF to binary (U-10%Zr) metallic fuel. The thermal output is assumed to be 300 MW, the cycle duration is 100 days, and the fuel average discharge burnup is about 10 atom%, achieved after 11 residence cycles. The 73 driver fuel assemblies are arranged in three enrichment zones, and a small number (six) of internal blanket assemblies are present; no radial or axial blankets are utilized.

The ALMR core is fueled with ternary (U-Pu-10%Zr) fuel, and its thermal output is 900 MW. The fuel residence time is 4 cycles with a cycle duration of 292 FPD, resulting in a fuel average discharge burnup of about 10 atom%. The core, whose planar layout is shown in Fig. 2, consists of 96 driver assemblies, 46 internal blanket assemblies, and is surrounded by one row of radial blanket assemblies and three rows of removable reflector and shield assemblies.

The fuel-cycle analysis of the FFTF and ALMR core models was performed using the equilibrium-cycle capability of the REBUS-3 code.<sup>13</sup> For the purpose of the nuclide transmutation calculations, each core was subdivided into relatively coarse depletion zones (e.g., a row of assemblies axially divided into five to seven segments). The flux within each zone was computed for a "stage-averaged" fuel composition determined by averaging the fuel nuclide densities of the successive batches that occupy each zone when a scatter reload approach of fuel management is implemented. Note that the explicit batch compositions thus result from a depletion performed using the flux appropriate to a batch-average composition, which requires an iterative approach to computing the stage-dependent fuel compositions (the cyclic mode

iteration in REBUS-3).

Because the depletion-dependent sensitivity code is currently limited to R-Z geometry, and because cross-section covariance data was available for a 21-group structure, the burnup swing sensitivity and uncertainty analyses were based on the results of 21-group, R-Z depletion calculations. The group cross sections are composition- and region-dependent, and were processed from the ENDF/B-V.2 nuclear data using the MC<sup>2</sup>-2<sup>14</sup> and SDX<sup>15</sup> codes.

Some key results of the equilibrium-cycle calculations performed for the FFTF and ALMR cores are given in Table I. The  $\delta k$  values for the two cores are 1.25% $\Delta k$  ( $1.25 \times 10^{-4} \Delta k/\text{day}$ ), and 0.185% $\Delta k$  ( $6.33 \times 10^{-6} \Delta k/\text{day}$ ), respectively. These values, and those of the other global performance parameters, are in good agreement with results determined by three-dimensional (Hex-Z) analyses. The R-Z representation does not, however, produce accurate power peaking results because of azimuthal nonuniformity of the core layout.

### III. SENSITIVITY AND UNCERTAINTY ANALYSIS METHODS

#### III.A DEPLETION-DEPENDENT SENSITIVITY COEFFICIENTS

The recent development of Depletion Perturbation Theory (DPT) for linear flux approximations<sup>8</sup> as implemented in the REBUS-3 code was used to generate nuclear data sensitivities for burnup-dependent responses. Validations of DPT have been reported previously<sup>8</sup> and in general, there is good agreement between the sensitivities generated by DPT and by the direct subtraction of forward calculations.

The response of interest in the analysis here is the burnup reactivity swing,  $\delta k$ . As shown in the Appendix, the burnup swing sensitivity  $S_{\delta k}$  (to some data parameter  $\alpha$ ) can be related to the beginning and end of cycle  $k_{\text{eff}}$  sensitivities ( $S_k^B$  and  $S_k^E$ , respectively) as;

$$S_{\delta k} = \frac{1}{\delta k} \left\{ k^B S_k^B - k^E S_k^E \right\} \quad (1)$$

where;

$$S_k^B = \frac{\alpha}{k^B} \frac{\partial k^B}{\partial \alpha}$$
$$S_k^E = \frac{\alpha}{k^E} \frac{\partial k^E}{\partial \alpha}$$

The sensitivities,  $S_{\delta k}$ , were validated for the 21-group, R-Z models of FFTF and the ALMR described in the previous section. Comparisons with direct subtraction are shown in Table II for several cross section variations of interest. The contributions of the various components to the

total sensitivity are also given in Table II. It is worth noting that for the cross section variations considered here, the number density term can dominate  $S_{\delta k}$ , which indicates the importance of accurately modeling the coupled neutron/nuclide field as in Depletion Perturbation Theory.<sup>6,7,8</sup>

We note here that the DPT approach provides accurate sensitivities of depletion-dependent responses to data variations  $\delta\alpha$  assuming the BOEC reactor loadings are independent of  $\delta\alpha$  (the adjoint system of equations does not require that the "cyclic-mode" constraint<sup>16</sup> be satisfied when the perturbation is made). In reality, however, the BOEC loadings are themselves affected by  $\delta\alpha$  (since the BOEC core contains partially depleted as well as fresh fuel), which to first order leads to an additional term in the expression for the sensitivity coefficient:

$$S_{\delta k}^{(e)} \equiv \frac{\alpha}{\delta k} \frac{d\delta k}{d\alpha} \approx S_{\delta k}^{(1)} + \frac{\alpha}{\delta k} \frac{\partial \delta k}{\partial N_b} \frac{dN_b}{d\alpha} \quad (2)$$

where  $S_{\delta k}^{(1)}$  is the DPT sensitivity neglecting the effect on the BOEC loading, and the second term on the right side accounts linearly for the effect of  $\delta\alpha$  on the BOEC nuclide state vector  $N_b$ . To our knowledge, this effect on the sensitivity coefficient of burnup-dependent responses has not been previously addressed. A comparison of single cycle  $S_{\delta k}^{(1)}$  and equilibrium-cycle  $S_{\delta k}^{(e)}$  sensitivities, determined by direct calculation for several important reactions, is summarized in Table III. These results suggest that the nuclide field perturbation can act to reduce the effect of  $\delta\alpha$  on the response.\*

While future efforts will be made to develop an adjoint system satisfying the cyclic mode (i.e., equilibrium) constraint, we are currently attempting to develop an efficient method, based on Eq. (2), for computing equilibrium-cycle sensitivities  $S_{\delta k}^{(e)}$ . Initial results have shown that:

1. If  $\frac{dN_b}{d\alpha}$  is determined by "brute-force," i.e., by performing the perturbed equilibrium-cycle calculation, then an excellent approximation of the equilibrium sensitivity  $S_{\delta k}^{(e)}$  can be obtained using the values of  $S_{\delta k}^{(1)}$  and  $\frac{\partial \delta k}{\partial N_b}$  now available from DPT.

\* For example, consider the single and equilibrium cycle burnup swing sensitivities to the U-238 capture cross section ( $\sigma_c^{238}$ ) shown in Table III. Most of the large negative value for the single cycle sensitivity can be attributed to the increased production of Pu-239 during the cycle (first term RHS of Eqn.2) resulting from an increase in  $\sigma_c^{238}$ . However, for the equilibrium cycle, the Pu-239 density is also increased at BOEC, which by itself would increase the burnup swing and thus provides a positive component to the sensitivity (second term RHS of Eqn.2). The net effect is a lower value for the equilibrium cycle sensitivity compared to the single cycle value computed by DPT.

2. Reasonably accurate estimates of  $\frac{dN_b}{d\alpha}$  can be obtained by simple methods using information available from DPT (e.g.,  $\frac{\partial N_e}{\partial \alpha}$ ), where  $\underline{N}_e$  represents the EOC nuclide state vector and from the unperturbed equilibrium-cycle calculation (e.g., the transmutation matrix relating the isotope densities of successive stages). More accurate and elaborate methods are also being investigated.

While the uncertainty results presented in Section IV are based on the single-cycle sensitivities  $S_{\delta k}^{(1)}$ , the effects of utilizing multi-cycle sensitivities (determined from a few direct equilibrium-cycle perturbation calculations) will also be briefly addressed.

### III.B UNCERTAINTY ANALYSIS

The sensitivity coefficients for a set of  $N_r$  reactor performance quantities (responses) can be assembled into a matrix  $\underline{S}$  of dimension  $N_r \times N_p$ , where  $N_p$  is the number of parameters (data variables such as group cross sections). We denote the  $r^{\text{th}}$  row of  $\underline{S}$  by  $\underline{S}_r$ , the sensitivity vector for response  $r$ . The correlated uncertainties of the different responses can be determined from;

$$\underline{V} = \underline{V}_p + \underline{V}_m = \underline{S} \underline{C}_p \underline{S}^T + \underline{V}_m$$

where  $\underline{V}_p$  and  $\underline{V}_m$  are relative covariance matrices (dimension  $N_r \times N_r$ ) for the  $N_r$  responses resulting from data-parameter and methods/modeling uncertainties, respectively; the  $N_p \times N_p$  matrix  $\underline{C}_p$  is the relative covariance matrix of the data parameters. Note that the relative standard deviation for response  $r$  is  $\sqrt{V_r}$ , where  $V_r$  is the  $(r,r)$  element of  $\underline{V}$ .

The use of integral experiments to derive adjustments of data parameters, performance quantities (responses), and their respective covariances, has been the subject of many studies (e.g., Refs. 5, 12, 17, 18), and so the techniques involved will not be addressed here. An important advantage of this approach is that it permits adjustment and uncertainty reduction for responses (such as the burnup reactivity swing) for which measurements may not be available. Results of the adjustment process (a vector of fractional adjustments to the data parameters,  $\delta_p$  and the associated adjustment,  $-\delta \underline{C}_p$ , of the data covariance matrix) can be used to determine the fractional adjustment  $B_r$  of a specified response (e.g.,  $\delta k$ )

$$B_r = \underline{S}_r \delta_p$$

and the relative variance  $V'_r$  of the adjusted response

$$V'_r = V_r - \underline{S}_r \delta \underline{C}_p \underline{S}_r^T$$

## IV. RESULTS

### IV.A. DATA FOR UNCERTAINTY ANALYSIS

Sensitivity coefficients were generated by DPT for the nuclides and reaction types listed in Tables IV and V for the FFTF and ALMR cores, respectively. For the U-fueled FFTF core, sensitivities to U-236 data and for Pu isotopes through 240 were obtained. For the Pu-fueled ALMR core, sensitivities were additionally generated for Pu-241 data, while U-236 data sensitivities were judged to be unimportant. The reaction types (i.e. data parameters) considered for each actinide are capture, fission, neutrons per fission ( $\nu$ ), elastic scattering, and inelastic scattering. Burnup swing sensitivities to fission-spectrum parameters have not yet been generated, and thus our error estimates do not include their contribution. For each core, sensitivities to the capture, elastic, and inelastic data were additionally generated for Zr (present in the fuel alloys), for Fe and Cr (the principal elements in the HT-9 structural material), for Ni (present in the inconel reflector adjacent to the FFTF driver assemblies), and for the Na coolant. Since incomplete scattering data were available for the lumped fission product (LFP) nuclides employed in the depletion analysis of the two cores, LFP sensitivities were only generated for the capture reaction.

The nuclear parameter covariance data utilized is described in Refs. 11 and 12. Additions to that data were needed for U-236 and the LFP. Covariance data for LFP capture were provided by Liaw,<sup>19</sup> based partly on ENDF/B-V and partly on WHC (formerly HEDL) evaluations. Since the ENDF/B-V files contain no covariance information for U-236, uncorrelated, sensitivity-averaged 1- $\sigma$  uncertainties of 60% (capture), 8% (fission), and 15% (elastic) were assigned, based on estimates by Poenitz;<sup>20</sup> uncertainties of 5% and 30% were assumed for the  $\nu$  and inelastic data, respectively.

### IV.B. UNCERTAINTY ANALYSIS RESULTS

Estimates of the relative uncertainties (i.e. standard deviations) in the burnup reactivity swing of the FFTF and ALMR core models are given in Tables IV and V, respectively. These uncertainties are those attributable to nuclear parameter uncertainties only. Also shown in Tables IV and V are the contributions to the relative variance by nuclide and reaction type, including cross correlation components represented in the covariance matrix. For FFTF, the overall uncertainty is 3.3%, with the largest contributions made by U-238 capture, U-235 fission and  $\nu$ , Pu-239 fission and  $\nu$ , and LFP capture. The next largest contributors to the error are U-236 capture, Pu-239 capture, U-238 inelastic, and Ni capture. For the ALMR core, the relative  $\delta k$  uncertainty is a factor of 40 greater (135%), with the dominant components being U-238 capture and Pu-239 fission, followed in importance by U-238 inelastic scattering, Pu-239 capture, Pu-240 capture, and Na elastic scattering.

The substantially larger relative  $\delta k$  uncertainty for ALMR compared to FFTF is a direct consequence of greater relative sensitivities.\* For example, as shown in Table II, the group-summed relative sensitivities of the ALMR  $\delta k$  to U-238 capture and Pu-239 fission, are -38.89 and 44.86, respectively, while the corresponding values for FFTF (U-238 capture and U-235 fission) are -0.9611 and 1.465, respectively. It should be noted, however, that when the sensitivities and uncertainties are converted from relative to absolute terms (via multiplication by  $\delta k$ ), we obtain:

$$\text{ALMR: } \delta k = 0.185\% \Delta k \pm 0.25\% \Delta k$$

$$\text{FFTF: } \delta k = 1.245\% \Delta k \pm 0.04\% \Delta k$$

i.e. a factor of six greater absolute uncertainty in the case of ALMR.

It appears that most of this difference can be explained by considering the absolute sensitivity of the burnup swing to the U-238 capture data on a group-summed basis and by focusing on the number-density component, which dominates the sensitivity (see Table II). This component of the absolute  $\delta k$  sensitivity can be written:

$$\underline{S}_N^E = \underline{S}_k^E * \underline{S}_N^E \quad (3)$$

where

$$\underline{S}_k^E = \underline{N}_E * \frac{\partial k^E}{\partial \underline{N}_E}$$

$$\underline{S}_N^E = \frac{\sigma}{\underline{N}_E} \frac{d\underline{N}_E}{d\sigma}$$

The vector  $\underline{S}_N^E$ , which expresses the effect of the cross-section change on the EOEC nuclide density vector, can be computed by DPT but was more conveniently determined (for a single reaction type) by direct burnup calculations in which the U-238 capture cross section was increased by 1% in each group. The vector  $\underline{S}_k^E$ , which specifies the effect of the altered state on

\* A far smaller role is played by (1) the higher uncertainty in the fission cross section of Pu239 compared to U235, which are the principal fissioning nuclides in the ALMR and FFTF cores, respectively, and (2) the small differences in the energy dependence of the sensitivity coefficients as shown in Figure 3.

EOEC core multiplication, is the adjoint number density term for the EOEC  $k_{\text{eff}}$  response and was thus available from DPT. The results shown in Table VI illustrate that the nuclide field perturbation contribution to the burnup swing sensitivity (Eqn.3) is greater by a factor of about six (last column of Table VI) for ALMR compared to FFTF. This is almost totally accounted for by the Pu-239 contribution alone (column 4 of Table VI). The worth,  $\frac{\partial k^E}{\partial N_E}$ , of Pu-239 is greater by a factor of 1.44 (first line in Table VI) in ALMR, primarily because the fractional change in the macroscopic cross section is greater in ALMR than FFTF for the same increase in fissile density. Moreover, the absolute Pu-239 nuclide field perturbation (product of lines 2 and 3 in Table VI) is greater by a factor of 4.54 in ALMR because of (a) the factor of nearly 3 longer burnup cycle, (b) the factor of 1.65 greater U-238 density (column 3, line 3 in Table VI) resulting from the larger internal blanket fraction and lower enrichment, and (c) the slightly higher neutron flux associated with the Plutonium fuel composition. The net effect is a factor of slightly more than 6 for the contribution of the Pu-239 nuclide field perturbation to the ratio of ALMR to FFTF burnup swing sensitivities, thus accounting for most of the difference in the absolute burnup swing uncertainty between the two systems.

It is also instructive to compare the  $\delta k$  uncertainty results with the uncertainty reported in Ref. 5 for a conventional 1000 MWe LMFBR. The relative  $\delta k$  uncertainty for that core, based on 4-group uncertainty analysis, was found to be 30% -- significantly lower than the ALMR value of 135% and significantly greater than the FFTF value of 3.3%. These differences are not entirely explained by differences in the magnitudes of the group-summed sensitivities to the important reactions (e.g. U-238 capture). For example, while the  $\delta k$  relative uncertainty of the 1000 MWe system is a factor of 4.5 smaller than ALMR, the U-238 capture sensitivity is a factor of 11.3 smaller. Similarly the factor of 9 greater  $\delta k$  uncertainty of the 1000 MWe system relative to FFTF exceeds the ratio (3.8) of U-238 capture sensitivities. In both cases, an increase by a factor of roughly 2.5 in the effective data-parameter uncertainty (defined loosely as the ratio of the net uncertainty to the total sensitivity) utilized in our analyses of ALMR and FFTF would produce results more consistent with those in Ref. 5. This difference of about 2.5 is largely attributable to the significantly smaller off-diagonal elements of the covariance matrix used in our uncertainty analysis. The smaller correlations are partly a result of alterations<sup>11,12</sup> made to the processed ENDF/B-V covariance data to obtain a positive definite covariance matrix, as required for use in data adjustment (and for physical validity). If no alterations are made to the covariance data (i.e. the processed ENDF/B-V values are used) the relative uncertainties in  $\delta k$  for ALMR and FFTF would increase by a factor of roughly 1.7 to about 230% and 5.6%, respectively. Conversely, if correlations among the data uncertainties are neglected (i.e. a diagonal covariance matrix is assumed) the uncertainties would decrease by a factor of roughly 1.3 to 98% and 2.5%, respectively.

The single-cycle  $\delta k$  sensitivity coefficients used in the above error estimates have been shown in the previous section to be larger in magnitude (at least for the important data) than the

equilibrium-cycle values which additionally account for the effect of data perturbations on the BOEC nuclide densities. This result leads to the interesting conclusion that the uncertainties in  $\delta k$  are smaller when the perturbations in reactor loading associated with cross-section variations are taken into account. The amount by which the uncertainties are reduced will be assessed when a complete set of equilibrium-cycle sensitivities become available.

#### IV.C. USE OF INTEGRAL EXPERIMENTS TO REDUCE UNCERTAINTIES

The data base and procedures developed for utilizing integral experiments in the adjustment of reactor performance quantities and their uncertainties<sup>10,11,12</sup> have been applied to the estimation of the adjustment in  $\delta k$  and its uncertainty for the ALMR and FFTF cores. The nuclear data parameters involved in the adjustment process are addressed in references 11 and 12. These parameters are substantially the same as those listed in Tables IV and V, with the following exceptions:

1. Data for U-236 and the LFP could not be adjusted since the integral experiment data base did not include integral parameters with appreciable sensitivities to these data. Consequently, their contribution to the  $\delta k$  uncertainty was not affected by the adjustment process.
2. Some data parameters whose FFTF and ALMR  $\delta k$  sensitivities have not been computed were involved in the adjustment (namely fission spectrum parameters, B-10 absorption, Mo capture). Thus  $\delta k$  uncertainty estimates before and after adjustment do not include contributions from these reactions.

The effect of data adjustment on the predicted values of  $\delta k$  for ALMR and FFTF and on their uncertainties is summarized in Table VII. These results were obtained using the  $\delta k$  sensitivity coefficients along with the data-parameter and covariance matrix adjustments obtained by applying the adjustment procedures and data base recommended by Poenitz.<sup>20</sup> For the FFTF core, the fractional adjustment in  $\delta k$  is seen to be approximately one standard deviation (3.0%). This increase in  $\delta k$  is caused primarily by the downward adjustment of the U-238 capture cross section which is only partly offset by other data adjustments, most notably the decrease in the U-235 fission cross section. Thus the adjusted value of  $\delta k$  is 1.283%  $\Delta k$  ( $= 1.03 \times 1.245\% \Delta k$ ). The relative uncertainty in  $\delta k$  is reduced from 3.3% to 1.7%, i.e. a factor of nearly 2. If the U-236 and LFP contributions are artificially excluded from the error estimates, the reduction in uncertainty is from 3.0% to 1.0%.

For the ALMR core, the adjustment in  $\delta k$  is approximately 1.3 standard deviations (181%). The upward adjustment is dominated by the downward adjustment of the U-238 capture cross section. The adjusted value of  $\delta k$  is thus 0.520%  $\Delta k$  ( $= 2.81 \times 0.185\% \Delta k$ ). The relative uncertainty in  $\delta k$  is reduced from 135% to 39% by applying integral-experiment data. The uncertainty reduction factor (3.5) is somewhat greater for ALMR than FFTF, in part because the error contributions of data parameters not involved in the adjustment are relatively less



important for ALMR. In absolute terms, the FFTF  $\delta k$  uncertainty is reduced by 0.020%  $\Delta k$  (from 0.041%  $\Delta k$  to 0.021%  $\Delta k$ ), whereas for ALMR, the reduction is 0.177%  $\Delta k$  (from 0.250%  $\Delta k$  to 0.073%  $\Delta k$ )

Results for two additional adjustment cases are compared to the reference case in Table VII. In the first additional case, correlations among the data-parameter uncertainties were neglected (i.e. the covariance matrix was assumed to be diagonal), while in the second, a subset of the available critical experiments data was utilized (only criticality and reaction rate ratio data were used; fission rate distributions, material worths, and energy spectra were excluded). The results for these cases suggest that the improvement in the prediction of  $\delta k$  is not very sensitive to assumptions concerning data-parameter correlations, and that the major portion of this improvement can be achieved by using a subset of the experimental data. However, no detailed analysis has been made (e.g. using the methods discussed in Reference 21) of the relative importance of different criticals systems or integral parameters to the overall improvement or of the potential for further uncertainty reduction by inclusion of additional integral experiment information.

## V. SUMMARY AND CONCLUSIONS

An analysis of the uncertainty in the burnup reactivity swing for two metal-fueled fast reactors with different characteristics has been performed using depletion-dependent sensitivity coefficients. The relative  $\delta k$  uncertainty for the Pu-fueled ALMR core was found to be approximately 135%, a factor of 40 greater than the corresponding value (3.3%  $\Delta k$ ) for the U-fueled FFTF model, reflecting the substantially larger  $\delta k$  sensitivities of the former to the important data parameters. The larger relative sensitivities in the case of ALMR were found to be attributable to (a) the lower value of the burnup reactivity swing, which magnifies the absolute  $\delta k$  sensitivities, and (b) the greater breeding efficiency and longer burn cycle, which cause a greater change in the EOC fissile mass when cross sections are perturbed. We thus conclude that the uncertainty in the  $\delta k$  of cores designed for a low  $\delta k$  by maximizing internal breeding is greater than the corresponding uncertainty in non-breeding systems, even when this uncertainty is expressed in absolute form. Additional work is needed, however, to elucidate the dependence of the burnup swing sensitivity on design options related to fuel type, core size and arrangement, and fuel management strategies.

The application of critical experiments integral data enabled reduction of the burnup swing uncertainties by factors of two and three for the FFTF and ALMR cores, respectively, with the fractional reduction being greater for the latter system in part because the data parameters not involved in the adjustment were relatively less important. Results of the adjustment process can be summarized as follows:

Burnup Swing and Standard Deviation (% $\Delta k$ )	ALMR	FFTF
Before Adjustment:	$0.185 \pm 0.250$	$1.245 \pm 0.041$
After Adjustment:	$0.520 \pm 0.073$	$1.283 \pm 0.021$

Possibilities for further reduction in these uncertainties by application of additional criticals data, as well as information from operating reactors should be explored in future work.

## VI. REFERENCES

1. D.C. WADE, Y.I. CHANG, "The Integral Fast Reactor (IFR) Concept: Physics of Operation and Safety," Proc. Int. Topl. Mtg. Advances in Reactor Physics, Mathematics and Computation, Paris, France, Vol. 1, p. 311, April, 1987.
2. R. T. LANCET, J.C. MILLS, Trans. Am. Nucl. Soc., 50, 336 (1985).
3. C.L. COWAN, et al., "Core Design and Performance Characteristics for the Sodium Cooled Power Reactor Inherently Safe Module (PRISM)," Proc. Int. Topl. Mfg. Advances in Reactor Physics, Mathematics and Computation, Paris, France, Vol. 1, p. 195, April 1987.
4. D.C. WADE. "Uncertainty Reduction Requirements in Cores Designed for Passive Reactivity Shutdown," Presented at this Meeting.
5. T. KAMEI et al., Nucl. Sci. Eng., 91, 11 (1985).
6. M. L. WILLIAMS, Nucl. Sci. Eng., 70, 20 (1979).
7. T. TAKEDA, T. UMANO, Nucl. Sci. Eng., 91, 1 (1985).
8. W. S. YANG, T. J. DOWNAR, Nucl. Sci. Eng., 99, 353 (1988).
9. T. KAMEI, T. YOSHIDA, Nucl. Sci. Eng., 84, 83 (1983).
10. P. J. COLLINS, W. P. POENITZ, H.F. McFARLANE, "Integral Data for Fast Reactors," Proc. Int. Conf. on Nuclear Data for Science and Technology, Mito, Japan, May 30-June 3, 1988.
11. P. COLLINS, et al., "A Data Base for the Adjustment and Uncertainty Evaluation of Reactor Design Quantities," Presented at this Meeting.
12. W. POENITZ, P. COLLINS, "Utilization of Integral Experimental Data for the Adjustment and Uncertainty Evaluation of Reactor Design Quantities," Presented at this Meeting.
13. B. J. TOPPEL, "A User's Guide to the REBUS-3 Fuel Cycle Analysis Capability," ANL-83-2, Argonne National Laboratory, March 1983.
14. H. HENRYSON II, B. J. TOPPEL, C. G. STENBERG, "MC<sup>2</sup>-2: A Code to Calculate Fast Neutron Spectra and Multigroup Cross Sections," ANL-8144, Argonne National Laboratory, June 1976.
15. W. M. STACEY, Jr. et al., Trans. Am. Nucl. Soc., 15, 292, 1972.
16. R. P. HOSTENY, "The ARC System Fuel Cycle Analysis Capability, REBUS-2," ANL-7722, Argonne National Laboratory, October, 1978.

17. J. B. DRAGT, et al., Nucl.Sci.Eng., 62, 117 (1977).
18. J. H. MARABLE, et al., Nucl.Sci.Eng., 75, 30 (1980).
19. J. LIAW, Argonne National Laboratory, Private Communication, November 6, 1987.
20. W. P. POENITZ, Argonne National Laboratory, Private Communication, June 30, 1988.
21. R. HWANG, "Topics in Data Adjustment Theory and Application," Presented at this Meeting.

## APPENDIX: THE BURNUP REACTIVITY SWING SENSITIVITY RESPONSE

In general for a response which is a function of two responses:

$$R = f(R_1, R_2)$$

the sensitivity coefficient is found by differentiating;

$$S = \frac{\alpha}{R} \frac{dR}{d\alpha} = \frac{\alpha}{R} \left[ \frac{\partial R}{\partial R_1} \frac{dR_1}{d\alpha} + \frac{\partial R}{\partial R_2} \frac{dR_2}{d\alpha} \right]$$

and rearranging terms to give;

$$S = \frac{R_1}{R} \frac{\partial R}{\partial R_1} S_1 + \frac{R_2}{R} \frac{\partial R}{\partial R_2} S_2$$

For the burnup reactivity swing response;

$$R = \delta k = k^B - k^E$$

the sensitivity coefficient becomes;

$$S_{\delta k} = \frac{k^B}{\delta k} \frac{\partial[\delta k]}{\partial k^B} S_k^B + \frac{k^E}{\delta k} \frac{\partial[\delta k]}{\partial k^E} S_k^E$$

or;

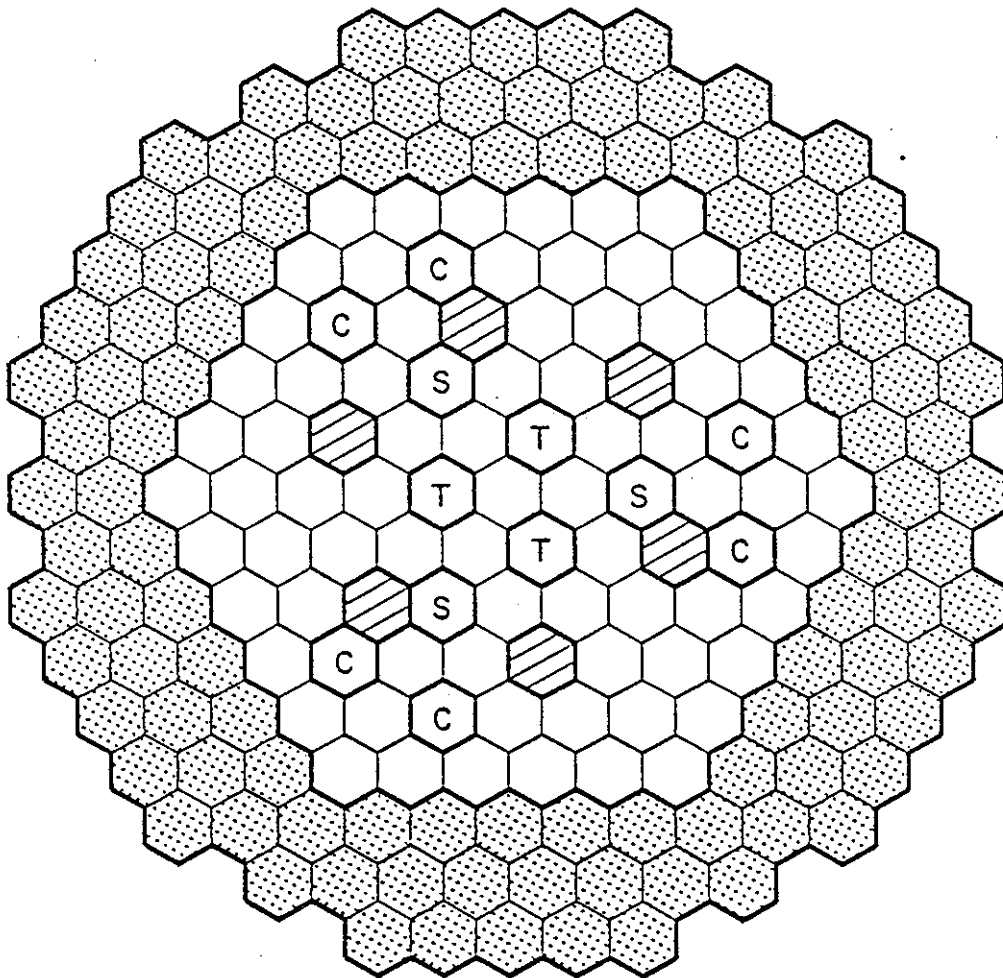
$$S_{\delta k} = \frac{1}{\delta k} \left\{ k^B S_k^B - k^E S_k^E \right\}$$

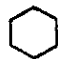
where;


$$S_k^B = \frac{\alpha}{k^B} \frac{\partial k^B}{\partial \alpha}$$


$$S_k^E = \frac{\alpha}{k^E} \frac{\partial k^E}{\partial \alpha}$$


Fig 1. FFTF Metal Core Planar Layout




 Driver (73)  
 Inner, Rows 1-4 (25)  
 Middle, Row 5 (18)  
 Outer, Row 6 (30)

 Inconel Reflector (108)  
 Type-1, Row 7 (36)  
 Type-2, Rows 8-9 (72)

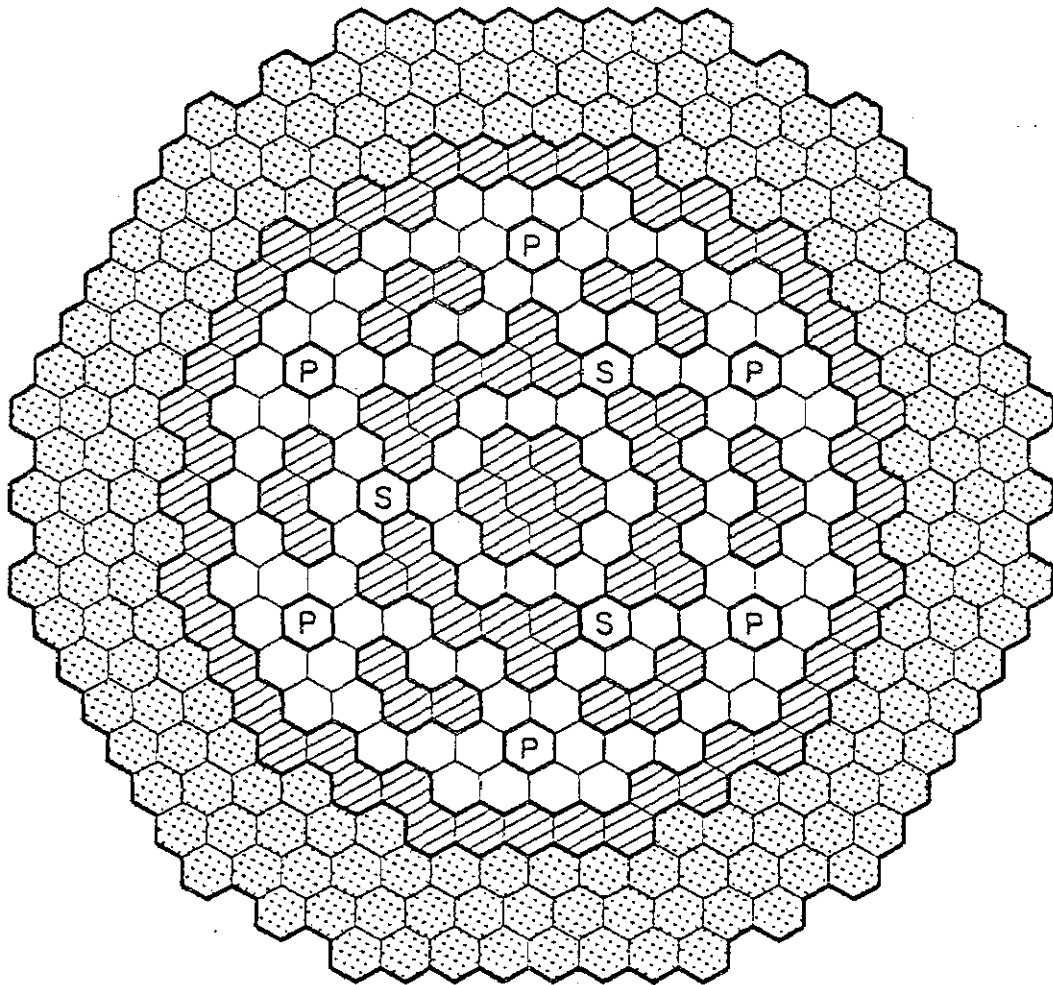
 Blanket (6)






 Control Rod (6)

 Test Location (3)

 Safety Rod (3)

Fig 2. ALMR Core Planar Layout



- |   |               |   |                               |
|---|---------------|---|-------------------------------|
|  | Driver (96)   |  | Primary Control (6)           |
|  | Blanket (94)  |  | Secondary Control (3)         |
|   | Internal (46) |  | Reflector/shield (180)        |
|   | Radial (48)   |   | 1 Row Steel (54)              |
|   |               |   | 2 Rows B <sub>4</sub> C (126) |

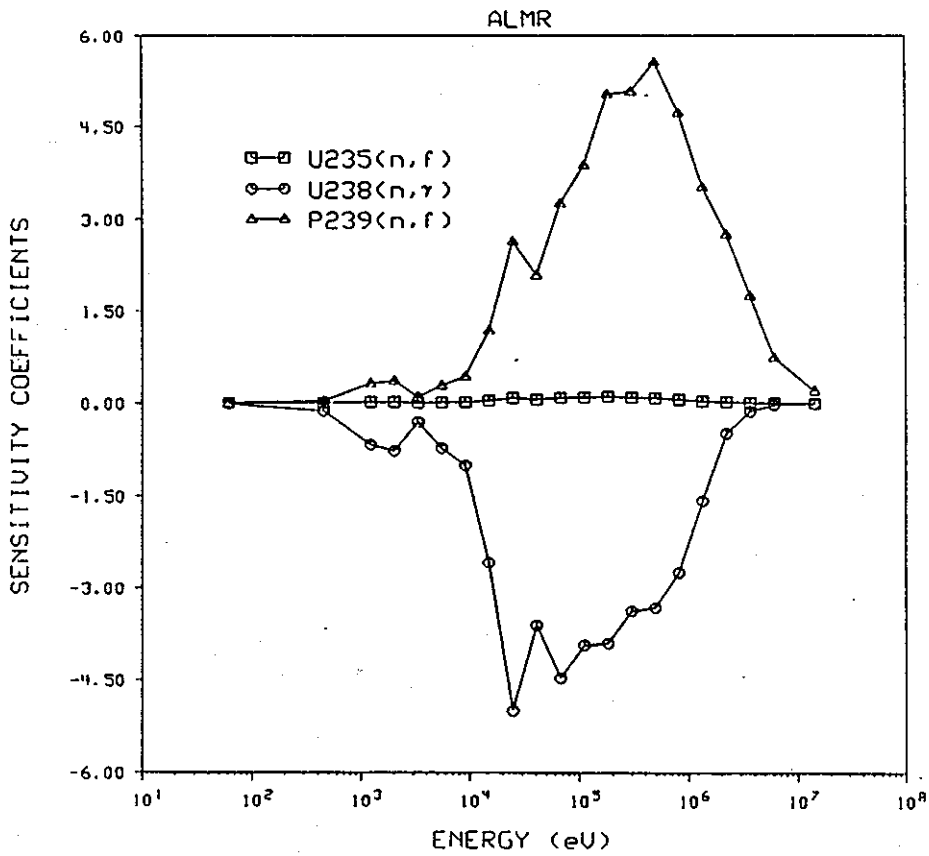
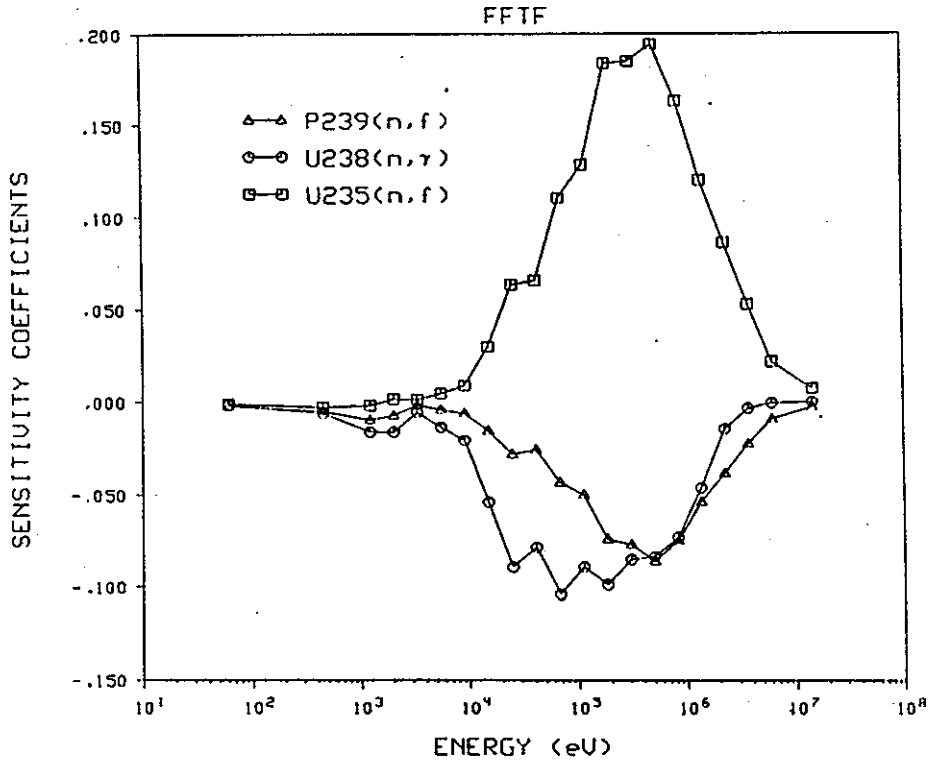


Fig.3 Burnup Reactivity Swing Sensitivity Profiles for FFTF and ALMR



Table I. Core Model Characteristics

	<u>FFTF</u>	<u>ALMR</u>
Power, MWth	300	900
Fuel Type	U-10%Zr	U-Pu-10%Zr
Structural Material	HT-9	HT-9
Fuel Residence Time, Number of Cycles	11	4
Cycle Length, fpd	100	292
Fuel Height, <sup>a</sup> in. (cm)		
Driver	36 (91.4)	38 (96.5)
Blanket	49 (124.5)	46 (115.8)
Lattice Pitch, in. (cm)	4.73 (12.0)	6.09 (15.5)
Volume Fractions (Fuel <sup>b</sup> /Steel/Na)		
Driver	0.350/0.272/0.378	0.385/0.256/0.359
Blanket	0.453/0.223/0.324	0.502/0.227/0.272
Fissile Enrichment, wt% Heavy Metal	32.0 <sup>c</sup> (U-235)	18.4 (Pu <sup>d</sup> )
Average Discharge Burnup, Atom%		
Driver	10.6	10.8
Internal Blanket	1.72	2.78
Radial Blanket	-	0.76
Burnup Reactivity Swing BOEC $k_{eff}$ -EOEC $k_{eff}$ , % $\Delta k$	1.245	0.185
Breeding Ratio/Conversion Ratio		
Driver	0.250/0.254	0.441/0.537
Internal Blanket	0.063/4.411	0.471/3.321
Radial Blanket	-	0.228/6.168

<sup>a</sup>Cold Dimensions

<sup>b</sup>Smear Fraction; Smear Density = 75% of Theoretical Density

<sup>c</sup>Average of Inner, Middle, and Outer Zone Enrichments (27.9%, 31.9%, and 35.6%, Respectively)

<sup>d</sup>Isotopic Split (238/239/240/241/242) = 0.004/0.724/0.233/0.027/0.012

Table II Components of Burnup Reactivity Swing Sensitivity Coefficients

<u>Cross Section</u>	<u>Reactor Core*</u>	<u>Direct Term</u>	<u>Density Term</u>	<u>Flux Term</u>	<u>Power Term</u>	<u>Total</u>	<u>Exact**</u>	<u>%Dif.</u>
U235(n,f)	FFTF	9.464-1	1.338+0	1.690-2	-8.188-1	1.465+0	1.460+0	0.3
U235(n,f)	ALMR	5.109-1	3.975-1	3.532-2	-3.620-3	9.360-1	-	-
U238(n, $\gamma$ )	FFTF	-8.061-2	-8.636-1	2.403-2	-9.945-3	-9.311-1	-9.605-1	2.9
U238(n, $\gamma$ )	ALMR	-1.517-1	-4.854+1	9.815+0	-8.620-3	-3.889+1	-3.832+1	1.4
Pu239(n,f)	FFTF	-7.486-1	1.747-1	3.722-3	-6.204-2	-6.322-1	-	-
Pu239(n,f)	ALMR	-2.420-1	4.041+1	4.918+0	-2.170-1	4.486+1	4.487+1	0.1

\*Note: FFTF:  $\delta k = 0.01245$  ( $1.245 \times 10^{-4} \Delta k/\text{day}$ )

ALMR:  $\delta k = 0.00185$  ( $6.33 \times 10^{-6} \Delta k/\text{day}$ )

\*\*Reaction cross sections perturbed +1% in all groups

Table III. Comparison of Equilibrium and Single-Cycle  
Burnup Reactivity Swing Sensitivity Coefficients

<u>ALMR</u>		
Case	$\delta k$	Sensitivity
Base	0.00185	-
Single cyc./Pu-239(n,f)*	0.00268	44.86
Equil. cyc./Pu-239(n,f)	0.00249	34.94
Single cyc./U-238(n, $\gamma$ )	0.00114	-38.38
Equil. cyc./U-238(n, $\gamma$ )	0.00146	-21.08

<u>FFTF</u>		
Case	$\delta k$	Sensitivity
Base	0.012451	-
Single cyc./U-235(n,f)	0.012631	1.4457
Equil. cyc./U-235(n,f)	0.012623	1.3814
Single cyc./U-238 (n, $\gamma$ )	0.012331	-0.9605
Equil. cyc./U-238(n, $\gamma$ )	0.012351	-0.8032

\*Reaction cross section perturbed +1% in all groups

Table IV. Components of the FFTF  $\delta k$  Uncertainty by Nuclide and Reaction Type

Nuclide, N	Reaction, R	Variance	Cross-Correlation Components		
		Component N, R	(N', R')		
U <sup>25</sup>	C	3.17-6	4.38-6	(U <sup>25</sup> F),	-4.91-5 (U <sup>28</sup> C)
	F	2.87-4	4.38-6	(U <sup>25</sup> C),	-6.43-6 (U <sup>28</sup> F),
			-3.45-5	(Pu <sup>49</sup> F),	-5.47-7 (Pu <sup>40</sup> F),
	v	1.18-4	1.78-7	(U <sup>28</sup> v),	-4.02-5 (Pu <sup>49</sup> v),
			-2.80-7	(Pu <sup>40</sup> v)	
	E	2.69-7			
	I	4.04-7			
U <sup>26</sup>	C	6.14-5			
	F	1.54-6			
	v	1.19-6			
	E	4.73-8			
	I	2.33-7			
U <sup>28</sup>	C	4.37-4	-4.91-5	(U <sup>25</sup> C)	
	F	2.82-6	-6.43-6	(U <sup>25</sup> F)	
	v	8.96-9	1.78-7	(U <sup>25</sup> v),	-2.67-7 (Pu <sup>49</sup> v),
			-1.92-9	(Pu <sup>40</sup> v)	
	E	2.62-8			
	I	1.19-5			
Pu <sup>49</sup>	C	1.30-5	-5.43-6	(Pu <sup>49</sup> F)	
	F	1.42-4	-3.45-5	(U <sup>25</sup> F),	-5.43-6 (Pu <sup>49</sup> C)
	v	1.11-4	-4.02-5	(U <sup>25</sup> v),	-2.67-7 (U <sup>28</sup> v),
			2.68-7	(Pu <sup>40</sup> v)	
	E	3.50-9			
	I	6.87-8			
Pu <sup>40</sup>	C	1.35-8	-1.04-13	(Pu <sup>40</sup> F)	
	F	5.31-8	-5.47-7	(U <sup>25</sup> F),	-1.04-13 (Pu <sup>40</sup> C)
	v	1.32-8	-2.80-7	(U <sup>25</sup> v),	-1.92-9 (U <sup>28</sup> v),
			2.68-7	(Pu <sup>49</sup> v)	
	E	1.59-10			
	I	2.22-10			
Fe	C	1.73-7	8.00-10 (FeE),	1.43-9 (FeI)	
	E	9.37-7	8.00-10 (FeC),	-5.03-7 (FeI)	
	I	3.94-6	1.43-9 (FeC),	-5.03-7 (FeE)	
Cr	C	2.60-7	2.99-11 (CrI)		
	E	7.48-7	-3.37-9 (CrI)		
	I	3.44-8	2.99-11 (CrC),	-3.37-9 (CrE)	

Table IV. Components of the FFTF  $\delta k$  Uncertainty by Nuclide and Reaction Type (Cont.)

Nuclide, N	Reaction, R	Variance Component N, R	Cross-Correlation Components (N', R')
Ni	C	1.17-5	
	E	4.10-7	
	I	2.18-7	
Na	C	8.23-10	4.88-12 (NaE)
	E	1.03-6	4.88-12 (NaC), -3.82-7 (NaI)
	I	1.57-6	-3.82-7 (NaE)
Zr	C	3.46-8	
	E	1.12-8	
	I	1.76-7	
LFP	C	1.22-4	

Total Variance = 1.069-3

Standard Deviation = 3.27%

C = Capture, F = Fission,  $\nu$  = Neutrons Per Fission,  
E = Elastic Scattering, I = Inelastic Scattering

Table V. Components of the ALMR  $\delta k$  Uncertainty by Nuclide and Reaction Type

Nuclide, N	Reaction, R	Variance	Cross-Correlation Components		
		Component N, R	(N', R')		
U <sup>25</sup>	C	1.78-5	2.20-5	(U <sup>25</sup> F)	
	F	1.32-4	2.20-5	(U <sup>25</sup> C),	-1.48-3 (U <sup>28</sup> C),
			-2.82-5	(U <sup>28</sup> F),	1.13-3 (Pu <sup>49</sup> F),
			4.15-5	(Pu <sup>40</sup> F),	5.21-5 (Pu <sup>41</sup> F)
	v	1.20-5	-1.13-5	(U <sup>28</sup> v),	1.69-5 (Pu <sup>49</sup> v),
			5.64-6	(Pu <sup>40</sup> v)	
	E	1.53-9			
	I	5.34-6			
U <sup>28</sup>	C	8.26-1	-1.48-3	(U <sup>25</sup> F)	
	F	1.22-4	-2.82-5	(U <sup>25</sup> F)	
	v	3.88-4	-1.13-5	(U <sup>25</sup> v),	-1.16-4 (Pu <sup>49</sup> v),
			-2.82-5	(Pu <sup>40</sup> v)	
	E	8.40-5			
	I	1.06-1			
Pu <sup>49</sup>	C	9.39-2	3.18-2	(Pu <sup>49</sup> C)	
	F	6.88-1	1.13-3	(U <sup>25</sup> F),	3.18-2 (Pu <sup>49</sup> C)
	v	1.16-3	1.69-5	(U <sup>25</sup> v),	-1.16-4 (U <sup>28</sup> v),
			3.49-5	(Pu <sup>40</sup> v)	
	E	7.80-7			
	I	2.24-3			
Pu <sup>40</sup>	C	2.61-2	1.09-13	(Pu <sup>40</sup> F)	
	F	1.55-3	4.15-5	(U <sup>25</sup> F),	1.09-13 (Pu <sup>40</sup> C)
	v	6.12-5	5.64-6	(U <sup>25</sup> v),	-2.82-5 (U <sup>28</sup> v),
			3.49-5	(Pu <sup>49</sup> v)	
	E	2.56-6			
	I	3.36-4			
Pu <sup>41</sup>	C	6.94-4	2.37-5	(Pu <sup>41</sup> F)	
	F	1.62-3	5.21-5	(U <sup>25</sup> F),	2.37-5 (Pu <sup>41</sup> C)
	v	1.35-6			
	E	1.48-8			
	I	4.70-6			
Fe	C	2.34-3	-4.54-8	(FeE),	8.38-7 (FeI)
	E	1.57-3	-4.54-8	(FeC),	5.55-4 (FeI)
	I	1.74-3	8.38-7	(FeC),	5.55-4 (FeE)
Cr	C	2.04-4	-1.76-9	(CrI)	
	E	2.52-3	-1.13-6	(CrI)	
	I	2.50-6	-1.76-9	(CrC),	-1.13-6 (CrE)

Table V. Components of the ALMR  $\delta k$  Uncertainty by Nuclide and Reaction Type (Cont.)

Nuclide, N	Reaction, R	Variance Component N, R	Cross-Correlation Components (N', R')
Ni	C	2.94-6	
	E	2.89-7	
	I	1.82-8	
Na	C	9.92-6	8.20-8 (NaE)
	E	1.08-2	8.20-8 (NaC), 1.18-4 (NaI)
	I	1.31-3	1.18-4 (NaE)
Zr	C	2.07-3	
	E	5.54-4	
	I	5.03-5	
LFP	C	3.27-4	
Total Variance		= 1.837	
Standard Deviation		= 135%	

C = Capture, F = Fission,  $\nu$  = Neutrons Per Fission,  
E = Elastic Scattering, I = Inelastic Scattering

Table VI. Nuclide Field Perturbation Contribution to Burnup Swing Sensitivities for the U-238(n, $\gamma$ ) Cross Section

	<u>FFTF</u>						Total
	U-235	U-236	U-238	Pu-239	Pu-240	Pu-241	
(1) $\frac{\partial k^{E*}}{\partial N_E}$	2.578-22***	-2.172-23	-1.227-23	3.928-22	7.459-23	4.938-22	-
(2) $\frac{\sigma}{N_E} \frac{\partial N_E}{\partial \sigma}$	0.0016	-0.0144	-0.0039	0.1715	-0.0179	-0.0487	-
(3) $N_E^{**}$	2.155+21	1.048+20	6.837+21	1.510+20	3.707+18	7.629+16	-
(4) $S_N$	8.888-4	3.278-5	3.272-4	1.017-2	-4.949-6	-1.835-6	1.142-2

	<u>ALMR</u>						Total
	U-235	U-236	U-238	Pu-239	Pu-240	Pu-241	
(1) $\frac{\partial k^E}{\partial N_E}$	4.069-22	-	-2.098-23	5.664-22	8.811-23	7.342-22	-
(2) $\frac{\sigma}{N_E} \frac{\partial N_E}{\partial \sigma}$	0.0350	-	-0.0096	0.1311	-0.0195	-0.0453	-
(3) $N_E^{**}$	1.726+20	-	1.131+22	8.959+20	2.743+20	3.194+19	-
(4) $S_N$	2.458-3	-	2.278-3	6.653-2	-4.713-4	-1.062-4	7.111-2

\* units = cm<sup>3</sup>/atom

\*\* units = atom/cm<sup>3</sup>

\*\*\* Read as 2.578 x 10<sup>-22</sup>

Note: All data is core averaged; notation is the same as Eqn. 3.



Table VII. Burnup Swing Adjustment and Adjusted Uncertainty  
Obtained by Application of Integral Experiment Data

	<u>Reference Adjustment Case</u>	<u>Cross Section Parameters Uncorrelated</u>	<u>Subset of Integral Data Utilized</u>
FFTF $\delta k$			
Fractional Adjustment, %	3.03 (0.93) <sup>a</sup>	2.84 (0.87) <sup>a</sup>	2.93 (0.90) <sup>a</sup>
Adjusted Relative Standard Deviation, <sup>b</sup> %	1.71	1.57	1.79
Adjusted Value, % $\Delta k$	1.283 $\pm$ 0.021	1.280 $\pm$ 0.020	1.281 $\pm$ 0.022
ALMR $\delta k$			
Fractional Adjustment, %	181 (1.34) <sup>a</sup>	197 (1.46) <sup>a</sup>	188 (1.39) <sup>a</sup>
Adjusted Relative Standard Deviation, <sup>b</sup> %	39.4	34.1	42.1
Adjusted Value, % $\Delta k$	0.520 $\pm$ 0.073	0.549 $\pm$ 0.063	0.533 $\pm$ 0.078

<sup>a</sup>Values in parentheses are the adjustments measured in standard deviations

<sup>b</sup>Value before adjustment = 3.27%

<sup>c</sup>Value before adjustment = 135%

NUCLEAR ENERGY AGENCY  
COMMITTEE FOR REACTOR PHYSICS TOPICAL MEETING  
JACKSON HOLE, WYO (USA)  
September 23-24, 1988

NUCLEAR DATA QUALIFICATION FOR THERMAL NEUTRON REACTORS

H. TELLIER

Service d'Etudes de Réacteurs et de Mathématiques Appliquées  
Centre d'Etudes Nucléaires de Saclay  
91191 - Gif-sur-Yvette (France)

## NUCLEAR DATA QUALIFICATION FOR THERMAL NEUTRON REACTORS

H. TELLIER

Service d'Etudes de Réacteurs et de Mathématiques Appliquées  
Centre d'Etudes Nucléaires de Saclay - 91191 Gif-sur-Yvette - France

### I - INTRODUCTION

Nowadays, the calculation of a nuclear reactor core is generally performed by solving the Boltzmann equation. According to the computer code we solve the integral form or the integrodifferential form of the transport equation. But in any case we need numerous numerical data: the geometrical and chemical data, and the neutron and nuclear data. The former data represent the dimensions of the cell and the core, the chemical and isotopic composition of the fuel, the structure and the moderator. They are generally known with a good accuracy. The latter data represent the neutron cross sections and the nuclear properties of the various nuclides. They are not always known with an accuracy as good as the reactor physicist wishes. The neutron data are generally deduced from direct nuclear measurements. These measurements give the variation of the nuclear properties of the nuclides versus the incoming neutron energy: they are the differential experiments. Very often, it is difficult to measure the cross sections with a very good accuracy. Consequently some of the best estimated values of the evaluated files have an uncertainty which is too large. To improve the knowledge of the neutron parameters, the reactor physicist must use another type of measurement: the integral experiments. In these experiments we use a mock-up of a reactor or the reactor itself and we measure some synthetic parameters which are representative of the neutron properties of the cell or of the reactor for the actual neutron spectrum. For example, we can measure criticality factor, buckling, reaction rates or irradiated fuel composition. If we choose integral experiments with a very simple geometry and an asymptotic neutron spectrum, such as uniform lattices or homogeneous media, we can perform the calculation of these experiments without numerical approximation. Therefore if we observe a difference between the computed value of a neutron parameter and the experimental value, this difference can be attributed to the uncertainties of the input neutron data. If we have at our disposal several integral experiments with different nuclear data sensitivities we can obtain informations or tendencies about the basic data. It is the tendency research method.

Generally the thermal neutron reactors are computed in a multigroup approximation and the nuclear data must be first processed to obtain multigroup cross sections. We must carefully check these multigroup libraries, to avoid the introduction of too much approximations with the processing codes which are used (modified NJOY or similar French codes). In the French Atomic Energy Commission the thermal neutron reactors calculations are performed which the APOLLO code which solves the Boltzmann equations by the collision probability method with ninety nine groups. Obviously it is not possible to obtain tendencies for all the cross sections and all the groups because the number of unknown quantities is too large. But we can choose a small number of synthetic parameters which represent the general trend of the cross sections versus energy. For the most part, it is sufficient for reactor physics.

We have used the tendency research method to validate the nuclear data of the major actinides: Uranium 235 and 238, Plutonium 239 and 240. Up to

now, the thermal reactors are not sensitive enough to Plutonium 241 and 242 to obtain accurate tendencies for all the cross sections of these isotopes. Nevertheless, the irradiated fuel analysis give us some informations about their capture cross sections.

## II - THE TENDENCY RESEARCH METHOD

In this section we will give a brief description of the tendency research method [1].

For each integral experiment (criticality factor, reaction rate, ...) we know the experimental result  $Y_i$  and the measurement uncertainty  $E_i$ . In any case we can compute the same quantity which is a function of the neutron parameters  $x_k$ . The result of this calculation is  $F_i$  (... ,  $x_k$ , ...). If we change the value of the neutron parameter  $k$ , which becomes  $x_k + \Delta x_k$ , the result of the computation is now  $F_i$  (... ,  $x_k + \Delta x_k$ , ...).

The principle of the tendency research method is to choose the modification  $\Delta x_k$  of the neutron parameters in such a way that the quantity

$$Q = \sum_i \frac{1}{E_i^2} [Y_i - F_i(\dots, x_k + \Delta x_k, \dots)]^2$$

for all the set of integral experiments becomes minimum. Nowadays the magnitude of the main neutron cross sections are more or less well known. So, the modifications  $\Delta x_k$  are expected to be small and we can make a first order expansion of the computed value

$$F_i(\dots, x_k + \Delta x_k, \dots) = F_i(\dots, x_k, \dots) + \sum_k \Delta x_k \frac{\partial F_i}{\partial x_k}$$

We can also replace the partial derivatives by the sensibility coefficients

$$S_{ik} = \frac{\Delta F_i}{\Delta x_k}$$

These sensibility coefficients (variation of the integral quantity  $F_i$  for a one per cent change of the parameter  $x_k$ ) can be computed by the perturbation theory or a variational method.

With these assumptions we must now minimize the quantity

$$Q = \sum_i \frac{1}{E_i^2} [Y_i - F_i(\dots, x_k, \dots) - \sum_k S_{ik} \Delta x_k]^2$$

or if  $\Delta Y_i$  represents the difference between the experimental result and the computed value for the integral experiment  $i$

$$Q = \sum_i \frac{1}{E_i^2} \left[ \Delta Y_i - \sum_k S_{ik} \Delta x_k \right]^2$$

The minimization is done with the least square method. That is why,

if we want to determine the modification  $\Delta x_k$  with a good accuracy, it is absolutely necessary to use a set of integral experiments for which the sensitivity coefficients are as different as possible. An illustration of this necessity is displayed on figure 1, in the case of a two parameter tendency research. When the sensibility coefficients are not very different, the slope of the curves which represent each integral experiment are almost the same. As in reality, these slopes are known with an uncertainty which depends on the integral experimental error bar  $E_i$ , the coordinates of the mean intersection point are not known with a very good accuracy. On the contrary if we use integral experiments with different sensitivity coefficients we can improve the accuracy of the intersection point coordinates. We can obtain different sensibility coefficients by using integral experiments corresponding to various types of reactors. As an example figure 2 shows the Uranium 235 sensibility profile for a typical pressurized water reactor and an advanced tight pitch water reactor. The importance of the thermal range is lower in the tight pitch reactor than in the standard pressurized water reactor.

From the mathematical point of view, the least square calculation leads to the  $\Delta x_k$  values which minimize the quantity Q. But we must take two remarks into account. First, the  $\Delta x_k$  are assumed to be small (don't forget that we have made a first order expansion of  $F_i$ ). Secondly the cross sections are measured by differential experiments with an experimental uncertainty  $\epsilon_k$ . The  $\Delta x_k$  must be lower or of the same order than  $\epsilon_k$ . This is why, instead of minimizing the Q value, we prefer minimize the following quantity:

$$Q' = \sum_i \frac{1}{E_i^2} \left[ \Delta Y_i - \sum_k S_{i,k} \Delta x_k \right]^2 + \lambda \sum_k \left( \frac{\Delta x_k}{\epsilon_k} \right)^2$$

In this expression,  $\lambda$  is the weighting coefficient of the microscopic data in the tendency research.

### III - INTEGRAL EXPERIMENT CHOICE

Three different kinds of integral experiments were used for the nuclear data qualification: critically measurements which give information about capture and production cross sections and moderator characteristics; reaction rate ratios and spent fuel analysis which give information about the capture cross section of the heavy isotopes.

Two essential conditions must be satisfied to obtain accurate tendencies: different sensibility coefficients and very simple experiments with an asymptotic neutron spectrum. For these two reasons we have carefully chosen critical facilities with uniform lattices for which the buckling was measured with a very good accuracy. To obtain various sensibility coefficients and various neutron spectra, we used three types of moderator (light water, heavy water and graphite) and for each moderator several moderating ratios overlapping a wide range of neutron spectra (from the very well thermalized lattices to the tight pitch lattices). Uranium fuels and Plutonium fuels are disconnected by using uranium lattices, mixed fuel (uranium and plutonium) lattice and multiplying media in which the fuel is only plutonium. The necessity to only use very clean experiments lead to reduce the critical measurements to the one for which the chemical and isotope composition, the geometrical dimensions and the buckling are very well known. Finally we used sixty one buckling measurements. They are splitted into two classes, the lattices without plutonium and the others. A part of them are international published results, French experiments constitute the remainder.

### III.1 - Uranium multiplying media

- 4 natural metal uranium lattices moderated by heavy water [2] which different moderating ratio. They are very well thermalized and are mainly sensitive to the low energy cross sections.

- 4 natural uranium graphite lattices [3] which are also sensitive to the low energy range but which allow, associated to the preceding ones, to disconnect the effect of the heavy water or the graphite.

- 3 enriched uranium lattices from American origin [4]. The enrichment is 2.7% and the moderator is light water.

- 1 metal uranium experiment [5]. The enrichment is 1.3% and the moderator is light water.

- 3 uranium dioxide light water lattices from English origin [6]. The enrichment is 1.4%.

- 2 homogeneous media which are constituted by a solution of uranyl nitrate in light water. The enrichment is 98% and these experiments, performed in Oak Ridge [7], are very few sensitive to  $^{238}\text{U}$ .

- 2 TRX lattices enriched at 1.5% and light water moderated [8].

- 1 Swedish critical experiment in which buckling measurements were carried out as a function of temperature [9].

- 6 enriched uranium light water lattices from Argonne [10]. In these lattices the importance of the epithermal range is enhanced by using various tight pitches.

- 8 French critical experiments performed from 1980 to 1984 in the frame of the pressurized water reactor studies.

All these experiments cover a wide range of neutron spectra. The slowing down density (number of neutron which reach the thermal energy range for one fission neutron) varies from 0.35 for the tight pitch lattices to 0.93 for the well thermalized lattices. The typical value of this spectrum index is 0.6 for a standard pressurized water reactor.

### III.2 - Mixed and plutonium media

- 6 heavy water moderated lattices. The fuel is metallic and is a mixture of 0.4% of plutonium and 99.6% of natural uranium. The amount of isotope 240 in the plutonium is equal to 6% [11].

- 6 light water moderated lattices, the fuel of which is made of 1.5 - 2 or 4% of plutonium with 8% of isotope 240 [12].

- 5 homogeneous multiplying media. They are made of solution of plutonium nitrate in light water. One is an American experiment in which the plutonium contains 4.8% of isotope 240 [13]. The four others are French critical experiments with 3.2% of plutonium 240 [14]. These five experiments are very interesting because they do not contain uranium and they allow us to disconnect the effect of uranium from the effect of plutonium.

- 4 Japanese lattices with light water and 8% of plutonium dioxide with 22% of Pu240 [15].

- 4 American lattices with light water and 2% of plutonium dioxide with 8% of Pu240. They cover a moderating ratio from 1 to 8 [16].

- 2 recent French experiments with tight pitches. The fuel is made of 11% of plutonium dioxide with 19% of isotope 240.

These plutonium experiments cover a neutron spectrum range a little bit harder than the range of the uranium experiments. The slowing down density varies from 0.25 to 0.87.

### III.3 - Spent fuel analysis

The variation, with the burn-up, of the chemical and isotopic composition of a spent fuel is a function of the capture cross sections. The experimental measurement of these compositions is an integral data which can supply informations about the capture cross sections of the heavy nuclei. But we absolutely need to be able to reproduce with a very good accuracy the burn-up story of the irradiated pellets. It is not always the case because the irradiations take place in power reactors which have a very complicated geometry. A good choice of the pellet in the pin, of the pin in the assembly and of the assembly in the core allows us to obtain irradiation conditions which can be well reproduced by the computation. We also need the power story of the reactor and the power shift inside the core as a function of the burn-up. These conditions were achieved in the case of the Tihange I power reactor. Thus we use the results of the analysis of fuel irradiated during one, two and three years in this reactor. Forty two results were used for the tendency research. They are relative to the isotopic composition of uranium and plutonium and the amount of plutonium in the spent fuel. The burn-up of the analyzed samples varies from 0.4 to 3.3 TJ/kg. The calculations are normalized to the experimental burn-up deduced from the measurement of the Nd148/U238 ratio.

### IV - SENSITIVE NUCLEAR PARAMETERS

Usually in France, we perform the transport calculation of the thermal neutron reactors with a 99 group library. That is to say that each cross section is represented by 99 values and that the neutron transfert from one group to another are represented by a very high order matrix. Obviously it is not possible to search for tendencies for each energy group of the cross sections or for each matrix element. But, fortunately, the difference between the computed values and the measured values of the integral quantities can be explained with the help of a more reduced number of neutron parameters. These parameters are commonly called synthetic parameters. It is for these synthetic parameters that we will search for tendencies and afterwards we will deduce informations about the neutron basic data. The choice of the synthetic quantities is favoured by the knowledge of the sensitivity profile of each integral experiment. For this purpose the whole energy range is divided into three parts:

- The fast energy range ( $E > 10$  keV) which is characterized by slight variations of the cross sections. It is mainly the fission cross sections which are important in this region.
- The resonance energy range ( $10$  keV  $> E > 1$  eV) which can be represented by the effective resonance integral or the effective average cross sections.

- The thermal range ( $E < 1$  eV) where the cross section can be represented by their shaped obtained from the microscopic data and the 0.025 eV value.

It is necessary to add to the preceding quantities, the  $\nu$  - bar for the fissile nuclei and the thermal cross sections and the migration area of the moderators. Finally we have used 23 synthetic parameters. They are:

- $\nu$  values for  $^{235}\text{U}$ ,  $^{238}\text{U}$ ,  $^{239}\text{Pu}$  and  $^{241}\text{Pu}$ ,
- thermal and epithermal capture and fission cross sections for  $^{235}\text{U}$  and  $^{239}\text{Pu}$ ,
- high energy fission cross section and effective capture integral of  $^{238}\text{U}$ ,
- thermal absorption cross section of  $^{240}\text{Pu}$  and  $^{241}\text{Pu}$ ,
- first resonance parameters for  $^{240}\text{Pu}$ ,
- thermal capture cross section and migration area of the moderators.

#### V - RESULTS AND ANALYSIS

From the mathematical point of view, the smallest value of the  $Q'$  sum is obtained when the degree of freedom number is maximal. That is to say, in the present case, the minimum is obtained when we accept to modify all the 23 synthetic parameters. A detailed analysis of these modifications shows that some of them are both small and unaccurate. Therefore, they do not have any physical meaning, and there is no objection to agree not to modify these parameters. It is easy to understand that the modifications of only some parameters can give a very good solution to our problem.

The tendency research method was used to qualify several set of nuclear data for the computation of the thermal neutron reactors. For example, in the case of the version 1 of the "Joint Evaluated File" we have obtained meaningful modifications for the following parameters of the heavy nuclei and moderators

- the neutron per fission yield of  $^{235}\text{U}$  and  $^{239}\text{Pu}$ ,
- the thermal fission cross sections of  $^{235}\text{U}$  and  $^{239}\text{Pu}$ ,
- the radiative width of the first  $^{240}\text{Pu}$  resonance,
- the effective integral of  $^{238}\text{U}$ ,
- migration and capture of the light water.

With these modifications the agreement between the computed values of the criticality factor and the experimental ones is better, on average, and the dispersion is smaller. The table I gives the average value and the dispersion of  $k_{eff}^c - 1$  in unit  $10^{-5}$ , separately for uranium experiments and plutonium experiments, after tendency research.

Uranium fuel	$26 \pm 490$
Plutonium fuel	$98 \pm 550$

TABLE I

$$\langle k_{eff}^c - 1 \rangle \pm \sigma$$

For all the experiments the differences between the computed value  $k_{eff}^c$  of the effective multiplication coefficient and the experimental ones



$(1 \pm \Delta k_{eff})$  are displayed on figures 3 for the uranium fuel and 4 for the plutonium fuel. Each integral experiment is identified by its slowing down density  $q$ . Taken into account the experimental uncertainties, the results seem to be satisfactory.

We obtain similar results in the case of the spent fuel analysis. As an example, figure 5 displays the comparison between the computed isotopic composition of the uranium and the measurements.

The proposed modifications of the initial JEF data which give the best agreement with all the integral experiments are given in table II for the heavy nuclei thermal data. We can make the following comments about the results of the tendency research method:

	ENDF/B5	Divadeenam [17] (1984)	Axton [18] (1986)	Tendency Research	
U235	$\nu$	2.4367	$2.4251 \pm 0.0034$	$2.4261 \pm 0.046$	$2.429 \pm 0.004$
	$\sigma_f$	583.6	$582.6 \pm 1.1$	$585.1 \pm 1.6$	$582.0 \pm 1.0$
	$\sigma_T$	98.4	$98.3 \pm 0.8$	$96.1 \pm 1.7$	$98.4 \pm 1.5$
Pu239	$\nu$	2.8914	$2.8768 \pm 0.0057$	$2.8794 \pm 0.0060$	$2.867 \pm 0.007$
	$\sigma_f$	741.7	$748.1 \pm 2.0$	$748.5 \pm 2.6$	$748.0 \pm 2.1$
	$\sigma_T$	270.2	$269.3 \pm 2.2$	$270.4 \pm 3.2$	$270.0 \pm 3.4$
Pu240	$\sigma_T$	292.7	-	-	$283.7 \pm 1.4$

TABLE II

Major actinides 0.025 eV neutron nuclear data

a) Uranium 235

The neutron per fission yield must be slightly decreased. It is better to use a 2200 m/s value equal to  $2.429 \pm 0.004$ . This value is significantly lower than the one of ENDF/B5. It is good agreement with the Devadeenam recommendation [17] but slightly different from the Axton one [18].

The thermal fission cross section must be also decreased and we propose  $582.0 \pm 1.0$  barn. No significant modification seems to be necessary for the thermal capture cross section and the epithermal fission and capture cross sections.

b) Uranium 238

The production cross section  $\nu\sigma_f$  must be kept unchanged in the fast neutron range but the self shielding capture cross section must be decreased by  $0.03 \pm 0.02$  barn in the resonance energy range. This corresponds to a decreasing of  $0.3 \pm 0.2$  barn for the effective integral. It is negligible for the infinite dilution resonance integral but it represents  $2 \pm 1.5\%$  for a 50 barn background cross section (average dilution for a pressurized water reactor), that is to say a  $200 \cdot 10^{-5}$  reactivity effect.

c) Plutonium 239

The plutonium 239 case is more difficult because, in all the evaluated files the  $\nu$  value is assumed to be roughly constant in the thermal energy range. But we know that the  $\nu$  value of plutonium 239 fluctuates from resonance to resonance. In particular, the  $\nu$  value of the 0.296 eV resonance is lower than the  $\nu$  value of the bound level. As the 0.296 eV resonance has an important weight in the thermal range, the  $\nu$  value cannot be constant. That is why we have modified the original shape of  $\nu$  versus energy according to Gwin results [19] and FORT evaluation [20]. It is with this modified shape that we performed the tendency research. With this assumption we recommend a  $\nu$  value equal to  $2.867 \pm 0.007$  for 0.025 eV neutron. It is lower but not too different from the Divadeenam and Axton recommendations but strongly discrepant with ENDF/B5. With these conditions we propose 748.0 for the fission cross section and 270.0 for the capture cross section.

It does not seem necessary to modify the epithermal cross sections.

d) Plutonium 240

It is essentially the spent fuel analysis which give some information about the  $^{240}\text{Pu}$  capture. For the radiation width of the first resonance, we obtained the value  $32.2 \pm 0.9$  meV. It is not very accurate and therefore the modification of the original value of the file is not significant. Our result is in agreement with the experimental result of Brookhaven [21] but in disagreement with the last result of Oak Ridge [22].

e) Moderators

Small modifications are suggested for the moderator neutron properties. It seems that the thermal capture of the light water must be slightly increased ( $0.6 \pm 0.4\%$ ). The proposed modification is a little more important for the migration area which must be decreased ( $2 \pm 1\%$ ). For the heavy water migration area, no modification seems to be useful ( $0. \pm 0.8\%$ ).

V - CONCLUSION

The use of integral experiments and tendency research method seems to be an very efficient tool to improve the neutron data and to achieve the accuracy which is required by the reactor physicists. But we imperatively must respect three stringent conditions.

- 1 - The integral experiments must be simple and clean from the neutron point of view, they must be computed without numerical or physical approximations. The best one are those which can be calculated with a one cell calculation in an asymptotic spectrum.
- 2 - In order to obtain the multigroup libraries, the evaluated data have to be process with a very accurate code. The Doppler broadening formalism, the energy mesh and the collapsing spectrum must be very carefully checked.
- 3 - It is necessary to have a "good shape" of the thermal neutron cross sections, because the magnitude of the 0.025 eV cross sections that we deduce from  $k_{eff}$  measurement can be depend on the shape of these cross sections in the thermal range. It can be shown, for example, that in the case of uranium 235 [23]: we can obtain results slightly different with the shape deduced from recent microscopic data than with the shape of the original versions of the Joint Evaluated File.

## REFERENCES

- [1] P. REUSS  
French Report CEA-N-2222 (1981).
- [2] Y. GIRARD and R. NAUDET  
IAEA Technical Report 20 (1963).
- [3] F. COGNE et al.  
French Report CEA-N-1344 (1970).
- [4] W.J. EICH et al.  
Report WCAP 3269-52 (1965).
- [5] R.L. HELLENS and G.A. PRICE  
Report USA EC-TID 8540, 529 (1964).
- [6] W. BROWN et al.  
Report AEEW-R-502 (1967).
- [7] R. GWIN and D.W. MAGNUSSON  
Nuclear Science and Engineering 12, 354 (1962).
- [8] J. HARDY et al.  
Nuclear Science and Engineering 40, 10 (1970).
- [9] R. PERSSON et al.  
Third International Nuclear Industries Fair Conf. 721062, 2, 11 (1972).
- [10] A.R. BOYNTON et al.  
Report ANL 7070, 33 (1963).
- [11] R. BIR et al.  
Report Euratom 4477 (1970).
- [12] L.C. SCHMID et al.  
Report BNWL-801 (1968).
- [13] R.C. LLYOD et al.  
Nuclear Science and Engineering 25, 165 (1966).
- [14] R. CAIZERGUES  
French Report CEA-R-3650 (1969).
- [15] I. KOBAYASHI et al.  
Nuclear Science and Technology, 15, 166 (1978).
- [16] R.D. LEAMER et al.  
Report WCAP-3726 (1967).
- [17] M. DIVADEENAM and J.R. STEHN  
Annals of Nuclear Energy, 11, 375 (1984).
- [18] E.J. AXTON  
Geel Report GE/PH/01/86 (1986).
- [19] R. GWIN et al.  
Nuclear Science and Engineering 87, 381 (1984).

- [20] E. FORT et al.  
Nuclear Science and Engineering 99, 375 (1988).
- [21] H.J. LIOU and R.E. CHRIEN  
Uranium and Plutonium Resonance Parameters, INDC 129, 438 (1981).
- [22] R.R. SPENCER et al.  
Nuclear Data for Basic and Applied Science - Santa Fé, I, 581 (1985).
- [23] H. TELLIER et al.  
"Internatioanl Reactor Physics Conference", Jackson Hole (1988).

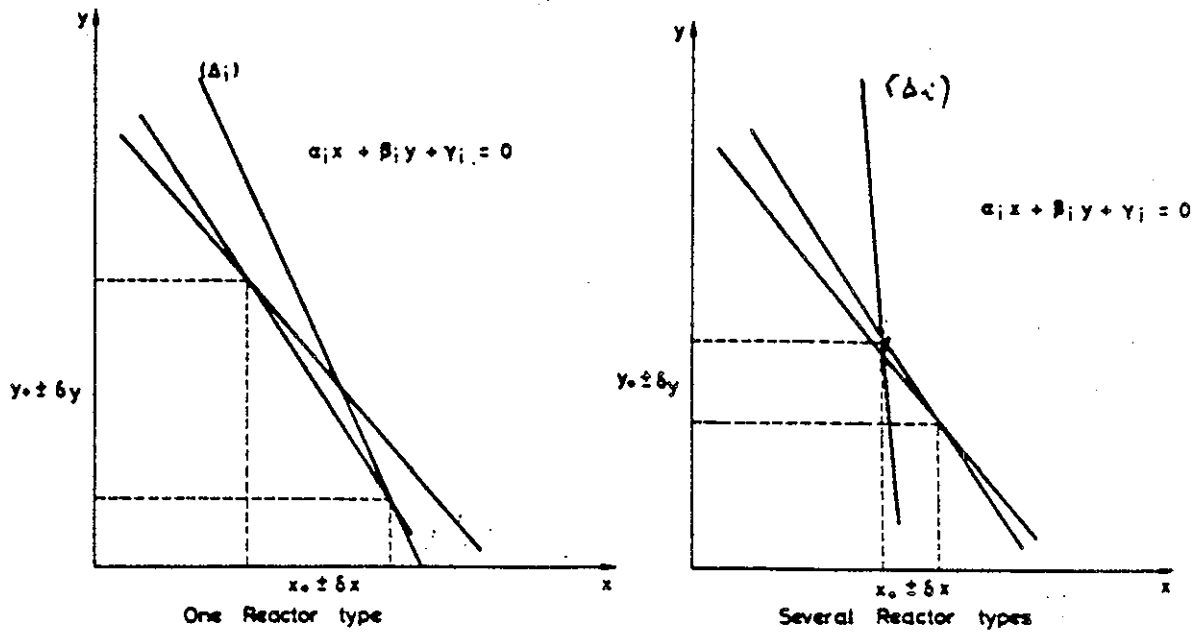


Figure 1

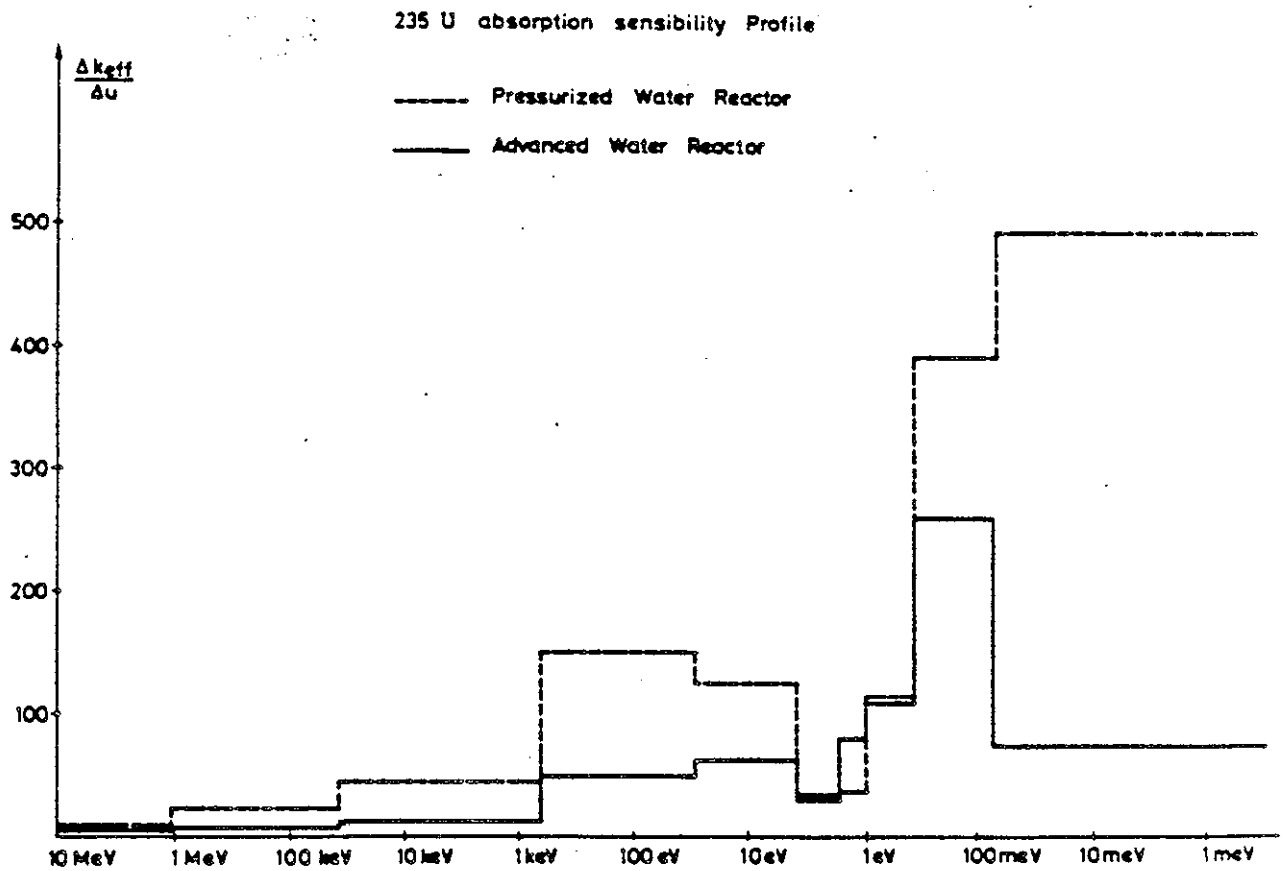


Figure 2

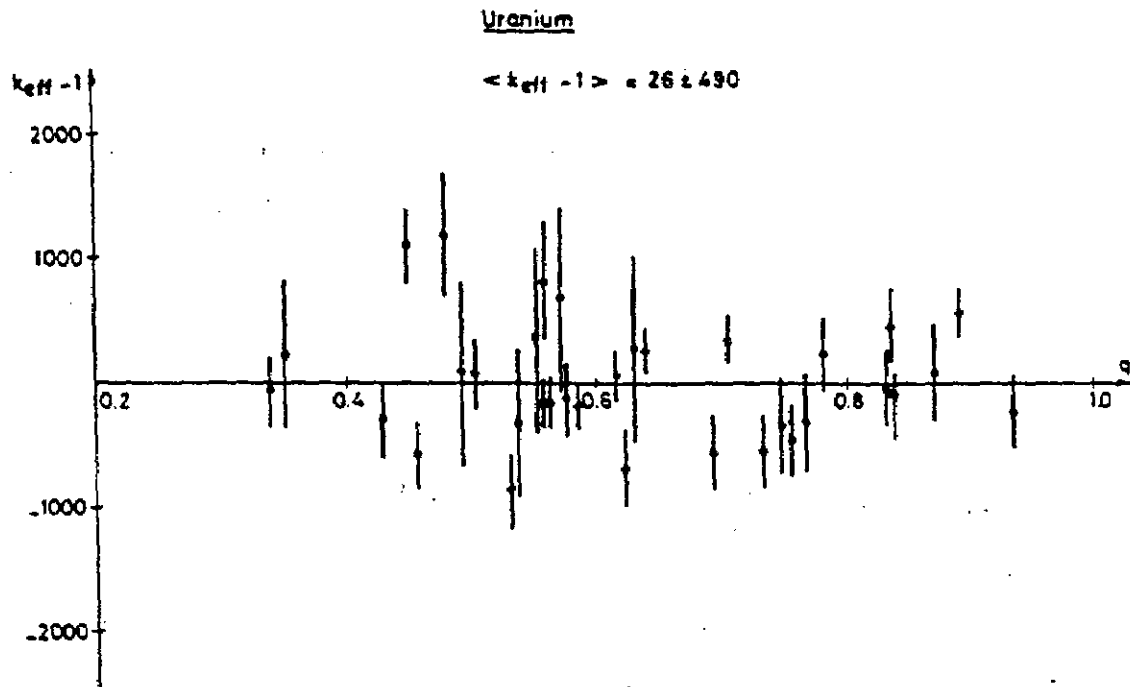


Figure 3

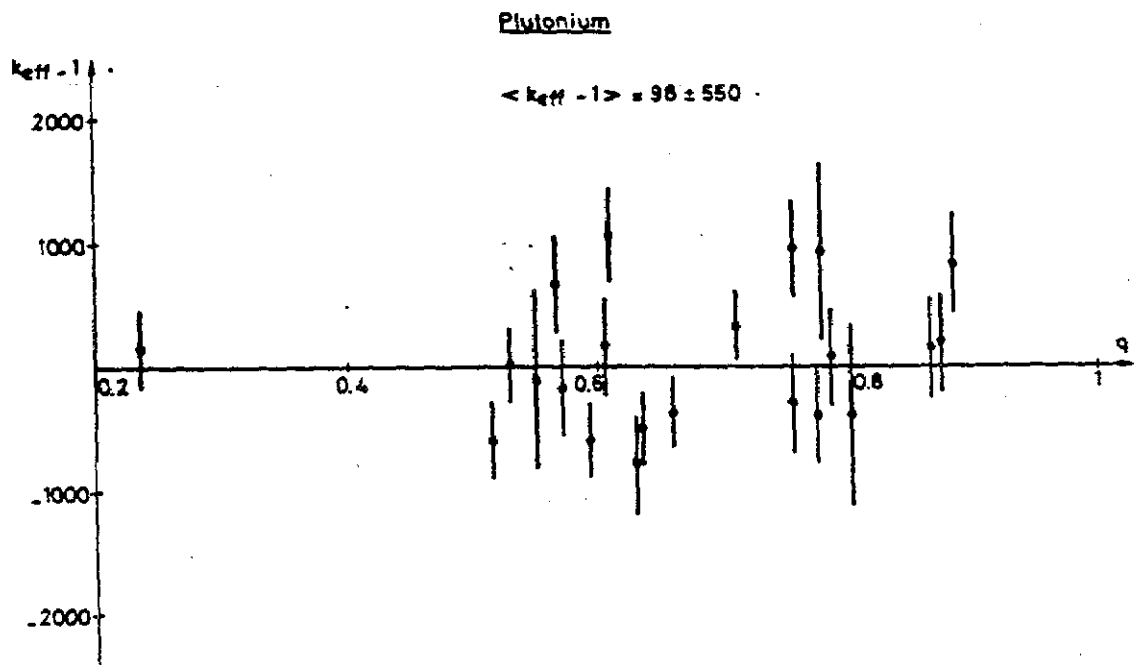


Figure 4

94050234

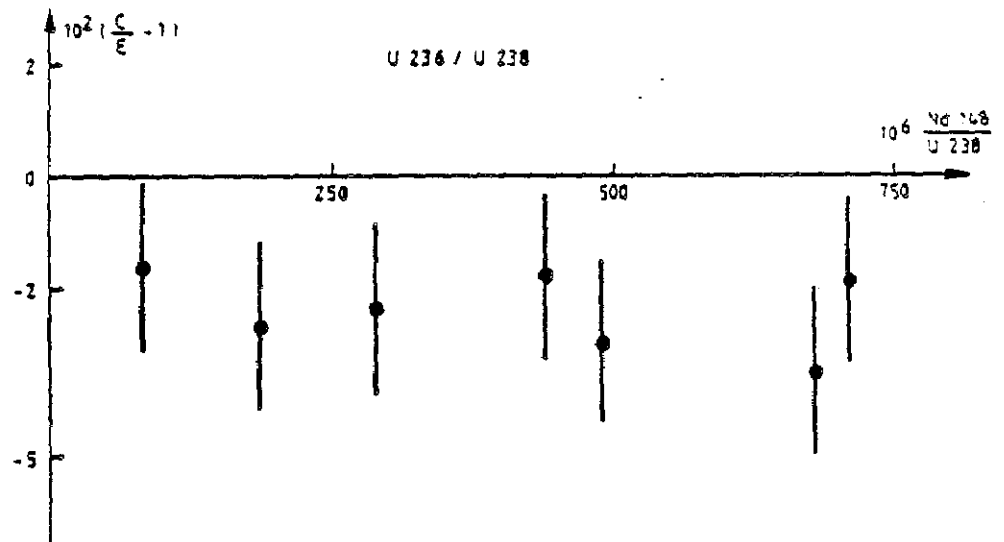
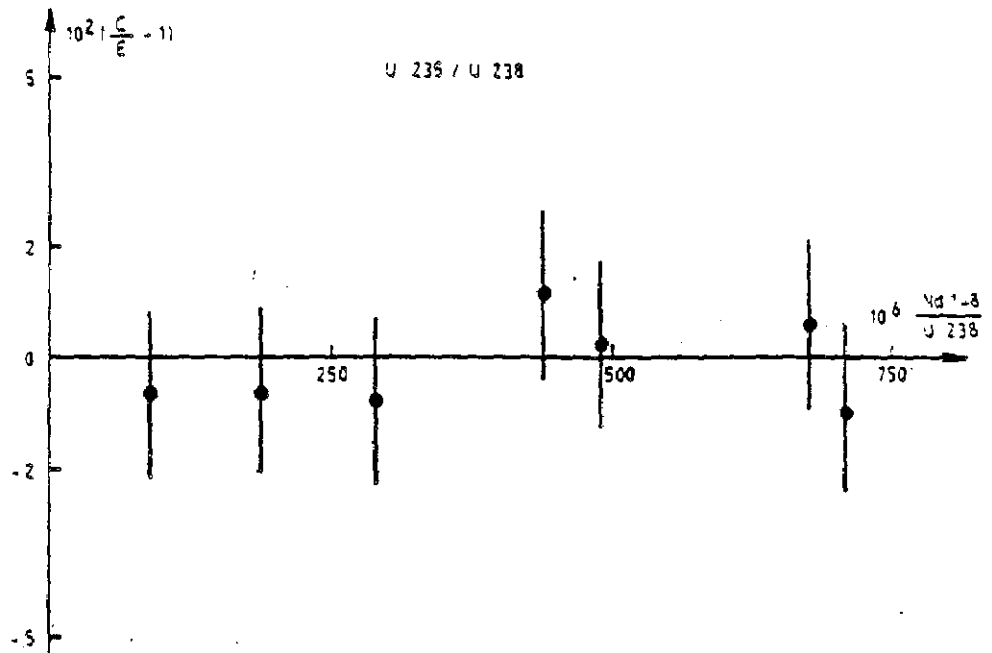


Figure 5

Summary of a paper submitted for presentation at the 1988 NEACRP Specialists' Meeting on the Application of Critical Experiments & Operating Data to Core Design Via Formal Methods of Cross Section Data Adjustments, September 18-21, in Jackson Hole, Wyoming.

TOPICS IN DATA ADJUSTMENT THEORY AND APPLICATIONS

by

R.N. Hwang

Applied Physics Division  
Argonne National Laboratory  
9700 S. Cass Avenue  
Argonne, Illinois 60439

\*Work supported by the U.S. Department of Energy, Nuclear Energy Programs under Contract W-31-109-ENG-38.



## I. INTRODUCTION

The methodologies of the uncertainty analysis and data adjustment have been well-developed and widely used abroad since the early 70's.<sup>1-7</sup> With limited amount of covariance data on the differential cross section and the integral experiments available at the time, their accomplishments are, indeed, astounding. One of the most comprehensive discussions on these subjects is believed to be given by Dragt et al.<sup>2-3</sup> Two fundamental adjustment equations that relate the posterior information (i.e., the adjusted cross section set and its covariance) to the prior information (i.e., the original cross section set along with the existing integral experiment data base and their covariances) are derived. Dragt<sup>2-3</sup> has shown that these equations can be derived either on the basis of the Bayes theorem or from the generalized linear least square approach usually referred to as the Gauss-Markov theorem. A rather elaborate code system has been developed at RCN (Reactor Centrum Nederland) to perform the adjustment calculations, centered around the STEK experiments.<sup>2</sup> More fundamental aspects of the pertinent theory were further examined by Peele<sup>8</sup> when the concerted efforts on the sensitivity analysis were carried out at ORNL in the middle and late 70's.<sup>8-11</sup> Many aspects of the Bayesian methodologies and the generalized least square approach have since been further explored by many others.<sup>12-19</sup> The fundamental adjustment equations, however, remain qualitatively unchanged.

For the past few years, extensive efforts on these subjects have also begun at ANL in order to utilize the massive amount of integral experiments accumulated over years to provide the basis for improving the reactor parameters encountered in various design calculations.<sup>20-22</sup> Pertinent covariance matrices and sensitivity matrices of the existing integral experiments have been evaluated and systematically compiled in the data files<sup>20-22</sup> along with the cross section covariance data derived from the ENDF-B/V for the 21 group structure currently under consideration. A production code GMADJ<sup>21</sup> that provides the adjusted quantities for a large number of cross section types has been developed by Poenitz<sup>21</sup> for routine applications.

The primary purpose of the present paper is to improve understanding of the application oriented issues important to the data adjustment theory and

the subsequent usage of the adjusted quantities in the design calculations in support of these activities.

In Section II, a brief review of the existing data adjustment theory is given along with the pertinent issues. One issue of particular interest is the treatment of the spatial and energy self-shielding effects. It is well known that such effects play an important role in the analysis of the integral experiments in the critical assemblies. The fact that these effects may have different characteristics in the power reactor systems presents potential difficulties in the applications of the adjusted quantities. It will be shown how these effects can be treated consistently by minor modification of the existing group constant processing code.

Section III discusses issues related to the interpretation and applications of the data adjustment theory. To address these issues, the characterization of the existing integral experiments and their potential connections to the design parameters of practical interest is essential. All these quantities are, in principle, characterized by their 'sensitivity profiles'. However, 'sensitivity profiles' are difficult to quantify especially when a large number of experiments and calculations involving many reaction types are considered. A simple yet effective alternative is to utilize the linear vector space concept. It is possible to define a reference sample space spanned by the sensitivity vectors characteristics of the existing integral experiments. A set of orthonormal basis which provides the connection between the vector space and the usual algebra can be obtained via the Gram-Schmidt process. The basis not only specifies the reference coordinate system but also provides the means of mapping the designer's sensitivity vectors into the reference vector space. Three criteria are proposed to estimate the potential impact of the adjusted quantities on the design parameters without having to go through the adjustment procedure. The proposed model can also help one to determine what types of future integral experiments are needed should the situation require. A multi-purpose code ADJUST has been developed to provide numerical means to quantize these criteria. Practical examples are given to illustrate how the proposed model can be carried out effectively. 18 FFTF responses were chosen as the user's quantities while 79 integral experiments carried out in three uranium-fueled and four plutonium-fueled critical assemblies were used as the reference systems for these purposes.

## II. Brief Review of the Data Adjustment Theory and Pertinent Issues

For our purpose here, a brief review on the fundamental aspects of the problem is believed to be helpful before the pertinent issues are addressed. In the following discussions the notations of Dragt, et al.<sup>2-3</sup> will be retained for convenience. It is important to realize, however, that the quantities defined by Dragt<sup>2-3</sup> must be modified slightly to be consistent with the data files currently available. Such modifications will be described after the adjustment equations are defined.

Consider a vector  $T$  with a set of  $n_t$  multigroup cross sections where  $n_t$  is the product of the number of groups, nuclides and reaction types of interest. The corresponding covariance matrix for the multigroup cross section of order  $n_t \times n_t$  is denoted by  $M$  to distinguish from the covariance matrix  $K$  for the infinitely dilute cross sections. The distinction is necessary when the question of the self-shielding effects are addressed in the discussions later. Let there be  $n_r$  integral quantities denoted by vector  $R$  with covariance matrix  $V$  of order  $(n_r \times n_r)$ . In the context of the methodologies currently in use,<sup>21</sup>  $V$  is the sum of  $V_E$ , covariance matrix of the integral experiments, and  $V_c$ , covariance attributed to model uncertainties in computing those integral experiments. The calculated values of the experiments are denoted by  $\bar{R}$  which is an implicit function of  $T$ . The sensitivity matrix of order  $(n_r \times n_t)$  obtained from the perturbation calculations is represented by  $G$ . The linearity assumption leads to

$$\delta \bar{R} = G \delta T \quad (1)$$

The derivation of the "best" estimate of cross sections  $T'$  and its covariance  $M'$  can be accomplished via either one of the two theoretical foundations.

### 1. Bayesian rule

The Bayes theorem<sup>23-24</sup> is also referred to as the principle of inverse probability that provides the rule in the process of learning from experience. It maybe stated formally as:<sup>23-24</sup> The posterior probabilities of the hypotheses are proportional to the product of the prior probabilities and the

likelihood. To translate the theorem into practical term of interest here, one can formulate it as

$$P(t_i | r_k) = P(t_i)P(r_k | t_i) \cdot \text{constant} \quad (2)$$

where the set of events (or cross sections)  $\{t_i\} = T$ ,  $P(t_i)$  is the probability of event  $t_i$ ,  $P(x|y)$  is the conditional probability and  $\{r_k\} = R$  are the existing integral experiment data. If the multivariate normal distributions are assumed for  $P(t_i)$ ,  $P(r_k | t_i)$  and  $P(t_i | r_k)$ , along with the linearity assumption of Eq-1, one has

$$\begin{aligned} P(t_i | r_k) &= \text{const.} \exp\left\{-\frac{1}{2}(T-\bar{T}')^T M'^{-1}(T-\bar{T}')\right\} \\ &= \text{const.} \exp\left\{-\frac{1}{2}(T-\bar{T}-\xi)^T (M^{-1} + G^T V^{-1} G)(T-\bar{T}-\xi)\right\} \end{aligned} \quad (3)$$

where the shift  $\xi$  is defined as

$$\xi = \frac{G^T V^{-1} (R-\bar{R})}{M^{-1} + G^T V^{-1} G} \quad (4)$$

Thus, to bring in additional information via the use of integral experiments amounts to the introduction of a shift factor and the reduction of the width of the original distribution function  $P(t_i)$  so that the expectation values of  $t_i$  become closer to the true value in the statistical sense. Eq-3 leads immediately to the adjustment equations

$$\bar{T}' - \bar{T} = \frac{G^T V^{-1} (R-\bar{R})}{M^{-1} + G^T V^{-1} G} \quad (5)$$

and

$$M' = (M^{-1} + G^T V^{-1} G)^{-1} \quad (6)$$

The posterior means  $\bar{T}'$  and its covariance  $M'$  can be found by solving these equations. Conceptually, the statistical origin of these quantities should be realized.

## 2. Generalized Least Square Approach

The emphasis of the least square approach is to find the "best" unbiased estimate of minimum variances to certain observed quantities with known errors.<sup>25</sup> Consider a observation vector consisting of  $n$  experiments with known random errors and assume that these observations are related linearly to a set of  $m$  physical parameters denoted by vector  $X$  with  $n > m$ . The matrix that relates the observations to the parameters in the over-determined system of linear equations is usually referred to as the design matrix. The objective is to find a best estimate  $X'$  corresponding to the best fit to the observations in the least square sense.

A direct analogy between the problem of interest and the above method is quite apparent. For the cross section adjustment purpose, however, the number of the available data base from the integral measurements  $n_p$  is usually much less than the number of cross sections to be adjusted. One way to avoid this problem is to picture the original set of group cross sections  $T = \{\tilde{\sigma}_i\}$  as if they were observed quantities. Thus, the number of parameters to be adjusted is  $m = n_t$  and the total observations are  $n = n_t + n_p$ . The design matrix is the union of an identity matrix  $I$  and sensitivity matrix  $G$ . The least square equation becomes

$$q^2 = (T' - T)^T M^{-1} (T' - T) + (\bar{R}' - R)^T V^{-1} (\bar{R}' - R) \quad (7)$$

where all the quantities were defined in the foregoing discussions. Upon minimization of  $q^2$  with respect to  $T'$ , one obtains the pair of adjustment equations same as Eq-5 and 6 except that  $\bar{T}$  and  $\bar{T}'$  are replaced by  $T$  and  $T'$  respectively.

Here, the physical meaning of the adjusted data is quite different from that based on Bayes theorem.  $T'$  is considered as a set of the auxiliary variables that can be used to provide the "best" calculated estimates of the experiments while the former is the mean value based on the normal distribution. Another distinction of theoretical interest is that the generalized least-square approach does not require the normality assumption of the distribution functions.

Both Eq. 5 and 6 involve the inversion of M which can present a practical problem if  $n_t$  is large. Dragt, et al.,<sup>2-3</sup> have shown, through simple matrix algebra, that they can be reduced to the much simpler forms.

$$T' - T = H (R - \bar{R}) \quad (8)$$

$$M' = P M \quad (9)$$

where

$$H = M G^T (G M G^T + V)^{-1} \quad (10)$$

$$P = I - H G \quad (11)$$

Here, the problem is reduced to that of the inversion of a  $(n_r \times n_r)$  matrix where  $n_r$  is usually smaller than  $n_t$ .

As mentioned earlier, various quantities defined by Dragt<sup>2-3</sup> must be modified somewhat to be consistent with the data files and methodologies currently in use. It is now customary to define the sensitivity coefficients as the fractional change in the calculated response in a given energy group corresponding to a fractional change in the cross section of the same group instead of the unnormalized version implied in Eq-1. The adjustment of cross sections and the uncertainties are also defined as the fractional values. Under these assumptions, the adjusted value  $T' - T$  and the discrepancy  $R - \bar{R}$  defined in Eq-8 should be replaced by  $(T' - T)/T$  and  $(\frac{R}{\bar{R}} - 1)$  respectively in the actual calculations. It is worth noting that the  $\frac{R}{\bar{R}}$  ratio implicitly requires the inclusion of all known corrections to the deficiencies of the calculational models based on the most rigorous methods available for the integral experiment analysis in accordance with their estimated 'covariance'  $V_c$  included in  $V$ . An alternative to treat the method deficiencies is the so-called 'bias' factor approach<sup>14</sup> where by the least squared equation must be modified slightly to accommodate the simultaneous adjustment of the 'bias' factors. In the present work, the 'bias' factor approach is not considered.

## 2. Pertinent Issues

From the practical point of view, there are three key issues in the applications of these equations. First concern is related to the availability

of detailed cross section covariance data required by the multigroup structure desirable for analysis of integral experiments. Second concern is the system dependent nature of the group cross sections characterized by the self-shielding effects in energy as well as in space. Third concern is the apparent lack of a general consensus on the treatment of the errors due to the calculational models in the adjustment process and in the subsequent applications of the adjusted data.

The energy group structure currently considered for the integral experiment analysis is 21 groups. The existing ENDF-B/V covariance data for various key cross sections are usually much coarser in structure. Consequently, the off-diagonal elements of the correlation matrix after processed through the NJOY code<sup>26</sup> can become unusually large as a result of going from the coarse structure to the finer structure. Although the process preserves the original data; the positive definite nature of the correlation matrix required on the physical grounds can no longer be maintained for most of the key actinides. Various remedies have been attempted in order to preserve the positive definite nature of the correlation matrix. One obvious method is to make the matrix more diagonally dominant by adding an additional term  $|\lambda_{\min}^-| I$  to the correlation matrix where  $|\lambda_{\min}^-|$  is slightly greater than the absolute magnitude of the smallest negative eigenvalue of the correlation matrix. Other options to scale down the off-diagonal elements were also discussed by Poenitz.<sup>21</sup> Such procedures, however, do not guarantee the preservation of the original errors inferred by the ENDF-B data unless the diagonal elements of the covariance are also modified accordingly. Recent applications of the adjusted data to the depletion-dependent perturbation calculations by Downar and Khalil<sup>29</sup> seem to indicate that the initial uncertainties of various responses prior to the adjustment obtained by using the 21 group data so produced are substantially lower than those obtained by Kamei and Yoshida<sup>15</sup> based on 4 groups with comparable diagonal elements. Aside from the possible differences in the basic off-diagonal elements assumed, the discrepancies can be attributed to the scaling process where the original ENDF/B data were not preserved. In lieu of detailed covariance information, the scaling process will be further examined. Another data related issue of practical interest is the lack of sufficient covariance data to represent the resolved resonances. The resolved energy region plays an important role in the self-shielding effects.

The cross section vector  $T$  and its covariance matrix  $M$  defined by Dragt<sup>2,3</sup> were meant for the self-shielded cross sections. Except for a handful of examples in earlier work,<sup>3,15</sup> no distinction is made on the shielded and the unshielded quantities in the current application of the adjustment theory. The use of the adjusted set deduced on the basis of the integral experiments of the zero power critical facilities for actual power reactors with somewhat different composition and geometric configurations can be controversial. The impacts of the self-shielding effect must be addressed in a broader context including the spatial self-shielding (or heterogeneity) effect that is known to play an important role in the analysis of the critical experiments. Our cross section sets generated by the MC<sup>2</sup>-2/SDX code<sup>28</sup> include corrections to both the high energy (flux peaking) and the low energy (flux depression) heterogeneity effects which are substantial in the plate geometries. For example, the spatial self-shielding factor for Pu<sup>239</sup> fuel plates in the ZPR-6/assembly 7 range from 1.35 to 1.15 between 14 meV and 1 meV region (or the first six groups of our standard 28 group set) where the peak of the fission spectrum occurs according to the calculations carried out by McKnight.<sup>29</sup> In contrast, the spatial self-shielding factor for the fuel rods in the closely packed lattice of a power reactor is not expected to be significantly different from unity in the same energy range. Similarly, the "disadvantage" factors in the low energy groups below 4 keV are substantially lower in the ZPPR systems than those expected in the fast power reactor systems. For the same reasons, the energy self shielding effects are also expected to be quite different. The latter is pertinent to reactor parameters that rely on the relatively low energy spectrum. The "Doppler Coefficient", for instance, is obviously the typical example. Although the use of the fractional change in the adjusted quantities softens the impact of the self-shielding effects, nevertheless, their potential roles can not be totally dismissed.

Without loss of generality, the self shielded cross section can be defined as<sup>30</sup>

$$\tilde{\sigma}_{ig} = \langle \sigma_{ig} \rangle f_{ig} = \langle \sigma_{ig} \rangle \left[ 1 + \frac{\text{COV}(\sigma_i, \phi)_g}{\langle \sigma_{ig} \rangle \langle \phi \rangle_g} \right] \quad (2)$$

where



$$\text{COV} (\sigma_i, \phi)_g = \langle \sigma_i \phi \rangle_g - \langle \sigma_{ig} \rangle \langle \phi \rangle_g \quad (3)$$

and the bracket  $\langle \rangle$  denotes the average over energy and space.

Thus, the degree of the self-shielding effect is physically a measure of the correlation between the basic cross section and neutron flux of a given environment in energy as well as in space. The multivariate nature of  $f_{ig}$  reflects the inter and intra correlations of the shielded cross sections in energy and in space.

Define  $\tau_{ik}^g$  be the sensitivity coefficient of the self-shielded cross section with respect to a particular parameter  $q_k$ . The computation of  $\tau_{ik}^g$  requires the detailed information of  $\phi$  as a function of  $\sigma_{ig}$ . Unlike the Bondarenko approach, such information, in principle, can be retrieved in the MC<sup>2</sup>-2/SDX code<sup>28</sup> when the group constants are generated. Once  $\tau_{ik}^g$  is obtained, little modification is needed to incorporate the self-shielding effects in the existing adjustment methodology. Work has been initiated in this area.

The issue concerning the 'uncertainties' of the calculational models is conceptually most difficult to resolve. With exception of the Monte Carlo approach, the deterministic nature of the model error pictured in statistical terms is not easy to grasp. Since the model errors in the calculated values of the same nature are highly correlated, both the diagonal and off-diagonal elements of the fictitious covariance must be assigned. The uncertainties assigned to the model errors can reflect a great deal of one's subjective judgment. The problem is the same whether one uses the direct approach or the 'bias' factor approach.<sup>14</sup> The fact that many method deficiencies are consequences of inadequate treatment of the group constants makes it even more difficult to rationalize. Heterogeneity effect and self-shielding effect are typical examples. From the theoretical point of view, it is clearly desirable to remove the model deficiencies if possible. In recent years, the methodologies in the analysis of the integral experiments have been significantly improved. The use of the Monte Carlo code VIM as a bench-mark tool has certainly improved our confidence of the methods currently in use. For  $k$  calculations at least, one can rely on many Monte Carlo results already in existence to infer the model uncertainties without ambiguity. The availability of the multi dimensional neutronic codes also softens the problem. This issue is likely to remain as long as the model deficiencies exist.

### III. INTERPRETATION OF THE ADJUSTMENT RESULTS AND ITS APPLICATIONS

#### 1. Geometric Considerations of the Adjustment Procedure

The essence of adjustment procedure can be best illustrated from the perspective of linear algebra. Of particular interest is the relationship of the responses and their corresponding covariance matrices before and after the adjustment. Using Eq-1 and Eq-8, one has

$$\bar{R}' - \bar{R} = [I - V(GMG^T + V)^{-1}](R - \bar{R}) \quad (14)$$

where I is the identity matrix.

Rearrangement of Eq-4 immediately leads to the relationship between the discrepancy vector after adjustment and that before adjustment

$$R - \bar{R}' = L(R - \bar{R}) \quad (15)$$

where

$$L = V (GMG^T + V)^{-1} \quad (16)$$

Similarly, it can be shown readily from Eq-9 that the covariance matrices of the response before and after the adjustment are related to each other precisely the same way.

$$GM'G^T = L(GMG^T) \quad (17)$$

Thus, the adjustment process amounts to finding an appropriate linear transformation L that transforms the known quantities into the adjusted quantities. Physical meaning of Eq-15 and Eq-17 is quite obvious. To achieve significant improvement in nominal values and uncertainties due to cross sections requires that the combination of covariances of the integral experiments and that due to the calculational models must be small compared to  $GMG^T$ . For integral experiments such as k, which can be measured and modeled accurately, the uncertainties due to nuclear data can be reduced up to one order of magnitude via the adjustment procedure. On the other hand, for measurements such as

localized flux ratios in which high degree of accuracy is more difficult to achieve, less impressive gain is expected.

Fig-1 shows the range of the fractional improvement in uncertainties due to cross sections for various responses after adjustment based on 79 integral measurements made in 3 uranium-fueled and 4 plutonium fueled systems. The calculations are based on extensive data files compiled at ANL using the multi-purpose code ADJUST which will be described later. By and large, the results indicate that the uncertainties of various responses after adjustment can become significantly lower when high quality integral measurements are available.

From a practical point of view, one is more interested in how the adjusted quantities (i.e.,  $T'$  and  $M'$ ) based on the existing integral experiments will help various design parameters that are not included in the fitting process. The design parameters, in principle, can cover a wide range of responses that may or may not bear any resemblance to the existing integral experiments. Two adjusted quantities that are passed on to the designers are the adjusted cross section set  $T'$  and its covariance matrix  $M'$ .

Unlike Eq-15 and Eq-17 the physical meaning of two adjustment equations that define  $T'$  and  $M'$  is more difficult to rationalize. From extensive calculations using the existing data files at ANL, it was found that most diagonal elements of  $M'$  are not significantly reduced for most of the key cross sections considered. Fig-2 and 3 shows the fractional improvement in various key cross sections as a function of energy groups (and energy) based on 79 experiments and ten reaction types described previously. The improvements in uncertainties of principal cross sections shown in Fig-2 are relatively insensitive to the number of experiments included. In contrast, their fractional changes  $(T'-T)/T$  not given here are extremely sensitive to the types of experiments included because of their explicit dependence of the discrepancy vector  $(R-\bar{R})$ . With the exception of  $U^{238}$  inelastic scattering cross sections which reflect the effect of the  $U^{238}$  fission rate related measurements and have relatively minor impact on the calculated quantities of practical interest as compared to other major reaction cross sections, the improvement in the cross section uncertainties via adjustment procedure is, at best, modest as compared to those in responses shown in Fig-1. To reconcile such differences, one is led to the conclusion that the improvement in

response uncertainties defined by Eq-17 and Fig-1 must, to a great extent, be attributed to the off-diagonal elements of  $M'$ . The alteration of the off-diagonal elements alone is equivalent to introducing a rotation in the original quadratic form  $GMG^T$  so as to enhance greater error cancellations. The calculated quantities can become much more tolerant of approximately the same uncertainties in cross sections through the rotation process.

The mechanism of rotation and its impact on the uncertainties can be best illustrated graphically. Consider a simplest possible case of a (2x2) covariance matrix and the sensitivity matrix of dimension of unity. The diagonal matrix  $D$  represents the square root of the variance of cross sections. The uncertainties before and after adjustment can be cast in terms of the well known law of cosine with the correlation coefficient equivalent to the cosine of the angle between two components as shown in Fig. 4. The adjustment of the correlation coefficient amounts to altering of the angle between two components via rotation.

From Fig-4, it is quite clear that  $\epsilon'$  can become significantly smaller than  $\epsilon$  via rotation although the  $D'$  remains substantially the same as  $D$  before the adjustment. Thus, the simple illustration is believed to be the plausible explanation the observed results summarized in Fig. 1, 2 and 3.

## 2. Questions of 'Similarity' Between the User's Quantities and the Reference Quantities

From the user's point of view, the best possible outcome is the dramatic improvement in  $D$  so that the adjustment data can be used for unlimited range of neutronic problems without any constraint. Since such expectation is unrealistic at this time, two obvious questions will arise. First, under what constraint, can the users expect very favorable results if the adjusted data are applied to their calculations? Secondly, what types of additional integral experiments (not necessarily the same types that they are trying to compute) should be considered to further improve the calculations? One obvious answer to these questions is that the "sensitivity profile" of their desired quantities must closely resemble those used in the adjustment procedures. However 'resemblance in sensitivity profile' is imprecise and difficult to quantify. It will be shown in the following discussion why the characterization of the relevant sensitivity vectors requires a more rigorous model.

(1) Sensitivity Profiles

The existing data file compiled at ANL primarily consists of experiments of reaction rate ratios, bilinear ratios, flux ratios, fission spectrum and delay neutron parameters. These measurements are characterized by the sensitivity vectors of key nuclides in the systems. By definition, the sensitivity coefficients of a given response  $R_x$  of type  $x$  with respect to a given cross section type  $z$  of the energy group  $i$  is proportional to  $\frac{\partial R_x}{\partial \sigma_{zi}}$ . For the reaction rate ratio related quantities which form the back-bone of the existing data file, the sensitivity vectors represent simple physical characteristics of the system. For

$$R_x^{(k)} = \sum_i N_x \sigma_{xi} \phi_i / \sum_j N_y \tilde{\sigma}_{yj} \phi_j,$$

the quantity  $\frac{\partial R_x^{(k)}}{\partial \sigma_{zi}}$  exhibits one of the following behavior:

(1)  $z \in x$

$$\frac{\partial R_x^{(k)}}{\partial \tilde{\sigma}_{zi}} \sim \text{Const. } \phi_i$$

to the first order.

(2)  $z \in y$

$$\frac{\partial R_x^{(k)}}{\partial \tilde{\sigma}_{zi}} \sim -\text{Const. } \phi_i$$

to the first order.

(3)  $z \notin x$  and  $z \notin y$

$$\frac{\partial R_x^{(k)}}{\partial \sigma_{zi}} \sim \text{const. } \frac{\partial \phi_i}{\partial \sigma_{zi}}$$

For  $k$ , C28/F49, and F25/F49 measurements, the sensitivity vectors for the key nuclides that explicitly appear in the ratio as (1) and (2) reflects the overall spectrum of the critical assemble under consideration. Similarly, for F28/F49, the sensitivity vectors of  $U^{238}$  fission reflect the high energy spectrum of the system. The sensitivity vectors that belong to the category (3) are of secondary importance. By and large, the central sample worth measurements also reflect the overall spectrum of the system. For flux ratios, the sensitivity vectors reflect only the derivatives of a certain portion of the spectrum of the given system. These quantities are not only difficult to measure but also difficult to calculate accurately. Fig-5 shows various 'sensitivity profiles' (defined as sensitivity vectors normalize to their norms) as function of energy groups for the ZPPR-15D used in the adjustment. Because of the current interest in the FFTF-calculations, ZPPR-15D, a  $U^{235}$  fueled system, is singled out for illustration purposes. It is worth noting that the behavior of major reaction rate ratios in Fig-5 are extremely similar to those of eigenvalue  $\kappa$  except for the signs in some cases. It is quite evident that various sensitivity profiles shown in this figure reflect the overall spectrum of the system. The impact of the Fe resonance at 28.8 keV (group 12) and the Na resonance at 2.85 keV (group 17) are visible. It should be noted that the eigenvalue related quantities are much more sensitive to  $\bar{v}$  than the reaction rate ratios because of the direct correlation of the  $\bar{v}\Sigma_f$  term and the eigenvalue  $k$  in the fundamental neutronic equation.

One brute force method for examining the 'similarity' between the user's 'sensitivity profiles' and those in the reference system is to compare their respective plots as a function of energy group (or energy) for each key reaction types. Fig-6 shows the 'sensitivity profiles' of various responses of the FFTF system of interest that are not included in the adjustment procedure. From Fig-6, it is clear that some are similar to the reference profiles given in Fig-5, but others are extremely difficult to assess. For quantities that reflects the overall spectrum of the system, it suffices to expect the 'similarity' as long as the spectrum of the user's system is, by and large, similar to that of some reference systems. For quantities that are sensitive to the localized regions on space and/or in energy of the user's system, the 'similarity' in the sensitivity profiles is less likely. In general, it is extremely difficult to assess the degree of 'similarity' on the basis of the

visual observations especially when many reaction types and a wide range of responses are considered.

A more plausible method to quantify the similarity between the user's sensitivity vectors and the reference sensitivity vectors is to define a set of correlation coefficients as proposed by Usachev.<sup>18</sup> If  $\vec{S}$  and  $\vec{C}$  are the user's sensitivity vector and reference sensitivity vector respectively, a characteristic parameter  $C_{12}$  is defined as the correlation coefficient deduced from the quadratic form of the union of  $\vec{S}$  and  $\vec{C}$  and the cross section covariance matrix. In the present notation, it is represented by

$$\begin{bmatrix} \vec{C} \\ \vec{S} \end{bmatrix}^T M \begin{bmatrix} G^T & S^T \end{bmatrix} = \begin{bmatrix} \sqrt{GMG^T} & 0 \\ 0 & \sqrt{SMS^T} \end{bmatrix} \begin{bmatrix} 1 \\ C_{21} \end{bmatrix} \begin{bmatrix} C_{12} \\ 1 \end{bmatrix} \begin{bmatrix} \sqrt{GMG^T} & 0 \\ 0 & \sqrt{SMS^T} \end{bmatrix} \quad (18)$$

where the correlation coefficient is defined as

$$C_{12} = \frac{\vec{C}^T \vec{S}}{\sqrt{GMG^T} \sqrt{SMS^T}} \quad (19)$$

Although the method has been used successfully in quantify the similarity between the user's sensitivity vectors and the reference ones for some cases, it does have its limitation especially in conjunction to one problem using the current covariance data. It will be shown that one necessary condition for the validity of the method is for M to be diagonal.

## 2. Issues Concerning Orthogonality and Correlation

Consider the example of a (2x2) covariance matrix previously described. There are three possible scenarios that can represent the geometric relationship between the user's sensitivity vector  $\vec{S}$  with respect to the reference vector  $\vec{C}$  used in the adjustment.

### (1) $\vec{S} \parallel \vec{C}$

It is obviously the most desirable situation if  $\vec{S}$  is parallel to  $\vec{C}$ . The resulting uncertainty is most likely to be benefited by the rotation process shown in Fig-4.

(2)  $\vec{S}D \perp \vec{G}D$

The most undesirable scenario is for  $\vec{S}D \perp \vec{G}D$ . It can be shown readily that the cross terms,  $S_1 d_1 S_2 d_2$  and  $g_1 d_1 g_2 d_2$ , must assume opposite sign.

Fig-7 illustrates graphically the situations before and after adjustment through rotation respectively when the user's error  $\epsilon_S$  is cast into the same form as that given in Fig-4. The orthogonality requires the angle between two components of  $\vec{S}D$  to be  $180^\circ$  out of phase with respect to those of  $\vec{G}D$ . Fig-7 is self-explanatory. The improvements of the user's quantities and the reference quantities may become mutually exclusive. In fact, the rotation may even result in adverse effect on  $\epsilon_S$ . This can be illustrated numerically by considering the following simple example with

$$\vec{G}D = [2 \quad 1]; \vec{S}D = [-1 \quad 2]$$

Table-1a shows the variances before and after the adjustment of  $r_{12}$  under various assumptions. The adjustment that helps  $GMG^T$  is no help for  $SMG^T$  for the cases included.

(3) Generally,  $\vec{S}D$  is neither parallel nor perpendicular to  $\vec{G}D$ . The vector in question can be decomposed into a parallel and a perpendicular components with respect to reference vector  $\vec{G}D$ .

From the above discussions, it is reasonable to conclude that the most desirable scenario from the user's point of view is when the parallel component dominates. One useful indicator is apparently the relative length of these two components. These simple examples provide the rational basis for generalization to be discussed. The question concerning the correlation coefficient  $C_{12}$  defined in Eq-19 can now be addressed in the same context. The example given above shows that the 'degree of orthogonality' of  $\vec{S}D$  with respect to  $\vec{G}D$  plays an important role in the assessment of the impact of the adjusted quantities on user's calculations. The question is whether  $C_{12}$  defined in Eq-19 can also serve as a reliable indicator under general condition. In general, the value of  $C_{12}$  reflects not only the 'degree of orthogonality' of  $\vec{S}D$  with respect to  $\vec{G}D$  but also the degree of correlation among the cross section data. These can be shown analytically



$$C_{12} \sim \sum_i (s_i d_i)(g_i d_i) + \sum_{i \neq j} (s_i d_i) r_{ij} (g_j d_j) \quad (20)$$

Clearly, the first term is a measure of orthogonality while the cross term strongly depends on correlation among the cross section data. Thus, orthogonality does not necessarily imply that  $C_{12}$  must vanish or vice versa. As a matter of fact,  $C_{12}$  can be very close to unity even if the first term in Eq-20 vanishes. For cases where the correlations of cross sections are not negligible, the use of  $C_{12}$  as the indicator of the correlation between user's quantities and the reference quantities may lead to unrealistic expectation. This can be illustrated by using the same example described in the previous section. Table 1b shows the values of  $C_{12}$  corresponding to various  $r_{12}$  values given in Table 1a. With exception of the case  $r_{12} = 0$ , large values of  $C_{12}$  clearly do not reflect the improvement in the uncertainties of the user's quantities after adjustment as shown in Table 1a.

Hence, one necessary condition for application of Eq-19 is that  $M$  must be diagonal. Unless the first term in Eq-20 is much greater than the second term in the same equation (or  $\vec{S}$  is 'similar' to  $\vec{G}$  to begin with), the correlation and orthogonality are not necessarily mutually exclusive. In the existing cross section covariance data compiled at ANL, the off-diagonal elements for key fissionable isotopes are not negligible.

### 3. Application of Vector Space Concept

The preceding rationale can be readily generalized within the context of the usual vector space concept. Consider matrices

$$A = GD \quad (21)$$

and

$$B = SD \quad (22)$$

that characterize the reference systems for integral experiments and the user's design parameters respectively prior to adjustment. The ranges of subspaces spanned by the row vectors of  $A$  and  $B$  are denoted by  $R\{A\}$  and  $R\{B\}$  respectively. Under the idealistic condition where an unlimited number of integral experiments is available, one has

$$R\{B\} \in R\{A\} \text{ as } R\{A\} \rightarrow \lim_{n \rightarrow \infty} R^n$$

i.e.  $R\{A\}$  spans the entire  $n$ -dimensioned real space. Physically, the reference vector space covers every conceivable calculations that the users can come out with. The adjusted data will always provide the users with desirable results, comparable to those for the reference systems.

In practice, however,  $R\{A\}$  clearly is not expected to span the entire real space. The predetermined integral data and the initial cross section uncertainties define the reference sample space  $R\{A\}$ . To quantify the 'similarity' between the user's quantities and the reference data, one only needs to know the relative importance of the projection of  $R\{B\}$  in  $R\{A\}$  with respect to its component orthogonal to  $R\{A\}$ .

One key step in connecting the geometries of vector space to the usual algebra in practical applications is to construct the orthonormal basis of the reference system. Given row vector space  $R\{A\}$  of  $A$  ( $n \times m$ ) of dimension  $r$ , the vector space spanned by a set of vectors  $\{\tilde{A}_i\}$  is also spanned by its orthonormal basis  $\{\tilde{U}_i\}$  obtained via the Gram-Schmidt process.  $\tilde{A}_i$  can be expressed as

$$\tilde{A}_i^T = \sum_j a_{ij} \tilde{U}_j^T \quad (23)$$

where  $a$  is a lower triangular matrix. For the data adjustment analysis, it is known that the accuracy of  $k_{eff}$  is by far the best both experimentally and computationally as compared to other integral measurements. Hence, the row vector of  $\tilde{A}$  of the best  $k$  calculation will be taken to be the first vector in the Gram-Schmidt process. The orthonormal basis  $\{\tilde{U}_i\}$  can be generated in the following way:

$$\tilde{W}_1 = \tilde{G}_k D \quad (24)$$

corresponding to one of the sensitivity vector  $\tilde{G}_k$  of the eigenvalue measurements, and

$$\tilde{W}_i = \tilde{A}_i - \frac{\tilde{W}_1^T \tilde{A}_i}{\tilde{W}_1^T \tilde{W}_1} \tilde{W}_1 - \dots - \frac{\tilde{W}_{i-1}^T \tilde{A}_i}{\tilde{W}_{i-1}^T \tilde{W}_{i-1}} \tilde{W}_{i-1} \quad (25)$$

for  $i > 1$ . The required orthonormal basis is

$$\vec{U}_i = \vec{W}_i / \|\vec{W}_i\| \quad (26)$$

In the practical applications, the sensitivity vectors of the same experiment measured in various critical assemblies of similar spectral characteristics will be grouped together when  $A$  is constructed for convenience.

The orthonormal basis  $\{\vec{U}_i\}$  not only defines the coordinate axes of the reference sample space of dimension  $r$  but also defines the projection matrix that maps the user's vector space  $R\{B\}$  of interest into the reference vector space  $R\{A\}$ .

If the orthonormal condition for  $\{\vec{U}_i\}$  is  $U^T U = I$ , the projection matrix  $P$  is

$$P = U U^T \quad (27)$$

Thus, for any give  $\vec{B} \in R\{B\}$ , the vector can be decomposed into a parallel and a perpendicular component with respect to the reference vector space  $R\{A\}$ .

$$\vec{B} = \vec{B}^{\parallel} + \vec{B}^{\perp} \quad (28)$$

where

$$\vec{B}^{\parallel} = P \vec{B} \quad (29)$$

With the reference sample space specified, pertinent criteria that define the relationship between the user's quantities and the reference quantities can be established. Three criteria of interest will be described. One obvious criterion to quantify the degree of 'similarity' between the user's vector  $\vec{B}$  and the reference vector space is the ratio  $\|\vec{B}^{\perp}\| / \|\vec{B}\|$ , the relative 'length' of the perpendicular component to that of the vector itself. One necessary but not sufficient condition for meaningful improvement in the user's quantities is that this ratio must be small. If the ratio is large, little improvement is expected. On the other hand, the extent of the improvement may still depend on other factors even if the ratio is small.

The orthonormal basis  $\{\vec{U}_i\}$  defines the coordinate system for the reference sample space. Given the orthonormal basis for the reference system

it is also possible to characterize the reference sample space in terms of simple patterns. Due to the limited variety of existing integral experiments measured in many systems of similar spectral characteristics, the sample points  $\{a_{ij}\}$  defined by Eq-23 in the  $r$ -dimensional space must appear in clusters as illustrated schematically in Fig-8(1).  $\vec{U}_1$ , the vector corresponding to the 'best'  $k$ -measurement, denotes the most preferential direction. Each cluster of points can be characterized by their arithmetic means which, in turn, define a handful of average vectors characteristics of various types responses i.e.

$$\langle \vec{A}_i^T \rangle = \sum_j^r \langle a_{ij} \rangle \vec{U}_j^T \quad (30)$$

where the index  $i$  denotes a specific 'cluster' of certain measurement.

The information given in Fig-1 can be used as the guidance on the relative importance of these average vectors. The preferential directions in vector space are determined by the good quality measurements. Fig-8(2) shows schematically the average values of  $\langle a_{ij} \rangle$  normalized to the norm of the corresponding average vectors are plotted vs the index of the basis. With such characterization, it is possible to probe the question of 'similarity' beyond the first criterion described earlier.

Since  $\vec{B}'' \in R\{A\}$ , it is expressible as a linear combination of the base vector  $\vec{U}_j$

$$\vec{B}_k''^T = \sum_j^r b_{kj} \vec{U}_j^T \quad (31)$$

To identify the 'resemblance' of  $\vec{B}''$  to each average vectors, the second criterion is to find its projections on these vectors similar to the procedure of the first criterion. The relative 'lengths' of its perpendicular component with respect to the vector itself is again a measure of 'similarly' between  $\vec{B}''$  and the average vector characteristics of a given cluster of data points. In particular, its direction with respect to  $\vec{U}_1$ , the 'most preferred' direction, is a good measure of whether the component  $\vec{B}''$  can achieve the maximum improvement via the adjustment process. Alternatively, the coefficients  $b_{kj}$  can be plotted vs the index of the basis similar to Fig-8(2). By directly comparing the pattern of  $b_{kj}$  in Fig-8(3) to various patterns of  $\langle a_{ij} \rangle$ , one can

determine whether the parallel components of  $\vec{B}$  is similar to the reference patterns characteristics of the 'preferential' directions.

The orthogonal component  $\vec{B}^\perp$  can be pictured as a linear combination of another set of orthonormal vectors not covered by the reference coordinate system as shown in Fig-8(3). In the event that  $\vec{B}^\perp$  is more important than  $\vec{B}^\parallel$ , the improvement of user's uncertainties requires additional integral experiments in order to enlarge the reference sample space. The proposed model can be used as a useful tool to provide a reasonable basis for choosing additional experiments effectively. From the discussions above, it is quite apparent that the additional experiments must be chosen such that  $\vec{B}^\perp$  with respect to the vector space spanned by the union of  $A$  and  $A_{\text{add}}$ , is as small as possible, where  $A_{\text{add}}$  is the product of the sensitivity matrix of the additional experiments in question and the square root of cross section variance  $D$ . The pertinent additional experiments do not necessarily have to be the same kind as the design parameters in question as long as they are of good quality and the above criteria are met when  $A_{\text{add}}$  is included.

Another useful criterion is to examine the relative contribution of two components of  $\vec{B}$  to the uncertainties directly. The quadratic form of interest can be represented by three terms:

$$\vec{B}\Gamma\vec{B}^T = \vec{B}^\parallel\Gamma\vec{B}^{\parallel T} + \vec{B}^\perp\Gamma\vec{B}^{\perp T} + 2\vec{B}^\parallel\Gamma\vec{B}^{\perp T} \quad (32)$$

where  $\Gamma$  is the correlation matrix.

For cases where the first term dominates, the use of the adjusted data is expected to improve the uncertainty significantly. On the other hand, little improvement is expected if the second term dominates. Whatever little improvement in the latter can only be attributed to the relatively small improvement in cross section variances alone but not to the adjustment of the correlation matrix of cross sections. For cases where the parallel and perpendicular components are comparable in magnitude, the sign of the cross term may play a role. As a general rule, the cross term with positive sign is likely to yield the more favorable results in the application of the adjusted data.

#### 4. Results in Practical Applications

To illustrate the practical application of the proposed method, calculations of various responses of interest for the FFTF analysis have been carried out using the ADJUST-code. The multipurpose code, ADJUST, not only provides the options to compute the adjusted quantities but also the capability of computing various quantities required by the vector space model.

One direct application the proposed model is to examine the impact of using the adjusted quantities on various design quantities of interest in the systems where integral measurements are not available. In the present work, 18 calculated FFTF quantities will be used for illustration purposes. For the reference systems, three uranium-fueled systems (ZPPR-15D, ZPR66A and ZEBRA-8H) and four plutonium-fueled systems (ZPR-6/7, ZPPR-12, ZPPR-12 V & ZPPR-15B) with total of 79 experiments are included in the adjustment procedure in which ten reaction types ( $\sigma_f^5, \sigma_\gamma^5, \bar{\nu}^5, \sigma_f^9, \sigma_\gamma^9, \bar{\nu}^9, \sigma_f^8, \sigma_\gamma^8, \sigma_{inel}^8, \sigma_{el}^8$ ) and 21 energy groups are considered. Although the criteria of interest do not require the information of the adjusted quantities, they are of interest in quantification of the degree of improvement in the design quantities for illustration purposes. The similar types of experiments are grouped according to the order given in Fig-1 for vector space calculations.

Table-2 gives the lengths and the ratio of the orthogonal component to the vector itself for various responses of interest. Also given is the fractional improvement in uncertainties of various responses when the adjusted data are used. These values provide good illustration of the Criterion I discussed earlier. With exception of few, most cases here show small orthogonal component so that the improvement is substantial. It should be noted, however, that the smaller ratio does not necessarily mean better improvement as shown. It is possible that  $\vec{B}$  may not fall into the 'preferential' directions even if  $\vec{B} \in R\{A\}$ . Hence, other criteria must also be examined.

Table-3 shows the relative length of the perpendicular components of each  $\vec{B}^n$  with respect to  $\vec{U}_1$ , the 'most preferred' direction, and the corresponding improvement after adjustment. Here, the 'most preferential' direction is taken to be proportional to the sensitivity vector corresponding to the k of ZPPR-15D. As one can see, all the eigenvalue related quantities examined show relatively small orthogonal component with respect to the direction of  $\vec{U}_1$ . Consequently, the resulting improvements in their uncertainties are substan-

tial. Similar ratios with respect to each average vectors characteristics of the reference vector space can also be obtained readily by the ADJUST-code. For illustration purposes, however, it suffices to show graphically the relevant patterns described in Fig. 8(2) and 8(3) under realistic conditions. Fig. 9 and 10 show the variation of each average sample point characteristics of the cluster of points representing the closely related experiments.  $\langle a_{ij} \rangle$  for eigenvalues, reaction rate ratios, and sample worths that reflect the overall spectral characteristics of the critical assemblies exhibit similar patterns except for the signs in some cases. The distribution of  $\langle a_{ij} \rangle$  for eigenvalues in the reference coordinate system is expected to be like a  $\delta$ -function center around  $\bar{U}_1$  whereas the reaction ratios spread out somewhat. The double peaks for  $k$  observed in Fig-9 are the consequences of inclusion of both uranium systems and plutonium systems in the ensemble in accordance to the groupings given in Fig-1. Strictly speaking, the characteristics of  $\langle a_{ij} \rangle$  can be better represented if the pertinent experiments of the u-fueled and Pu-fueled systems are grouped separately. The patterns for flux ratios are significantly different from the others considered in this study. As discussed earlier, the sensitivity coefficients of the latter quantities reflect the derivatives of the spectrum in the prescribed energy region. Fig-10 shows the large fluctuations of the patterns corresponding to the high energy and the intermediate energy flux ratios.

Fig-11 and Fig-12 show the coefficients  $b_{ij}$  of the 'parallel' components of  $\vec{B}$  vectors for various FFTF-quantities of practical interest. Quantities strongly dependent on the overall spectrum of the system given in Fig-11 show striking similarity to those given in Fig-9 for the reference systems. The results along with the ratios given in Table-2 provide the explanation for the substantial improvement in these quantities given in the last column of Tables. 'FFTF DEL-K' represents the reactivity swing after a fuel cycle time of 100 days based on the depletion dependent perturbation calculations provided by Downar and Khalil.<sup>27</sup> Other quantities of the FFTF system are given in Fig-12. Of particular interest is the pattern representing the 'parallel' component of the low energy flux ratios at the beginning of fuel cycle denoted by 'FFTF-FL3FLT-B' (below 9 keV). Since none of the measurements included are good measure of the low energy spectrum, the latter shows the least similarity to the reference patterns and, therefore, shows the least improvement.

To quantify the similarity of  $\hat{B}$  and the reference quantities  $\{\hat{A}_i\}$  directly, Criterion III is needed. Table-4 shows various components of the variance of the FFTF parameters before and after the adjustment along with the corresponding fractional improvement as obtained by the ADJUST-code. The standard deviations of various components are also listed below their variances. As expected, the standard deviations of the orthogonal components are insensitive to the data adjustment. Whatever change one observes is attributed primarily to the small improvement in the uncertainties in cross sections but not to the rotation caused by the alternation of the off-diagonal elements of the cross section correlation matrix. It is quite evident from Table-4 that the relative importance of the parallel components prior to the adjustment determine the outcome of the fractional improvement. The use of Criterion III along with Criterion II provides explanation of why the improvement of some parameters are better than others.

Because the FFTF system is not fundamentally different from the reference critical assemblies used and the parameters examined are not too different from the measured quantities, no big surprises were observed in the examples given. For design calculations that involve parameters dependent on complex configurations of the reactor and local spectra that are difficult to reproduce in the existing critical assemblies, the situations can be quite different. The proposed model can be better utilized under those conditions.

#### IV Conclusions

The recently compiled information of the integral experiment evaluations and covariances for both integral experiments for zero power reactors and nuclear data derived from ENDF-B/V along with the advances in sensitivity and uncertainty analysis make possible the routine applications of the data adjustment theory to various fast reactor design calculations. One essential consideration of the fast reactor calculations and the integral experiment analysis is the accurate treatment of the detailed spectrum of the system. It is especially so when the safety related parameters are considered. The detailed treatment of the spectrum requires the use of fine group structures and accurate calculational models which, in turn, will impact our thinking on the application of the data adjustment theory. From a practical point of view, improvements in the following areas are believed to be desirable. To reflect the group structure commonly used in the fast reactor calculations, the extension of the existing covariance information for nuclear data is



desirable. The question concerning the covariance of nuclear parameters in the resolved energy region also requires more attention. It is believed that the data adjustment theory can be further enhanced if one includes the relevant system-dependent characteristics of the group cross sections in the calculations. Work has been initiated so that the sensitivity matrices for the spatial and energy self-shielding effects can be treated consistently in the MC<sup>2</sup>-2/SDX code<sup>28</sup> when the group constants are generated. Some general consensus on how the deficiencies of the calculational models should be treated in the adjustment process is also needed.

From the perspective of the users of the adjusted data, the questions concerning the interpretation and appropriate utilization of these data are equally important as those concerning the data adjustment theory itself. Calculations based on numerous integral experiments currently available have shown that the calculated values of these experiments can be significantly improved while the improvement in the cross section uncertainties is, at best, modest. Such phenomena are attributed to the rotation process manifested through the adjustment of the off-diagonal elements of the initial cross section covariance and have been illustrated geometrically by using a simple example. Consequently, the 'similarity' between the user's sensitivity vectors to those reference vectors used in the adjustment is essential to ensure the meaningful improvement when the adjusted quantities are applied to the design calculations. The simple model based on the linear vector space concept provides the means for characterization of the reference sample space and for quantification of the 'similarity' between the user's parameters and the reference measurements. The proposed method can also be used to help determine what types of future experiments are most beneficial to the design parameters which may not be improved satisfactorily by the adjusted data within the constraint of the existing experiments. A multi-purpose code ADJUST has been developed for these purposes.

## REFERENCES

1. J. L. Rowlands and B. A. McDougall, Proc. Int. Conf. Physics of Fast Reactor Operation and Design, London, p.115, British Nuclear Energy Society (1969).
2. J. B. Dragt, "Statistical Considerations on Techniques for Adjustment of Differential Cross Sections with Measured Integral Parameters," in M. Bustraan et al., "STEK, The Fast-Thermal Coupled Facility of RCN at Petten," RCN-122, p. 85, Reactor Centrum Nederland (1970).
3. J. B. Dragt, W. M. Dekker, H. Gruppelaar, and A. J. Janssen, Nucl. Sci. Engr., 62, 117-129 (1977).
4. H. Hggblom, "Adjustment of Neutron Cross Section Data by a Least Square Fit of Calculated Quantities to Experimental Results, Part I, Theory," AE-422, A. B. Atomenergi (1971).
5. H. Mitani and H. Kuroi, J. Nucl. Sci. Tech.; 9, 383 (1972) and 9, 642 (1972).
6. L. N. Usachev and Yu. Bobkov, "Planning an Optimum Set of Microscopic Experiments and Evaluations to Obtain a Given Accuracy in Reactor Parameter Calculations", INDC CCP-19/U, International Nuclear Data Committee (1972).
7. A. Gandini, "Nuclear Data and Integral Measurements Correlation for Fast Reactors, Part 2: Review of Methods," RT/FI (73) 22, Comitate Nazionale Nucleare (1973).
8. R. W. Peele, "Uncertainty in the Nuclear Data Used for Reactor Calculations," Adv. in Nucl. Sci. Tech., Vol. 14, 11-84 (1982).
9. F. G. Perey, Proc. Conf. Nuclear Cross Section and Technology, Washington, D.C. 1975. NBS-SP425, Vol. 2, p. 842 (1975).
10. F. G. Perey, "The Data Covariance Files for ENDF/B-V," ORNL/TM-5938, ENDF-249, (1977).
11. C. R. Weisbin, E. M. Oblow, J. H. Marable, R. W. Peele, and J. L. Lucius, Nucl. Sci. Engr., 66, 307-333 (1978).
12. F. Schmittroth, Nucl. Sci. Engr., 72, 19-34 (1979).
13. W. P. Poenitz, "Covariances for Adjusted Derived Quantities," IAEA Meeting on Covariance Methods and Practices in the Field of Nuclear Data, Rome, Nov. 17-19 (1986); also, W. P. Poenitz and R. W. Peele. Covariances of Evaluated Nuclear Data Based on Experimental Data Uncertainties and Nuclear Model."
14. J. H. Marable, C. R. Weisbin and G. deSaussau, Nucl. Sci. Engr., 75, 30-55 (1980).
15. T. Kamei and T. Yoshida, Nucl. Sci. Engr., 91, 11-33 (1985).

16. E. Greenspan, "Sensitivity Functions for Uncertainty Analysis," Adv. in Nucl. Sci. Tech., Vol. 14, 193-249 (1982).
17. Y. A. Chao, Nucl. Sci. Engr. 72, 1-8 (1979).
18. L. N. Usachev et al., Proc. Int. Conf. Neutron Physics and Other Applied Purposes, Harwell, Sept 25-29 1978, Conf-780921, p. 181, International Atomic Agency (1978).
19. G. Palmiotti and M. Salvatores, Nucl. Sci. Engr., 87, 333-348 (1984).
20. P. J. Collins, "Integral Experiment Information for Fast Reactors," Adv. in Nucl. Sci. Tech., Vol. 14, 159 (1982).
21. W. P. Poenitz, Unpublished Information (1987).
22. P. J. Collins, W. P. Poenitz, H. F. McFarlane, "Integral Data for Fast Reactors", Proc. Int. Conf. on Nucl. Data for Sci & Tech., Mito, Japan, May 30 - June 3, 1988.
23. T. Bayes, "Essay Toward Solving a Problem in Doctrine of Chance," Phil. Trans., Royal Soc. London 53, p. 376 (1763).
24. H. Jeffries, "Theory of Probability," 3rd Ed. Oxford Univ. Press, (1961).
25. W. C. Hamilton, "Statistics in Physical Science," Ronald Press Co., New York (1964).
26. D. W. Muir and R. E. MacFarlane, "The NJOY Nuclear Data Processing System, Vol. IV: The ERRORR and COVR Modules," LA-9303, Vol. IV (ENDF-324) (1985).
27. T. Downar and H. Khalil, "The Application of Time-Dependent Sensitivity Theory and Data Adjustment Methods to Uncertainty Analysis of a Metal-Fueled FFTF Core" Proc. of this meeting.
28. H. Henryson, B. J. Toppel, and C. G. Stenberg, "MC<sup>2</sup>-2: A Code to Calculate Fast Neutron Spectra and Multigroup Cross Sections," ANL 8144 (1976).
29. R. E. McKnight, Private Communication (1987).
30. R. N. Hwang, Ann. Nucl. Energy, 9, 33-44 (1982).

FIGURE 1

# IMPROVEMENT IN UNCERTAINTIES AFTER ADJUSTMENT

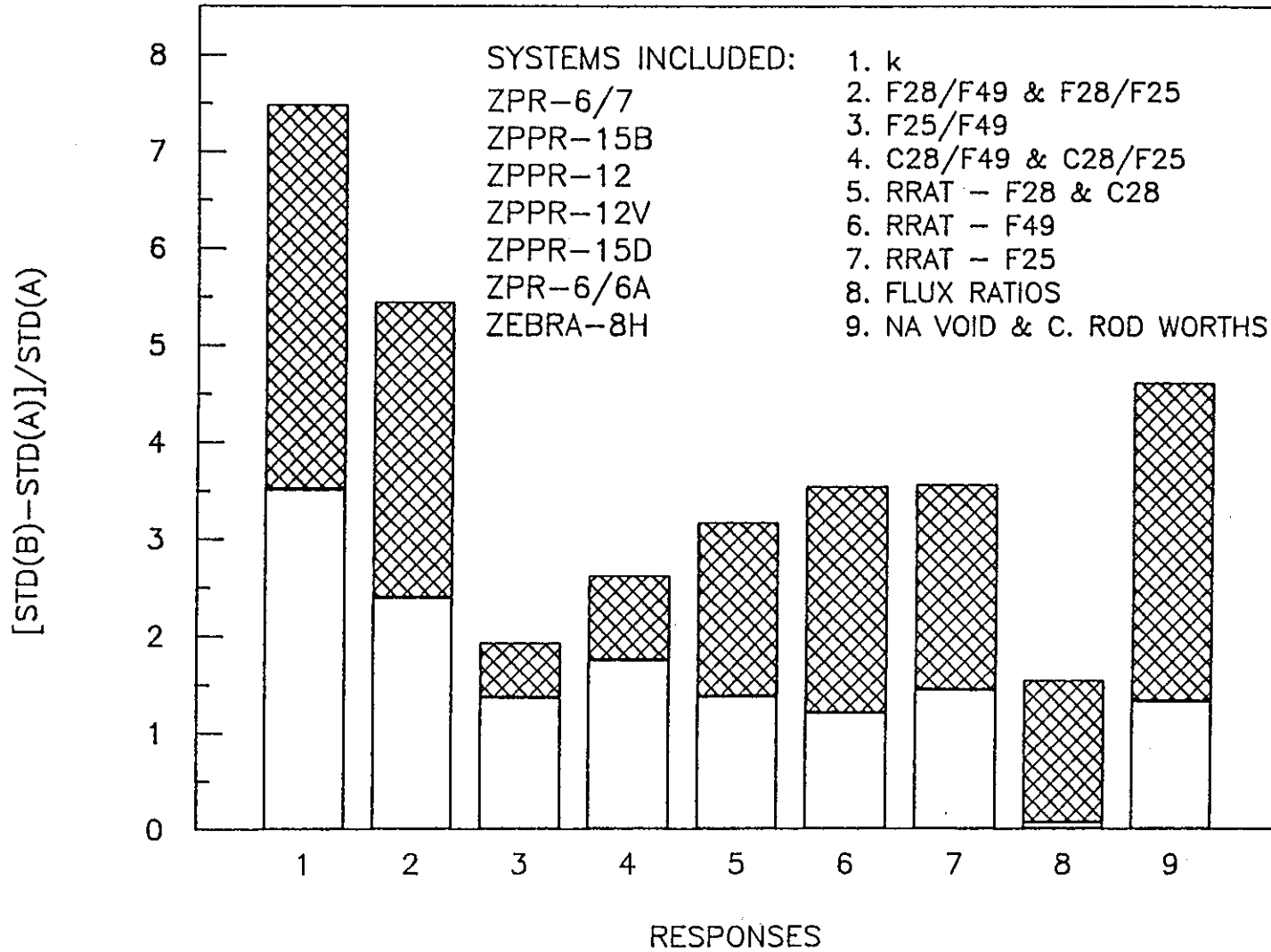


FIGURE 2

IMPROVEMENT IN CROSS SECTION UNCERTAINTIES  
(U & Pu - SYSTEMS)

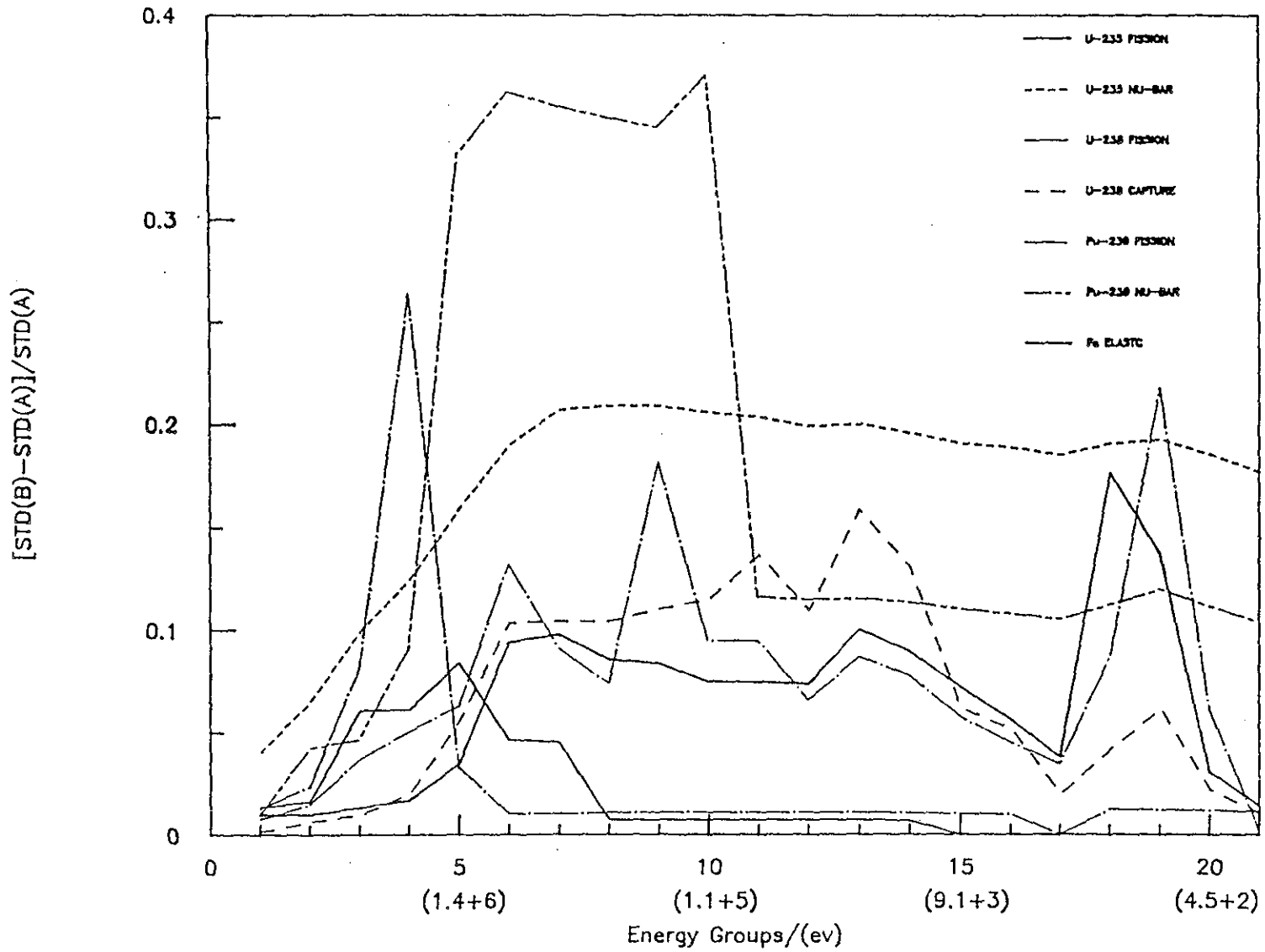


FIGURE 3

IMPROVEMENT IN CROSS SECTION UNCERTAINTIES  
(Pu - SYSTEMS)

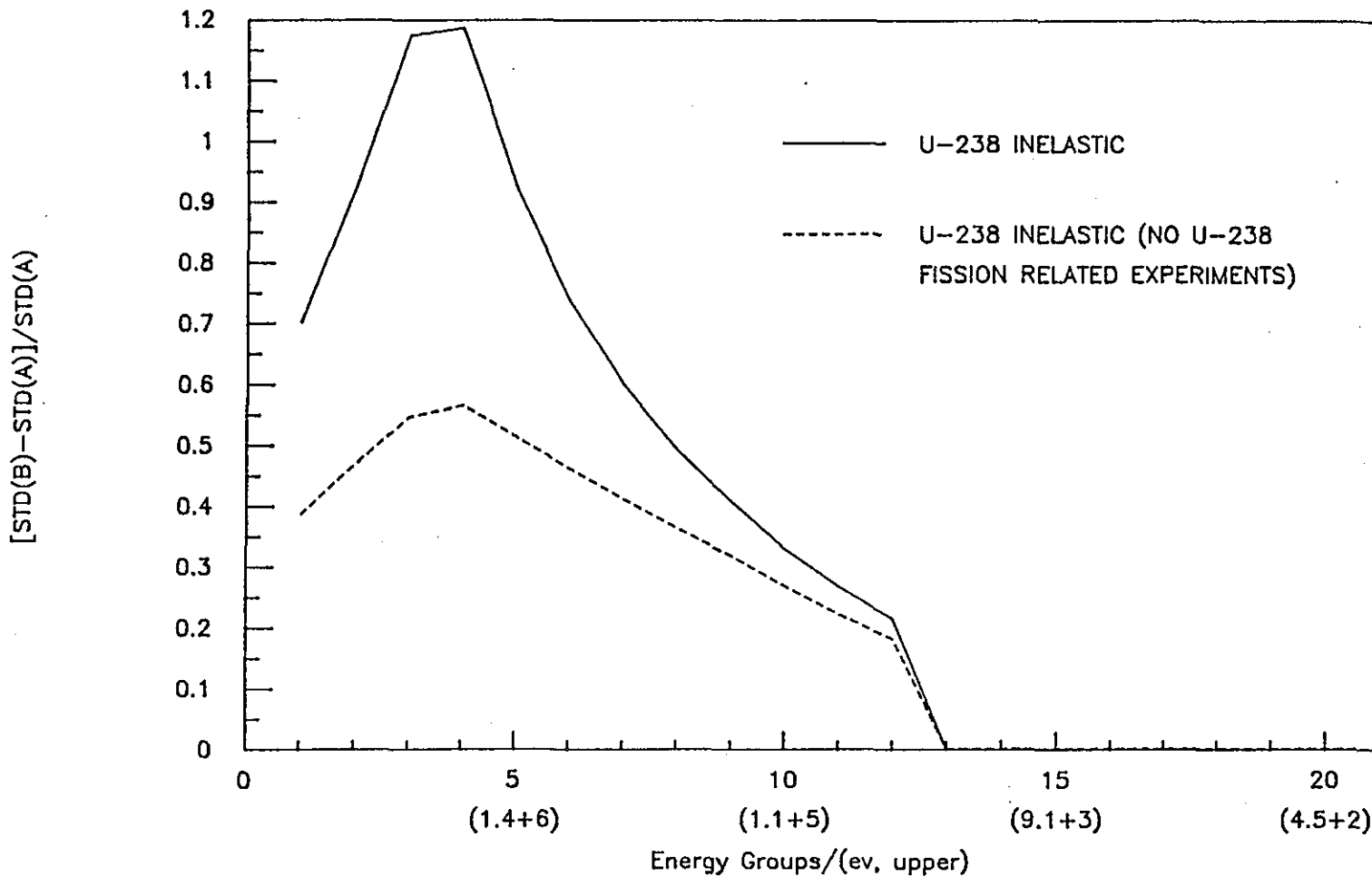
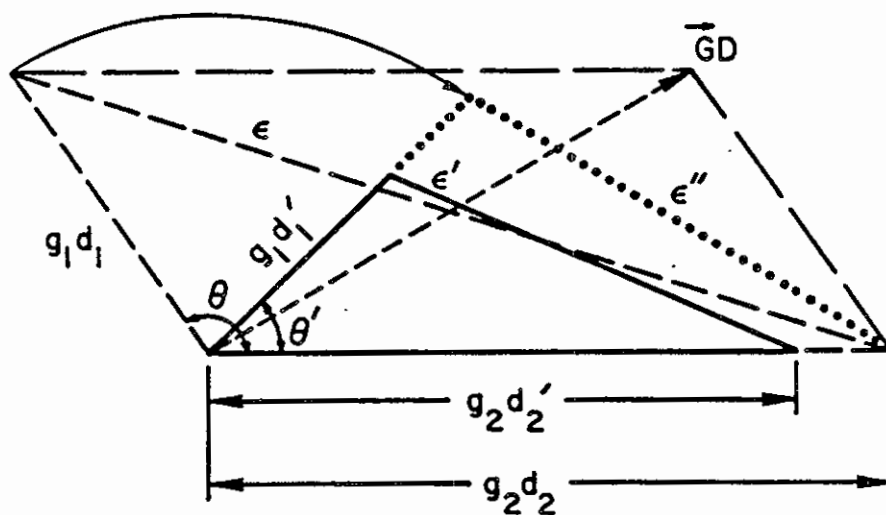


FIGURE 4

QUADRATIC FORM  $GMG^T = \epsilon^2$  BEFORE AND AFTER ADJUSTMENT--  
(2 x 2) EXAMPLE.



$$M = DRD$$

$$\epsilon = \sqrt{(g_1 d_1)^2 + (g_2 d_2)^2 - 2(g_1 d_1 g_2 d_2) \cos \theta} \quad (\text{BEFORE})$$

$$r_{12} = -\cos \theta$$

$$\epsilon', d_1', d_2', \text{ \& } \theta' \quad (\text{AFTER})$$

FIGURE 5

INTEGRAL EXPERIMENTS FROM ZPPR-15D

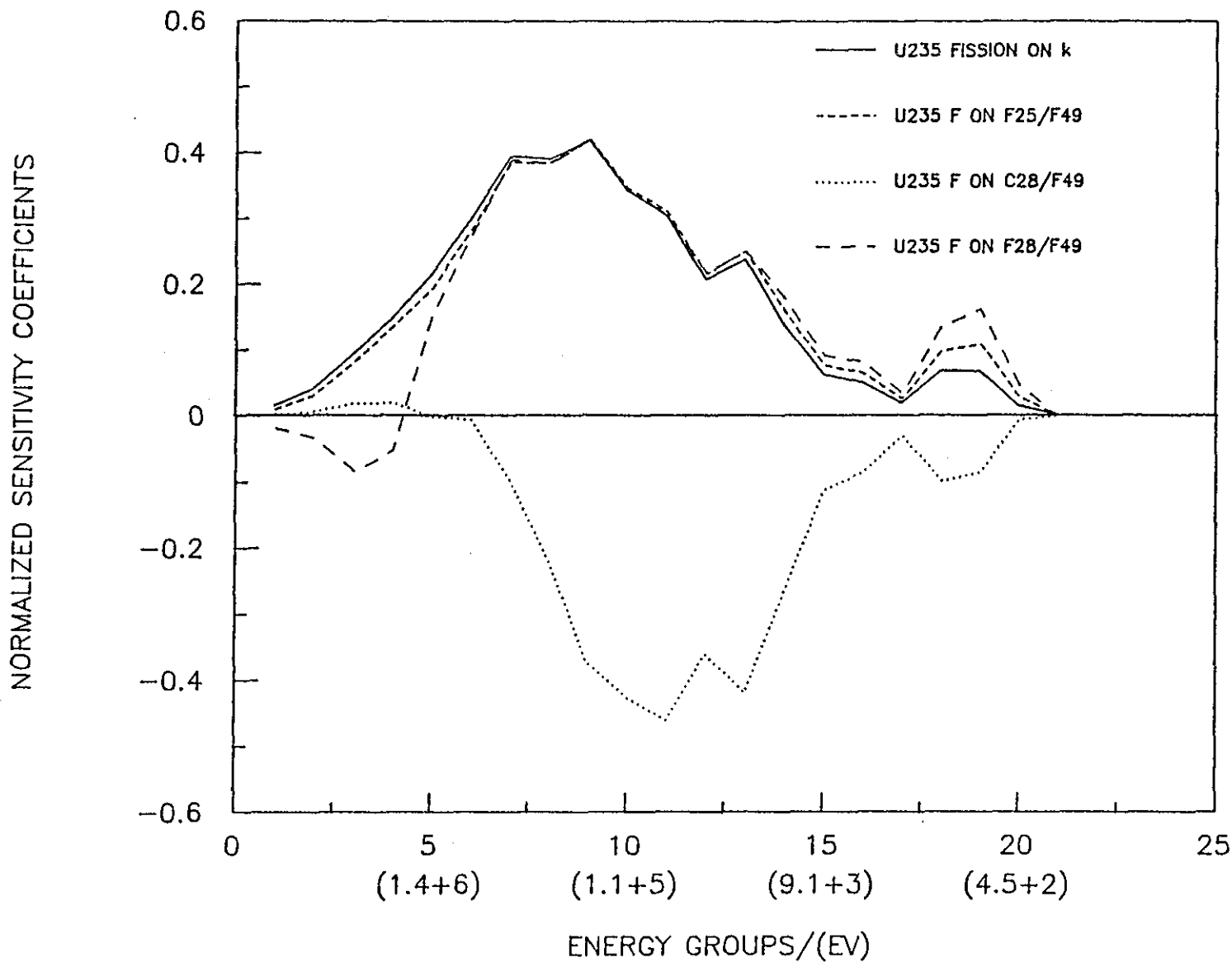




FIGURE 6  
U-235 FISSION FOR FFTF

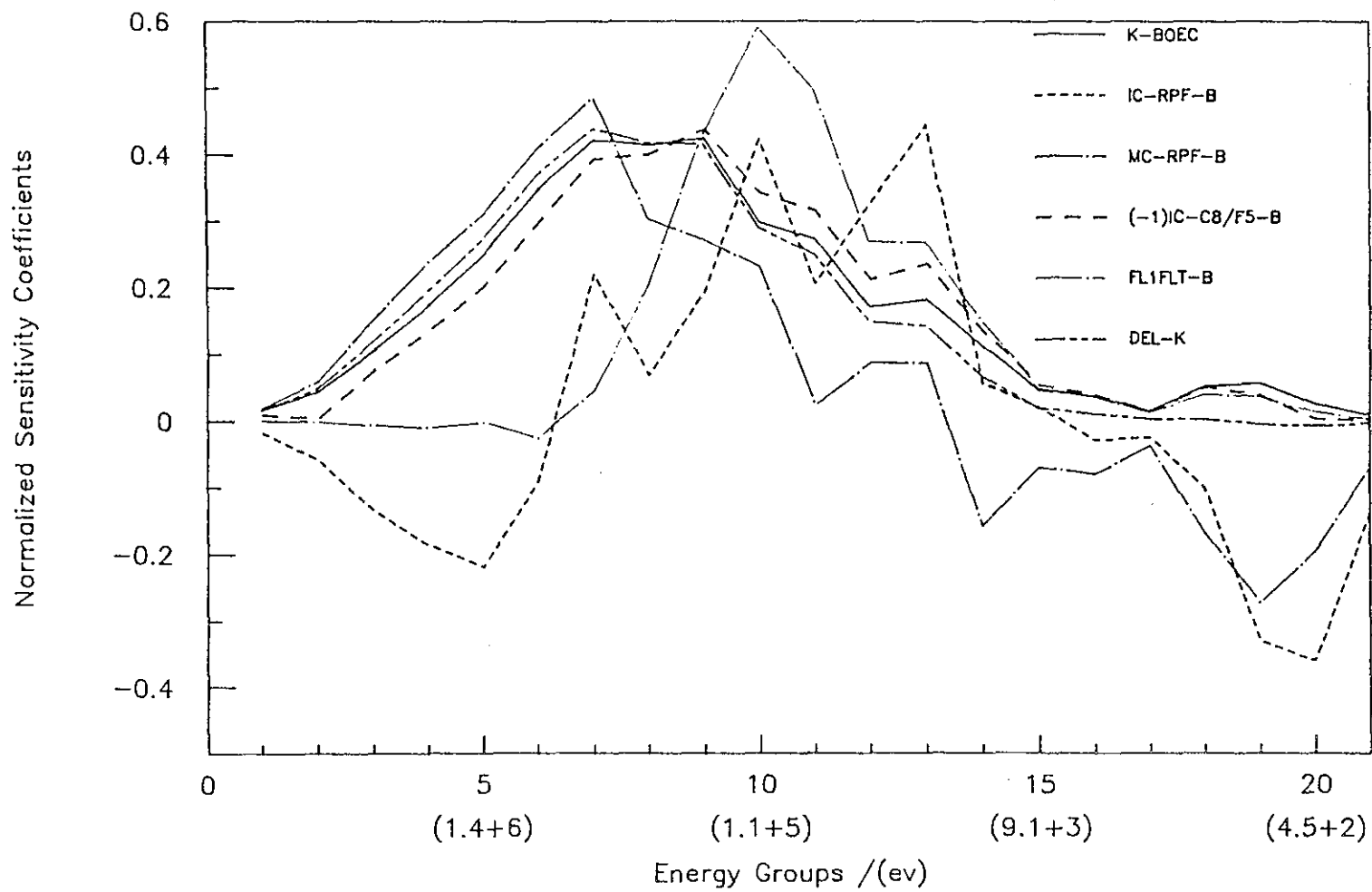
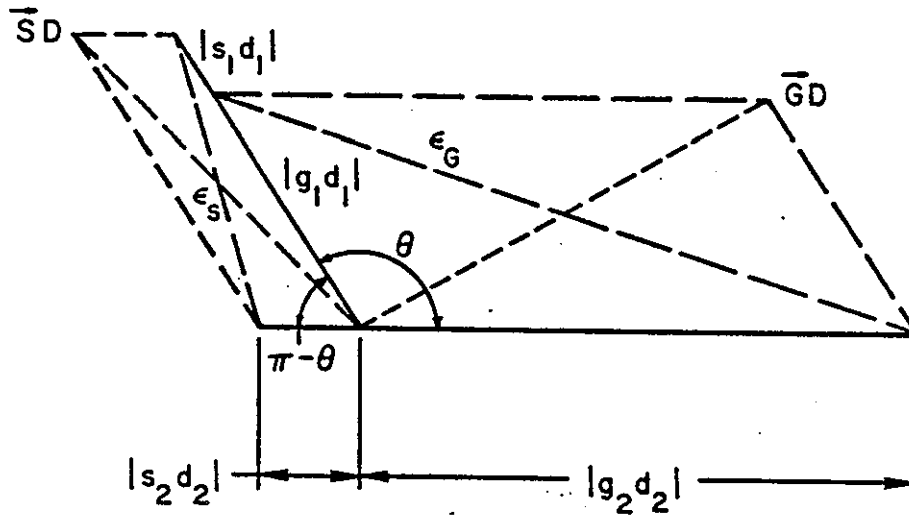


FIGURE 7

$\overline{SD} \perp \overline{GD}$

BEFORE ADJUSTMENT:



$$\epsilon_s = \sqrt{(s_1 d_1)^2 + (s_2 d_2)^2 - 2 |s_1 d_1| \cdot |s_2 d_2| \varsigma \cos(\pi - \theta)}$$

$$\varsigma = \text{sgn}(g_1 d_1 g_2 d_2)$$

AFTER ADJUSTMENT:

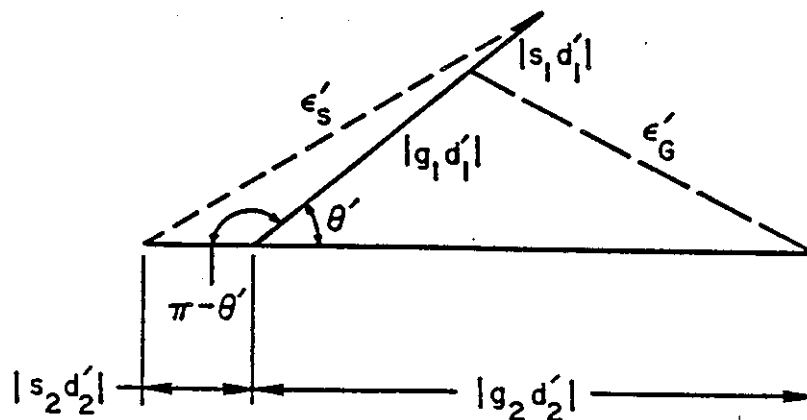
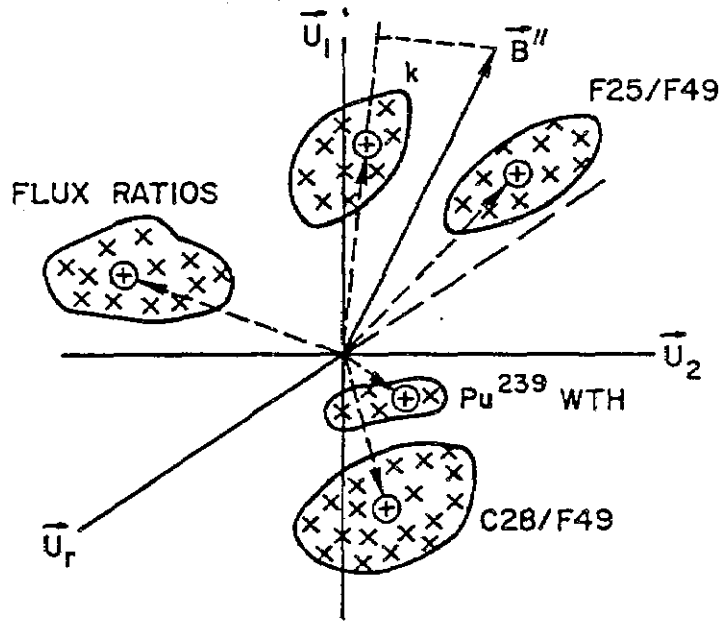


FIGURE 8

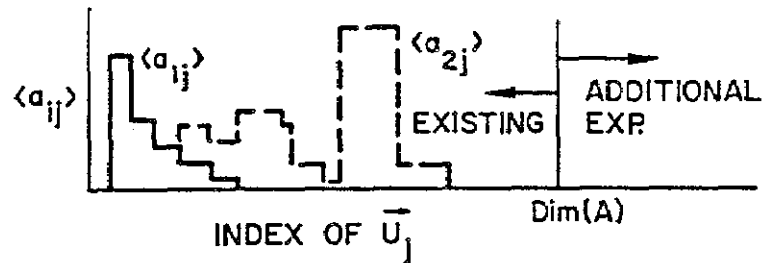
CHARACTERIZATION OF REFERENCE SAMPLE SPACE:

(1) CLUSTERS IN REFERENCE SAMPLE SPACE



(2) PATTERNS CHARACTERISTICS OF REFERENCE

$$\text{SYSTEM: } \langle \bar{A}_i^T \rangle = \sum \langle a_{ij} \rangle \bar{U}_j^T$$



(3) PATTERNS CHARACTERISTICS OF USER'S

$$\text{PARAMETER: } \bar{B}_i''^T = \sum b_{ij} \bar{U}_j^T$$

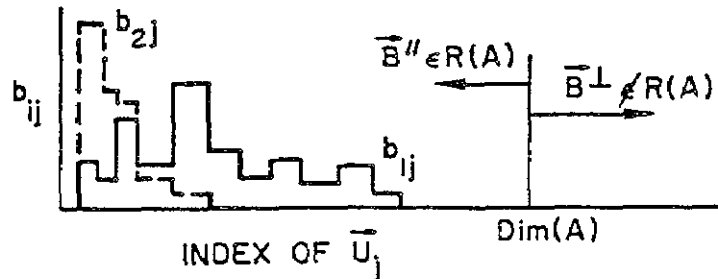


FIGURE 9

PATTERNS IN PREDETERMINED SAMPLE SPACE(PU & U )

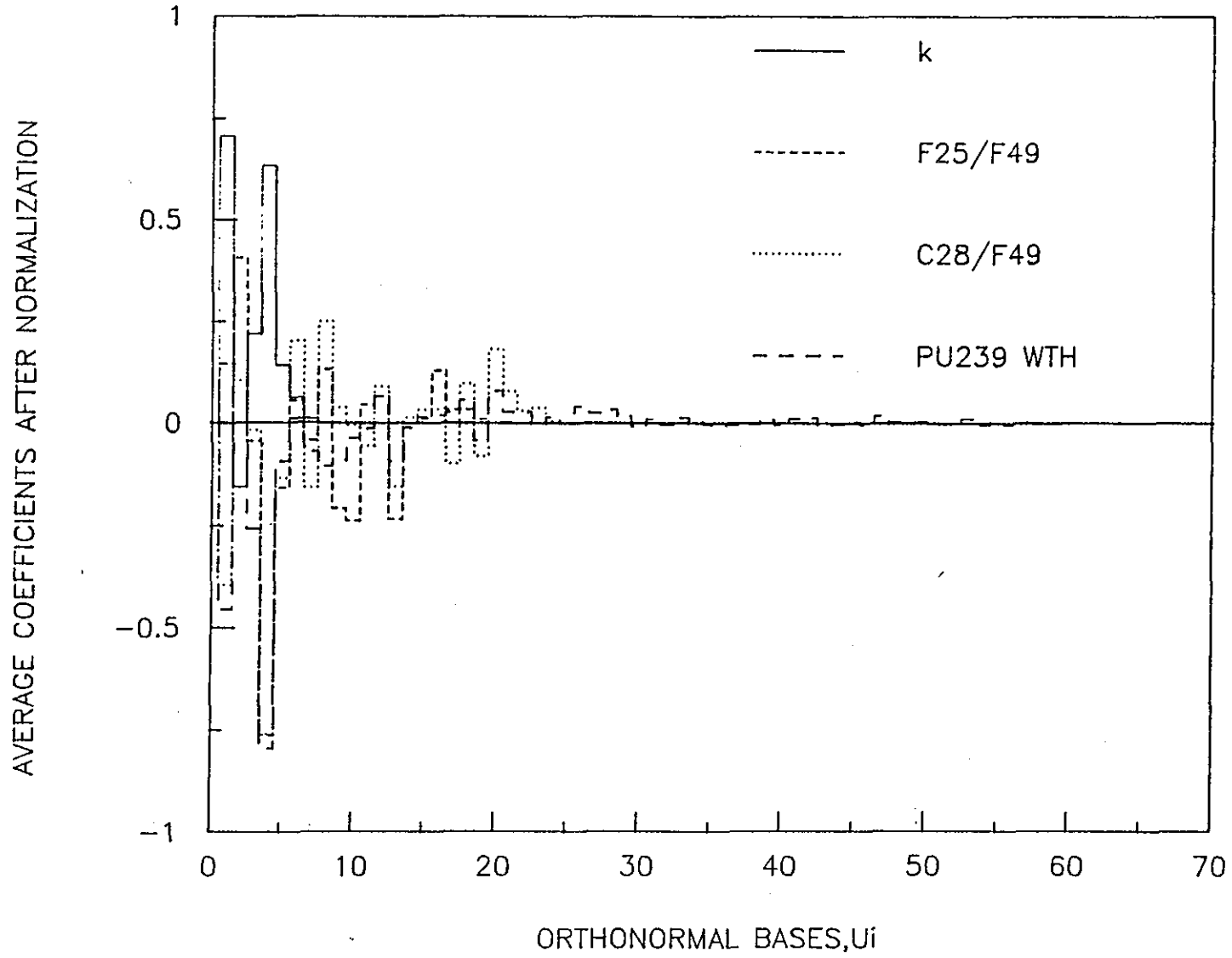


FIGURE 10

PATTERNS IN PREDETERMINED SAMPLE SPACE(PU & U )

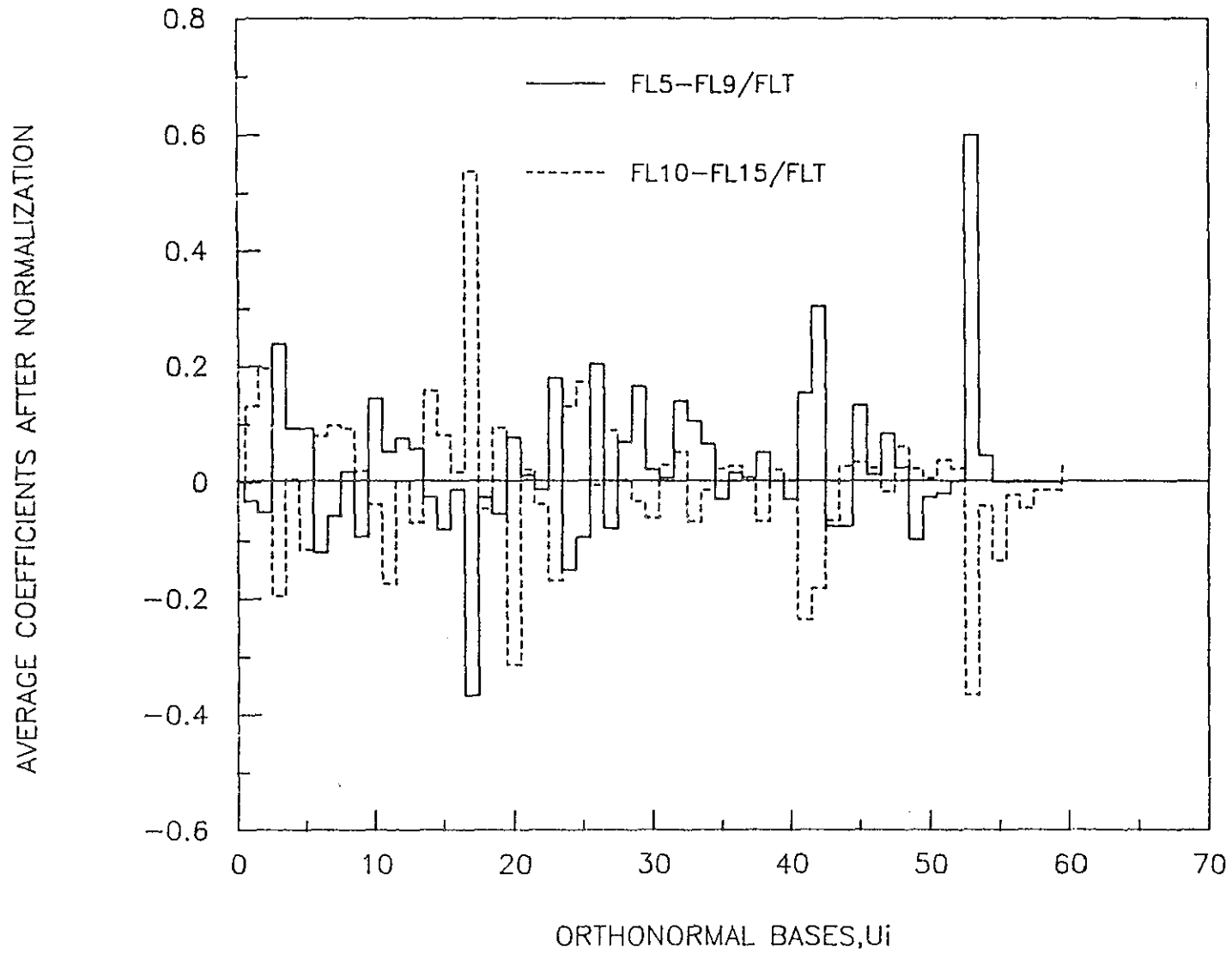


FIGURE 11

PARALLEL COMPONENTS OF USER'S QUANTITIES

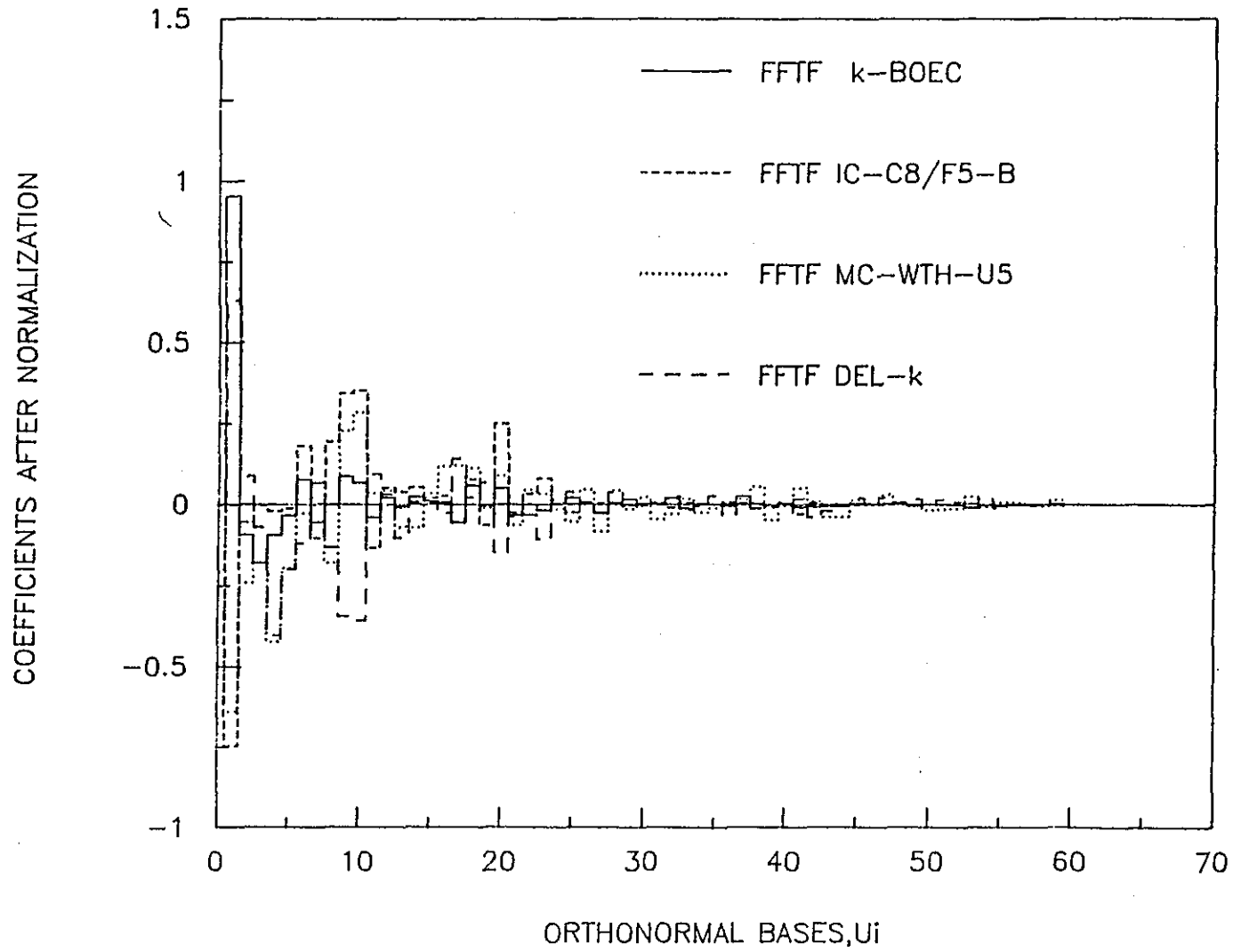


FIGURE 12

PARALLEL COMPONENTS OF USER'S QUANTITIES

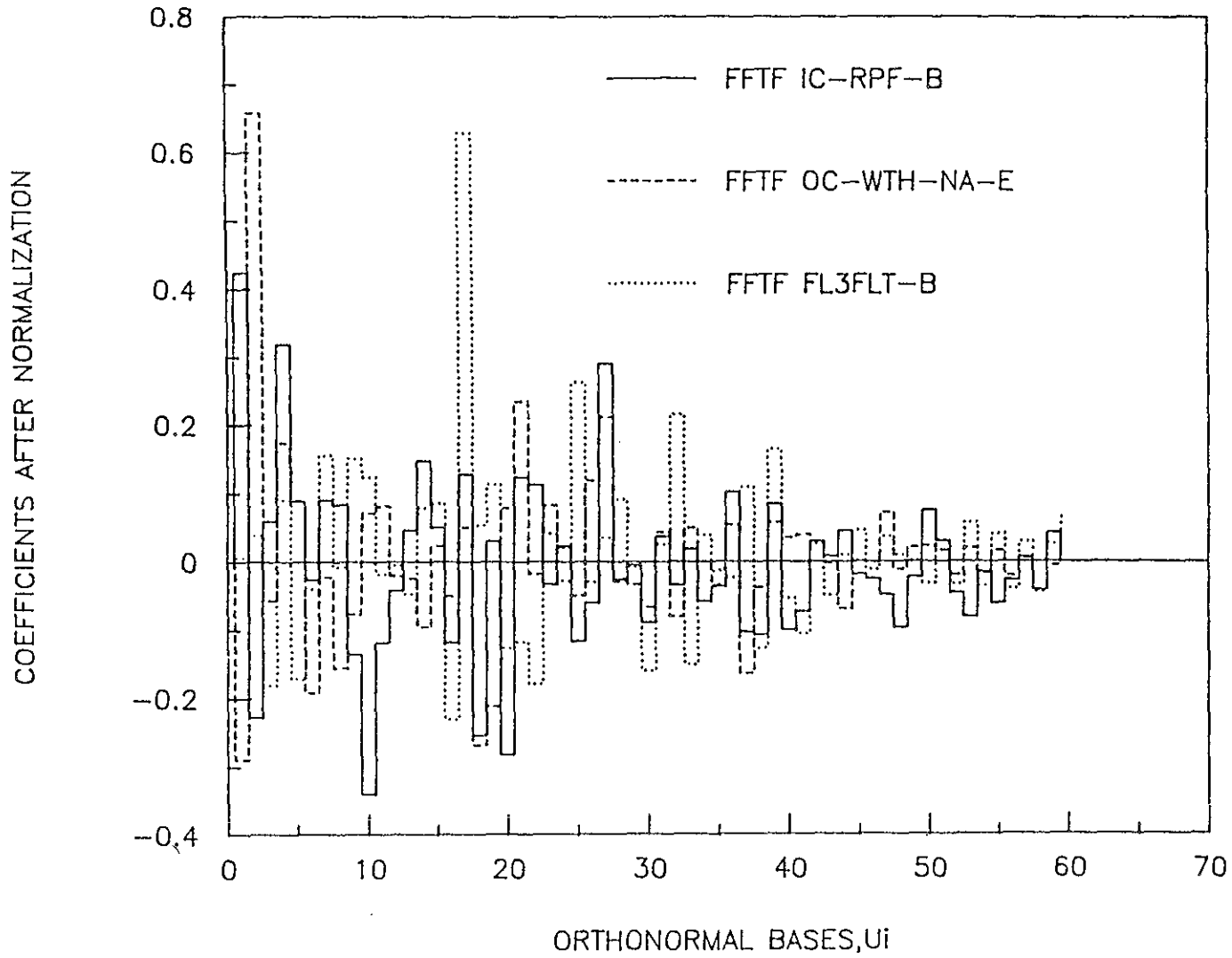


Table 1a. Illustration of the Effect of Rotation on Two Orthogonal Vectors

$$\vec{A} = \{2 \ 1\}; \vec{B} = \{-1 \ 2\}$$

Before Adjustment			After Adjustment		
$r_{12}$	$ARA^T$	$BRB^T$	$r_{12}$	$AR'A^T$	$BR'B^T$
1.0	9.0	1.0	-0.1	4.6	5.4
0.5	7.0	3.0	-0.5	3.0	7.0
0.0	5.0	5.0	-1.0	1.0	9.0

Table 1b. Illustration of Situation that Orthogonality and Correlation are not Necessarily Mutually Exclusive ( $\vec{A}$  &  $\vec{B}$  same as Table 1-a)

$r_{12}$	$ARB^T$	$C_{12}$
1.0	3.0	1.0
0.5	1.5	0.327
0.0	0.0	0.0



TABLE 2. Estimation of Projection of Users SEN. Vectors on R(G) - Criterion 1  
 Lengths of Perpendicular Component/Vector Itself/Their Ratio/Fractional  
 Improvement in Uncertainties.

		PERPEND.	VECTOR	RATIO	(STD(B)-STD(A))/STD(B)
FFTF-CON	K-BOEC	0.220370-03	0.647860-02	0.340150-01	0.701130+00
FFTF-CON	IC-RPF-B	0.395200-03	0.122090-02	0.323700+00	0.314250+00
FFTF-CON	MC-RPF-B	0.207090-03	0.103870-02	0.199380+00	0.491490+00
FFTF-CON	OC-RPF-B	0.490060-03	0.160320-02	0.305660+00	0.422630+00
FFTF-CON	IC-C8/F5-B	0.287370-03	0.181350-01	0.158460-01	0.653900+00
FFTF-CON	MC-C8/F5-B	0.290210-03	0.182190-01	0.159290-01	0.646570+00
FFTF-CON	OC-C8/F5-B	0.978230-03	0.170270-01	0.574520-01	0.636370+00
FFTF-CON	IC-WTH-U5-E	0.772890-03	0.897510-02	0.861150-01	0.592050+00
FFTF-CON	MC-WTH-U5-E	0.891630-03	0.105460-01	0.845460-01	0.590310+00
FFTF-CON	OC-WTH-U5-E	0.941200-03	0.108270-01	0.869300-01	0.549950+00
FFTF-CON	IC-WTH-NA-E	0.134230-01	0.797580-01	0.168290+00	0.540550+00
FFTF-CON	MC-WTH-NA-E	0.963080-02	0.472800-01	0.203700+00	0.452010+00
FFTF-CON	OC-WTH-NA-E	0.393900-02	0.223660-01	0.176110+00	0.457180+00
FFTF-CON	FL1FLT-B	0.249960-03	0.401210-02	0.623000-01	0.514690+00
FFTF-CON	FL2FLT-B	0.647750-03	0.112000-01	0.578370-01	0.520360+00
FFTF-CON	FL3FLT-B	0.451680-02	0.171960-01	0.262670+00	0.298820+00
FFTF-CON	EOC-K	0.235670-03	0.642740-02	0.366670-01	0.702800+00
FFTF-CON	DEL-K	0.163350-02	0.222180-01	0.735230-01	0.567760+00

TABLE 3. Direction of the Projections in the Reference Coordinate System Relative to the Preferred Direction - Criterion 2 Lengths of Perpendicular Component/Vector Itself/their Ratio/Fractional Improvement in Uncertainties.

		MOST PREFERENTIAL DIRECTION			FRA. IMPROVEMENT
		PERPEND.	VECTOR	RATIO	(STD(B)-STD(A))/STD(B)
FFTF-CON	K-BOEC	0.19390D-02	0.64749D-02	0.29946D+00	0.70113D+00
FFTF-CON	IC-RPF-B	0.10464D-02	0.11551D-02	0.90584D+00	0.31425D+00
FFTF-CON	MC-RPF-B	0.10097D-02	0.10178D-02	0.99203D+00	0.49149D+00
FFTF-CON	OC-RPF-B	0.14662D-02	0.15265D-02	0.96046D+00	0.42263D+00
FFTF-CON	IC-C8/F5-B	0.12042D-01	0.18133D-01	0.66409D+00	0.65390D+00
FFTF-CON	MC-C8/F5-B	0.12258D-01	0.18217D-01	0.67289D+00	0.64657D+00
FFTF-CON	OC-C8/F5-B	0.11499D-01	0.16999D-01	0.67646D+00	0.63637D+00
FFTF-CON	IC-WTH-U5-E	0.66021D-02	0.89418D-02	0.73834D+00	0.59205D+00
FFTF-CON	MC-WTH-U5-E	0.80786D-02	0.10508D-01	0.76878D+00	0.59031D+00
FFTF-CON	OC-WTH-U5-E	0.82501D-02	0.10786D-01	0.76488D+00	0.54995D+00
FFTF-CON	IC-WTH-NA-E	0.78084D-01	0.78621D-01	0.99317D+00	0.54055D+00
FFTF-CON	MC-WTH-NA-E	0.45852D-01	0.46288D-01	0.99057D+00	0.45201D+00
FFTF-CON	OC-WTH-NA-E	0.21069D-01	0.22017D-01	0.95696D+00	0.45718D+00
FFTF-CON	FL1FLT-B	0.40020D-02	0.40043D-02	0.99942D+00	0.51469D+00
FFTF-CON	FL2FLT-B	0.11174D-01	0.11181D-01	0.99935D+00	0.52036D+00
FFTF-CON	FL3FLT-B	0.16591D-01	0.16592D-01	0.99998D+00	0.29882D+00
FFTF-CON	EOC-K	0.18824D-02	0.64231D-02	0.29306D+00	0.70280D+00
FFTF-CON	DEL-K	0.17184D-01	0.22157D-01	0.77555D+00	0.56776D+00

TABLE 4. Components of User Variances with Respect to R(G\*) and Fractional Improvement in Uncertainties - Criterion 3.

		PARALLEL		PERPENDICULAR		CROSS TERMS		FRA. IMP.
		BEFORE	AFTER	BEFORE	AFTER	BEFORE	AFTER	(STD(B)-STD(A))/STD(B)
FFTF-CON	K-BOEC	0.64553D-04 0.80345D-02	0.57117D-05 0.23899D-02	0.42090D-07 0.20516D-03	0.41543D-07 0.20382D-03	0.20872D-06	0.35290D-07	0.70113D+00
FFTF-CON	IC-RPF-B	0.19519D-05 0.13971D-02	0.85805D-06 0.92631D-03	0.14282D-06 0.37792D-03	0.13917D-06 0.37306D-03	0.86063D-07	0.28303D-07	0.31425D+00
FFTF-CON	MC-RPF-B	0.19220D-05 0.13863D-02	0.47323D-06 0.68792D-03	0.41232D-07 0.20306D-03	0.38757D-07 0.19687D-03	0.21043D-07	0.10983D-08	0.49149D+00
FFTF-CON	OC-RPF-B	0.28181D-05 0.16787D-02	0.79658D-06 0.89251D-03	0.21452D-06 0.46316D-03	0.20841D-06 0.45652D-03	-0.25268D-07	-0.24938D-08	0.42263D+00
FFTF-CON	IC-C8/F5-B	0.62891D-03 0.25078D-01	0.76107D-04 0.87240D-02	0.93771D-07 0.30622D-03	0.82013D-07 0.28638D-03	0.11754D-05	-0.70313D-06	0.65390D+00
FFTF-CON	MC-C8/F5-B	0.63076D-03 0.25115D-01	0.79353D-04 0.89080D-02	0.85100D-07 0.29172D-03	0.78677D-07 0.28049D-03	0.56479D-06	-0.55997D-06	0.64657D+00
FFTF-CON	OC-C8/F5-B	0.55331D-03 0.23523D-01	0.72909D-04 0.85387D-02	0.87122D-06 0.93339D-03	0.86395D-06 0.92949D-03	-0.30426D-05	-0.89969D-06	0.63637D+00
FFTF-CON	IC-WTH-U5-E	0.17185D-03 0.13109D-01	0.28041D-04 0.52954D-02	0.61722D-06 0.78563D-03	0.59358D-06 0.77044D-03	0.51383D-06	0.15285D-06	0.59205D+00
FFTF-CON	MC-WTH-U5-E	0.22784D-03 0.15094D-01	0.37350D-04 0.61115D-02	0.86474D-06 0.92992D-03	0.81376D-06 0.90209D-03	0.10673D-05	0.40239D-06	0.59031D+00
FFTF-CON	OC-WTH-U5-E	0.23746D-03 0.15410D-01	0.47292D-04 0.68769D-02	0.85179D-06 0.92292D-03	0.79174D-06 0.88980D-03	0.32766D-05	0.84823D-06	0.54995D+00
FFTF-CON	IC-WTH-NA-E	0.87149D-02 0.93354D-01	0.17458D-02 0.41783D-01	0.15142D-03 0.12305D-01	0.14887D-03 0.12201D-01	-0.22864D-04	-0.27917D-04	0.54055D+00
FFTF-CON	MC-WTH-NA-E	0.31078D-02 0.55747D-01	0.88608D-03 0.29767D-01	0.79041D-04 0.88905D-02	0.78399D-04 0.88543D-02	0.75220D-05	-0.52288D-05	0.45201D+00
FFTF-CON	OC-WTH-NA-E	0.75502D-03 0.27478D-01	0.21293D-03 0.14592D-01	0.12928D-04 0.35956D-02	0.12721D-04 0.35666D-02	0.13685D-04	0.46621D-05	0.45718D+00
FFTF-CON	FL1FLY-B	0.41111D-04 0.64118D-02	0.95873D-05 0.30963D-02	0.56394D-07 0.23748D-03	0.52098D-07 0.22825D-03	0.83324D-06	0.25289D-06	0.51469D+00
FFTF-CON	FL2FLY-B	0.30237D-03 0.17389D-01	0.69086D-04 0.83118D-02	0.35000D-06 0.59161D-03	0.33454D-06 0.57840D-03	0.42247D-05	0.11937D-05	0.52036D+00
FFTF-CON	FL3FLY-B	0.82322D-03 0.28692D-01	0.39232D-03 0.19807D-01	0.25602D-04 0.50598D-02	0.22784D-04 0.47733D-02	0.55854D-04	0.29684D-04	0.29882D+00
FFTF-CON	EOC-K	0.64539D-04 0.80336D-02	0.56462D-05 0.23762D-02	0.48165D-07 0.21946D-03	0.47749D-07 0.21852D-03	-0.24108D-07	0.85886D-08	0.70280D+00
FFTF-CON	DEL-K	0.79303D-03 0.28161D-01	0.13875D-03 0.11779D-01	0.42113D-05 0.20521D-02	0.36104D-05 0.19001D-02	0.21935D-04	0.10695D-04	0.56776D+00

**SESSION IV**

**September 24, 1988**

**Chairman: D. Wade (ANL, U.S.A.)**

**Rapporteur: D. Hwang (ANL, U.S.A.)**



# ADJUSTMENT METHODS FOR SYSTEM DESIGN AND OPERATION IMPROVEMENT

A. Gandini

ENEA - Fast Reactor Department  
CRE Casaccia, Rome (Italy)

## ABSTRACT

Adjustment methods aimed at differential data and/or system operation improvement basing on experimental integral data are commented. Consideration is given to systematic errors, to sensitivity coefficient calculation methods, to nonlinear adjustment procedures. Problems relevant to system modelling, integral data transposition, burnup and thermohydraulic field analysis, are also discussed.

## 1. INTRODUCTION

The methodology of fitting starting differential data values with integral data measured on critical facilities is at present well established and has been widely used in the last decade in the reactor domain to assist the core physics design. Its widespread adoption occurred particularly after the so called generalized perturbation theory methods have become of general use, enabling the calculation of the sensitivity coefficients required.

An alternative use of the above methodology could be that of fitting the detections made on line on an operating power reactor, represented by a somewhat simplified model, so that continuous improvements of the operation strategy can be obtained.

It is the object of the present paper to review and comment on the adjustment methods so far developed, aimed both at differential data improvement basing on experiments in critical facilities, and at fitting data obtained in power systems in order to adjust performance parameters (e.g., power distribution, control rod worths, etc.) and then enhance system operation. Topics covered include:

1. Identification of systematic errors;
2. Recent advancements of generalized perturbation theory (GPT) methods. The EGPT technique, enabling the use of standard codes for the calculation of the importance function;
3. Nonlinear adjustment procedures. The global detector technique, of interest when a large number of integral measurements have to be analysed;
4. System modelling, in view of the scope of the adjustment exercise. The Kalman filter concept;
5. Correlation coefficients and their use in optimal experiment design and data transposition. The bias factor transposition method;
6. Lognormal and truncated data distributions;

7. Nonlinear GPT techniques to be used in the analysis of:

- a) burnup and buildup measured quantities, such as material concentrations, d.p.a. values and the residual reactivity at end of cycle,
- b) thermohydraulic/physics quantities (temperatures, pressures, etc.) at steady state conditions, aimed at obtaining adjusted data relevant to engineering/physics system parameters.

Before going into the details of above topics, a short description and nomenclature definitions relevant to the GPT method and adjustment methodologies are presented.

## 2. GPT

Let us consider a generic physical system defined by a number of parameters  $p_j$  ( $j=1,2,\dots,J$ ) and described by an  $N$ -component vector field  $\underline{f}$  obeying equation (in vector notation)

$$\underline{m}(\underline{f}|\underline{p}) = 0 \quad (2.1)$$

Vector  $\underline{f}(\underline{\theta}, t)$  generally depends on the phase-space coordinates  $\underline{\theta}$  and time  $t$ . Vector  $\underline{p}$  represents the set of parameters  $p_j$  ( $j=1,2,\dots,J$ ) fully describing the system and entering into Eq.(2.1). Their values generally determine physical constants, initial conditions, source terms, etc. Eq.(2.1) can be viewed as an equation comprehensive of linear, as well as nonlinear, operators and is assumed to be derivable with respect to parameters  $p_j$  and, in the Frechet sense, to component functions  $f_n$  ( $n=1,2,\dots,N$ ).

Consider now a response of interest, or functional,  $Q$  given by the expression, linear with respect to  $\underline{f}$  (we can always reduce to this condition),

$$Q = \int_{t_0}^{t_1} \langle \underline{h}^+, \underline{f} \rangle dt \equiv \langle \langle \underline{h}^+, \underline{f} \rangle \rangle \quad (2.2)$$

where  $\underline{h}^+$  is an assigned vector function,  $t_0$  and  $t_1$  represent given time

limits, while brackets  $\langle \rangle$  represent integration over the space-phase, whereas the double ones  $\langle \langle \rangle \rangle$  also over time.

In the following, we shall look for an expression giving the sensitivity coefficients  $\partial Q / \partial p_j$  relevant to each parameter  $p_j$ .

According to an extension of the GPT method /1/, Eq.(2.1), or its linearized form (if dealing with a nonlinear problem), is heuristically interpreted as governing some density field. The concept of importance,  $f^*(\theta, t)$ , can then be introduced, corresponding to the contribution to the given functional due to the insertion of a particle (or pseudo-particle) in the phase-space position  $\theta$  and time  $t$ .

Expanding Eq.(2.1) around a reference solution gives

$$\sum_{j=1}^N (H \frac{f}{\sim/j} + \frac{m}{\sim/j}) \delta p_j + O_2 = 0 \quad (2.3)$$

where  $O_2$  is a second, or higher, order term, and where

$$\frac{f}{\sim/j} = \frac{df}{dp_j} \quad (2.4)$$

$$\frac{m}{\sim/j} = \frac{\partial m}{\partial p_j} \quad (2.5)$$

Operator H is given by the Jacobian matrix

$$H = \begin{vmatrix} \frac{\partial m}{\partial f} & \frac{\partial m}{\partial f} & \dots & \frac{\partial m}{\partial f} \\ 1 & 2 & \dots & N \\ \dots & \dots & \dots & \dots \\ \frac{\partial m}{\partial f} & \frac{\partial m}{\partial f} & \dots & \frac{\partial m}{\partial f} \\ N & N & \dots & N \\ \dots & \dots & \dots & \dots \\ \frac{\partial m}{\partial f} & \frac{\partial m}{\partial f} & \dots & \frac{\partial m}{\partial f} \\ 1 & 2 & \dots & N \end{vmatrix} \quad (2.6)$$



where  $\bar{\partial}/\partial f_n$  generally denote Frechet derivatives. Since in Eq.(2.3) the parameters  $p_j$ , and then their changes  $\delta p_j$ , are assumed independent from each other, it must be

$$H \frac{f}{/j} + \frac{m}{/j} = 0 , \quad (2.7)$$

which represents the (linear) equation governing the (pseudo)-density  $\frac{f}{/j}$ . The source term  $\frac{m}{/j}$  is here intended to account also, via appropriate delta functions, of initial conditions.

Consider now functional

$$Q_j = \langle \langle h^+ , \frac{f}{/j} \rangle \rangle . \quad (2.8)$$

Adopting the concept of importance to field  $\frac{f}{/j}$ , if we weight with it space- and time-wise the source term  $\frac{m}{/j}$  (inclusive of delta functions accomodating initial conditions), this amounts to a result equivalent to functional  $Q_j$ , i.e.,

$$Q_j = \langle \langle f^* , \frac{m}{/j} \rangle \rangle , \quad (2.9)$$

where  $f^*$  is the importance function obeying equation /1/

$$H^* f^* + h^+ = 0 , \quad (2.10)$$

$H^*$  being obtained reversing operator  $H$ . This implies transposing matrix elements, changing sign of the odd derivatives, inverting the order of operators.

We can easily see that the sensitivity,  $s_j$ , of functional  $Q$  with respect to parameter  $p_j$  can be written

$$s_j = \langle \langle \frac{\partial h^+}{\partial p_j} , \frac{f}{/j} \rangle \rangle + \langle \langle f^* , \frac{\partial m}{\partial p_j} \rangle \rangle , \quad (2.11)$$

where the first term at the right hand side represents the so called, easy to calculate, direct term.

The GPT methodology, on which the above sensitivity expression is based, is quite general and can be applied to any response defined in a linear or nonlinear, time dependent or stationary, field.

It may occur, in certain circumstances, that one or more components [e.g.,  $f_n$ ] of vector field  $\underline{f}$  do not depend on all the space-time coordinates [e.g.,  $x, t$ ]. Consistently with viewing components of  $\underline{f}$  as pseudo-density functions, and without alteration of the problem specifications and results, this, or these, variables may be interpreted as averaged quantities and then replaced by the proper averaging operator [e.g.,  $\langle \cdot \rangle_{(x) \ x} / V$ ] applied to the corresponding extended variables [so obtaining, to exemplify,  $\langle f_n(x) \rangle_{(x) \ x} / V$ ].

These will then be assumed dependent on all coordinates, although only their average values are of interest and no further specification for them is required. This rule is referred to as "coordinate dependence complementation". Its use is required in order that a correct operation reversal is made to obtain the operator governing the importance function  $1/\cdot$ .

### 3. PARAMETER ADJUSTMENT PROCEDURE

The adjustment methodology is well known (see, for example, Ref. /2-4/). Consider starting values  $p_o$  of parameters  $p_j$  ( $j=1,2,\dots,J$ ) represented by vector  $p$  and characterizing the systems considered, and experimental integral data  $Q_1^{ex}$  ( $l=1,2,\dots,L$ ), represented by vector  $Q^{ex}$  and relevant to these same systems. To these quantities variance/covariance matrices  $B_Q$  and  $B_P$ , respectively, are associated. With the definitions

$$Q_1^{cal} = Q_1(p_o) \quad (l=1,\dots,L) \quad (3.1)$$

$$y_{Q,l} = \frac{Q_1^{ex} - Q_1^{cal}}{Q_1^{cal}} \quad (l=1,\dots,L) \quad (3.2)$$

$$y_{P,j} = \frac{P_j - P_{oj}}{P_{oj}} \quad (j=1, \dots, J) \quad (3.3)$$

$$s_{lj} = \frac{P_{oj}}{Q_1} \frac{\partial Q_1}{\partial p_j} \Big|_{P_o} \quad \left. \begin{array}{l} l=1, \dots, L \\ j=1, \dots, J \end{array} \right\} \quad (3.4)$$

and the first order vector relationship

$$y_Q = S y_P, \quad (3.5)$$

S being the sensitivity matrix with elements  $s_{lj}$ , the best estimates  $\tilde{y}_P$  result given by imposing the maximization of the likelihood function, i.e., the minimization of

$$F(y_P) = (y_Q - S y_P)^T B_Q^{-1} (y_Q - S y_P) + y_P^T B_P^{-1} y_P. \quad (3.6)$$

The following equivalent expressions are obtained:

$$\tilde{y}_P = B_P^{-1} S^T (S B_P^{-1} S^T + B_Q^{-1})^{-1} B_Q^{-1} y_Q \quad (\text{method of the Lagrange multipliers}) \quad (3.7)$$

$$\tilde{y}_P = (S B_Q^{-1} S^T + B_P^{-1})^{-1} S B_Q^{-1} y_Q \quad (\text{method of reduction by elements}) \quad (3.8)$$

where the components of vector  $y_Q^{\text{ex}}$  are obtained from Eq.(3.2) with  $Q_1^{\text{ex}}$  in place of  $Q_1$ .

For the adjusted dispersion matrix  $\tilde{B}_P$ , the following equivalent expressions correspondingly result:

$$\tilde{B}_P = B_P - B_P S^T (B_Q + S B_P S^T)^{-1} S B_P \quad (3.9)$$

$$\tilde{B}_P^{-1} = B_P^{-1} + S B_Q^{-1} S^T. \quad (3.10)$$

Pieces of different integral information can be added subsequently, adopting at each stage the latest up-dated dispersion matrix  $\tilde{B}_p$ , and assuming no correlation exists among different pieces of information.

The choice of one, or the other, method depends upon the problem being considered. Generally, that method is chosen which involves the inversion of the smallest matrix. So, if  $J < L$ , the Lagrange multipliers method is preferable, if  $J > L$ , then the method of reduction by elements should be adopted.

Criteria for establishing the degree of confidence can be adopted, for example  $\chi^2$  tests, since it results that the residual quantity

$$\tilde{R} = \mathbf{y}_Q^{\text{ex},T} (\mathbf{B}_Q + \mathbf{S} \mathbf{B}_P \mathbf{S}^T)^{-1} \mathbf{y}_Q^{\text{ex}} \quad (3.11)$$

is distributed as  $\chi^2_L$  (i.e., with  $L$  degrees of freedom). Its expected value is, therefore, equal to  $L$ .

#### 4. SYSTEMATIC ERRORS

The adjustment methodology described in previous section presupposes that the errors are normally distributed and the absence of systematic ones. If there is the suspect that these latter are present in the system parameters  $p_{oj}$ , a method similar to that suggested by Mitani and Kuroi (see Ref./5/ and comment in Ref./6/) could be employed, as shown in the following.

Consider the data  $p_{oj}$ , or, better, the relative values  $y_j^{\text{ex}}$  (identically zero) obtained from Eq.(3.3) in which  $p_j$  are replaced with the starting values (the "a priori" information)  $p_{oj}$ . Let us assume we can set

$$\mathbf{y}_P^{\text{ex}} = \mathbf{y}'_P + \mathbf{R} \bar{\mathbf{p}} \quad (4.1)$$

$\mathbf{y}'_P$  representing normally distributed quantities,  $\bar{p}_k$  ( $k=1, \dots, K$ ) being systematic (or negligence) errors and  $\mathbf{R}$  a  $J \times K$  assigned matrix reflecting the

structure which is suspected characterizing the systematic errors (for instance, a normalization parameter affecting a set of data). The data adjustments result then given by the same formulation relevant to the method of reduction by elements (which has to be used in this case, rather than that of the Lagrange multipliers, to avoid singularities) where, in place of  $B_P^{-1}$ , the matrix

$$(\bar{B})_P^{-1} = B_P^{-1} - B_P^{-1} R (R^T B_P^{-1} R)^{-1} R^T B_P^{-1} \quad (4.2)$$

is used. In this case, the quantity  $R$  given by Eq.(3.11) results distributed as  $\chi_r^2$ , with

$$r = \text{rank}(S) - \text{rank}(R) \quad (4.3)$$

If  $K \geq J$ , the number of the degrees of freedom will then become zero (all the information being used to identify the systematic errors).

Finally, for what concerns the possibility of sorting out possible systematic errors within the integral data experimental information, this can be effected by adding separately the suspected data and then try to identifying them by possible abrupt, significant, increases of the  $\chi^2$  value well above its expected value.

## 5. RECENT ADVANCEMENTS OF GPT METHODS

In order to calculate the sensitivity coefficients required in the adjustment methodology, the solution of the importance functions entering expression (2.11) has to be obtained. This may pose some difficulties if two or three dimension problems have to be run and an ad hoc program is not available. In the following, a method to reduce these difficulties is commented. By this method, known under the name EGPT (Equivalent GPT), a generally inhomogeneous problem is transformed into an homogeneous one, so that standard, generally available, codes can be used.

Consider Eq.(2.10) governing the importance function  $f^*$  relevant to the

response, Eq.(2.2) in which function  $\underline{h}_A^+$  is given. To this importance function we may associate function  $\underline{f}_A^*$  governed by the equation:

$$H^* \underline{f}_A^* + \underline{h}_A^+ = 0, \quad (5.1)$$

with  $\underline{h}_A^+$  arbitrarily chosen.

Let us consider the identity

$$\underline{h}_A^+ \equiv \tau D_{cA}^* \underline{f}_A^*, \quad (5.2)$$

where  $\tau$  is an arbitrarily large, positive, coefficient, and  $D_c^*$  a suitable matrix operator (correspondingly proportional to  $1/\tau$  and, therefore, arbitrarily small). A factorization of this type could be obtained, for instance, setting  $D_c^*$  equal to a diagonal matrix with the  $g, g'$ th component equal to  $\underline{h}_{A,g}^+ / \tau \underline{f}_{A,g}^*$ .

Let us consider then function  $\underline{f}_{A(c)}^*$  governed by the equation

$$(H^* + D_c^*) \underline{f}_{A(c)}^* + \underline{h}_A^+ = 0. \quad (5.3)$$

It can be shown [7] that the following sensitivity expression can be written, equivalent to Eq.(2.11) (apart from a negligible quantity, vanishing with  $1/\tau$ ),

$$s_j = \left\langle \left\langle \frac{\partial \underline{h}_A^+}{\partial p_j}, \underline{f}_{A(c)}^* \right\rangle \right\rangle + \tau \left\langle \left\langle (\underline{f}_{A(c)}^* - \underline{f}_A^*), \frac{\partial \underline{h}_A^+}{\partial p_j} \right\rangle \right\rangle, \quad (5.4)$$

Now, if we choose a source  $\underline{h}_A^+$  of the type

$$\underline{h}_A^+ = \underline{h}_{A,0}^+ \delta(t - t_F), \quad (5.5)$$

Eqs.(5.1) and (5.3) result homogeneous equations [with "final" condition  $\underline{f}_{A,F}^*(t) \equiv \underline{f}_{A(c),F}^*(t) = \underline{h}_{A,0}^+$ ].  $t_F$  here represents an asymptotic time.

As we have seen, by this choice we have transformed the difficulty of solving the generally inhomogeneous equation (2.10) of the importance

function into that of solving the homogeneous ones (5.1) and (5.3). This can be of interest in those circumstances in which standard (up to 3D) codes already exist for the solution of the homogeneous solution of the latter ones (as is the case for the neutron field in a critical system). Such choice cannot obviously be applied to source driven (subcritical) cases [e.g., to shielding problems] in which Eqs.(5.1) and (5.3) would not have nonvanishing solutions in the range of time considered.

We note that if the response is given by a ratio

$$R = \frac{\langle \tilde{h}_1^+, f \rangle}{\langle \tilde{h}_2^+, f \rangle} \equiv \frac{Q_1}{Q_2}, \quad (5.6)$$

this can be reduced, by a proper linearization, to the condition previously considered /7/.

## 6. NONLINEAR ADJUSTMENT PROCEDURES

In the previous derivations of adjustment methods we have assumed that the quantities  $Q_l$  ( $l=1,2,\dots,L$ ) could be adequately expanded to first order around given values  $Q_l^{cal}$ . If the dependence of  $Q_l$  from parameters  $p_j$  ( $j=1,2,\dots,J$ ) is significantly nonlinear, relatively to the amount of the expected adjustments, this assumption may lead to some more or less serious inaccuracy in the adjustment procedure. In order to avoid it, two approaches may be adopted, as shown in the following.

By the first approach use is made of second order sensitivities and an iterative procedure /8/ is adopted, replacing at each  $r$ 'th iteration the sensitivity coefficient  $s_{lj}$ , Eq.(3.4), with

$$s_{lj}^{(r)} = s_{lj} + \sum_{i=1}^J s_{l,ij} \tilde{y}_{p,i}^{(r-1)} \quad (6.1)$$

where  $\tilde{y}_{p,i}^{(r-1)}$  represents the  $i$ 'th parameter adjustment at the  $(r-1)$ st

iteration, while

$$s_{l,ij} = \frac{p_{oi} p_{oj}}{q_1} \frac{\partial^2 Q}{\partial p_i \partial p_j} \Big|_p \quad \left. \begin{array}{l} l=1, \dots, L \\ j=1, \dots, J \end{array} \right\} \quad (6.2)$$

The above iteration methodology may be unpractical and, moreover, it might not converge. Another approach is then suggested in which the constraints, rather than those given by Eq.(3.5), should be maintained in the original form, Eq.(3.1). The solution for the optimal estimates  $\tilde{y}_p$  results then satisfying the equation

$$\begin{aligned} F(\tilde{y}_p) &= (y_Q^{\text{ex}} - D^{-1} [Q(\tilde{p}) - Q(p_o)])^T B_Q^{-1} (y_Q^{\text{ex}} - D^{-1} [Q(\tilde{p}) - Q(p_o)]) \\ &\quad + y_p^T B_p^{-1} y_p = \text{min.} \end{aligned} \quad (6.3)$$

where D represents the diagonal matrix

$$D = \text{diag} \left| \begin{array}{cccc} q_1 & & & \\ & q_2 & & \\ & & \dots & \\ & & & q_L \end{array} \right| \quad (6.4)$$

This translates into the equation

$$-S_Q^{-1} (y_Q^{\text{ex}} - D^{-1} [Q(\tilde{p}) - Q(p_o)]) + B_p^{-1} y_p = 0 \quad (6.5)$$

from which we can obtain the expression, for  $\tilde{y}_p$ ,

$$\tilde{y}_p = B_p^{-1} S_Q^{-1} (y_Q^{\text{ex}} - D^{-1} [Q(\tilde{p}) - Q(p_o)]) \quad (6.6)$$

One could then adopt iteratively the (linear) adjustment methods described previously to increasingly improve the parameter estimates  $\tilde{p}$  until they coincide with the solution within a convergence criterion. At each iteration step, new values  $\tilde{p}$  of the parameters and, correspondingly, new values  $Q(\tilde{p})$  and a new sensitivity matrix S would be introduced at the right hand side of above equation.



### 6.1. The Global Detector Technique

There are cases in which the number (L) of the quantities  $Q_l$  to be considered is too high to make practicable the calculation of all the sensitivity coefficients required with the method described above. To overcome this difficulty, the global detector technique can be used, as described in the following. This technique follows an original idea proposed by McCracken /9/ and successively developed by Matthes /10/ and Gandini /11/ in relation to neutron propagation experiments in metal blocks.

For simplicity, let assume that the quantities  $Q_l$  represent functionals linear with respect to  $f$  (and then relevant to the same system), of the form

$$Q_l = \langle \langle h_l^{+T}, f \rangle \rangle \quad (l=1,2,\dots,L) \quad (6.7)$$

$h_l^{+T}$  representing known functions.

Let us then define the (L-component) vector

$$\underline{t} = B^{-1} \{ y_Q^{ex} - D^{-1} [Q(\tilde{p}) - Q(\tilde{p}_0)] \} \quad (6.8)$$

so that we can write

$$S B^{-1} \{ y_Q^{ex} - D^{-1} [Q(\tilde{p}) - Q(\tilde{p}_0)] \} = \sum_{l=1}^L \begin{pmatrix} s & t \\ 1,1 & l \\ s & t \\ 1,2 & l \\ \cdot & \cdot \\ \cdot & \cdot \\ s & t \\ 1,J & l \end{pmatrix} \quad (6.9)$$

At this point it is clear that the quantity

$$s_j^* = \sum_{l=1}^L s_{l,j}^t \quad (6.10)$$

represents the sensitivity, with respect to the j'th parameter, of a (global) functional  $Q^*$  represented by a linear combination (with coeffi-

icients  $t_1$ ) of all functionals  $Q_1$  considered. i.e.,

$$Q^* = \sum_{l=1}^L t_l Q_l \quad (6.11)$$

Eq.(6.6) can then be written

$$\tilde{y}_p = B_p \underline{s}^*(p) \quad (6.12)$$

i.e., recalling Eq.(3.3),

$$\tilde{p} = p_o + p_{o,j} \sum_{i=1}^J b_{p,ji} s_i^*(p) \quad (6.13)$$

where  $b_{p,ji}$  represents the  $ji$ 'th element of matrix  $B_p$ .

The adjustment process starts setting  $\tilde{p}_o = p_o$  and then calculating  $\underline{t}_{(o)}$  along with Eq.(6.8). This allows the definition of the global detector  $Q^*$  and, correspondingly, of the sensitivities  $s_j^*$ , given by the expression

$$s_j^* = \left\langle \left\langle f_{(o)}^* , \frac{\partial m}{\partial p_j} \right\rangle \right\rangle \quad (6.14)$$

where  $f_{(o)}^*$  represents the first iteration importance relevant to  $Q^*$ .

Since vector  $\underline{s}^*$  depends on the solution  $\tilde{y}_p$ , it is clear that an iterative procedure should be adopted, starting from the initial values  $p_{o,j}$ , i.e., iterating along with approximations  $\underline{t}_{(r)}$  of vector  $\underline{t}$  [using Eq.(6.8)] by which, via the above method, the  $(r+1)$ 'st-iteration adjusted values  $\tilde{p}_{(r+1)}$  are obtained.

In order to help reach convergence, recalling the minimization condition expressed by Eq.(6.3), a procedure is suggested implying further inner iterations. Let us consider at each  $(r-1)$ 'st iteration the corresponding quantity  $F(\tilde{y}_{p(r-1)})$  as defined in Eq.(6.3) (which, for simplicity, we

shall denote  $F_{(r-1)}$ . If the convergence has not yet been reached, we proceed to the next iteration and evaluate a new vector  $\underline{t}'_{(r)}$  (where the prime denotes the first inner iteration). Correspondingly, new values  $\bar{y}'_{p(r)}$  and  $F'_{(r)}$  will be obtained. If the difference

$$\Delta'_{(r)} = F'_{(r)} - F_{(r-1)} \quad (6.15)$$

is such that  $|\Delta'_{(r)}| \leq \epsilon$ ,  $\epsilon$  being a given small positive quantity, the iterative process will be considered converged. If  $\Delta'_{(r)} < -\epsilon$ , no other inner iterations being needed, we define

$$\tilde{y}_{p(r)} \equiv \bar{y}'_{p(r)} \quad (6.16)$$

(and, consequently,  $F_{(r)} \equiv F'_{(r)}$ ) and proceed to the next  $(r+1)$ 'st iteration. If, on the other hand,  $\Delta'_{(r)} > \epsilon$ , a further inner iteration is needed. We consider, then, new adjustments

$$\tilde{y}''_{p(r)} = \frac{1}{2} (\bar{y}'_{p(r)} + \bar{y}_{p(r-1)}) \quad (6.17)$$

With these new values we calculate  $F''_{(r)}$  and the new difference

$$\Delta''_{(r)} = F''_{(r)} - F_{(r-1)} \quad (6.18)$$

If necessary, new values

$$\tilde{y}'''_{p(r)} = \frac{1}{2} (\bar{y}''_{p(r)} + \bar{y}_{p(r-1)}) \quad (6.19)$$

can be considered and so proceed up to a point at which the condition

$\Delta_{(r)} < -\epsilon$  is verified, and, consequently, the  $r$ 'th iteration vector  $\bar{y}_{p(r)}$

(and the corresponding value  $F_{(r)}$ ) obtained.

## 7. SYSTEM MODELLING. THE KALMAN FILTER

System modelling should be adequate to the purpose of the adjustment exercise. So, if this is oriented to the improvement of the basic data, the inaccuracies inherent in model simplifications should be minimized by a proper detailed description of the geometrical, material, etc. properties. On the other hand, if it is oriented to the improvement of the constants to be adopted for the operation of a specific system, a coarse model can be adopted. The adjustment methodology described previously, which in this case would take advantage of the on line information (such as power distribution, control worths, etc) which becomes available as the system operates, can be complemented by the so called Generalized Bias Operators (GBO) transposition method, proposed by Ronen et al. /12/. By this method, benchmark reference (multigroup, transport) calculations are used to adjust the (generally, few-group, diffusion) operator governing the neutron density, and entering into the equation adopted for project, or operation, practical purposes. After this first adjustment is effected, new subsequent adjustments making use of the on line data obtained from the operating system should be made.

Since in this case it is likely that the number of physical parameters (due to the coarseness of the model) is less than that of the measured quantities, the method of reduction by elements (see Section 3) would be preferable. If we assume that the subsequent pieces of information used are independent from each other, this updating process can be assimilated to the so called Kalman filter /13/, generally applied to dynamic systems in which independent observations are made at subsequent times. The Kalman filter process has in fact strong analogies with the adjustment process described in section 3, as shown below.

Let us consider that added experimental information has to be included, besides that which has been used to obtain the adjusted quantities  $\tilde{q}$  and  $\tilde{B}_p$ .

This new experimental information will be represented by the quantities

$Q_1^{\text{ex}}$  ( $l=L+1, L+2, \dots, \bar{L}$ ), to which the error covariance matrix  $\hat{B}_Q$  is associated.

It can be easily shown that the updated parameter relative adjustments

$\bar{y}_p$  and the corresponding covariance matrix  $\bar{B}_p$  may be written as

$$\bar{y}_p = \bar{y}_p + B_p^{-1} S^T (B_Q + S B_p S^T)^{-1} (y_Q^{\text{ex}} - S y_p) \quad (7.1)$$

$$\bar{B}_p = B_p - B_p S^T (B_Q + S B_p S^T)^{-1} S B_p \quad (7.2)$$

(method of the Lagrange multipliers), or

$$\bar{y}_p = (B_p^{-1} + S^T B_Q^{-1} S)^{-1} (B_p^{-1} y_p + S^T B_Q^{-1} y_Q^{\text{ex}}) \quad (7.3)$$

$$\bar{B}_p = B_p^{-1} + S^T B_Q^{-1} S \quad (7.4)$$

(method of reduction by elements), where  $S$  represents the sensitivity matrix relevant to the added integral quantities, while the elements of vector  $y_Q^{\text{ex}}$  are obtained from Eq. (3.2) with  $Q_1$  replaced by  $Q_1^{\text{ex}}$  [ $l=L+1, L+2, \dots, L$ ].

So, as mentioned in Section 3, new (independent) information can be added for readjustment without the need of rerunning the entire problem.

Consider now vectors  $y_Q^{\text{ex}}$  and  $y_Q^{\text{ex}}$  as vectors of quantities determined by measurements at times  $t_{T-1}$  and  $t_T$ , respectively. Eqs.(7.1) and (7.2) (limiting consideration to the Lagrange multipliers method) can then be rewritten in the form:

$$y_{p,T} = y_{p,T-1} - K_T (y_{Q,T}^{\text{ex}} - S_{T-1} y_{p,T-1}) \quad (7.5)$$

$$B_{p,T} = B_{p,T-1} - K_T S_{T-1}^T B_{p,T-1} \quad (7.6)$$

where

$$K_T = B_{p,T-1} S_{T-1}^T (S_{T-1}^T B_{p,T-1} S_{T-1}^T + B_{Q,T})^{-1} \quad (7.7)$$

Matrix  $K_T$  is referred to as the "Kalman gain", whereas the difference  $(y_{Q,T}^{ex} - S_{T-1}^T y_{p,T-1})$  is called the "filter innovation" since it represents the new information incorporated in the measurements at  $t_T$ , which are potentially of use in estimating  $y_{p,T}$ .

As expected, with increasing added information, the influence of the initial, "a priori", dispersion matrix  $B_p$  on the adjusted parameters, and corresponding dispersion matrix, gradually decreases. This can be easily verified observing the original expressions, Eqs.(3.8) and (3.10), of the adjusted parameter changes  $\tilde{y}_p$  and corresponding (inverted) error matrix  $B_p^{-1}$ , respectively: as the size of the error dispersion matrix  $B_Q$  (and then of matrix  $B_Q^{-1}$ ) increases with the increasing number of experiments considered, the matrix corresponding to the product at the right hand side of the above equations,  $S_Q^T B_Q^{-1} S_Q$ , tends to prevail over  $B_p^{-1}$  (due to the increasingly number of addend terms, definite positive at diagonal positions, at each element of that same matrix), so that the relative contributions from  $B_p^{-1}$  to  $B_p^{-1}$  correspondingly tend to decrease.

## 8. CORRELATION COEFFICIENTS. THEIR USE IN INTEGRAL DATA TRANSPOSITION

The importance of experimental campaigns in relation to the design of a specific reference project is well recognized. In these cases, a number of quantities, significant with respect to the major integral parameters relevant to the reference system, are measured on an experimental facility and then transposed to the reference system itself. In cases in which the experimental facility is very close to it and similar quantities are considered in the two systems, only minor corrections of the measured data are generally necessary. In particular, the simple, well known bias-factor transposition (BFT) method can be successfully adopted. However, if the two systems differ to some extent and/or quantities in the experimental facility somehow different from those of the reference design are considered, although the useful information contained in the measurements remains significant, making full use of it may become a problem. A number of methods can be envisaged to this purpose. We shall here show here a method /14/ based on the adjustment methodology described in Section 3.

For the general case in which the integral experimental information contained in measurements  $Q_{A,l}^{ex}$  ( $l=1,2,\dots,L$ ) performed on an experimental facility has to be transposed to a set of quantities  $Q_{B,m}$  ( $m=1,2,\dots,M$ ) relevant to a reference system, let us define the  $L \times J$  and  $M \times J$  sensitivity matrices  $S_A$  and  $S_B$ , respectively, with elements

$$S_{A,lj} = \frac{p_{oj}}{Q_{A,l}} \frac{\partial Q_{A,l}}{\partial p_j} \quad \left| \begin{array}{c} p \\ o \end{array} \right. \quad (8.1)$$

$$S_{B,mj} = \frac{p_{oj}}{Q_{B,m}} \frac{\partial Q_{B,m}}{\partial p_j} \quad \left| \begin{array}{c} p \\ o \end{array} \right. \quad (8.2)$$

The vector  $\bar{y}_B$  of the estimates  $\bar{y}_{B,m}$ , defined as

$$\tilde{y}_{B,m} = \frac{\tilde{Q}_{B,m}^{cal} - Q_{B,m}^{cal}}{Q_{B,m}^{cal}}, \quad (8.3)$$

results, recalling Eqs.(3.5) and (3.7),

$$\tilde{y}_B = S_B^T (S_B S_B^T + B_A)^{-1} y_A^{ex}, \quad (8.4)$$

where  $y_A^{ex}$  is a vector of elements

$$\tilde{y}_{A,l}^{ex} = \frac{Q_{A,l}^{ex} - Q_{A,l}^{cal}}{Q_{A,l}^{cal}}. \quad (8.5)$$

The corresponding evaluated covariance matrix results

$$\tilde{B}_B = S_B S_B^T - S_B S_B^T (B_A + S_B S_B^T)^{-1} S_B S_B^T. \quad (8.6)$$

To see these relationships in more detail, let us consider the case in which a single quantity  $Q_B$  relevant of a reference system has to be evaluated, based on the information contained in the measurements  $Q_{A,l}^{ex}$  of  $L$  quantities  $Q_{A,l}$  ( $l=1,2,\dots,L$ ), more or less correlated with  $Q_B$ , made in an experimental facility at somehow different geometry and composition conditions. Having determined the adjustments  $\tilde{y}_p$ , the relative correction to be applied to  $Q_B^{cal}$  is given by the expression

$$\tilde{y}_B = S_B \tilde{y}_p, \quad (8.7)$$

where  $S_B$  is the one-row matrix

$$S_B = |s_{B,1} \quad s_{B,2} \quad \dots \quad s_{B,J}|. \quad (8.8)$$



Let us define the correlation coefficients

$$r_{ls} = \frac{\epsilon_{ls}}{\epsilon_l \epsilon_s} \quad (8.9)$$

$$r_{B,l} = \frac{\epsilon_{B,l}}{\epsilon_B \epsilon_l} \quad (8.10)$$

where

$$\epsilon_{ls} = S_{A,l}^T B_{A,s} S_{A,l} \quad (\text{a priori covariance associated to } Q_{A,l}^{\text{cal}} \text{ and } Q_{A,s}^{\text{cal}}) \quad (8.11)$$

$$\epsilon_{B,l} = S_{B,l}^T B_{A,l} S_{B,l} \quad (\text{a priori covariance associated to } Q_B^{\text{cal}} \text{ and } Q_{A,l}^{\text{cal}}) \quad (8.12)$$

and

$$S_{A,l} = \begin{vmatrix} s_{A,l1} & s_{A,l2} & \dots & s_{A,lJ} \end{vmatrix} \quad (8.13)$$

We define also the quantities

$$\epsilon_l^2 = \epsilon_{ll} \quad (\text{a priori variance, assumed } \neq 0, \text{ associated to } Q_{A,l}^{\text{cal}}) \quad (8.14)$$

$$\epsilon_B^2 = S_{B,l}^T B_{B,l} S_{B,l} \quad (\text{a priori variance, assumed } \neq 0, \text{ associated to } Q_B^{\text{cal}}) \quad (8.15)$$

The amount of fractional change of  $Q_B^{\text{cal}}$  consequent on the information contained in measurements  $Q_{A,l}^{\text{ex}}$  and relative to the a priori error  $\epsilon_B$  can then be written, recalling Eq.(8.4), disregarding fourth (and higher) order correlation terms, and assuming that the covariance matrix  $B_A$  can be neglected with respect to  $S_{A,l}^T B_{A,l} S_{A,l}$  (a condition which usually justifies an experimental campaign),

$$\frac{\tilde{y}_B}{\epsilon_B} = \frac{1}{1 - \sum_{l < s} (r_{ls}^2 - 2r_{ls} \sum_{t > s} r_{lt} r_{st})} \left[ \sum_{l < s} (1 - \sum_{t > s} r_{st}^2) r_{B,l} \frac{y_{A,1}^{ex}}{\epsilon_1} - \sum_{s < t} (r_{st} - \sum_{l \neq s,t} r_{sl} r_{tl}) \left( r_{B,t} \frac{y_{A,s}^{ex}}{\epsilon_s} + r_{B,s} \frac{y_{A,t}^{ex}}{\epsilon_t} \right) \right] \quad (8.16)$$

As far as the error  $\tilde{\epsilon}_B$  to be associated with the updated estimate  $\tilde{Q}_B$  is concerned, the following expression can likewise be obtained

$$\frac{\tilde{\epsilon}_B^2}{\epsilon_B^2} = 1 - \frac{1}{1 - \sum_{l < s} (r_{ls}^2 - 2r_{ls} \sum_{t > s} r_{lt} r_{st})} \left[ \sum_{l < s} r_{B,l}^2 (1 - \sum_{t > s} r_{st}^2) - 2 \sum_{s < t} r_{B,s} r_{B,t} (r_{st} - \sum_{l \neq s,t} r_{sl} r_{tl}) \right] \quad (8.17)$$

It is easy to see the relationship between the BFT and the above methods. In fact consider one single experiment  $Q_{A,1}^{ex}$ . Eqs. (8.16) and (8.17) become

$$\frac{\tilde{y}_B}{\epsilon_B} = r_{B,1} \frac{y_{A,1}^{ex}}{\epsilon_1} \quad (8.18)$$

$$\frac{\tilde{\epsilon}_B^2}{\epsilon_B^2} = 1 - r_{B,1}^2 \quad (8.19)$$

Assume now  $r_{B,1} \approx 1$  (and then  $\epsilon_B \approx \epsilon_1$ ). Recalling the definition, Eq. (8.18), we obtain then the BFT expression

$$\tilde{Q}_B = Q_B^{\text{cal}} (1 + y_{A,1}^{\text{ex}}) \equiv Q_B^{\text{cal}} \frac{Q_{A,1}^{\text{ex}}}{Q_{A,1}^{\text{cal}}} \quad (8.20)$$

(with error  $\epsilon_B$  negligible). For  $r_{B,1}$  significantly different from unity, Eqs.(8.18) and (8.19) should be, instead, adopted.

### 9. LOGNORMAL AND TRUNCATED GAUSSIAN DISTRIBUTIONS

There may be circumstances in which, although physically known as positive, some parameters might result negative after the adjustment procedure. This can be due, for example, to large inaccuracies associated with the starting, a priori, parameters. In these circumstances, in order to make use of the information concerning the positiveness of the parameters themselves, their logarithmic value

$$t_j = \ln\left(\frac{p_j}{p_{o,i}}\right) \quad (j=1,2,\dots,J) \quad (9.1)$$

has been considered /15/ and the quantities

$$t_j^{\text{ex}} = \ln\left(\frac{p_j^{\text{ex}}}{p_{o,i}}\right) \quad (j=1,2,\dots,J) \quad (9.2)$$

are assumed normally distributed. The distribution function in this case reads

$$f(p)_j = \frac{1}{\sqrt{2\pi} \alpha_j p_j} \exp\left\{-\frac{[\ln(p_j/\beta_j)]^2}{2 \alpha_j^2}\right\}, \quad (9.3)$$

where  $\ln p_j$ , its average value (expressed as  $\ln \beta_j$ ) and its variance  $\alpha_j^2$

replace  $p_j$ ,  $\bar{p}_j$  and  $\sigma_j^2$ , respectively. The presence of the  $1/p_j$  coefficient at the right hand side is due to the fact that the argument  $p_j$ , rather than  $\ln p_j$ , is maintained, i.e., the distribution has been multiplied by  $d \ln p_j / dt_j$  ( $\equiv 1/p_j$ ). In this case the average value ( $\bar{p}_j$ ) and the variance ( $\sigma_j^2$ ) are given by the expressions

$$\bar{p}_j = \beta_j e^{\alpha_j^2/2} \quad (9.4)$$

$$\sigma_j^2 = \beta_j^2 e^{\alpha_j^2} (e^{\alpha_j^2} - 1) \quad (9.5)$$

and, conversely, if  $p_j$  and  $\sigma_j^2$  are known, the corresponding coefficients  $\beta_j$  and  $\alpha_j^2$  may be obtained by the expressions

$$\alpha_j^2 = \ln(1 + \frac{\sigma_j^2}{p_j^2}) [\equiv \overline{(\ln p_j)^2} - (\ln \beta_j)^2] \quad (9.6)$$

$$\beta_j = p_j e^{-\alpha_j^2/2} \quad (\ln p_j = \ln \beta_j) \quad (9.7)$$

Even though the use of the lognormal distribution answers the problem of avoiding negative values of parameters (known to be positive) out of an adjustment exercise, it is difficult to justify it on pure statistical grounds. A more correct approach can in fact be proposed, based on arguments relevant to the information theory /16/. Along with this theory, the distribution that makes the best use of the information on the first and second moments and on the positiveness of the distributed quantity, in the sense that it maximizes the so called information entropy, is the (left) truncated Gaussian. More generally, if we assume that a given quantity, say  $p_j$ , lies within the limits  $\epsilon_1$  and  $\epsilon_2$ , the following distribution function should be

used

$$f(p_j) = \begin{cases} \frac{1}{\sqrt{2\pi} \sigma_j} e^{-\frac{(p_j - \bar{p}_j)^2}{2\sigma_j^2}} & \text{for } \epsilon_1 \leq p \leq \epsilon_2 \\ 0 & \text{otherwise} \end{cases} \quad (9.8)$$

Parameters  $\bar{p}_j$  and  $\sigma_j^2$  can be related to the average values  $\bar{p}_j$  and the variances  $\sigma_j^2$  by means of the expressions

$$\bar{p}_j \equiv \int_{\epsilon_1}^{\epsilon_2} p f(p_j) dp = \bar{p}_j + \frac{\sigma_j^2 \mu_{j,0}}{\sqrt{2} \mu_{j,1}} \quad (9.9)$$

$$\sigma_j^2 \equiv \int_{\epsilon_1}^{\epsilon_2} (p - \bar{p}_j)^2 f(p_j) dp = 2 \left[ \frac{\sigma_j^2 \mu_{j,2}}{\mu_{j,1}} + \bar{p}_j \bar{p}_j - \frac{\bar{p}_j^2 + \bar{p}_j^2}{2} \right] \quad (9.10)$$

where

$$\mu_0 = e^{-\frac{t_1^2}{2}} - e^{-\frac{t_2^2}{2}} \quad (9.11)$$

$$\mu_1 = \int_{t_1}^{t_2} e^{-\frac{t^2}{2}} dt \quad (9.12)$$

$$\mu_2 = \int_{t_1}^{t_2} t^2 e^{-\frac{t^2}{2}} dt \quad (9.13)$$

and

$$t_1 = \frac{1}{\sqrt{2}} \frac{\epsilon_1 - \bar{p}_j}{\sigma_j}, \quad t_2 = \frac{1}{\sqrt{2}} \frac{\epsilon_2 - \bar{p}_j}{\sigma_j} \quad (9.14)$$

We can then write

$$\bar{p}_j = \bar{p}_j - \frac{\bar{\sigma}_j \mu_{j,0}}{\sqrt{2} \mu_{j,1}} \quad (9.15)$$

$$\frac{\bar{\sigma}_j^2}{\mu_{j,2}} = \frac{\mu_{j,1}}{\mu_{j,2}} \left[ \frac{\sigma_j^2}{2} - \bar{p}_j \bar{p}_j + \frac{\bar{p}_j^2 + \bar{p}_j^2}{2} \right] \quad (9.16)$$

The procedure to be followed for the latter type of adjustment consists in the following simple steps:

1. Determine the parameters  $\bar{p}_j$  and  $\bar{\sigma}_j^2$  via the Eqs. (9.15) and (9.16). A simple iteration routine may be adopted, starting with values  $\bar{p}_j = \bar{p}_j$  and  $\bar{\sigma}_j = \bar{\sigma}_j$  at the right hand side of these equations.
2. Adopt the standard adjustment technique, as described in Section 3, to determine the optimal values  $\tilde{p}_j$  and  $\tilde{\sigma}_j^2$ .
3. Obtain the optimal, adjusted, parameters  $\bar{p}_j$  and  $\bar{\sigma}_j^2$  using equations (9.9) and (9.10).

To exemplify, consider the simple case of one parameter,  $p$ , of which two experimental values are available, .5 and .3, to which variances  $.3^2$  and  $.2^2$  are associated. The quantity  $p$  is assumed positive, so that  $\epsilon_1 = 0$  and  $\epsilon_2 = \infty$ .

Following the usual adjustment (least squares) technique, we easily obtain:

$$\bar{p} = .362 \quad \bar{\sigma}^2 = .166^2$$

Adopting the lognormal distribution it results

$$\bar{p} = .364 \quad \bar{\sigma}^2 = .156^2$$

while, adopting the truncated Gaussian distribution,

$$\bar{p} = .317 \quad \bar{\sigma}^2 = .174^2$$

## 10. NONLINEAR GPT SENSITIVITY TECHNIQUES

As shown in Section 2, the GPT methodology can easily be adopted to cope with nonlinear problems. There are two main areas of interest to the adjustment methodology which are of particular interest: the first one concerns the exploitation of the information contained in burn-up and build-up experiments, the second one that contained in thermohydraulic ones.

In the following, techniques relevant to the evaluation of the sensitivities required to adjustment exercises are commented.

### 10.1. Burnup Field

A GPT related perturbation methodology relevant to the nuclide field has been developed in 1975 /17/. Kallfeltz et al. /18/ coupled it with the GPT methodology relevant to the neutron field to account for nonlinear effects inherent in burnup problems. Other efforts in the nonlinear domain have been made by Harris and Becker /19/, who arrived at a still crude formulation, and, successively, by Williams /20/ and Gandini /21/. Williams used variational techniques starting from the nuclide and (time-wise discretized) neutron density equations, along with the quasi-static approximation. Gandini used the heuristically based GPT method after having formally extended the neutron and nuclide field to a control (intensive) variable (determined by imposing that the power history is conserved). A rule which has played a crucial role for simply determining the operator governing the importance function with this latter method has been that of the coordinate dependence complementation mentioned at the end of Section 2. The equations obtained governing the (time-wise continuous) importance function result relevant to the physical solution. <sup>(see Appendix 1)</sup> Different integration schemes can then be defined /21/.

An integration scheme equal to that suggested by Williams could be as well easily obtained /22/ using this GPT methodology by selecting as (fictitious) control variable the eigenvalue,  $\lambda$ , multiplying the fission source in the (quasi-static) equation governing the neutron density and by making a proper use of the above mentioned variable complementation rule (the complementation in this case affecting also the time variable).

Typical quantities which can be analysed with these methodologies are:

- the amount of a material specified in a given region at the end of the reactor life cycle;
- the d.p.a. of a specific material and at a given position;

For what concerns the residual reactivity at the end of the reactor life cycle, two approaches have been developed: one proposed by Takeda et al. /23/, based on Williams' variational method, and another one based on GPT /24/ theory. The first one assumes as response to be studied  $1/\lambda$ , the second one the very expression of the control material worth at end of the fuel cycle, with reversed sign (which amounts to the true residual reactivity worth). Both of these methods call for an extension of the field to the conventional adjoint function. It is interesting to note that the two corresponding perturbation expressions differ from each other of a quantity proportional to the macroscopic absorption cross-section of the control material at the end of the fuel cycle /24/. So, in those cases in which this is expected to be negligible, this difference tends also to vanish.

## 10.2. Thermohydraulic Field

A major effort is presently underway, aiming at constructing a code by which a multi-channel thermohydraulic problem can be perturbatively analyzed. The governing equations to be solved have been obtained starting from those coded in the COBRA IV-I program /25/. These equations have been written in the form of a nonlinear matrix operator governing, within each channel, the compound field including fuel, clad, coolant and wall temperatures, coolant pressure and density, and cross-flow. Adopting the simple rules for reversing the Jacobian matrix around a reference solution has made it possible to obtain the equation governing the importance function relevant to the response to be analysed. A scheme of the calculational procedure can be found in Ref./26/. A rule which also here played a crucial role has been that of the coordinate dependence complementation mentioned in Section 2. Interface and/or limit conditions between different regions have been accommodated in the governing equations by means of appro-



appropriate delta functions (see Appendix 2).

Once this methodology will be implemented, adjustment exercises could as well be made in relation to thermohydraulic experiments (for example, at different steady state conditions) to adjust the data base. To this purpose the methodology illustrated in Section 3 can be very well used, interpreting parameters  $p_j$  as characterizing the thermohydraulic system considered and the responses  $Q_1$  as temperature and/or pressure detections at specified positions.

## APPENDIX 1

To illustrate the GPT methodology for burnup analysis, consider the field equations governing the neutron density  $[n(r,t)]$ , the nuclide density  $[c(r,t)]$  and the (intensive) control variable  $[p(t)]$  depending on the strategy chosen to maintain the overall power [an equation governing the neutron adjoint flux  $\phi^*$  could as well be considered in case a functional depending on it has to be studied]:

$$\underline{m}_{(n)} \equiv -\frac{\partial n}{\partial t} + B(c, \rho | p)n = 0$$

$$\underline{m}_{(c)} \equiv -\frac{\partial c}{\partial t} + E(n | p)c + \underline{h}_c(p) = 0$$

$$\underline{m}_{(\rho)} \equiv \langle c, S(p)n \rangle + W(p) = 0$$

where  $W$  is the overall, generally time dependent, power,  $p$  is a vector representing the system parameters,  $\underline{h}_c$  is a fuel source term generally given by a sum of delta functions defined at  $t_0$  and at each fuel feed operation time,  $S$  is a given matrix containing the microscopic fission cross-sections of the fuel materials.

Setting  $\underline{m} = \begin{bmatrix} \underline{m}_{(n)} \\ \underline{m}_{(c)} \\ \underline{m}_{(\rho)} \end{bmatrix}$  and following the simple rules of the GPT

methodology described in Section 2 [and then replacing  $\rho(t)$  with  $\langle \tilde{\rho}(r,t) \rangle / V$ ], to the

field  $\underline{f} = \begin{bmatrix} n \\ c \\ \tilde{\rho} \end{bmatrix}$  we can associate the derivative field  $\underline{f}/j = \begin{bmatrix} n/j \\ c/j \\ \tilde{\rho}/j \end{bmatrix}$  governed by the equation

$$\begin{pmatrix} \frac{\partial}{\partial t} + B & \frac{\partial(Bn)}{\partial c} & \frac{\partial(Bn)}{\partial \varphi} & \langle \cdot \rangle \\ \frac{\partial(Ec)}{\partial n} & \frac{\partial}{\partial t} + E & 0 & \\ \langle c, S(\cdot) \rangle & \langle (\cdot), Sn \rangle & 0 & \end{pmatrix} \begin{pmatrix} n/j \\ c/j \\ \tilde{\rho}/j \end{pmatrix} + \begin{pmatrix} m_{(n)}/j \\ m_{(c)}/j \\ m_{(\rho)}/j \end{pmatrix} = 0 ,$$

$\bar{\partial}/\partial n$  and  $\bar{\partial}/\partial \varphi$  representing Frechet derivatives. In turn, to the field  $f/j$  we can

associate the importance  $f^* = \begin{pmatrix} n^* \\ c^* \\ \tilde{\rho}^* \end{pmatrix}$  obeying the equation [recalling that in response  $Q_j$  (see Eq.(2.8)), for consistency with the complementation rule,  $\varphi_{/j} h_{\varphi}^+$  is replaced by  $\langle \tilde{\varphi}_{/j}, \frac{h_{\varphi}^+}{V} \rangle$ ]

$$\begin{pmatrix} \frac{\partial}{\partial t} + B^* & \left[ \frac{\partial(Ec)}{\partial n} \right]^T & S^T c \langle \cdot \rangle & \\ \left[ \frac{\partial(Bn)}{\partial c} \right]^* & \frac{\partial}{\partial t} + E^T & Sn \langle \cdot \rangle & \\ \langle n, \left( \frac{\partial B}{\partial \varphi} \right)^* (\cdot) \rangle & 0 & 0 & \end{pmatrix} \begin{pmatrix} n^* \\ c^* \\ \tilde{\rho}^* \end{pmatrix} + \begin{pmatrix} h_n^+ \\ h_c^+ \\ h_{\varphi}^+ \end{pmatrix} = 0 ,$$

$h_n^+$ ,  $h_c^+$  and  $h_{\varphi}^+$  depending on the response considered. The bottom row equation

corresponds to the relationship

$$\langle n^*, \left( \frac{\partial B}{\partial \varphi} \right)^* n \rangle = h_{\varphi}^+(t) ,$$

which transforms into an ( $\rho$ -mode) orthogonality relationship when  $h_{\varphi}^+ = 0$ .

Integrating the equations relevant to the importances  $n^*$  and  $c^*$  gives their physical solution. A variety of integration schemes can then be derived [21], depending on the problem considered [setting  $\varphi^*$  in place of  $\langle \varphi^* \rangle$ ].

## APPENDIX 2

To show the basic features of the GPT methodology, we shall consider here the simple steady state fuel/coolant heat balance equations, in cylindrical (two regions)  $r, z$  geometry,

$$m_1 \equiv \frac{1}{r} \frac{\partial}{\partial r} \left( rK \frac{\partial T_f}{\partial r} \right) - \left[ K \frac{\partial T_f}{\partial r} + h(T_f - T_c) \right] \delta(r - R^-) + s_f = 0 \quad (a)$$

$$m_2 \equiv \frac{2\pi R}{A} h [T_f(R) - T_c] - \frac{\partial(v\gamma_c T_c)}{c \partial z} + s_c = 0, \quad (b)$$

where  $T_f$  (fuel temperature) depend on  $r$  and  $z$ , whereas  $T_c$  (coolant temperature) only on  $z$ .  $R$  is the radius at the interface between fuel and coolant regions,  $A$  the transverse coolant area,  $K$  the thermal conductivity in the fuel,  $h$  the heat transfer coefficient,  $v$  the coolant speed,  $\gamma_c$  the volume heat capacity in in the coolant region,  $s_f$  and  $s_c$  heat source terms.

Usually the source term  $s_c \equiv s_{c,0} \delta(z - z_0)$ ,  $z_0$  being the inlet coolant position.

In Eq.(a) by an appropriate delta function the interface condition (at  $R$ )

$$-K \frac{\partial T_f}{\partial r} \Big|_{r=R} = h [T_f(R) - T_c]$$

has been incorporated, so that the correct overall heat balance is maintained. In fact space integrating over  $r$  between 0 and  $R$  would give the correct heat leakage,  $-2\pi R h [T_f(R) - T_c]$  [ $\equiv K(\partial T_f / \partial r)$ ], from the fuel region.

In accordance with the coordinate dependence complementation rule, sub-

stituting in Eqs. (a) and (b)  $T_c(z)$  with  $\langle T_c(r,z) \rangle / A$  [and in Eq. (b)  $T_f(R,z)$  with the equivalent expression  $\langle T_f(r,z)\delta(r-R) \rangle / 2\pi R$ ], they can be written

$$\left\{ \begin{array}{l} \frac{1}{r} \frac{\partial}{\partial r} \left( rK \frac{\partial}{\partial r} \right) - \left[ K \frac{\partial}{\partial r} + h \right] \delta(r-R) \\ \frac{h}{A} \langle \delta(r-R) \rangle \end{array} \right\} \frac{h \delta(r-R)}{A} \begin{array}{c} \langle \cdot \rangle \\ (c) \\ T_f \\ S_f \end{array} + \left\{ \begin{array}{l} \frac{2\pi R}{A} h - \frac{\partial(v\gamma)}{\partial z} \\ \frac{h}{A} \langle \delta(r-R) \rangle \end{array} \right\} \frac{\partial(v\gamma)}{A} \begin{array}{c} \langle \cdot \rangle \\ (c) \\ T_c \\ S_c \end{array} = 0.$$

Going through the GPT methodology [1], the (linear) operator governing

the derivative functions (in vector form)  $\begin{bmatrix} T \\ f/j \\ \sim \\ T \\ c/j \end{bmatrix}$  [defined by Eq. (2.4)] result, recalling Eq. (2.6),

$$H = \left\{ \begin{array}{l} \frac{1}{r} \frac{\partial}{\partial r} \left[ r \frac{\partial(K \cdot)}{\partial r} \right] - \left[ -K \frac{\partial}{\partial r} + h \right] \delta(r-R) \\ \frac{h}{A} \langle \delta(r-R) \rangle \end{array} \right\} \frac{h \delta(r-R)}{A} \begin{array}{c} \langle \cdot \rangle \\ (c) \\ T \\ S \end{array} + \left\{ \begin{array}{l} \frac{2\pi R}{A} h - \frac{\partial(v\gamma)}{\partial z} \\ \frac{h}{A} \langle \delta(r-R) \rangle \end{array} \right\} \frac{\partial(v\gamma)}{A} \begin{array}{c} \langle \cdot \rangle \\ (c) \\ T \\ S \end{array}$$

with  $\bar{h} = h - [T_f(R) - T_c] (ah / \partial T_c)$  and  $\bar{v}\gamma = v\gamma + T_c [\partial(v\gamma) / \partial T_c]$ .

By operation reversal, the following operator, governing the importance

functions (in vector form)  $\begin{bmatrix} T^* \\ f \\ \sim \\ T^* \\ c \end{bmatrix}$ , is obtained

$$H^* = \left\{ \begin{array}{l} \left( K \frac{1}{r} \frac{\partial}{\partial r} \left( r \frac{\partial}{\partial r} \right) - \left[ -K \frac{\partial}{\partial r} + h \right] \delta(r-R) \right) \\ \frac{\bar{h}}{A} \langle \delta(r-R) \rangle \end{array} \right\} \frac{h \delta(r-R)}{A} \begin{array}{c} \langle \cdot \rangle \\ (c) \\ T \\ S \end{array} + \left\{ \begin{array}{l} \frac{2\pi R}{A} \bar{h} + \frac{\partial(v\gamma)}{c \partial z} \\ \frac{\bar{h}}{A} \langle \delta(r-R) \rangle \end{array} \right\} \frac{\partial(v\gamma)}{A} \begin{array}{c} \langle \cdot \rangle \\ (c) \\ T \\ S \end{array}$$

94050312

The following equations then result [setting  $T^*(z) \equiv \langle T^*(r,z) \rangle / A$ ]

$$K \frac{1}{r} \frac{\partial}{\partial r} \left( r \frac{\partial T^*}{\partial r} \right) - \left[ -K \frac{\partial T^*}{\partial r} + h(T^* - T^*_c) \right] \delta(r-R^-) + h^+ = 0 \quad (c)$$

$$\frac{2\pi R}{A} \bar{h} [T^*(R) - T^*_c] + \sqrt{V} \frac{\partial T^*}{\partial z} + h^+ = 0 \quad (d)$$

$h^+$  and  $h^+_c$  being source terms associated with the response considered.

To note that Eq.(c) incorporates also the interface condition (at R)

$$K \frac{\partial T^*}{\partial r} \Big|_{r=R} = h [T^*(R) - T^*_c]$$

#### REFERENCES

1. A. GANDINI, "Generalized Perturbation Theory (GPT) Methods. A Heuristic Approach," in *Advances of Nuclear Science and Technology*, vol. 19, J. Lewins and M. Backer Eds., Plenum Press, N.Y., 1987.
2. Y.V. LINNIK, *Method of Least Squares and Principles of Theory of Observations*, Pergamon Press, Elmsford, N.Y., 1961.
3. A. GANDINI, CNEN Report, RT/FI(73)5, 1973.
4. J.B. DRAGT, *Nucl. Sci. Eng.*, **62**, 117 (1977).
5. M. MITANI and H. KUROI, *J. of Nucl. Sci. and Techn.*, **2**, 383 (1972).
6. A. GANDINI, CNEN Report, RT/FI(73)22, 1973.
7. A. GANDINI, G. PALMIOTTI, M. SALVATOIRES, *Ann. Nucl. En.*, **13**, 109 (1986).
8. A. GANDINI, CNEN Report, RT/FI(78)10, 1978.
9. A.M. MCCRACKEN, NEA Specialists Meeting on Sensitivity and Shielding Benchmarks, Paris, Nov. 17, 1977.
10. W. MATTHES, *Annals Nucl. Energy*, **6**, 103 (1979).
11. A. GANDINI, *Annals Nucl. Energy*, **10**, 443 (1983).
12. Y. RONEN, D.G. CACUCI, J.J. WAGSCHAL, *Nucl. Sci. Eng.*, **77**, 426 (1981).
13. R.E. KALMAN, *Trans. ASME, J. Basic Eng.*, **82**, 36 (1960).
14. A. GANDINI, "Uncertainty Analysis and Experimental Data Transposition Methods ...", in *Uncertainty Analysis*, Y. Ronen Edr., CRC Press (1988).
15. R. SCHMITTROTH, *Nucl. Sci. Eng.*, **72**, 19 (1979).
16. M. TRIBUS, "The Use of the Maximum Entropy Estimate in the Estimation of Reliability", in *Recent Developments in Information and Decision Processes*, R.E. Machol and P. Gray, Eds., MacMillan, New York, 1962, p.102.
17. A. GANDINI, CNEN Report, RT/FI(75)4, Rome (1975)
18. J.M. KALLFELTZ, G.B. BRUNA, G. PALMIOTTI, M. SALVATOIRES, *Nucl. Sci. Eng.*, **62**, 304 (1977).
19. D.R. HARRIS, M. BECKER, *Trans. Am. Soc.*, **23**, 534 (1976).
20. M.L. WILLIAMS, *Nucl. Sci. Eng.*, **70**, 20 (1979)
21. A. GANDINI, *Trans. Am. Nucl. Soc.*, **45**, 325 (1983). See also: *Ann. Nucl. Energy*, **14**, 273 (1987).
22. F. CARVALHO DA SILVA, private communication (1988)
23. T. TAKEDA, A. HARA, T. UMANO, Sensitivity Coefficient of Neutronic Property in a Fast Reactor Based on Depletion Perturbation Theory, Proceed. Top. Meet. on Reactor Physics and Shielding, Sept. 1984, Chicago, p.829.
24. A. GANDINI, *Advances in Generalized Perturbation Methods for Reactor Evolution Studies*, *Ibid.*, p.841. See also: *Ann. Nucl. En.*, **15**, 327 (1988).
25. COBRA IV Code, Report BNWL-2214.
26. A.C.M. ALVIM, F.R. ANDRADE LIMA, A. GANDINI, Application of the Heuristically Based GPT Theory to Thermohydraulic Problems", Proceed. II Congresso Geral de Energia Nuclear, Rio de Janeiro, April 1988.

## EXTENDED COVARIANCE DATA FORMATS FOR THE ENDF/B-VI DIFFERENTIAL DATA EVALUATION\*

Robert W. Peelle  
Oak Ridge National Laboratory  
P. O. Box 2008, Oak Ridge, TN 37831-6354

Douglas W. Muir  
Group T-2, MS-B243  
Los Alamos National Laboratory\*\*  
Los Alamos, NM 87545

### ABSTRACT

The ENDF/B-V included cross section covariance data, but covariances could not be encoded for all the important data types. New ENDF-6 covariance formats are outlined including those for cross-file (MF) covariances, resonance parameters over the whole range, and secondary energy and angle distributions. One "late entry" format encodes covariance data for cross sections that are output from model or fitting codes in terms of the model parameter covariance matrix and the tabulated derivatives of cross sections with respect to the model parameters. Another new format yields multigroup cross section variances that increase as the group width decreases. When evaluators use the new formats, the files can be processed and used for improved uncertainty propagation and data combination.

### INTRODUCTION

The formal methods of data adjustment require representation of the variance-covariance matrix of all data used. If this requirement is not met in a realistic way, the results are not likely to have the value expected by the analyst. All workers in the field have found substantial challenge in satisfying this criterion for integral as well as differential data.

For the ENDF/B-V differential data evaluation,<sup>1</sup> much effort was expended in the development of formats to permit the inclusion of covariance data,<sup>2</sup> and the evaluators for many of the most important cross sections made serious efforts to use these formats. The main goal was to allow propagation of the differential data uncertainties to yield responsible uncertainty estimates for parameters calculated from the data base.

\*Research sponsored by the Division of Nuclear Physics, U. S. Department of Energy, under contract No. DE-AC05-84OR21400 with Martin Marietta Energy Systems, Inc.

\*\*Operated by the University of California for the U. S. Department of Energy under contract W-7405-ENG-36.

Formally, this information is the same as that required for data adjustment,<sup>3</sup> though the level of detail required may be less demanding for simple uncertainty propagation.

The evaluation of covariance data for ENDF/B-V was difficult in part because of the lack of complete uncertainty estimates in the experiments and model calculations that underpin evaluations. In addition, provision was not included in ENDF/B-V formats to encode all the types of covariance data expected to be of importance to applications.

Since the release of ENDF/B-V, techniques for data evaluation that include covariance information have been more fully developed and tested at several installations, and a greater number of experimenters and model code users have taken pains to include covariance information with their results.<sup>4</sup>

Even when covariance data have been treated fully in a differential data evaluation, significant problems can occur in the development of the corresponding ENDF-format covariance files. For example, in the recent evaluation of standards and other important energy-dependent cross sections for ENDF/B-VI, the total of 800-odd output cross section values for ten reactions are correlated, but inclusion of 300,000 covariance elements in the evaluated file would be unsupportable. Our knowledge about such a variance-covariance matrix must be representable with a small fraction of this many parameters, particularly since the whole analysis is based on about 10,000 experimental data points.<sup>5</sup> The originally planned approach was to collapse the matrix strongly except near the diagonal; the method is untested as of this writing.

The approved ENDF-6 formats contain many options for easing and making more complete the representation of covariance data. Some are quite new in concept. Since one of the striking inadequacies was the inability to represent covariances of energy or angle distributions, the new formats include two general approaches to solving these problems.

The covariance representations outlined in this paper are new since publication of the format manual for ENDF/B-V.<sup>6</sup> The text below draws heavily on material prepared for the preliminary ENDF-6 format and procedure manual.<sup>7</sup>

## COVARIANCES FOR THE PRODUCTION OF RADIOACTIVE NUCLEI

A new MF-40 file is provided in ENDF-6 formats to contain covariance data for the neutron activation cross section information that is in File 10. The formats and procedures are based on a proposal by F. Mann.<sup>8</sup> The formats and procedures are very similar to those for smooth cross sections in File 33, except that there is an additional level of indexing corresponding to the indicator LFS, the identifier of the final state of the activation reaction.

## EXTENSIONS TO SOME EXISTING COVARIANCE FORMATS

Some relatively minor extensions have been included in the ENDF-6 formats to strengthen capabilities and avoid conflicts that arose in the development of uncertainty files for ENDF/B-V.

In the previous formats there were no provisions for encoding covariances between cross sections represented in ENDF files having different values of MF. One conflict arose concerning the thermal cross section parameters, for which tabulated covariances between neutron multiplicity

(File 1) and fission cross section (File 3) could not be represented.<sup>9</sup> Covariance quantities interrelating fission neutron multiplicity, fission cross sections, and activation cross sections can now be given, even though the quantities themselves appear in Files 1, 3, and 10, respectively. The extra labels required in the files are arranged so that zeros imply covariances among quantities in the same file.

Formerly, it was possible to indicate in "NC-type" sub-subsections that a particular smooth (e.g., File 3) cross section within a given energy region was evaluated entirely with respect to an indicated standard cross section. Now, an evaluated cross section can be recognized to depend on a standard with relative weight less than unity. This capability might be useful if some but not all of the underlying experiments recorded the ratio of the indicated cross section to a standard one. For a given energy region, two different standards can be referenced, provided the sum of their weights is no more than unity. Because it is necessary to "find" the variety of correlations introduced by the use of standards, it is hoped that evaluators will clearly document the cases in which they have employed such NC-type sub-subsections.

Consistent with the above paragraphs, an activation cross section in File 10 can now be recognized as a "standard" for purposes of covariance representation of a smooth cross section in File 3.

#### UPDATED RESONANCE-REGION COVARIANCE REPRESENTATIONS

The ENDF-6 formats include new options for both the resolved and the unresolved resonance regions. It is hoped but not yet proven that these relatively complex new formats will allow what is known about resonance region covariances to be treated for those nuclides where the uncertainty in resonance self shielding is important to applications.

##### The Resolved Resonance Region

The ENDF/B-V covariance formats allowed covariances among the parameters of the same resonance to be encoded provided one of the Breit-Wigner formats was used for the parameters themselves. This restricted approach is sufficient where only a few isolated resonances are of importance for resonance self protection. ENDF-6 formats contain a compatibility option so that existing evaluations can be employed with minimum alteration.

The resonance parameter formulations for which covariance data are permitted are no longer confined to the Breit-Wigner options, and off-diagonal elements are no longer restricted to parameters of the same resonance. Covariances between resonance energies and widths are also now allowed. In addition to the two Breit-Wigner descriptions, covariances can be given among Reich-Moore or Adler-Adler parameters. Any desired covariance terms among the parameters of arbitrarily selected sets of resonances can be given in a matrix format. As another option, all the parameters of a given type in a particular energy region may be treated as having an indicated covariance pattern.

No provisions are yet made to handle correlations among the parameters of resonances in different isotopes of an element or those of different materials. Successful covariance evaluation is not assured even though one can obtain a parameter covariance matrix from resonance fitting programs. For nuclides with many resonances, such as U-238, the problem of estimating and representing the important covariance elements provides a strenuous challenge.



## The Unresolved Resonance Region

There was no provision for uncertainties for the unresolved resonance region in ENDF/B-V formats, except that relative uncertainties in File 33 for such energy regions refer to the sum of the smooth cross sections given in File 3 and the cross sections reconstructed from the resonance parameters in File 2. Such an approach for the unresolved resonance region is sufficient for applications in which the nuclide in question has a low enough concentration that uncertainties in self-shielding factors are small compared to those in the average cross sections at infinite dilution.

An ENDF-6 format is defined for covariances in the unresolved resonance region. It may be used when self shielding can be important in this energy range. In File 32 the covariance matrix of one set of average Breit-Wigner resonance parameters is given for the whole region, and in File 33 are found the covariance data for the infinite dilution average cross section. The cross section processor obtains the covariance matrix of the shielded or effective cross sections by combining these two types of information. (Note that the File 32 average parameters themselves do not need to reproduce the self-shielding factors.) A means for this combination in a slightly less restricted case has been demonstrated by de Saussure and Marable.<sup>10</sup> In one test case using their results, Broadhead and Dodds found that the covariances of effective cross sections were only weakly affected by uncertainties in the average cross sections.<sup>11</sup> While it is unclear what the quantitative outcome will be for other cases, it is clear that no better approach has been identified. The idea is similar to the new ENDF-6 unresolved resonance region representation for the cross sections themselves, in which infinite dilution cross sections are given in the necessary detail, but average parameters are given at only a few energy points and are used only for the calculation of self shielding.

## SECONDARY ENERGY AND ANGLE DISTRIBUTIONS

Simplified representations are now provided for covariances of secondary angle and energy distributions that are contained in Files 4 and 5. These files are being replaced by File 6 in many evaluations for ENDF/B-VI because Files 4 and 5 do not permit the secondary energy variation of the angular distributions of outgoing particles that is usually observed for incident and secondary energies above a few MeV.

Covariance data for angular distributions of secondary particles can be encoded in File 34 in terms of covariances among Legendre coefficients. Energy-dependent correlations of the magnitude of the cross section with the angular dependence can be recognized using covariances of the  $a_0$  coefficient even though its nominal value is unity in the ENDF formats. Covariances are expected to be encoded for only one or two Legendre moments. The original expectation was that this format would be used at least for the scattering of neutrons on hydrogen, but the formulation of the next Section should permit more direct evaluation.

Based on a proposal by Perey,<sup>12</sup> a simplified covariance format is provided in File 35 for energy distributions of secondary neutrons. Covariance matrices for secondary neutron energy distributions may be tabulated for a few large primary neutron energy bands. It is assumed (not realistic) that there is full correlation for a given secondary energy within each primary energy band. The secondary energy distributions are

however assumed to be completely uncorrelated between the various primary energy bands (equally unrealistic). No covariances linking different materials or reaction types are allowed. Furthermore, no covariances with information in other files are allowed, for example smooth cross sections in File 3 or fission neutron multiplicities in File 1. The usefulness of this new format will depend on the evaluator judiciously balancing the effects of the incorrect assumptions. Note that the ENDF/B-V assumption of zero uncertainty in File 5 energy distributions is even more incorrect.

#### COVARIANCES OF QUANTITIES FROM MODEL CODES

Covariance data for cross sections and angular distributions that are output from any model or fitting code can in principle be represented by the model parameter covariance matrix and tabulated derivatives (sensitivities) of cross sections etc. with respect to key model parameters.<sup>5</sup> In favorable cases where relatively few parameters represent some cross sections over broad energy ranges, the representation can be quite compact as well as general. The details of the formulation and even the meaning of the parameters need not appear in the evaluated file. An advantage of such generality is that the results of a wide variety of evaluation methodologies can be described.

The idea of a covariance file structure based on this idea was explored by Muir,<sup>13</sup> who observed that multigroup averages of sensitivities are identical to the parameter sensitivities of the corresponding multigroup data; the latter are needed for most applications. To take full advantage of this equivalence, the sensitivities must be represented in a format as close as possible to that for the data itself, so that the sensitivities can be retrieved and integrated by processing codes that have received minimum modification. A proposal for such a format was presented by Muir at the May, 1988 CSEWG meeting.<sup>14</sup> Subsequently an ENDF-6 format modification was proposed<sup>15</sup> and accepted by the CSEWG Methods and Formats Committee for allowing the needed information to be placed in File 30.<sup>16</sup> The new approach may mitigate the considerable difficulty otherwise experienced in representing covariances for correlated energy-angle distributions and multiplicities, and should simplify covariance evaluation whenever the evaluated cross sections etc. have been derived from a theoretical formula using parameters among which the covariance matrix is known.

The potential value of a covariance format of this type became especially clear in connection with the R-matrix analysis of the light-element reaction systems for ENDF/B-VI,<sup>17</sup> in particular for the evaluation of the light-element neutron standards.<sup>18</sup> The parameters in this example describe levels (resonances) in the relevant compound systems. Where all resonances can be enumerated, the formulation can be considered exact and, if the relevant experimental data are consistent, the parameter covariance matrix can be trustworthy.

Much of the angle-energy dependent data being encoded in File 6 for the 1-20 MeV region is derived from optical and statistical-preequilibrium theoretical models. Relevant parameters for this case include the optical and level-density parameters, pre-equilibrium matrix elements, and gamma-ray strength functions. Parameter covariance matrices for similar models have been demonstrated in a few cases based on the experimental data used to define the parameters.<sup>19</sup> While such model parameter covariance data are not available for current U. S. evaluations of this type, developments elsewhere suggest that the general model parameter covariance propagation

technique will be applicable to a broad range of cross sections in the future. This prospect places certain difficulties in our path, since the resulting propagated uncertainties in individual differential cross sections would doubtless be smaller than systematic discrepancies observed in some angle and energy ranges.

Since the idea of the ENDF File 30 is somewhat new, it seem worthwhile to outline the approach. In the context of File 30 the term "sensitivity" is defined as the derivative  $\sigma'$  of an evaluated quantity, say  $\sigma$ , with respect to the logarithm of one of the model parameters  $\alpha_i$ , i.e.,

$$\sigma'_i = \alpha_i \partial\sigma/\partial\alpha_i .$$

An advantage of employing such derivatives in File 30 is that the  $\sigma'_i$  are expressed in exactly the same units as  $\sigma$  whether it be an actual cross section or a distribution quantity. This means that integrations over energy and angle can be performed with minimal changes in multigroup processing codes. Therefore, an ENDF/B processing program that calculates multigroup cross sections can be used with few modifications to obtain the parameter sensitivities of the multigroup constants using data encoded in File 30. The use of derivatives with respect to the logarithms of the parameters also meshes nicely with the use of relative parameter covariance matrices. It is understood that the data fields normally used to store information on cross sections etc. are used in File 30 to record the corresponding sensitivity information, but that other quantities have standard (MF/30) ENDF-6 definitions.

The first section, MT=1, of File 30 contains a directory that displays the contents and ordering of information that is recorded in other sections of the file. (Note that in File 30 the MT-values do not correspond to reaction types.) It also contains an optional cross-material and cross-sublibrary correspondence table that may be utilized if the same parameter values are important for covariance data outside the sublibrary/material in which a particular File 30 is placed. The directory serves as a guide for the processing codes and provides also an eye-readable list of the files and sections elsewhere in the current evaluation that are significantly sensitive to the parameters under consideration. A series of pointers for each parameter indicates the sections (MFSEN, MTSEN) of data in the main body of the evaluation that are sensitive to that parameter. MFSEN and MTSEN also determine the formats to be used to represent the dependence of the sensitivities on the applicable independent variables such as energy, angle, etc.

The second section of File 30, MT=2, contains the relative covariance matrix of the model parameters. The upper half of the symmetric matrix is encoded by rows in a way that saves space if the last elements in a row are null.

Sections MT=3 through MT=10 are set aside for possible future assignment, and those from 11 to 999 are used for the sensitivities. A single section in this range of MT values is the collection of all the sensitivities relevant to a given model parameter MP. The section number is determined by the parameter index, using the relation  $MT=MP+10$ . Each subsection corresponds to a record in the MT=1 directory, and contains the derivatives of the cross section etc. quantities in the referenced section (MFSEN, MTSEN) of the main file to the model parameter identified in that record.

The information in File 30 is considered to describe sources of uncertainty that are independent of those described in Files 31-40.

Therefore, for a given set of multigroup cross sections, the multigroup covariance matrix obtained from File 30 should be added to any such matrix derived from the other files.

In addition to the utility of File 30 that is directly apparent, some possibilities exist that are less obvious. (a) To permit covariance data for a smooth cross section evaluated from experiments to appear in File 30, an evaluator could set up an ad hoc "nuclear model" in which the model parameters are just the cross section values at particular grid points; for linear interpolation the sensitivity functions would be triangles centered on each grid point and reaching zero at the next adjacent grid points. (b) To seek more compact storage for any nuclear model, one could diagonalize the parameter covariance matrix and compute linear combinations of the original sensitivities using the resulting transformation matrix. If the transformed sensitivities interpolate as well as the original ones, at least for the important eigenvalues, the result would be useful and elegant. However, adjustment of parameters might become more complicated. (c) Another idea is for a processing code to store only the multigroup sensitivities and the original parameter covariance matrix rather than expand this information into the full multigroup covariance matrix which can be very large. For a particular applied problem, matrix products might be computed and stored that are the sensitivities of integral parameters (e.g. Doppler coefficients) to the nuclear model parameters. The same point is valid here as has been recognized for resonance parameters:<sup>20</sup> whenever practicable, formal adjustment can better proceed using the model parameters as variables rather than the intervening group cross sections.

#### A SELF-SCALING MINIMUM VARIANCE FOR GROUP CROSS SECTIONS

Up to now, ENDF covariance files processed on a sufficiently fine energy mesh yielded physically unreasonable full correlation between adjacent group cross sections; these singular multigroup covariance matrices caused distress in some mathematical manipulations and were conceptually objectionable. A "minimum variance" format has now been approved<sup>16</sup> to assure that, if an evaluated covariance matrix on the evaluator's grid is positive definite, the multigroup cross section covariance matrix on any user's grid will also enjoy this property. A second goal is to allow the evaluator to represent the effect of the underlying unresolved resonance structure on the uncertainty in the cross section averaged over regions smaller than those otherwise considered in the evaluation. The new format does not address minimum uncorrelated variances for energy or angle distributions.

Under this new procedure, diagonal (variance) components are added to the overall multigroup covariance matrix. These components can be small enough to make no unwarranted change to a propagated uncertainty averaged over a broad spectrum, but large enough to assure that multigroup covariance matrices are positive definite even for fine energy groups.

The covariance evaluator specifies values of  $F_k$  for selected energy intervals  $E_k$  in an LB-8 "NI-type" sub-subsection of e.g., File 33. The magnitude of the resulting variance component for a processed average cross section depends strongly on the size of the energy group as well as on the values of  $F_k$  in the sub-subsection. For the simplest case of a multigroup covariance matrix processed on the energy grid of this sub-sub-

section with a constant weighting function, the variance components  $VAR_{kk}$  contributed by the LB-8 component are just  $F_k$ ; the off-diagonal contributions are zero. LB-8 sub-subsections cannot be used to represent cross-reaction or cross-material covariances.

In general, each  $F_k$  characterizes a contribution to the absolute variance of the indicated cross section averaged over any energy interval (sub-group)  $\Delta E_j$  that lies completely within the energy interval  $\Delta E_k$  and that is narrow with respect to variations in the energy-dependent multigroup weight functions utilized in the intended applications. The variance contribution  $VAR_{jj}$  from an LB-8 sub-subsection to the processed group variance for the energy group  $(E_j, E_{j+1})$  is inversely proportional to its width  $\Delta E_j$  and is obtained from the relation

$$VAR_{jj} = F_k \Delta E_k / \Delta E_j$$

where  $E_k \leq E_j < E_{j+1} \leq E_{k+1}$ . Note that the  $VAR_{jj}$  are variances in average cross sections. No contributions to off-diagonal elements of the multigroup covariance matrix are generated by LB-8 sub-subsections.

In contrast to other processing laws to date, the law for processing LB-8 sub-subsections directly references the variance of an average cross section rather than the variance of a pointwise cross section. If a fine-grid covariance matrix is developed and then collapsed to the evaluator's LB-8  $E_k$  grid, the resulting variance components are just the  $F_k$ .

The values of  $F_k$  may be chosen by the evaluator to account for the statistical fluctuations in fine-group average cross sections that are induced by the width and spacing distributions of the underlying resonances. Values may also be chosen to represent the uncertainty inherent in estimating the average cross sections for small energy intervals where little or no experimental data exist and smoothness is not certain.

The LB-8 sub-subsections help prevent mathematical difficulties when multigroup covariance matrices are generated on an energy grid finer than that used by the evaluator, but  $F_k$  values must be chosen carefully to avoid accidental significant dilution of the evaluated covariance patterns represented in the other sub-subsections. If no physical basis is apparent for choosing the  $F_k$  values, they may be given values about 1% as large on the evaluator's grid as the combined variance from the other sub-subsections. Such values would be small enough not to degrade the remainder of the covariance evaluation, and large enough to assure that the multigroup covariance matrix will be positive definite for any energy grid if the matrix on the evaluator's energy grid is positive definite.

The requirement to include LB-8 sub-subsections should relieve numerical problems encountered by data adjusters whether the adjustments are based on integral data or on new differential data. However, even if  $F_k$  values are very carefully chosen, problems are inherent in covariance evaluations that utilize extremely coarse energy grids and thereby imply unphysical high correlations among cross sections for large energy regions. Some such evaluations were provided in ENDF/B-V because the main purpose of the covariance information was to permit the propagation of nuclear data uncertainties for applications with broad neutron spectra. However, some users who have employed the adjustment equations to update an existing evaluation by "adding" new data and their associated covariances have needed to modify certain ENDF/B-V covariance files onto a finer grid.<sup>21</sup> To minimize the extent to which such users will be tempted to make ad hoc changes to covariance files, ENDF-VI covariance evaluators for

reactions of particular importance are now being asked to employ narrower energy meshes than in the past in order to reduce the difficulties to be encountered by future evaluator-users of the covariance files.<sup>22</sup> Overlapping structures in energy and other techniques are suggested to reduce the occurrence of large changes in correlation as one crosses an arbitrary energy boundary.

### CONCLUSION

Broadened format capabilities and the increased experience with covariance data that is now possessed by measurers, evaluators, and users should facilitate the generation of new evaluated covariance files that better meet the requirements for formal data adjustment. It remains for evaluators to employ the newly available techniques to determine if they meet the needs. Since some of these formats have become available only after most of the evaluation work on ENDF/B-VI is completed, they may not be so widely used for the first version of the new evaluated file.

### ACKNOWLEDGEMENT

The authors acknowledge the significant contributions to the work described here by many other present and past members of the CSEWG Covariance Subcommittee. We also acknowledge the stimulating suggestions and requests brought to this subcommittee by analysts and nuclear data providers worldwide.

### REFERENCES

1. R. KINSEY, ed., ENDF/B Summary Documentation, BNL-NCS 17541 (ENDF 201), 3rd ed. (ENDF/B-V), a library coordinated by the National Nuclear Data Center, Brookhaven National Laboratory (July 1979).
2. F. G. PEREY, "The Data Covariance Files for ENDF/B-V," Oak Ridge National Laboratory Report ORNL/TM-5938 (ENDF-249), 1978. See also Ref 6.
3. R. W. PEELE, "Uncertainty in the Nuclear Data Used for Reactor Calculations," Chapter II of Sensitivity and Uncertainty Analysis of Reactor Performance Parameters, in Advances in Nuclear Science and Technology, Vol 14, Lewins and Becker, eds., Plenum Press, 1982. Compare Eqs. 8 (beware misprint) and 38.
4. D. L. SMITH, "Examination of Various Roles for Covariance Matrices in the Development, Evaluation, and Application of Nuclear Data," paper IC01(33), Proc. of the International Conference on Nuclear Data for Science and Technology, Mito, Japan, June 1988.

5. R. W. PEELLE, "Evaluating Nuclear Data Uncertainty: Progress, Pitfalls, and Prospects," p. 68, Proc. IAEA Specialists' Meeting on Covariance Methods and Practices in the Field of nuclear Data, Rome, Italy, November 1986, V. Piksaikin, ed., International Atomic Energy Agency Report INDC(NDS)-192/L (January 1988).
6. R. KINSEY, ed., "Data Formats and Procedures for the Evaluated Nuclear Data File ENDF/B-V," Brookhaven National Laboratory report, BNL-NCS-50496 (ENDF-102), 1979. Revised November 1983, B. Magurno, ed. See also Ref. 2.
7. P. F. ROSE and C. L. DUNFORD, "Preliminary Data Formats and Procedures for Evaluated Nuclear Data File ENDF-6," National Nuclear Data Center, Brookhaven National Laboratory, May 1988. Also, CSEWG communication of R. W. Peelle to C. L. Dunford and R. W. Roussin offering format and procedure modifications covering the LB-8 short range variance component and the File 30 option for use of nuclear model covariance matrices. (July 1988).
8. F. MANN, Hanford Engineering Development Laboratory, private CSEWG communication reproduced as Appendix 5B-2 in the Summary of the May 1984 CSEWG meeting, Charles Dunford, ed., Brookhaven National Laboratory (July 1984).
9. E. J. AXTON, "Evaluation of the Thermal Constants of U-233, U-235, Pu-239, and Pu-241 and the Fission Neutron Yield of Cf-252," p. 9, Central Bureau for Nuclear Measurements Report GE/PH/01/86, June 1986.
10. G. de SAUSSURE and JAMES MARABLE, Oak Ridge National Laboratory, private communication (1981). Also, submitted to Nucl. Sci. Eng. for publication (1988).
11. B. L. BROADHEAD and H. L. DODDS, Trans. Am. Nucl. Soc., Vol. 39, 929 (1981).
12. F. G. PEREY, Oak Ridge National Laboratory, private communication (1983).
13. D. W. MUIR, Proc. IAEA Specialists' Meeting on the Fusion Evaluated Nuclear Data Library, Vienna, Austria, November 1987.
14. D. W. MUIR, Format Proposal for File 30: Parameter Covariances and Sensitivities, Attachment B to Enclosure 5, "Summary of the CSEWG Meeting of May 10-12, 1988," Charles L. Dunford, ed., Brookhaven National Laboratory, July 1988.
15. D. W. MUIR, Los Alamos National Laboratory, private communication to R. Peelle, June 1988. The proposal was forwarded to the CSEWG Methods and Formats Committee July 15, 1988. See Ref. 7.
16. R. W. ROUSSIN, Oak Ridge National Laboratory, private communication as Chair of the CSEWG Methods and Formats Committee to C. Dunford of the National Nuclear Data Center, Brookhaven National Laboratory. August 30, 1988.

17. G. M. HALE Los Alamos National Laboratory, private communication (1988).
18. R. PEELLE and H. CONDE, "Neutron Standard Data," Paper IH01(020), Proc. of the International Conference on Nuclear Data for Science and Technology, Mito, Japan, June 1988.
19. UENOHARA, KANDA, YUGAWA, and YOSHIODA, "Estimation of Level Density Parameters and Energy Shifts With Bayesian Method," Proc. Intern. Conf. on Nuclear Data for Basic and Applied Science, p. 1201, Santa Fe NM, 1985. Y. KANDA and Y. UENOHARA, "Covariances of Nuclear Model Parameters Generated From Experimental Information," "Covariance Methods and Practices in the Field of Nuclear Data," Proc. of IAEA Specialists' Meeting, Rome, Italy, p. 98, November 1986, V. Piksaikin, ed., International Atomic Energy Agency Report INDC(NDS)-192/L (January 1988). UENOHARA, TSUJI, and KANDA, "Estimation of Parameters in Nuclear Model Formula for Nuclides of Structural Materials," paper BD05(112), Proc. International Conference on Nuclear Data for Science and Technology, Mito, Japan, June 1988.
20. A. GANDINI and M. SALVATORES, "Nuclear Data and Integral Measurements Correlation for Fast Reactors, Part 3, The Consistent Method," CNEN-RT/FI (74) 3, Comitato Nazionale Energia Nucleare, 1974. M. SALVATORES et al., "Resonance Parameter Data Uncertainty Effects on Integral Characteristics of Fast Reactors," p. 31, Proc. of the IAE Consultants Meeting on Uranium and Plutonium Isotope Resonance Parameters, October 1981, D.E. Cullen, ed., International Atomic Energy Agency report INDC(NDS)-129/GJ. B. L. BROADHEAD, "A Nuclear Data Adjustment Methodology Utilizing Resonance Parameter Sensitivities and Uncertainties," Dissertation, University of Tennessee, Knoxville, TN (1983).
21. C. Y. FU and D. M. HETRICK, "Experience in Using the Covariances of Some ENDF/B-V Dosimetry Cross Sections: Proposed Improvements and Addition of Cross-Reaction Covariances," p. 877 in Proc. of the Fourth ASTM-EURATOM Symposium on Reactor Dosimetry, Vol II, National Bureau of Standards, Gaithersburg, Md, (March, 1982). D. L. SMITH, "Some Comments on the Effects of Long-range Correlations in Covariance Matrices for Nuclear Data," p. 18, Argonne National Laboratory Report ANL/NDM-99 (March 1977)
22. P. F. ROSE and C. L. DUNFORD, eds., "Preliminary Data Formats and Procedures for the Evaluated Nuclear Data File ENDF-VI," op. cit., p 30.4 (May, 1988).





NEACRP Specialists' Meeting on the Application of Critical Experiments and Operating Data to Core Design Via Formal Methods of Cross Section Data Adjustments

Session 1 (Morning Session, Friday 23, September, 1988)

The first session dealt with the derivation and performances to two well established group cross section sets, CARNAVAL-IV and FGL-5, with the adjustments of JENDL-2 for uncertainty analysis, and a presentation on the requirements for uncertainty reductions of parameters of cores designed for passive reactivity shutdown.

M. Salvatores reported that the successive CARNAVAL sets were derived from previous versions by enlarging the experimental data base, with version IV developed for SUPERPHENIX applications. Three different categories of experimental data were distinguished which were analyzed in terms of spectrum-dependent parameters. The residual C/E-1's then permitted interpolation for the determination of the bias factors and their associated uncertainties for the reactor design configuration. CARNAVAL-IV performed very well for the prediction of the critical mass bias of SUPERPHENIX; however, a 8-10% bias was observed for the control rod worth. Underestimation of the capture and transport cross sections of Iron, non-adjustment (and underestimation) of the transport cross section of Oxygen, as well as overestimation of the  $^{10}\text{B}(n,\alpha)$  cross section have been identified as possible sources of errors. An integral data bank has been developed at Cadarache which will contain recent and new integral experimental data. The presently developed evaluated nuclear data file JEF-2 together with this integral experimental data bank are expected to provide improved versions of CARNAVAL.

The considerations which had been involved in the derivation of the adjusted group cross sections set FGL-5, and its performance were discussed by J. Rowlands. FGL-5 had been developed ~ 15 years ago and thus was constrained by the data available at that time, as well as the calculational methods which were not as refined as they are today. For these reasons data on reaction rate distributions, sodium void reactivity and control rod worth were not included in the adjustment process.  $k_{\text{eff}}$ , buckling, reaction rate ratios, spectra and small sample reactivities were used in an iterative process in order to avoid problems associated with the non-linearities. Recent reaction rate intercomparisons (IRMA) might (though with substantial reservations) indicate that uncertainties for reaction rate ratios may have been underestimated, and the C/E discrepancies for small sample worth, which existed then, has been found later to be due to calculational approximations. In spite of these problems, good consistency was found for the calculations of  $k_{\text{eff}}$  values and reaction rate ratios for all plate geometry ZEBRA assemblies which indicates high correlation of experimental techniques and calculational methods within one program. The FGL-5 set also provided good predictions for a wide range of other parameters, e.g. within  $\pm 5\%$  for control rod worth,  $\pm 5\%$  for sodium void,  $\pm 15\%$  for Doppler (SEFOR) and  $\pm 2\%$  for reaction rate distributions. However, problems due to the approximations for plate geometry calculations resulted in overpredictions of  $k_{\text{eff}}$  for pin geometry cores.

The adjustments of JENDL-2 cross sections with experimental data from the JUPITER-I and -II programs, and their use for the estimation of the prediction uncertainties of a 1000 MWe FBR core were discussed by T. Takeda. The C/E's obtained with JENDL-2 show good predictions for the criticality but derivations from 1 by 4-12% for spatial control rod worth and up to 28% for sodium void. The use of JENDL-3T did not improve these discrepancies and the use of data adjustment was decided. The C/E's were substantially improved after adjustments to the 29 experimental data from ZPPR-9, -10A, -10D and -13A. The uncertainties were evaluated for the derivation of bias factors using three different methods. The uncertainties for  $k_{eff}$ , control rod worth (central and 3rd ring), and the  $^{239}\text{Pu}$  fission rate ratio (edge to center) were considered for 1) the bias method, 2) the adjustment method, and 3) the combined adjustment and bias method. The latter involved the use of benchmark experiments for the adjustment of group cross sections and subsequent use of the adjusted set for the analysis of the experimental data from a mockup core and application of the bias method. Surprisingly, the uncertainties were found to be rather similar for all three methods but the uncertainties were reduced significantly compared with the uncertainties if integral experimental data were not used.

Finally, D. Wade summarized reductions of uncertainties required for core designs with passive reactivity shutdown features. Anticipated transients without scram (LOF, LOHS, TOP) were considered and it was shown that the asymptotic consequences of these events can be characterized by the change of the outlet temperature,  $\delta T_{out}$ . The uncertainties of the  $\delta T_{out}$  due to uncertainties of the neutronics parameters benefit substantially from partial self-cancellation of uncertainty components, which was shown for the LOHS. However, this type of cancellation fails for a TOP event. Consequently, several quantities of importance to TOP events were specified for which reductions of the uncertainties are required. Specifically, reduced uncertainties are required for quantities traditionally measured in critical assemblies, with emphasis on worth data.

In summary, various data adjustments have performed reasonably well and problems which occurred with the adjusted group cross section sets are associated with less refined calculational methods and poorer experimental values of the past. Correlations between experimental data from specific experimental programs and between calculational methods might have contributed to a false sense of security. Recent improvements of evaluated nuclear data files (JEF-2, ENDF/B-VI) should provide a sound basis for the utilization of accurate integral experimental data in order to improve and to reduce the uncertainties of predicted reactor design parameters. For this to become a reality, a high-quality integral experimental data base is required which contains a large range of different types of data and is as uncorrelated as possible. The latter can be achieved only by international cooperation.

W. P. Poenitz  
Argonne National Laboratory

September 23 PM session

The cross Section adjustment is effective to get reliable prediction for both static and burnup core performance parameters. A large number of integral data are required to cover wide range of neutron spectra. "Bad" data can be eliminated from the adjustment. The estimation of calculation method (model) errors and experimental errors should be carefully performed; rather large systematic differences were found among data measured by various organizations for a MASURCA assembly (IRMA campaign); correlations between different measured data may be large.

The adjustment method can be combined with the bias factor method. The reasonability of use of mockup critical both to adjustment and bias factor calculations should be discussed in more detail from theoretical and numerical points of view.

Measured data from power reactor operation may be useful in addition to critical assembly data. Sensitivity differences between mockup criticals and real cores should be discussed. Furthermore, data from transmission experiments and shielding experiments may be useful for the adjustment of specified elements.

To select a large number of reliable measured data, world-wide cooperation is desirable.

T. Takeda  
Osaka University

94050328



NEACRP Specialist's Meeting on the Application of Critical Experiments and Operating Data to Core Design Via Formal Methods of Cross Section Data Adjustments

Session 3 (Morning Session, Saturday 24 September)

Paper 3.1 Salvatores and A. D'Angelo

The variation of reactivity with burnup is a particularly important parameter in reactor optimization, and it is necessary to improve the data for both heavy isotopes and fission products to meet the accuracy requirements. The paper by Salvatores and D'Angelo describes measurements made for U-238, Pu-239, Pu-240 and Pu-241 and the consequent improvements in accuracy of prediction of heavy isotope reactivity effects. Although the heavy isotope contribution to the loss of reactivity with burnup is typically only 20% of the total loss, it is the net result of positive and negative components and the uncertainty in calculations of this component made before taking account of these new measurements is estimated to contribute 25% in the uncertainty in the calculation of the total reactivity loss with burnup.

Three types of measurement have been made:

- (a) Changing the type of plutonium fuel used in a central zone of a Masurca core (the BALZAC HI phase). Five configurations were studied:
  - (i) the reference core
  - (ii) plutonium fuel having three different isotopic ratios, including one with a high Pu-240 content ~45%.
  - (iii) as increase in the UO<sub>2</sub> content of the zone.
- (b) The PROFIL irradiation experiments in PHENIX for separated isotopes. These were analyzed by mass spectrometry and give values for the capture cross sections (relative to U-235 fission), with accuracies typically of about ±1%.
- (c) The TRAPU irradiation experiments for mixed-oxide pins in PHENIX. Fuel pins having three differing compositions were irradiated (two with Pu-240 contents of about 20% and one of about 40%).

The data sensitivities of these experiments are given in the paper. Since the spectra are essentially the same for all of the experiments, only one-group adjustments to the data are possible (treating these measurements in isolation). It is intended to use them with the JEF-2 library but to illustrate the importance of the measurements, calculations of the improvements in accuracy resulting from an independent adjustment of CARNAVAL-IV data are given. They show that the heavy isotope contribution to the uncertainty is reduced from 27% to 7%, the TRAPU experiments having the largest effect in reducing the uncertainty. There was good consistency between the results of the different types of experiment.

### Paper 3.2 H. Khalil and T. J. Downar

This paper also examines the uncertainty in the prediction of the variation of reactivity with burnup and how it can be reduced by taking account of fast critical integral data. The importance of an accurate knowledge of the reactivity variation and consequent control requirements in determining passive accommodation of transient over-power accidents in ALMR designs is emphasized. The paper extends an earlier study made for a 1000 MWe LMFBR to a uranium metal/Zr fuelled FFTF core (with 11 cycles) and an ALMR design having U-Pu-10% Zr fuel and sodium cooling (with 4 cycles). This core has internal radial breeders and a blanket. Discharge burnup is about 10.5% for both cores. A new method for calculating depletion-dependent sensitivity coefficients is described (Depletion Perturbation Theory, DPT). This single cycle method has been implemented in the REBUS-3 code. It is shown that burnup-reactivity change can be related to the difference between the beginning and end of cycle reactivity sensitivities. Comparisons are made with direct sensitivity calculations and the agreement is good. Further developments are being made to improve the efficiency of the method for equilibrium core calculations. It was necessary to modify the ENDF/B-V covariance data to ensure that these are positive definite. The covariance data were supplemented by data for the capture cross-sections of a lumped fission product by Liaw and also data for U-236. Tables of the contributions to the uncertainty in the burnup/reactivity swing for a single cycle,  $\delta k$ , are given (by isotope and reaction) for both FFTF and ALMR, the uncertainty being 3.27% for FFTF and 125% for ALMR. The large difference is a consequence of the different sensitivities, (a factor of 40 for U-238 capture, for example). However, when expressed in absolute rather than percentage terms, this ratio is reduced by a factor of about 7 to a factor of about 6. The changes in nuclide densities are the main sources of uncertainty. For the 1000 Mwe LMFBR, the uncertainty was estimated to be 30%. The uncertainties would be smaller for an equilibrium cycle.

The effect of using the ANL data adjustments (Collins and Poenitz), which are based on zero power critical experiments, is calculated. These do not include adjustments for fission products, U-236, B-10 absorption nor Mo capture but result in significant improvements in the accuracy of prediction, by a factor of 2 for FFTF and a factor of 3.5 for ALMR. The most relevant items of integral data are the K values and reaction rate ratios.

### Conclusions from papers 3.1 and 3.2

Even on the basis of zero power critical experiments, a useful reduction in the uncertainty in burnup/reactivity variations can be obtained. However, irradiation experiments measuring the composition change in well characterized fuel pins irradiated in the spectrum of interest given the most significant improvement (for the heavy element contribution). More experiments of this type (and complementary to them) would be valuable to improve the accuracy further and provide a test of the consistency.

### Paper 3.3 H. Tellier

An adjustment procedure is used for nuclear data in the thermal energy range. This procedure, called the Tendency Research Method, gives a relative weighing,  $\lambda$ , to the nuclear data adjustment term in the least-squares minimization expression ( $\lambda$  is usually taken to be unity). The importance of using systems with a wide range of spectra and relative compositions in such a procedure is emphasized.

Three types of measurements are taken into account:

- (a) criticality measurements (61 buckling measurements)
- (b) reaction rate ratios
- (c) analysis of the composition of spent fuel from Tihange I. This gives information about capture cross sections of heavy isotopes. It is emphasized that the irradiation conditions must be well known for the data to be useful.

Experiments on uniform lattices with accurately measured bucklings, and compositions are chosen for the analysis (including light water, heavy water and graphite moderated lattices with differing fuel/moderator ratios and both uranium and plutonium fuel and mixed fuel). The characteristics of the lattices are described in the paper. (A general problem is that most clean experiments are old and unreliable and new experiments are in complex geometry).

For the uranium systems, the slowing down density (probability of thermalization of a fission neutron) ranges from 0.35 to 0.93 the value for a typical PWR being 0.6. For the plutonium systems, the range is 0.25 to 0.87.

The burnup of the 42 irradiated fuel samples ranges from 0.4 to 3.3 TJ/kg with burnup being measured by the  $Md148/U238$  ratio. Although the calculations are carried out in 99 groups, the number of variable parameters can be reduced to just a few, being factors applied in 3 energy ranges: fast ( $>10$  keV), resonance (1 eV - 10 keV) and thermal. There are 23 variable parameters in all, 2 for each moderator, and the remainder for U-235, U-238, Pu-239, Pu-240 and Pu-241. (Cross-sections shapes are not varied in these ranges.) However, many of the parameter changes are small and inaccurate and so these are then fixed instead of being variable. All the adjustments are small and so the sensitivity equations can be linearized.

Following adjustment, the dispersion between calculated and measured values of  $k$  is reduced to 0.49% for uranium fuelled systems and 0.55% for plutonium fuelled systems (the values for individual systems being illustrated in figures in the paper).

The values of the thermal constants  $\nu$ ,  $\sigma_{gf}$  and  $\sigma_{gc}$  derived in this way for U-235 and Pu-239 are compared with the values of Divadeenam (1984) and Axton (1986). The accuracies are similar but there are one or two significant differences. In particular, for Pu-239 the value  $\nu$  is about 0.01 (or 0.3%) smaller. A value for Pu-240 capture which is about 3% lower than the ENDF/B-V value is obtained. Relative to JEF-1, other parameters have been adjusted, including Pu-240 1 eV resonance parameters.



Tellier's study is better than that of Divadeenam and Axton in the respect that it isn't limited to the use of thermal Maxwellian averages derived from reactor spectrum measurements and to assumptions that cross section shapes in the thermal region can be treated by means of Westcott g factors. However, the cross section shapes are assumed fixed in Tellier's study. His values could be revised following the completion of further measurements of these shapes. More detail of the differential data used in his fitting, and the treatment of covariances (for example with respect to reaction rate ratio measurements, and their dependence on half-life values and the systematic error etc.) and details of the integral measurements and uncertainties should be published so that the relative merits of the evaluations can be judged. In principle, his data should be better than that of Divadeenam and Axton because the integral data analyzed are more comprehensive and more rigorously analyzed, but it is not clear that this is also the case of the differential data included.

#### Paper 3.4 R. Hwang

The presentation began with a brief description of a proposed method for relating sensitivities involving resonance shielded cross sections to basic parameters. This will be important for Doppler coefficient sensitivity calculations.

The paper emphasized the role of integral data in improving the accuracy of prediction of integral properties and demonstrates this for a range of properties. Improvements in differential cross sections are few, an example being U-238 (n,n'). This is dependent on F8 ratio measurements.

The relationship between integral measurements and a property which is to be predicted is considered in terms of the perpendicular component of the sensitivities of the property relative to those of the integral data. For an improvement in accuracy of prediction, the perpendicular component should be as small as possible and the parallel component as large as possible. A code called ADJUST has been written to calculate the projection of the sensitivities of the property to be predicted on those of the integral data. On the basis of these components, the fractional improvement in accuracy is calculated and this is illustrated by calculations for a number of properties of FFTF.

The method can be used to evaluate the potential value of an integral experiment in improving the accuracy of prediction of properties.

In the following discussion Salvatores and Gandini described similar procedures which they have used for estimating the value of an experiment in improving the accuracy of predictions. The sensitivities themselves can give ideas about the type of experiment which could be of value but the reactor physicist must still think up experiments which he considers will help to reduce uncertainties in the properties of interest.

John Rowlands  
9-24/88

September 24 p.m. Session

(Rapporter: R. N. Hwang)

The first paper given by A. Gandini covers a wide range of topics of interest in the application of the data adjustment theory. Seven topics described are summarized as follows:

### 1. Identification of Systematic Error

The presence of systematic errors (in cross sections and/or other source) can impact the adjusted quantities. One commonly used method to test the statistical consistency is the  $\chi^2$ -test. If the value of  $\chi^2$  per degrees of freedom significantly exceeds unity, systematic errors in one or more quantities and/or basic parameters are present. If the systematic errors are attributed to a given integral experiment, the removal of such experiment from the adjustment procedure should bring the  $\chi^2$ -values down to the acceptable range. On the other hand, if the systematic errors are attributed to the basic parameters a more rigorous criterion is needed.

A method similar to that of Mitani and Kuroi has been developed to test the systematic error hypothesis. The method is based on the linearity assumption between the parameter deviations and the systematic error deviations with the coefficients denoted by a matrix R. Thus, an optimal estimate of the component due to the systematic errors can be obtained via the least square method. Consequently, it is possible to define a normal likelihood function and the corresponding  $\chi^2$  with the degree of freedom r equal to the difference between the rank of the sensitivity matrix and that of the matrix R. The new  $\chi^2$  with r degrees of freedom can then be used to test the systematic error hypothesis considered.

### 2. Recent Development in the Generalized Perturbation Theory

The calculations of the sensitivity coefficients via the GPT methodologies require the computation of the importance functions defined by an inhomogeneous equation. It may become a problem when two or three dimensional configurations are considered. An alternative method referred to as EGPT (equivalent GPT) was proposed whereby the inhomogeneous equation of interest is transformed into a homogeneous one so that many existing codes can be utilized.

### 3. Nonlinear Adjustment Procedure

The usual data adjustment theory is primarily based on the linearity assumption that defines the relationship between the change in a given response and the adjustment in cross sections. For some cases, the higher order effects may become important. Two iterative methods that treat the non-linear effect were reviewed. From a practical point of view, such methods generally require an excessive amount of computation when a large number of integral experiments are included. Furthermore, the convergence of such process is not guaranteed.

An alternative based on the so-called global detector technique was proposed. The optimal estimates under consideration can be expressed in terms

of a vector  $S^*$  physically equivalent to the sensitivity vector for the "global" functional  $Q^*$  defined as a linear combination of all functionals considered. An iterative method has also been developed to implement the method proposed.

#### 4. System Modelling

The data adjustment method can be extended to provide a useful tool for improving the accuracy of the estimated responses of interest in a specific operating system utilizing the on-line experimental information of the system measured at different time intervals. This new experimental information along with the adjusted quantities obtained in the usual approach provides a means for updating the quantities of interest and their uncertainties for the operating reactor. The processes are analogous to the well-known Kalman filter concept for dynamic systems in which independent observations are made at various time intervals.

Analytical expressions have been derived to incorporate the new information in the estimation of the quantities of interest and their uncertainties at a given time. It is seen that the influence of the "a priori" information on the adjusted quantities decreases as more additional information is added in the process.

#### 5. Correlation Coefficients and Their Use in Data Transposition

The question concerning whether and how the adjusted quantities based on the existing integral experiments are applicable to the design calculations is of great practical interest. It is especially important if the characteristics of the reference systems and their measured quantities do not resemble those in the design calculations. One useful criterion in treating the data transposition problem and optimal experiment design is to examine the correlation coefficients that relate these errors of the reference quantities to those of the quantities under consideration. It was shown that the ratio of the adjusted to the unadjusted variances for a given design parameter of interest can be expressed as a function of the correlation coefficients with respect to the reference quantities. The magnitude of the ratio provides a useful indicator whether the design parameter under consideration can be improved by the adjusted quantities based on the reference experiments. In the limit when one reference experiment is considered, the proposed expression becomes identical to that obtained by Usachev et al.

#### 6. Lognormal and Truncated Gaussian Distributions

The assumption of normal distribution for the quantities to be adjusted, in principle, renders the possibility that the adjusted quantities may become negative upon adjustment. One way to avoid the problem is to assume a normal distribution for the logarithm of the quantities (or lognormal distribution) instead. Thus, the adjusted quantities so obtained are always positive. The assumption, however, is clearly questionable on the statistical grounds. A more rigorous method consistent with the information theory was proposed as an alternative. The distribution that best preserves the first and second order moments and the positive nature of the quantity is the (left)

truncated Gaussian. The pertinent average and variances can still be obtained readily within any given range of interest.

A simple example was given to illustrate the impact on the adjusted quantities when the usual least square technique, the lognormal distribution and the truncated Gaussian were used respectively.

#### 7. Comments on Application of the Non-linear GPT Methodologies

Two main areas currently of interest that require the non-linear GPT methodologies are the burn-up calculations and calculations including the thermohydraulic considerations.

For burn-up calculations, two approaches are currently in use. One is the improved method proposed by Takeda et al, based on the variational method of Williams developed earlier. The other is the one proposed by Gandini based on the GPT. The former considers the eigenvalue  $\lambda$  as the adjustable quantity while the latter relies on the control rod positions. The difference between the perturbation expressions of the two methods is proportional to the macroscopic cross section of the control rod at the end of the fuel cycle. Hence, the difference may not be significant in many practical applications.

Applications of the GPT to the multi-channel thermohydraulic problem is also under consideration. A numerical method is being developed to treat the problem with a non-linear operator with the compound fields including fuel, clad, coolant and wall temperatures, coolant pressure and density, and cross flow. Applications of the adjustment methodologies in conjunction to various thermohydraulic experiments are anticipated upon completion of the code development.

The second paper given by R. Peele described the new covariance data formats for the forthcoming ENDF/B-VI data file with several improved features to accommodate various data required in the uncertainty analysis.

A new MF=40 file is provided to contain covariance data for the neutron activation cross section information in File 10. In addition the covariance quantities interrelating fission neutron multiplicity, fission cross sections and activation cross sections, which were not permitted in ENDF/B-V, can now be given even though these quantities themselves appear in Files 1, 3 and 10 respectively.

The new ENDF/B-VI formats also include new options for both the resolved and unresolved energy regions. For the resolved energy range, the covariance data are no longer confined to the Breit-Wigner options. Covariance data for the Reich-Moore or Adler-Adler parameters can also be accommodated. At present, no provisions are yet made to cope with the inter-correlations among resonance parameters of different nuclides. For the unresolved energy range, a covariance format is defined for the treatment of the self-shielding effect. The covariance matrix of one set of average Breit-Wigner parameters is given in File 32 while the covariance data for the infinitely dilute average cross sections are given in File 33. Thus, the user can obtain the covariance of the self-shielded cross sections of interest by combining these two types of information.

One striking new feature in the new ENDF/B-VI formats is the options that permit a more rigorous representation of the covariance of energy and angle distributions not permitted in ENDF/B-V. One "late entry" format allows for covariance data for cross sections from model or fitting codes in terms of the model parameter covariance matrix and the tabulated derivatives of cross sections with respect to the model parameters (or sensitivity coefficients).

Another welcome addition is the self-scaling scheme whereby the fine meshes in the covariance of the multigroup cross sections derived from the relatively coarse meshes given in the data file will not yield physically ambiguous full correlation among the adjacent groups. A minimum variance format based on simple energy scaling has been included to ensure the positive definite nature of the covariance matrix for any grid that the user chooses.

Third paper by Y. Orechwa addressed the target accuracy considerations for U.S. advanced LMR core designs. The basic philosophy of the U.S. advanced LMR design concept has been significantly affected by the changing socio-economic climates. The earlier perception of the need for LMFBRs to meet rapidly growing demand for electricity no longer exists. The loss of faith by public in nuclear power particularly in the areas of safety related issues and cost escalation has further compounded the problem. The conventional concept starting with the deployment of demonstration plant to the series production is no longer viable.

A promising alternative to cope with the change in the US is the IFR concept currently under consideration. The main characteristics of this new design are focused on inherent safety, reduced cost and closed fuel cycle with waste disposal capabilities. The accuracy of a core performance parameter for such reactor will undoubtedly be affected by the new operational modes of the fuel cycle. Like the traditional LMFBR designs, there is incentive for improvement of basic data as long as the data uncertainties are still dominant.

Numerical examples from the considerations of uranium startup, actinide self-consumption, the negative reactivity feedback mechanism due to radial expansion of the core, and the roles of neutron and  $\gamma$ -heating rate pertinent to the IFR designs are given to illustrate their importance in the design considerations.

In conclusion, Orechwa believes that the target accuracies are likely to play an important role in the IFR design although the evaluations of "useful" target accuracies may be a formidable task. There appears to be a trade-off between the inherent safety features and the degree of self-sufficient recycle. Critical areas are believed to be in the material accountancy and the burnup swing prediction.

Participants  
NEACRP Specialists' Meeting  
September 23-24, 1988

**CANADA**

A. R. Dastur  
Atomic Energy of Canada, Ltd.  
Canada Operations  
Sheridan Park Research Community  
2285 Speakman Drive  
Mississauga, Ont. Canada, L5K1B2

416/823-9040 - ext. 450

J. V. Donnelly  
Atomic Energy of Canada, Ltd.  
Whiteshell Nucl. Research Establishment  
Pinawa, Manitoba ROE 1 LO, Canada

204/753-2311 - ext. 3025

**FRANCE**

J. C. Cabrilat  
CEA - DRP/SPRC - Bldg. 230  
CEN/Cadarache  
13108 Saint Paul Lez Durance Cedex  
France

42.25.33.65

J. Mondot  
CEA - DRP/SPRC - Bldg. 230  
CEN/Cadarache  
13108 Saint Paul Lez Durance Cedex  
France

42.25.33.65

M. Roshd  
FRAMATOME  
Manager, Methods & Develop.  
Nuclear Design  
Tour Fiat - Cedex 16  
92084 Paris la Defense  
France

(1) 796-31-40

**FRANCE (cont.)**

M. Salvatores  
CEA - DRP/SPRC - Bldg. 230  
CEN/Cadarache  
13108 Saint Paul Lez Durance Cedex  
France

42.25.33.65

H. Tellier  
DEMT/SERMA/LENR  
CEN Saclay  
B.P. No. 2  
91190 Gif-sur-Yvette, France

**ITALY**

Augusto Gandini  
Comitato Nazionale Energia  
Nucleare e Energie Alternative (ENEA)  
CRE Casaccia  
Casella Postale 2400  
00100 Roma, A.D., Italy

(6) 30483459

**JAPAN**

Takanobu Kamei  
Nippon Atomic Industry Group Co., Ltd.  
NAIG Nuclear Research Laboratory  
4-1, Ukishima-cho, Kawasaki-ku  
210 Kawasaki-shi, Japan

044-277-3131

Iwao Otake  
ISL Inc.  
1-26-6 Higashi-Azabu  
Minato-ku Tokyo 106, Japan

03-583-6728

**UNITED STATES (cont.)**

P. B. Hemmig  
Office of Nuclear Energy  
NE-462  
U.S. Department of Energy  
Washington D.C. 20585

**UNITED STATES (cont.)**

D. C. Wade  
Argonne National Laboratory  
Applied Physics Division  
Building 208  
9700 S. Cass Avenue  
Argonne, IL 60439

**JAPAN (cont.)**

Fumiaki Nakashima  
Power Reactor and Nuclear Fuel  
Development Corporation  
9-13, 1-Chome Akasaka  
Minato-ku Tokyo 107, Japan

03-586-3311

Toshio Sanda  
Power Reactor and Nuclear Fuel  
Development Corporation  
9-13, 1-Chome Akasaka  
Minato-ku Tokyo 107  
Japan

03-586-3311

Keisho Shirakata  
Power Reactor and Nuclear Fuel  
Development Corporation  
9-13, 1-Chome, Akasaka  
Minato-ku Tokyo 107  
Japan

03-586-3311

Toshikazu Takeda  
Osaka University  
Department of Nucl. Engineering  
Yamadaoka 2-1, Suita  
Osaka, Japan

06-877-5111

**SWITZERLAND**

Hans-Dieter Berger  
Paul Scherrer Institute  
CH-5303 Wurenlingen  
Switzerland

056-99 28 94

**UNITED KINGDOM**

John L. Rowlands  
Room 220, Building B21  
Atomic Energy Establishment  
Winfrith  
Dorchester, Dorset DT2 8DH  
England

305 6311 - ext. 2051

**UNITED STATES**

Carol Atkinson  
Argonne National Laboratory  
P. O. Box 2528  
Idaho Falls, ID 83403-2528

208/526-7083

Peter J. Collins  
Argonne National Laboratory  
P. O. Box 2528  
Idaho Falls, ID 83403-2528

208/526-7479

Thomas Downar  
Purdue University  
& Argonne National Laboratory  
Applied Physics Division  
Building 208  
9700 S. Cass Avenue  
Argonne, IL 60439

312/972-7266

Edward K. Fujita  
Argonne National Laboratory  
Applied Physics Division  
Building 208  
9700 S. Cass Avenue  
Argonne, IL 60439

312/972-4866

**UNITED STATES (cont.)**

P. B. Hemmig  
Office of Nuclear Energy  
NE-462  
U.S. Department of Energy  
Washington D.C. 20585

R. N. Hwang  
Argonne National Laboratory  
Applied Physics Division  
Building 208  
9700 S. Cass Avenue  
Argonne, IL 60439

312/972-4877

Hussein Khalil  
Argonne National Laboratory  
Applied Physics Division  
Building 208  
9700 S. Cass Avenue  
Argonne, IL 60439

312/972-7266

Yuri Orechwa  
Argonne National Laboratory  
Applied Physics Division  
Building 208  
9700 S. Cass Avenue  
Argonne, IL 60439

312/972-4876

Robert W. Peelle  
Oak Ridge National Laboratory  
P. O. Box 2008  
Building 6010  
MS 354  
Oak Ridge, TN 37831-6354

615/574-6113

Wolfgang P. Poenitz  
Argonne National Laboratory  
P. O. Box 2528  
Idaho Falls, ID 83403-3538

208/526-7092

**UNITED STATES (cont.)**

D. C. Wade  
Argonne National Laboratory  
Applied Physics Division  
Building 208  
9700 S. Cass Avenue  
Argonne, IL 60439

312/972-4858

John R. White  
Mechanical & Energy Eng. Dept.  
University of Lowell  
Lowell, MA 01854

617/452-4530

David W. Wootan  
Westinghouse Hanford Company  
P. O. Box 1970  
MSIN L7-25  
Richland, WA 99352

509/376-4635

W. S. Yang  
School of Nuclear Engineering  
Purdue University  
West Lafayette, IN 47809

317/743-6356

Claes Nordberg  
NEA Data Bank  
Organization for Economic  
Cooperation and Development  
Nuclear Energy Agency  
91191 Gif-sur-Yvette Cedex  
France

94050340